# A STUDY OF THE CALCIUM-INDUCED MORPHOLOGICAL TRANSITIONS OF HUMAN ERYTHROCYTES

Jacqueline Linda Whatmore

Doctor of Philosophy

THE UNIVERSITY OF ASTON IN BIRMINGHAM

October 1991

The University of Aston in Birmingham

# A STUDY OF THE CALCIUM-INDUCED MORPHOLOGICAL TRANSITIONS OF HUMAN ERYTHROCYTES

Jacqueline Linda Whatmore
Doctor of Philosophy
1991

**SUMMARY**

An examination was made of the morphological transitions induced in human erythrocytes by the elevation of cytosolic calcium, and of the biochemical mechanisms responsible. The loss of the discocyte morphology and the sequential progression of cells through the echinocyte stages 1, 2, 3 and sphereo-echinocyte was found to occur in both a calcium concentration- and a time-dependent manner.

SDS-PAGE analysis of cytoskeletal proteins prepared from intact cells loaded with 150uM or 1mM calcium revealed the partial proteolytic loss of proteins 2.1, 2.2 and 4.1. The rate of proteolysis was not paralleled by that of echinocytosis, making a causative relationship unlikely. Cytoskeletal integrity did appear to influence shape reversal from the echinocyte to the discocyte morphology after removal of the calcium and ionophore A23187. The loss of 80% protein 4.1, 40% 2.1 and 30% 2.2 was associated with, although not necessarily the sole cause, of irreversible sphereo-echinocytosis. Pre-treatment of cells with wheat germ agglutinin preserved the discocyte morphology despite continued cytoskeletal proteolysis during calcium-loading.

All observations were made on cells incubated either in the presence or absence of glycolytic substrates, effectively altering cell metabolic status. This influenced the rate of progression of cells through the echinocyte stages, the rate of proteolysis of cytoskeletal proteins, and the extent and kinetics of shape reversal from cells transformed to the sphereo-echinocyte morphology. The stage 1 to discocyte transition was the rate limiting step of this shape recovery. In contrast the rate of loss of the discocyte morphology was independent of cell metabolic status during exposure to calcium, as was the extent of restoration of the discocyte morphology from cells transformed to stage 1 echinocytes. An hypothesis is presented that echinocytosis is a discontinuous process with discrete steps initiated by different biochemical mechanisms varying in their dependence on metabolic energy.

**KEYWORDS** Erythrocyte shape; calcium; proteolysis; cytoskeletal proteins.

An experiment is a device to make Nature speak intelligibly. After that one only has to listen.

George Wald
1967 Nobel Lecture

**ACKNOWLEDGEMENTS**

I wish to express my gratitude to Professor John Hickman for his guidance throughout the project and the preparation of this thesis, and also to Dr. Alan Perris for his valued advice.

I wish to thank my fellow members of the CRC research group for their friendship and help, and also uncomplaining donation of blood samples. In addition I wish to acknowledge the technical support of Jan Pargeter, Rose Hunt and Paul Fundak; the assistance of Beci Holt and Lesley Tomkins with the electron microscopy; the advice of Dr. G. Nash, and Dr. Jennifer Pinder for the kind donation of antibodies.

I am also grateful to the SERC, and Aston University for their support of the project.

Finally I wish to thank Darran, without who's encouragement these studies would never have been possible.

**CONTENTS**


| | | Page |
|---|---|---|
| SUMMARY | | 2 |
| ACKNOWLEDGEMENTS | | 4 |
| CONTENTS | | 5 |
| LIST OF FIGURES | | 10 |
| ABBREVIATIONS | | 14 |
| CHAPTER 1: INTRODUCTION | | 16 |
| 1.1 | Aims of this study | 17 |
| 1.2 | Introduction; the human erythrocyte | 18 |
| 1.3 | The molecular architecture of the human erythrocyte | 21 |
| | Erythrocyte plasma membrane | 21 |
| | Integral membrane proteins | 23 |
| | Erythrocyte cytoskeletal proteins | 24 |
| 1.4 | Analogues of erythrocyte cytoskeletal proteins in nonerythroid cells | 32 |
| 1.5 | The importance of calcium regulation in biological systems | 34 |
| 1.6 | Calcium regulation in the human erythrocyte | 36 |
| | Passive $Ca^{2+}$ permeability | 38 |
| | The erythrocyte membrane $Ca^{2+}$-ATPase | 38 |
| 1.7 | Intracellular consequences of a disturbance in calcium homeostasis | 42 |
| | Effects on cellular potassium | 42 |
| | Effects on cell shape | 42 |
| | Effects on cell enzyme systems | 44 |
| 1.8 | Shape transformations of human erythrocytes | 44 |
| 1.9 | The role of the plasma membrane in the control of erythrocyte shape | 46 |
| | The bilayer-couple hypothesis and the | 46 |

control of erythrocyte shape

The importance of membrane inositol lipids in the control of erythrocyte shape 47

1.10 The role of the cytoskeletal complex in the control of erythrocyte shape 49

Shape regulation by phosphorylation of cytoskeletal proteins 50

Shape regulation by proteolysis of cytoskeletal proteins 52

Shape regulation by calmodulin 56

The possible role of a contractile system in the control of erythrocyte shape 58

1.11 The role of co-ordinated membrane/cytoskeleton changes in the control of erythrocyte shape 58

1.12 Summary 61

CHAPTER 2: EXPERIMENTAL MATERIALS AND METHODS 64

2.1 Source of experimental materials 65

2.2 Buffers 67

2.3 Gel electrophoresis buffers 69

2.4 Preparation of erythrocytes 73

2.5 Induction of morphological transitions by elevation of intracellular free calcium 74

2.6 Cell fixation and quantitation of morphologies 75

2.7 Preparation of samples for scanning electron microscope 76

2.8 Examination of the effect of calcium concentration on the rate of echinocyte formation 77

2.9 Examination of time-dependent echinocytosis 77

2.10 Reversal of calcium-induced echinocytosis 78

| | | |
|---|---|---|
| 2.11 | Density separation of erythrocytes into populations of different ages | 80 |
| 2.12 | Examination of time-dependent echinocytosis in erythrocyte populations enriched in young or old cells | 82 |
| 2.13 | Examination of the reversal of calcium-induced echinocytosis in erythrocyte populations enriched in either young or old cells | 82 |
| 2.14 | Examination of the effect of incubation in buffer A at 37°C on subsequent calcium-induced morphological transitions | 83 |
| 2.15 | Uptake of $^{45}Ca^{2+}$ by erythrocytes in the presence of calcium ionophore | 84 |
| 2.16 | Preparation of erythrocyte ghosts to examine the effect of calcium on cytoskeletal proteins of intact cells | 86 |
| 2.17 | Modulation of calcium-induced morphological transitions by wheat germ agglutinin (WGA) | 88 |
| 2.18 | Examination of the effect of pre-treating cells with wheat germ agglutinin on calcium -induced cytoskeletal proteolysis | 90 |
| 2.19 | Trypsin-mediated proteolysis of erythrocyte ghost proteins | 91 |
| 2.20 | Estimation of protein concentration | 92 |
| 2.21 | Sodium dodecyl sulphate polyacrylamide gel electrophoresis (SDS-PAGE) | 92 |
| 2.22 | Immunological detection of ankyrin by Western blotting | 95 |
| 2.23 | Extraction and quantitiation of ATP | 97 |
| 2.24 | Examination of cellular ATP levels in cells maintained in either buffer A or B at 37°C | 98 |
| 2.25 | Estimation of cellular ATP levels during calcium loading of erythrocytes in buffer A, containing metabolic substrates | 99 |
| CHAPTER 3: | RESULTS AND DISCUSSION | 100 |
| 3.1 | An investigation into the progression of the calcium-induced morphological transitions of | 101 |

human erythrocytes and their relationship to both calcium concentration and the metabolic status of the cell

3.1.1 Introduction; calcium-induced transitions of erythrocyte morphology 101

3.1.2 The progression of echinocytosis in a metabolically replete environment 105

3.1.3 The progression of echinocytosis in erythrocyte populations enriched in either young or old cells 109

3.1.4 The progression of echinocytosis in a Tris buffer containing no metabolic substrates 113

3.1.5 Discussion 119

3.2 An investigation into the role of cytoskeletal proteolytic cleavage in the initiation of calcium-induced echinocytosis, and the importance of cytoskeletal integrity to the restoration of the discocyte form during shape reversal 123

3.2.1 Introduction; calcium-induced proteolytic event 123

3.2.2 Proteolytic events associated with time-dependent echinocytosis in erythrocytes loaded with either 150μM or 1mM calcium in a metabolically replete media 127

3.2.3 Proteolytic events associated with time-dependent echinocytosis in erythrocytes loaded with 1mM calcium in the absence of metabolic substrates (buffer B) 137

3.2.4 Proteolytic events associated with the trypsin digestion of erythrocyte ghost proteins 142

3.2.5 The reversal of calcium-induced shape transitions, and the relationship between the restoration of the discocyte morphology and cell metabolic status 144

3.2.6 The reversal of calcium-induced shape transitions in populations of erythrocytes enriched in either young or old cells 157

3.2.7 Electron micrographic examination of erythrocyte shape reversal 160

3.2.8 Discussion 160

3.3 The modulating effects of lectin binding on cell shape and cytoskeletal integrity during the loading of erythrocytes with calcium 165

3.3.1 Introduction; the effects of extracellular ligand binding on erythrocyte morphology 165

3.3.2 Modulation of the calcium-induced shape transitions of human erythrocytes by the extracellular binding of wheat germ agglutinin (WGA) 167

3.3.3 The effect of extracellular WGA binding on the proteolytic cleavage of protein 4.1 resulting from the loading of erythrocytes with calcium 172

3.4 The effects of long term pre-incubation in replete media on the progression of erythrocyte shape transitions induced by calcium-loading 178

3.4.1 Introduction 178

3.4.2 The effects of pre-incubation in replete media on echinocytosis induced by increasing calcium concentrations 179

3.4.3 The effects of pre-incubation in replete media on time-dependent echinocytosis 182

3.4.4 The effects of pre-incubation in replete media on the rate of accumulation of $^{45}Ca^{2+}$ in erythrocytes following permeabilization with A23187 186

3.4.5 The effects of pre-incubation in replete media on the rate of accumulation of $^{45}Ca^{2+}$ in erythrocytes following permeabilization with ionomycin 193

3.4.6 Discussion 200

CHAPTER 4: CONCLUSIONS 202

CHAPTER 5: REFERENCES 214

APPENDIX I: Shape reversal from the echinocyte form in erythrocyte populations enriched in either young or old cells 235

## LIST OF FIGURES


| Figure number | | Page |
|---|---|---|
| 1 | The surface architecture of the undisturbed human erythrocyte | 19 |
| 2 | The major red cell integral and cytoskeletal proteins | 22 |
| 3 | A schematic cross-sectional representation of the human erythrocyte and its association with the lipid bilayer membrane | 24 |
| 4 | A schematic representation of the spatial organisation of the major proteins of the human erythrocyte cytoskeleton | 26 |
| 5 | Simplified diagrammatic representation of the physiological consequences of a disturbance in erythrocyte calcium homeostasis | 43 |
| 6 | Simplified scheme of the phosphoinositide signalling cascade and its relationship to the regulation of other cellular processes | 48 |
| 7 | A summary of the distinguishing characteristics of each echinocyte stage | 76 |
| 8 | The progression of echinocytosis, illustrating the morphological characteristics of each echinocyte stage | 103 |
| 9 | Progression of echinocytosis induced by increasing calcium concentrations | 106 |
| 10 | The progression of time-dependent echinocytosis induced by 150μM calcium in erythrocytes held in buffer A | 107 |
| 11 | The progression of time-dependent echinocytosis induced by 1mM calcium in erythrocytes held in buffer A | 108 |
| 12 | A comparison of the levels of different echinocyte stages induced by 150μM calcium in populations of human erythrocytes enriched in either young or old cells | 112 |
| 13 | The influence of the availability of metabolic substrates during prolonged incubation on erythrocyte morphology and metabolic status | 115 |

| | | |
|---|---|---|
| 14 | The progression of time-dependent echinocytosis induced by 150μM calcium in erythrocytes held in buffer B | 117 |
| 15 | The progression of time-dependent echinocytosis induced by 1mM calcium in erythrocytes held in buffer B | 118 |
| 16 | The relationship between the morphology transitions induced by calcium and cell ATP levels | 120 |
| 17 | The electrophoretic separation of erythrocyte ghost proteins by SDS-polyacrylamide gel electrophoresis | 126 |
| 18 | Time-dependent proteolytic modification of cytoskeletal proteins in erythrocytes loaded with 150μM calcium | 128 |
| 19 | Time-dependent proteolytic modification of cytoskeletal proteins in erythrocytes loaded with 1mM calcium in the presence of glycolytic substrates (buffer A) | 132 |
| 20 | Time-dependent proteolytic modification of cytoskeletal proteins in erythrocytes loaded with 1mM calcium in the absence of glycolytic substrates (buffer A) | 138 |
| 21 | Densitometric analysis of protein cleavage in erythrocytes loaded with 1mM calcium in either the presence (buffer A) or absence (buffer B) of metabolic substrates | 139 |
| 22 | The proteolysis of erythrocyte ghost proteins during digestion with trypsin | 143 |
| 23 | The quantitation of cell morphologies during shape reversal from echinocytosis induced in absence of glycolytic substrates (buffer B); shape reversal attempted in the presence of metabolic substrates | 147 |
| 24 | The quantitation of cell morphologies during shape reversal from echinocytosis induced in absence of glycolytic substrates (buffer B); shape recovery also attempted in buffer B | 149 |
| 25 | The quantitation of cell morphologies during shape reversal from echinocytosis induced in presence of glycolytic substrates (buffer A); shape recovery also attempted in buffer A | 152 |

| | | |
|---|---|---|
| 26 | The quantitation of cell morphologies during the attempted shape reversal of erythrocytes previously loaded with 1mM calcium for 60 minutes | 156 |
| 27 | SEM analysis of shape reversal from echinocytosis induced by loading cells held in buffer A with 150µM calcium for 10 minutes; shape recovery also attempted in buffer A | 161 |
| 28 | SEM analysis of shape reversal from echinocytosis induced by loading cells held in buffer A with 1mM calcium for 15 minutes; shape recovery also attempted in buffer A | 162 |
| 29 | A comparison of the extent of erythrocyte shape modulation by WGA at 25°C and 37°C | 169 |
| 30 | Time-dependent proteolytic modification of human erythrocyte cytoskeletal proteins in intact cells loaded with 1mM calcium at 25°C | 174 |
| 31 | Time-dependent proteolytic modification of human erythrocyte cytoskeletal proteins in intact cells loaded with 1mM calcium at 25°C after pre-treatment with WGA | 175 |
| 32 | Densitometric quantitation of the rate and extent of the cleavage of protein 4.1 in erythrocytes loaded with 1mM calcium with (+WGA), or without (-WGA) prior treatment with WGA | 176 |
| 33 | Total echinocytosis induced by increasing calcium concentrations in erythrocytes incubated in buffer A at 37°C prior to calcium loading | 180 |
| 34 | A comparison of the time-course of echinocytosis before and after 6 hours incubation in buffer A when A23187 is used to facilitate calcium entry | 183 |
| 35 | The time-course of formation of different stage echinocytes in erythrocytes treated with 150µM calcium and 5µM A23187 after 6 hours incubation in buffer A at 37°C | 184 |
| 36 | A comparison of the rate of accumulation of $^{45}Ca^{2+}$ during the treatment of erythrocytes with 150µM calcium and A23187 before and after 6 hours incubation in buffer A | 188 |

| | | |
|---|---|---|
| 37 | A comparison of the rate of accumulation of $^{45}Ca^{2+}$ during the treatment of erythrocytes with 1mM calcium and A23187 before and after 6 hours incubation in buffer A | 190 |
| 38 | The rate of accumulation of $^{45}Ca^{2+}$ during the treatment of erythrocytes with 150µM calcium in the absence of ionophore | 191 |
| 39 | A comparison of the time-course of echinocytosis before and after 6 hours incubation in buffer A when ionomycin is used to facilitate calcium entry | 195 |
| 40 | The rate of accumulation of $^{45}Ca^{2+}$ during the treatment of erythrocytes with calcium and ionomycin before and after 6 hours incubation in buffer A | 196 |
| 41 | A comparison of the time-course of echinocytosis in erythrocytes incubated in buffer A for 6 hours at 37°C and then resuspended in either fresh buffer or the buffer used for incubation, before treatment with 150µM calcium and 5µM A23187 | 199 |
| 42 | The quantitation of cell morphologies during reversal from echinocytosis induced in an erythrocyte population enriched in young cells while held in buffer B; shape recovery attempted in buffer A | 236 |
| 43 | The quantitation of cell morphologies during reversal from echinocytosis induced in an erythrocyte population enriched in old cells while held in buffer B; shape recovery attempted in buffer A | 238 |
| 44 | The quantitation of cell morphologies during reversal from echinocytosis induced in an erythrocyte population enriched in young cells while held in buffer A; shape recovery attempted in buffer A | 240 |
| 45 | The quantitation of cell morphologies during reversal from echinocytosis induced in an erythrocyte population enriched in old cells while held in buffer A; shape recovery attempted in buffer A | 242 |

**ABBREVIATIONS**

| | |
|---|---|
| A23187 | Calcium Ionophore A23187 |
| APS | Ammonium persulphate |
| ATP | Adenosine-5'-triphosphate |
| BSA | Bovine serum albumin |
| $Ca^{2+}$ | Calcium ion |
| $Ca^{2+}$-ATPase | Calcium adenosine-5'-triphosphatase |
| $CaCl_2$ | Calcium chloride |
| Calpain | Calcium activated neutral protease |
| cDNA | copy deoxyribonucleicacid |
| Conc | concentration |
| DAG | 1,2-diacylglycerol |
| $dH_2O$ | Distilled water |
| DMSO | Dimethyl sulfoxide |
| DNA | Deoxyribonucleic acid |
| DPM | Disintegrations per minute |
| DTT | Dithiothreitol |
| ECL | Enhanced chemiluminescence |
| EDTA | Ethylenediaminetetraacetic acid |
| EGTA | Ethyleneglycol-bis-(ß-aminoethyl ether)N,N,N',N'-tetraacetic acid |
| G3PD | Glyceraldehyde 3-phosphodehydrogenase |
| Gly | Glycine |
| HCl | Hydrochloric acid |
| $HCO_3^-$ | Bicarbonate |
| Hct | Haematocrit |
| $H_2O_2$ | Hydrogen peroxide |
| IMP | Inosine monophosphate |
| Ins | Inositol |
| $InsP_3$ | Inositol 1,4,5-trisphoshate |
| K | Potassium |
| KCl | Potassium chloride |
| Kd | Kilodalton |
| L | litre |
| MCV | Mean cell volume |
| $Mg^{2+}$ | Magnesium ion |
| $MgCl_2$ | Magnesium chloride |
| mRNA | Messenger ribonucleic acid |
| Mw | Molecular weight |
| Na | Sodium |
| NaCl | Sodium chloride |
| NAG | N-acetylglucosamine |
| $NaH_2PO_4$ | Sodium dihydrogen phosphate |
| NaOH | Sodium hydroxide |
| PA | Phosphatidic acid |
| PAGE | Polyacrylamide gel electrophoresis |
| PBS | Phosphate buffered saline |
| PC | Phosphatidylcholine |
| PCA | Perchloric acid |
| PE | Phosphatidylethanolamine |
| PtdIns | Phosphatidylinositol |
| PtdIns4P | Phosphatidylinositol 4-phosphate |
| $PtdIns(4,5)P_2$ | Phosphatidylinositol 4,5-bisphosphate |

| | |
|---|---|
| PKC | Protein kinase C |
| PLC | $Ca^{2+}$-dependent polyphosphoinositide phosphodiesterase (phospholipase C) |
| PMSF | Phenylmethylsulphonylfluoride |
| PS | Phosphatidylserine |
| rpm | revolutions per minute |
| SEM | Scanning electron microscope |
| SDS | Sodium dodecylsulphate |
| SDS-PAGE | Sodium dodecylsulphate polyacrylamide gel electrophoresis |
| SM | Sphingomyelin |
| TEMED | N,N,N',N',-tetramethylethylenediamine |
| Tris | Tris[(hydroxymethyl)aminoethane] |
| WGA | Wheat germ agglutinin |

# CHAPTER 1: INTRODUCTION

## 1.1 Aims of this study

This thesis describes detailed examinations of the morphological and biochemical changes initiated in the mature human erythrocyte by a rise in intracellular free calcium levels. A range of intracellular physiological processes which are triggered by a rise in cytosolic calcium are accompanied by the morphological transition of the erythrocytes from normal discocytes to crenated echinocytes (figure 5). A greater understanding of the relationship between the two may thus provide information on both the pathophysiological effects of an abnormal calcium load and on the regulatory mechanisms controlling erythrocyte cytoskeletal and cytoskeleton/membrane associations. The experiments described in this thesis are essentially studies on the physiological effects of raising erythrocyte intracellular calcium to a level where shape transitions are induced. The cellular mechanisms responsible for these calcium-induced shape changes can then be examined. Therefore, experiments were designed with several specific aims:

1. To more fully understand the relationship between calcium concentration and the extent of the echinocytic morphological transition. Erythrocytes pass through several defined echinocytic stages as the shape transition progresses: a detailed study of the calcium loading conditions inducing each echinocyte stage during the discocyte - echinocyte transformation was made to provide

morphological information which could be related to the biochemical mechanism or mechanisms involved.

2. To examine possible sites of calcium action which maybe associated with cytoskeletal integrity. To continue previous work begun in this laboratory, the relationship between calcium-induced morphological transitions and cytoskeletal proteolysis was examined. Particular attention was paid to the key membrane/cytoskeleton linkage proteins, ankyrin and protein 4.1.

3. To examine the possible role of a transmembrane signalling pathway in the control of morphological transitions induced by calcium.

4. To provide information relevant to the pathophysiological effects of an increase in intracellular calcium in more complex cells. Analogues of erythrocyte cytoskeletal proteins have been identified in a variety of non-erythroid cells suggesting that the molecular processes controlling erythrocyte cell shape may have some general relevance in cell biology.

## 1.2. Introduction

The mature human erythrocyte contains no internal organelles or transcellular cytoskeletal structures. In comparison with more complex, nucleated cells the red cell thus appears to have a relatively `simple' molecular architecture. However, it is capable of surviving approximately 200,000 circuits through the bloodstream

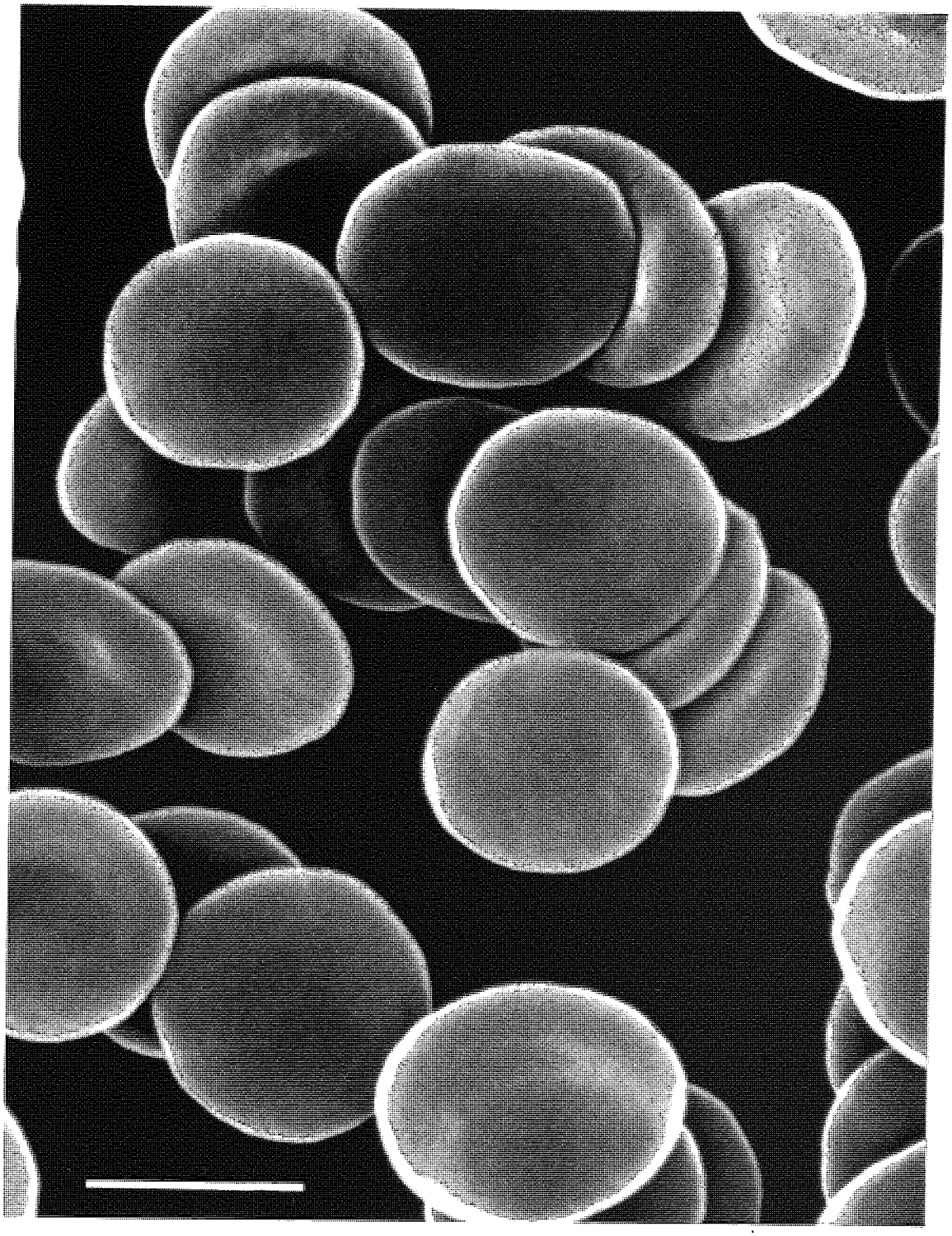

**FIGURE 1** The surface architecture of undisturbed human erythrocytes.
Cells were washed, fixed and photographed by scanning electron microscopy. Calibration bar, 5μM.

during its 120 day lifespan. The cell possesses remarkable physical properties: in the vasculature, erythrocytes survive continual deformation with immeasurably low levels of intravascular rupture and, when undisturbed, the cell immediately recovers its characteristic biconcave discoid morphology which is illustrated in figure 1. Less transient morphological changes can however be induced by a variety of chemical or environmental treatments.

Erythrocyte shape and durability is thought to be conferred jointly by the two major structural components of the cell: the lipid bilayer membrane and the two dimensional lattice of proteins forming a membrane-associated cytoskeleton on the cytoplasmic surface of the plasma membrane (Elgsaeter et al., 1986, Steck, 1989). Hypotonic lysis of erythrocytes removes contaminating haemoglobin and cytosolic elements, resulting in a membrane ghost in which the plasma membrane and cytoskeleton remain closely associated through the interactions of proteins which bind to both membrane spanning proteins and cytoskeletal components. Two such linkage proteins, ankyrin and protein 4.1 have been identified, (Bennett and Stenbuck, 1979, Anderson and Lovrien, 1984) and they will be described in greater detail later in this introduction. The key structural position of these proteins suggests that they may make an important contribution to the physical properties of erythrocytes.

## 1.3. The molecular architecture of the human erythrocyte

Since the lipid bilayer and the associated cytoskeleton contribute jointly to erythrocyte physical properties, this introduction will begin with a summary of the relevant characteristics of these two components.

### Erythrocyte plasma membrane

The erythrocyte plasma membrane is a lipid bilayer which, like many other biological membranes, has an asymmetric distribution of phospholipids between the two leaflets (Op den Kamp, 1979, Devaux, 1991). In the erythrocyte, the uncharged phospholipids which contain choline; sphingomyelin (SM) and phosphatidylcholine (PC), are preferentially located in the outer leaflet. In contrast the inner leaflet is rich in anionic lipids such as the aminophospholipids, phosphatidylethanolamine (PE) and phosphatidylserine (PS). Phosphatidylinositol (PtdIns) and its phosphorylated derivatives phosphatidylinositol 4-phosphate (PtdIns4P) and phosphatidylinositol 4,5-bisphosphate (PtdIns(4,5)$P_2$), account for 3-4% of total membrane lipid and are also concentrated in the inner leaflet of the bilayer (Butikofer, 1990). This asymmetry is thought to be maintained, at least partially by the active transport of the aminophospholipids from the outer, to the inner leaflet by an ATP-dependent carrier protein (Seigneuret and Devaux, 1984).

**FIGURE 2** Major red cell integral and cytoskeletal proteins

| Protein | Identification | Mol. wt. | Copies/cell |
|---|---|---|---|
| Cytoskeletal proteins | | | |
| 1 | Spectrin-alpha | 240,000 | 200,000 |
| 2 | -beta | 225,000 | 200,000 |
| 2.1 | Ankyrin | 215,000 | 100,000 |
| 2.2 | | 190,000 | |
| 2.3 | | 180,000 | |
| 2.6 | | 150,000 | |
| | Adducin-alpha | 103,000 | 30,000 |
| | -beta | 97,000 | 30,000 |
| 4.1a | | 80,000 | 100,000 |
| 4.1b | | 78,000 | 100,000 |
| 4.2 | | 72,000 | 200,000 |
| 4.9 | | 48,000 | 100,000 |
| 5 | Actin | 43,000 | 500,000 |
| 6 | G3PD | 35,000 | 500,000 |
| 7 | | 29,000 | 400,000 |
| 7a | Tropomyosin-a | 29,000 | 60,000 |
| 7b | -b | 27,000 | 60,000 |
| 8 | | 24,000 | 200,000 |
| Integral proteins | | | |
| 3 | Anion transporter | 95,000 | 1,000,000 |
| GPA | Glycophorin A | 43,000 | 600,000 |
| GPB | Glycophorin B | 39,000 | 50,000 |
| GPC | Glycophorin C | 25,000 | 80,000 |

Nomenclature based on electrophoretic mobility of proteins on SDS-PAGE (Fairbanks et al., 1971)

Integral membrane proteins

The close association between the lipid bilayer and the cytoskeletal network is the result of interactions between cytoskeletal components and the cytoplasmic domain of integral membrane proteins. The molecular weight and relative abundance of the major species of these proteins are identified in figure 2.

Two major species of integral proteins are present in the erythrocyte membrane, notably band 3 and the glycophorins. Band 3 is a glycoprotein present in about 1 X $10^6$ copies per cell (see Jennings, 1989 for a current review). The membrane spanning domain functions as an anion transport channel. The N-terminal 43kd segment however, forms a water soluble domain that is localized on the cytoplasmic surface of the membrane (Bennett and Stenbuck, 1980). This region contains a binding site for the cytoskeletal protein ankyrin (Bennett and Stenbuck, 1979) and therefore provides a major site of association between the membrane and the cytoskeleton.

The glycophorins A, B, C and D are a family of glycoproteins containing sialic acid. All except glycophorin B have extracellular, transmembrane and cytoplasmic domains. The cytoplasmic domains of both glycophorin A (Anderson and Lovrien, 1984) and glycophorin C (Reid et al, 1990) are able to bind to the cytoskeletal protein 4.1, providing a second group of membrane and cytoskeleton linkage sites. The associations between the

plasma membrane and the underlying cytoskeleton are illustrated below in figure 3.

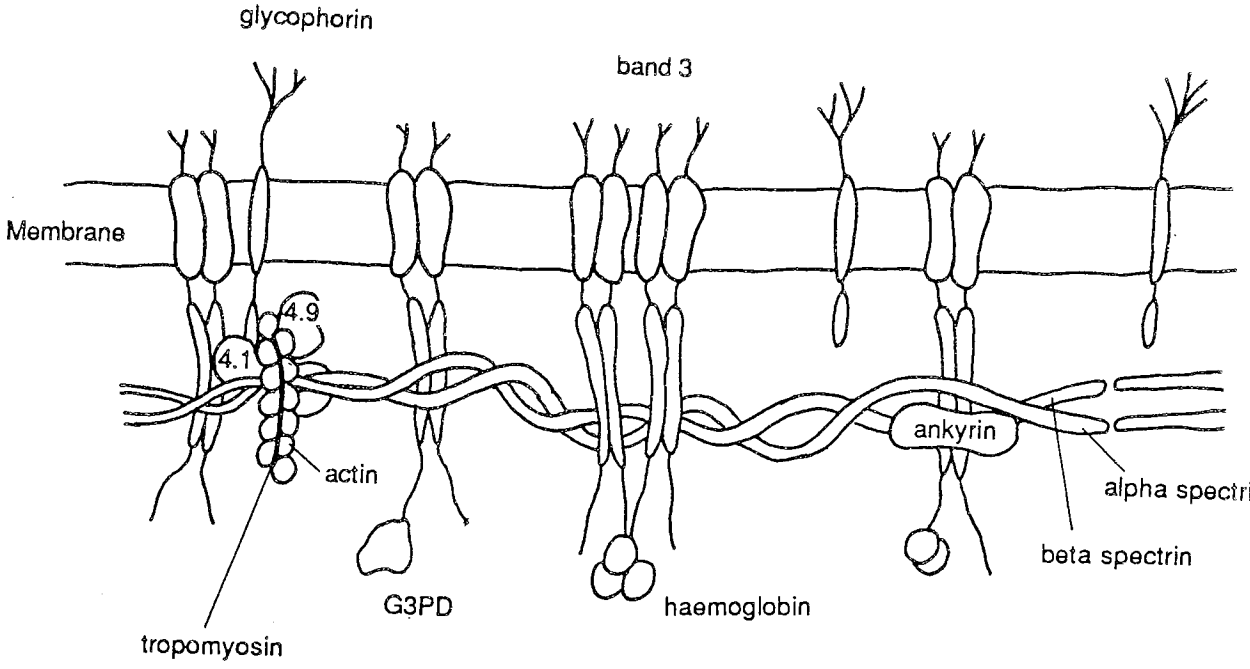


**FIGURE 3** A schematic cross-sectional representation of the erythrocyte cytoskeletal network and its association with the lipid bilayer membrane.

## Erythrocyte cytoskeletal proteins

When erythrocyte ghosts are treated with a nonionic detergent the membrane lipids and integral proteins can be selectively solubilized to reveal the cytoskeletal network as a fibrous insoluble residue (Yu et al., 1973). The structure of this isolated skeleton and its component proteins have both been extensively reviewed (Bennett,

1985, 1989, Marchesi, 1985). Three principle cytoskeletal proteins have been identified; spectrin, actin and protein 4.1. In addition, several accessory proteins are present, including ankyrin, protein 4.9, protein 4.2, adducin and tropomyosin. Electron microscopy has revealed the organisation of these proteins as junctional nodules linked by filamentous molecules to form a continuous, planar, roughly hexagonal lattice of proteins (Shen et al., 1986). The interrelationship of these proteins is shown in figure 4.

**Spectrin** Spectrin is the major protein of the erythrocyte cytoskeleton (reviewed by Goodman et al., 1988). It has two component polypeptides of 250kd (alpha) and 225kd (beta), which associate along their length in an antiparallel fashion to form heterodimers. End to end association of the dimers results in the formation of flexible, rod-shaped tetramers with a maximum, mean length of 194nm (Shotton et al., 1979), which are the principle form of spectrin present in the cytoskeleton (Ungewickell and Gratzer, 1978). The tetramers exist as helical structures, essentially forming weak, two stranded springs which are transiently extended when the cell is subject to mechanical forces. This confers elasticity and therefore durability to the cell which immediately recovers when the mechanical stress is relaxed (McGough and Josephs, 1990).

Spectrin displays the ability to bind to three other

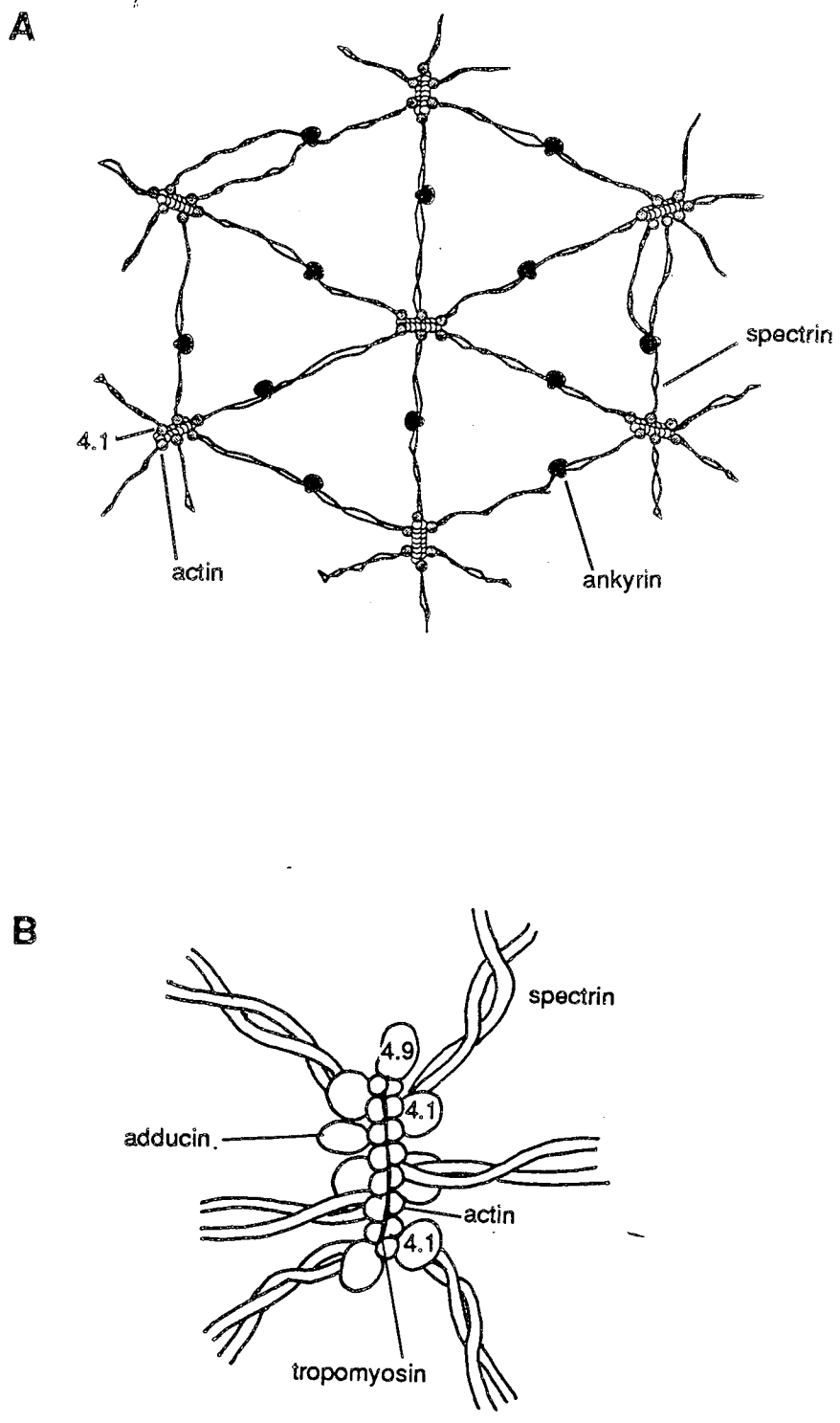


**FIGURE 4** A schematic representation of the spatial organisation of the major proteins of the human erythrocyte cytoskeleton.

**A** The arrangement of cytoskeletal proteins into a roughly hexagonal, two-dimensional lattice on the cytoplasmic surface of the erythrocyte plasma membrane. (Modified from Mangeat, 1988).

**B** The organisation of proteins within the junctional nodes of the protein lattice.

cytoskeletal proteins; actin, protein 4.1 and ankyrin. Rotary shadowing indicates that the actin-binding site of spectrin is close to the two tail ends of each tetramer (Cohen et al., 1980). This region contains the C terminus of the alpha subunit and the N terminus of the beta subunit, and sequence homology data has indicated that the actin-binding site is localized on the latter (Karinch et al., 1990, Winkelmann et al., 1990). However, Cohen et al. (1984), observed that only intact heterodimers exhibit actin-binding and therefore the interaction may also be dependent on alpha spectrin. The association between actin and spectrin is further promoted by protein 4.1 (Ungewickell et al., 1979) which interacts with the same terminal segment of spectrin that has shown to associate with actin (Winkelmann et al., 1990).

**Actin** Erythrocyte actin is organised into short, uniform filaments of approximately 12 G-actin monomers (Shen et al., 1986). The constant length and stability of these filaments is probably attributable to tropomyosin which is present in red cells with sufficient abundance to just cover both of the helical grooves of each actin filament (Fowler and Bennett, 1984). This interaction may in turn be regulated by the tropomyosin-binding protein, tropomodulin (Fowler, 1990). Also associated with actin are proteins 4.9 and 4.2 and adducin which are all thought to contribute to the assembly and/or stabilization of the

filaments. This complex of proteins based around actin forms the junctional nodes observed in isolated erythrocyte cytoskeletons. The tail ends of several spectrin tetramers interact with each actin filament (see figure 4), effectively cross-linking individual complexes and therefore providing the basic structure of the erythrocyte cytoskeleton.

**Protein 4.1** As mentioned previously protein 4.1 provides an important key linkage between the membrane and the cytoskeleton. In addition to its association with spectrin, protein 4.1 has a membrane binding site, for which several integral proteins have been proposed. Anderson and Lovrien (1984) observed that 4.1 specifically associates with glycophorin A on inside-out erythrocyte membranes, an interaction which has been shown to be regulated by PtdIns(4,5)$P_2$ (Anderson and Marchesi, 1985). An additional site of lower affinity binding has been associated with band 3 (Pasternack et al., 1985). However, recently Reid et al. (1990), have suggested that the interaction of 4.1 with the cytoplasmic domain of glycophorin C is the functionally important linkage in intact erythrocytes. This proposal is supported by the observation that erythrocytes deficient in glycophorin C have decreased membrane stability under conditions where glycophorin A deficient cells are normal (Reid et al., 1987).

On SDS gels protein 4.1 is visualised as a doublet containing two polypeptides of molecular weight 80kd and 78kd, known as 4.1a and 4.1b. The difference between the two is probably due to a post-translational modification that occurs during the maturation of erythrocytes since 4.1b predominates in young erythrocytes, while the higher molecular weight 4.1a is the major form found in older cells (Mueller et al., 1987).

**Ankyrin** Ankyrin provides the second important linkage between the erythrocyte cytoskeleton and membrane, by possessing binding sites for both spectrin and the cytoplasmic domain of the integral protein band 3 (Tyler et al., 1979, Bennett and Stenbuck, 1979). Rotary shadowing indicates that ankyrin binds approximately midway along the spectrin tetramers, about 20nm from the head of the spectrin molecules at which dimers associate to form tetramers (Tyler et al., 1979).

Ankyrin is present in erythrocytes as a family of closely related proteins, the largest of which has a molecular weight of 215kd on SDS gels and is known as protein 2.1. Antibodies raised against this protein also recognise the lower molecular weight polypeptides of the series; 2.2, 2.3 and 2.6 (Bennett and Stenbuck, 1979), and the close relationship of all four proteins is demonstrated by the similarity of their tryptic and chymotryptic peptide maps (Luna et al. 1979, Yu and Goodman, 1979). All of

these polypeptides are seen even when extreme care is taken to prevent proteolysis during preparation, and therefore are apparently present in intact erythrocytes. The lower molecular weight proteins are thought to be derived either by in situ proteolysis of the largest (Yu and Goodman, 1979), or by alternative mRNA processing (Hall and Bennett, 1987).

From the above discussion it can be seen that the two linkage proteins, ankyrin and 4.1, attach different domains of the cytoskeletal protein spectrin to the cytoplasmic surface of the plasma membrane. Therefore, close associations between these two erythrocyte structural components regularly occur over the entire cytoskeletal network. This suggests that the cleavage of either linkage protein during calcium loading of erythrocytes could weaken these associations and therefore have profound effects on erythrocyte shape.

**Other cytoskeletal proteins** In addition to the major structural components described above several other skeletal proteins have been identified whose role within the intact erythrocyte is still not fully understood.

At least two of these proteins are associated with the spectrin-actin junctions; protein 4.9 and adducin. The former has been shown to bind to, and bundle actin filaments in in vitro assays (Siegel and Branton, 1985), and it has been suggested that this protein may play some

role in cytoskeletal assembly during cell development (Siegel and Branton, 1985). Adducin may also be involved in the assembly of the cytoskeleton since the purified protein has been shown to bundle actin filaments. In addition, adducin promotes the association between spectrin and actin independently of protein 4.1 (Mische et al., 1987).

Protein 4.2 accounts for approximately 5% of the total membrane protein mass, and has even been cloned and sequenced (Korsgren et al., 1990, Sung et al., 1990) and yet its function in the intact cell remains unknown. Evidence for a structural role has been obtained from in vitro binding assays which indicate that 4.2 is capable of multiple interactions with other cytoskeletal proteins: it binds to purified ankyrin and 4.1, and also to the cytoplasmic domain of band 3 at a site distinct from that of ankyrin binding (Korsgren and Cohen, 1988). Recent clinical evidence supports a stabilizing role for protein 4.2 since individuals whose red cells are deficient in this protein suffer various levels of anaemia, with increased erythrocyte fragility (Rybicki et al., 1988).

Studies using monoclonal antibodies raised against platelet myosin have identified an erythrocyte form of this protein (Wong et al., 1985). More recent investigations have suggested that erythrocyte myosin is both anchored to the cytoskeleton and, is regulated by an interaction with protein 4.1 (Pasternack and Racusen, 1989).

## 1.4. Analogues of erythrocyte cytoskeletal proteins in non-erythroid cells

Analogues of erythrocyte cytoskeletal proteins have been found in many other cell types and throughout the animal kingdom (for review see Coleman et al., 1989). So far, proteins closely related to spectrin, ankyrin, protein 4.1, protein 4.2 and adducin have been identified in non-erythroid cells. These discoveries, in addition to the presence of actin, myosin and tropomyosin in erythrocytes and the similarity in spatial organisation of these proteins in erythroid and non-erythroid cells indicate that at least some aspects of the molecular structure of the erythrocyte cytoskeleton have a general relevance in cell biology.

Ankyrin was the first erythrocyte protein to be identified in non-erythroid cells. In 1979, Bennett prepared antibodies against a fragment of erythrocyte ankyrin and used this to demonstrate the presence of a related protein in a range of human and rat cells and tissues. Since then, ankyrin analogues have been purified from a variety of mammalian tissues including brain (Davis and Bennett, 1984), kidney (Drenckhahn et al., 1985) and endothelial cells (Ketis et al., 1986). Recently, the primary amino acid sequence of ankyrin has been derived (Lambert et al., 1990, Lux et al., 1990) and it has been found to have homology with several invertebrate, yeast and viral proteins. Interestingly, most of the homologous

proteins are involved with tissue differentiation and cell-cycle control, although the relevance of this is not yet known (Lux et al., 1990).

The discovery of non-erythroid ankyrins was followed in the early 1980's by the isolation of spectrin-like proteins from mammalian brain tissue (Levine and Willard, 1981, Bennett et al., 1982) and intestinal brush borders (Glenney et al., 1982). Antibodies raised against brain spectrin (fodrin) were subsequently used to identify related proteins in a whole spectrum of cultured cells (Burridge et al., 1982, Levine and Willard, 1981). In addition to mammalian spectrins, related proteins have been found in many avian cells (Repasky et al., 1982), and also in invertebrates such as Drosophila (Byers et al., 1987) and Acanthamoeba (Pollard, 1984).

Most mammalian erythroid and non-erythroid spectrins share certain structural characteristics: they are composed of two non-identical, high molecular weight subunits, they share some antigenic determinants, and amino acid and peptide sequencing has indicated a common structural motif (Coleman et al., 1989). Similarities in biological function also exist; all mammalian spectrins examined so far are capable of binding actin, often in association with protein 4.1. More recently, homology has been shown between the amino acid sequence of spectrin and both alpha-actinin and the human Duchenne muscular dystrophy protein (Davison and Critchley, 1988), which suggests that

spectrin is only one member of a large family of related proteins.

Proteins which react with antibodies raised against erythrocyte protein 4.1 have also been discovered in a diverse range of mammalian cells, including brain (Goodman et al., 1984), lens (Aster et al., 1986), fibroblasts (Cohen et al., 1982) and several blood cell types (Spiegel et al., 1984). In addition, Conboy et al. (1986) demonstrated that erythrocyte 4.1 cDNA hybridizes to non-erythroid mRNAs from liver, pancreas and intestine, further indicating a widespread distribution of 4.1 analogues. In most cases the functional role of these analogues is not clear. However, in lymphocytes this protein may play a role in the transmission of external stimuli into the cell (Kroczek et al., 1986).

Finally, non-erythroid forms of both protein 4.2 and adducin have been identified. Friedrichs et al., (1989), have demonstrated immunoreactive forms of erythrocyte 4.2 associated with the membranes of platelets, brain and kidney. Likewise, Bennett et al., (1988), have purified from brain tissue a protein closely related to, and having similar properties to erythrocyte adducin.

## 1.5. The importance of calcium regulation in biological systems

The precise regulation of cytosolic $Ca^{2+}$ levels is essential to the physiological welfare of all eukaryotic

cells (for review see Carafoli, 1987). Intracellular ionised calcium is maintained at micromolar levels whereas the extracellular concentration is in the millimolar range. Controlled gating across the membrane enables this ion to function as a messenger in the transduction of physiological stimuli after agonist receptor binding (reviewed by Rasmussen and Waisman, 1983). Cytosolic levels are then restored by sequestration or extrusion. If this homeostatic system is disrupted such that intracellular $Ca^{2+}$ rises excessively, several pathological consequences ensue. Not surprisingly therefore, many toxicological processes are frequently attributed to an impairment of calcium control mechanisms.

The role of calcium in cell death induced by toxic agents has been widely investigated. An early consequence of such injury is an increase in the cytosolic concentration of the ion (Schanne et al., 1979, Jewell et al., 1982). A relationship has been reported between this rise and the change in plasma membrane morphology resulting in cell surface `blebbing', which is an early cytotoxic event during cell death induced by many toxic agents (Jewell et al., 1982, Lemasters et al., 1983). However, this mechanism of bleb formation is not thought to be universal, in hepatocytes at least, depletion of cellular ATP appears to be a sufficient stimulus for cell surface changes, and calcium does not play a role in cell death until rupture of the `blebs' destroys the ionic gradients

across the plasma membrane (Lemasters et al., 1987, Nieminen et al., 1988, Harman et al., 1990).

Orrenius and colleagues (1989) have identified a number of biochemical mechanisms that are stimulated by sustained increases in cytosolic calcium. Several of these have the potential to induce cell surface `blebbing' and finally cell death through the disruption of membrane and cytoskeletal integrity. These processes include cytoskeleton weakening and dissociation by calcium-activated proteases and also the calcium-activated attack of phospholipases on membrane lipids (Nicotera et al., 1986, Orrenius et al., 1989). Interestingly, similar biochemical mechanisms have been implicated in the formation of spicules during the echinocytic morphological transition of human erythrocytes, as will be discussed later in this introduction. Therefore, examination of the mechanisms initiated during a rise in erythrocyte cytosolic calcium may provide information on some of the processes which mediate cell death in nucleated cells, following a disturbance of calcium homeostasis.

## 1.6. Calcium regulation in the human erythrocyte

For the human erythrocyte, in common with all living cells, the precise regulation of intracellular calcium concentration is essential for survival (for reviews see Schatzmann and Burgin, 1978, Carafoli, 1987, Lew, 1990). The intracellular environment of human erythrocytes is

maintained virtually $Ca^{2+}$ free. The total intracellular calcium content of erythrocytes from healthy donors estimated by atomic absorption spectroscopy is in the range 0.9 to 2.8μmol/L cells (Engelmann and Duhm, 1987). Of this, ionized calcium comprises only a small fraction and is maintained at a concentration of about 10-30nM (Lew et al., 1982, Rhoda et al., 1985). Most of the calcium present in erythrocytes is associated with the membrane since the amount estimated in ghost membranes is similar to that in whole cells (Harrison and Long, 1968). A number of membrane binding sites have been identified including the membrane calcium pump (Al-Jobore et al., 1984), the $Na^{+}$-$K^{+}$ pump (Brown and Lew, 1983) and proteins phosphorylated in the presence of ATP (Porzig and Stoffel, 1978). Cytosolic calcium may be bound by chelators such as 2,3-diphosphoglycerate (Collier and Lam, 1970). It is also possible that a fraction of total intracellular calcium is stored in vesicles (Engelmann et al., 1990) similar to those present in sickle erythrocytes (Lew et al., 1985).

Since plasma $Ca^{2+}$ concentrations are approximately 1.2mM a calcium gradient in excess of 10,000 fold exists across the erythrocyte membrane. The maintenance of this gradient is achieved by two contributing systems; a low passive membrane permeability to calcium and the active transport of the ion out of the cell.

Passive $Ca^{2+}$ permeability

At physiological external $Ca^{2+}$ concentrations, the low passive influx is saturated and reaches a maximum of 40-50µM/L cells per hour (Lew et al., 1982, Tiffert et al., 1984, McNamara and Wiley, 1986). Even if the external $Ca^{2+}$ concentration is raised far above the normal range, little increase in the passive influx into the erythrocyte is observed (Tiffert et al., 1984).

The erythrocyte membrane $Ca^{2+}$-ATPase

Erythrocytes possess a powerful membrane bound, ATP-driven $Ca^{2+}$ pump which extrudes calcium ions from the intracellular environment (for reviews see Carafoli et al., 1982, Schatzmann, 1983, Garrahan and Rega, 1990). Magnesium-dependent ATPase enzymes of this type have been reported in a wide variety of cells and are probably essential to calcium homeostasis in all eukaryotic cells (Garrahan and Rega, 1990).

Erythrocyte pump activity is stimulated directly by cytosolic free $Ca^{2+}$. The ion concentration required for half-maximal activation is 3.2µM in the presence of calmodulin (see below) and 24.5µM in its absence (Garrahan and Rega, 1990). Calcium extrusion is accompanied by the hydrolysis of ATP with a Ca:ATP stoichiometry of 1:1 in intact cells (Dagher and Lew, 1988). The saturated $Ca^{2+}$ extrusion capacity of the erythrocyte pump at non-limiting ATP concentrations is in the range 4-24mmol/L cells per

hour (Dagher and Lew, 1988). This is 2-3 orders of magnitude larger than the passive calcium influx, and the erythrocyte therefore maintains the pump-leak turnover of 40-50µmol/L cells per hour with a huge spare pump capacity.

Although the $Ca^{2+}$-ATPase is active at cytosolic calcium levels a number of factors have been shown to enhance the activation of the pump during a rise in intracellular calcium, including the calcium-binding protein calmodulin (Jarret and Penniston, 1978), limited proteolysis (Wang et al., 1988) and interaction of the pump with phospholipids (Roelofsen and Schatzmann, 1977, Carafoli et al., 1982). Of these mechanisms only activation by calmodulin has been demonstrated under physiological conditions (Muallem and Karlish, 1982)

**Pump stimulation by calmodulin** Calmodulin is a $Ca^{2+}$-binding protein that mediates the biological action of the ion in many calcium dependent reactions. The protein is found ubiquitously in eukaryotic cells and is highly conserved throughout evolutionary development, as is its general mechanism of action (for reviews see Klee et al., 1980, Cheung, 1982). Briefly, each calmodulin molecule possesses four calcium binding sites and the association of calcium with these sites is dependent on the concentration of $Ca^{2+}$ ions within the intracellular environment (Cheung, 1982). Upon the binding of $Ca^{2+}$ to inactive calmodulin the protein becomes activated and undergoes a large

conformational change (Dedman et al., 1977, Seamon, 1980). The activated $Ca^{2+}$-calmodulin complex is then able to bind to and activate the target enzyme which in the case of erythrocytes is most notably the $Ca^{2+}$-ATPase.

The cytosol of human erythrocytes contains relatively high concentrations of calmodulin; between 3-5μM (Foder and Scharff, 1981). It stimulates the activity of the $Ca^{2+}$-ATPase by increasing the apparent affinity of the enzyme for $Ca^{2+}$ by between 5 and 9 fold (Gietzen et al., 1980, Enyedi et al., 1987). However, although calmodulin stimulates pump activity it is not essential. The binding of calmodulin to the pump requires a calcium ion concentration of 1-10μM (Foder and Scharff, 1981) and therefore resting cytosolic calcium levels are insufficient. In addition, calcium transport still persists in the complete absence of the modulator.

**Pump stimulation by partial proteolysis** Partial proteolysis of the $Ca^{2+}$-ATPase by calpain (calcium activated neutral protease, see later) in the presence of calcium not only produces a calmodulin-like activation of the pump but also abolishes its sensitivity to calmodulin (Wang et al., 1988). The same effects are observed following limited trypsin treatment (Sarkadi et al., 1986) and it may be that proteolysis interferes with calmodulin activation by removing a regulatory domain that inhibits the system in the absence of the modulating protein

(Falchetto et al., 1991). Wang and co-workers (1988), have suggested that *in vivo* calpain may irreversibly activate the $Ca^{2+}$-ATPase in response to prolonged and/or uncontrolled intracellular calcium rises, thus providing the cell with a last defence mechanism against an otherwise lethal calcium influx.

**Pump stimulation by interaction with phospholipids** The activity of the erythrocyte $Ca^{2+}$ATPase is also modified by phospholipids in an *in vitro* environment. When purified pump preparations are reconstituted into lipid vesicles containing acidic phospholipids, enzyme activity is similar to that stimulated by calmodulin and, as with proteolysis, calmodulin sensitivity is lost (Niggli et al., 1981). In addition PtdIns(4,5)$P_2$ has been reported to stimulate calmodulin activation (Choquette et al., 1984). In spite of this evidence the relevance of lipid activation in the intact cell is not known.

The most likely explanation for the above observations is that the $Ca^{2+}$-ATPase has two functional forms (Scharff and Foder, 1978): a low affinity, low activity form and a high affinity, high activity form. Calmodulin, acidic lipids and partial proteolysis would induce the transformation of the pump to the latter form by either interacting with an inhibitory domain in the pump or, as in the case of proteolysis by removal of this domain.

## 1.7. Intracellular consequences of a disturbance in erythrocyte calcium homeostasis

The disturbance of erythrocyte calcium homeostasis results in a range of physiological effects which are summarised in figure 5. These include an increase in the K permeability of the membrane, the activation of a host of enzymes dependent on calcium, and gross morphological changes which are probably mediated by these enzymes.

### Effects on cellular potassium

Even a relatively small rise in the intracellular $Ca^{2+}$ concentration to 40-100nM is sufficient to activate the $Ca^{2+}$-sensitive K channels of intact erythrocytes (Tiffert et al., 1988). This leads to the rapid loss of intracellular potassium which in turn causes cell dehydration (Gardos, 1958, Lew and Ferreira, 1978). From the above data it appears that the activation threshold for these events is only just above physiological $Ca^{2+}$ levels and this may be one reason why erythrocytes maintain such low cytosolic concentrations of the ion.

### Effects on cell shape

A rise in internal $Ca^{2+}$ concentration from 10nm to 10-100μM leads to the morphological transition of the erythrocyte from the discocyte to a crenated echinocyte form (Sarkadi et al., 1976, Shimizu, 1988). This transformation involves a progression of morphological

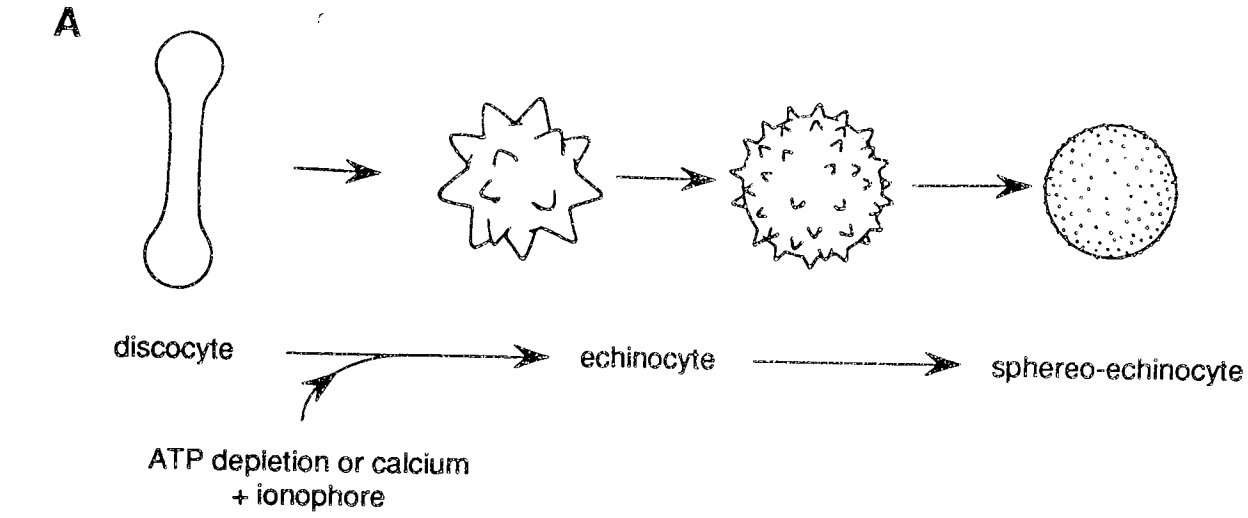


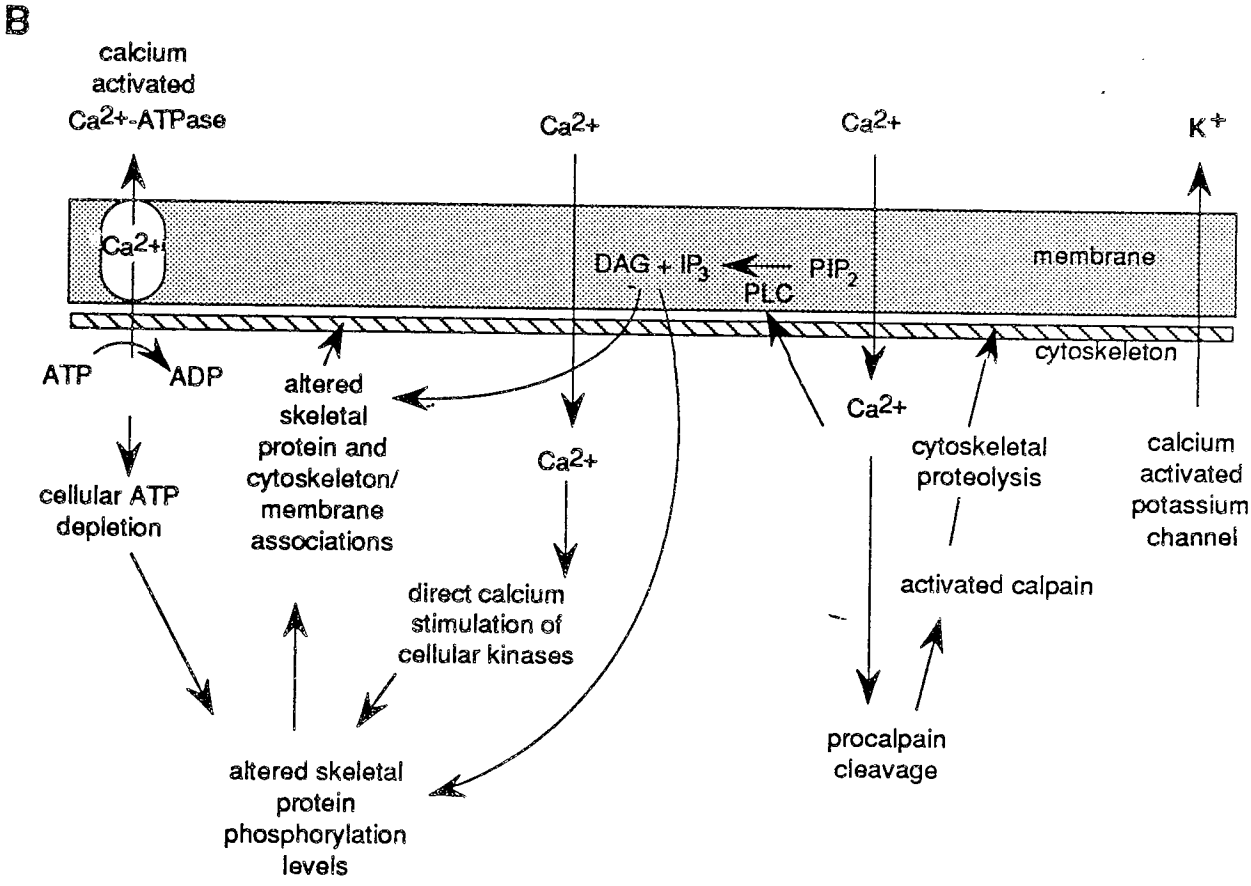


**FIGURE 5** Simplified diagrammatic representation of the physiological consequences of a disturbance in erythrocyte calcium homeostasis

**A** Morphological transformation of the discocyte to the echinocyte form.

**B** Stimulation of calcium-activated intracellular processes.

changes. Initially spicules appear on the surface of the membrane, followed by the disappearance of discoid morphology as the cells become spherical. Eventually the spicules separate leading to membrane loss and the formation of smooth sphereo-echinocytes (Bessis, 1973). This shape change is accompanied by a loss of cell deformability (Weed, et al. 1969).

Effects on cell enzyme systems

The entry of calcium into the erythrocyte activates a whole range of calcium stimulated enzymes; either directly, indirectly or via calmodulin. Many of these are described in greater detail in other sections of this introduction along with their possible relevance to shape changes. Briefly however, amongst the enzymes calcium is known to activate are, cell proteases which degrade cytoskeletal components, a phosphodiesterase which attacks membrane lipids and kinases which alter the phosphorylation of skeletal components. In addition, ATP consumption by the $Ca^{2+}$-ATPase may lead to cellular ATP depletion which would in turn affect the phosphorylation levels of both cytoskeletal and membrane components.

## 1.8. Shape transformations of human erythrocytes

Human erythrocytes can be induced to undergo shape transitions from the native discocyte to a crenated echinocyte form (figure 5) by a number of in vitro

manipulations. In the early 1960's Nakao and his co-workers (1960, 1961) noticed that if erythrocyte ATP levels fell below a certain threshold the cells became echinocytes and therefore concluded that ATP was necessary for the maintenance of the discoid form. Similar shape changes were found to be induced by certain anionic amphiphilic compounds (Deuticke, 1968). In addition, as indicated above, intracellular calcium accumulation has also been associated with the echinocytic shape transformation (Weed et al. 1969). Under in vitro conditions this can be artificially achieved by facilitating calcium entry with a specific ionophore such as A23187 (White, 1974, Edmondson and Li, 1976). Prior to the point of major membrane loss the shape transition can be reversed and the discocyte morphology regained if the causative agent is removed and/or the cell is allowed to resynthesize ATP (Feo and Leblond, 1974, Palek et al, 1978, Anderson and Lovrien, 1981). The cellular events which result in the discocyte-echinocyte transformation are still not fully understood. Although several theories have been proposed over the years, workers are still divided over the issue of whether shape changes are a function of the membrane or the cytoskeleton, or,as is more likely due to co-ordinated changes occurring in both.

## 1.9. The role of the plasma membrane in the control of erythrocyte shape

### The bilayer-couple hypothesis

The bilayer-couple hypothesis was proposed by Sheetz and Singer (1974, 1976) to explain the shape changes induced by amphiphilic agents. Briefly, this hypothesis states that when such an agent interacts with a membrane, it will partition into either the inner or outer half of the lipid bilayer, thus causing an expansion of this leaflet relative to the other. If the two halves remain coupled then the cell would change shape to accommodate this. In the erythrocyte, anionic compounds partition into the outer leaflet, due to the electrostatic repulsion of the predominantly negatively charged phospholipids in the cytoplasmic leaflet. This causes an expansion of the outer lipid layer thus causing the crenation of the membrane and leading to echinocytosis. Cationic compounds will distribute preferentially into the inner leaflet due to electrostatic attraction, leading to an increase in the area of this lipid layer, and therefore invagination and stomatocytosis. The same shape changes would be observed if a compound accumulated in either leaflet as a result of a slow rate of diffusion through the membrane.

This model does successfully predict the action of many drugs on erythrocyte morphology and has been supported experimentally (Sheetz and Singer, 1976). Under experimental conditions the cationic, tertiary amine

chlorpromazine diffused rapidly across the membrane and induced stomatocytosis within 10 minutes. However, metachlorpromazine; a quarternary amine of the same series could not diffuse as rapidly and produced echinocytosis due to its accumulation in the outer leaflet. In erythrocyte ghosts both compounds had access to the inner lipid layer and both induced stomatocytosis.

The importance of membrane inositol lipids in the control of erythrocyte shape

The underlying principles of the bilayer-couple hypothesis have been adopted by later workers to explain echinocyte formation under other conditions. These workers have suggested that the shape changes are mediated by effects on membrane lipids; principally the phosphoinositides; PtdIns, PtdIns4P, and PtdIns(4,5)$P_2$. These lipids form a widespread receptor-coupled transmembrane signalling pathway, which is summarised in figure 6. Agonist-induced hydrolysis of PtdIns(4,5)$P_2$ by phospholipase C (PLC) generates two interacting second messengers; diacylglycerol (DAG) and inositol(1,4,5) trisphosphate ($InsP_3$), (Berridge, 1984, 1987). In the erythrocyte the inositol lipids are concentrated at the cytoplasmic surface of the membrane and a proportion of cellular ATP is expended in maintaining the rapid steady-state removal and replacement of the monoester phosphate groups of the three lipid species.

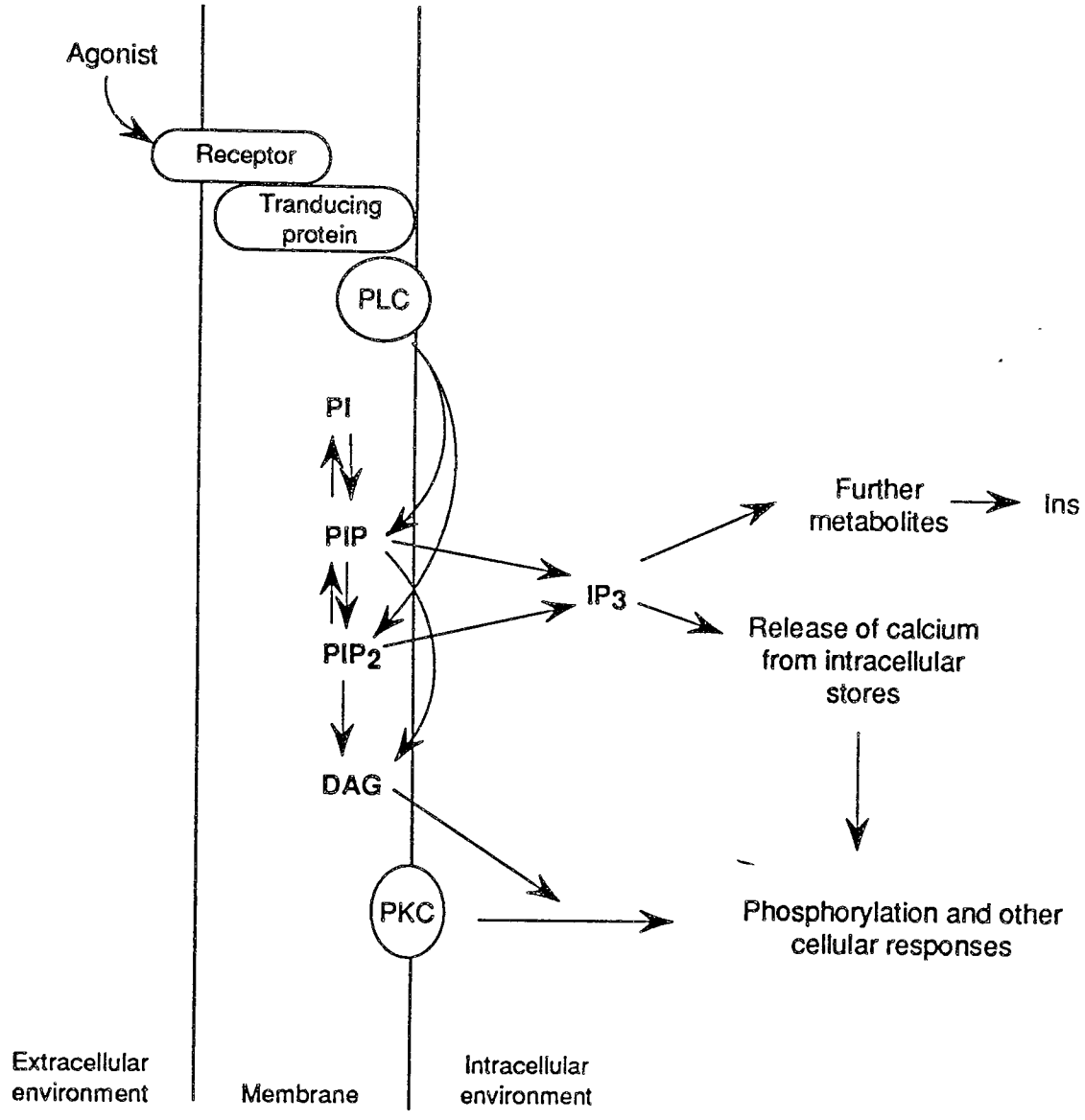


**FIGURE 6** Simplified scheme of the phosphoinositide signalling cascade and its relationship to the regulation of other cellular processes.

In 1975, Allan and Michell found that echinocytosis due to both calcium loading and ATP depletion was accompanied by an increase in membrane DAG levels. Later it was discovered that during calcium loading the DAG was a product of the breakdown of both PtdIns4P and PtdIns(4,5)$P_2$ by a calcium activated polyphosphoinositide phoshophodiesterase (PLC) (Downes and Michell, 1981). DAG is converted to phosphatidic acid (PA) in the presence of ATP, but if conditions of metabolic depletion exist the DAG rapidly redistributes over both halves of the membrane, this results in a net loss of lipid from the inner leaflet, causing shrinkage and therefore echinocytosis (Allan et al., 1978). Echinocytosis induced by metabolic depletion is accompanied by the dephosphorylation of PtdIns(4,5)$P_2$ to PtdIns and also of PA to DAG. Since PtdIns has a smaller headgroup than PtdIns(4,5)$P_2$, and the DAG will become redistributed, both reactions will result in a relative decrease in area of the inner leaflet, therefore inducing crenation (Ferrell and Huestis, 1984, Backman, 1986).

## 1.10. The role of the cytoskeletal complex in the control of erythrocyte shape

In spite of the persuasive evidence not all features of erythrocyte morphology can be explained by a membrane based model. For instance, studies on patients suffering from certain haemolytic anaemias have indicated that the abnormal erythrocyte shape associated with these diseases

can be attributed to skeletal defects; either through a deficiency of a particular protein or defective association between proteins (reviewed by Palek and Lux, 1983). In addition, several morphological studies have been carried out on intact isolated cytoskeletons (prepared by Triton extraction of erythrocyte ghosts), which retain the size and shape of the intact cell (Lange et. al., 1982). Jinbu and co-workers (1984, 1984b) discovered that these Triton shells changed shape and volume when calcium treated, and that these effects were reversed upon incubation in the presence of ATP. Data such as this together with a growing understanding of cytoskeletal structure and regulation has lead many workers to propose that changes in the erythrocyte cytoskeleton are responsible for shape transitions, leaving the membrane to passively accommodate these changes. It has been suggested that conditions which induce morphological changes would lead to the modification of the physiological processes which normally regulate the protein associations within the cytoskeleton and several of these processes have been suggested as targets.

Shape regulation by phosphorylation of cytoskeletal proteins

All of the major erythrocyte cytoskeletal proteins with the exception of actin, are known to be substrates for one or more protein kinases and phosphatases (reviewed by Boivin, 1988 and Cohen et al., 1990). A continuous, steady

-state turnover of phosphate groups within the cytoskeleton appears to exist. However, the physiological role of this in the regulation of protein-protein associations is not known.

In spite of detailed investigations, there appears to be no direct linkage between phosphorylation of any one protein and cell shape change (Anderson and Tyler, 1980, Patel and Fairbanks, 1981, Reinhart et al., 1986). However, evidence indicates that the phosphorylation status of skeletal proteins does affect the relative strength of protein interactions under in vitro conditions. Under such conditions phosphorylation of protein 4.1 reduces its binding to spectrin, actin and the cytoplasmic domain of band 3 (Eder et al., 1986, Ling et al., 1987, Danilov et al., 1990). If this occurs in intact cells, then it may have some relevance in calcium-induced echinocytosis since the phosphorylation level of 4.1 is increased under these conditions (Tang, 1988). In addition, the phosphorylation of ankyrin decreases its affinity for spectrin tetramers (Lu et al., 1985) and also for the cytoplasmic portion of band 3 (Soong et al., 1987). It is interesting to note that the binding affinities of both the key proteins which link the plasma membrane and the cytoskeleton are altered by increased phosphorylation. More recently it has been demonstrated that the phosphorylation of protein 4.9 abolishes its actin bundling activity (Husain-Chishti, et al., 1988). However, the relevance of these regulatory

mechanisms to erythrocyte shape changes are speculative because, so far, no phosphorylation events have been linked to the regulation of protein interactions in the intact cell. Indeed, Backman (1988) has suggested that phosphorylation/dephosphorylation reactions are important for skeletal assembly during erythroid development, but play no functional role in the mature cell.

Shape regulation by proteolysis of cytoskeletal proteins

Proteolytic enzymes are known to play an important role in cellular processes in a variety of cells (reviewed by Pontremoli and Melloni, 1986). These enzymes catalyze the essentially irreversible cleavage of a limited number of peptide bonds of a target protein. The proteolytic systems of the human erythrocyte have been studied extensively, and protease activity has been found to be associated with both the membrane and cytosolic compartments. Three proteolytic enzymes have been isolated from erythrocyte membranes, all belonging to the acidic endopeptidase family (Pontremoli et al., 1979). In addition, at least six proteinases have been identified in the cytosol, including three which have almost identical characteristics to those found in the membrane, two dipeptidyl aminopeptidases and one neutral endopeptidase. This latter shows maximum activity at pH 7.5 and appears to be activated by calcium (Pontremoli et al., 1980). More recently this enzyme has been classified as a member of a

family of calcium-activated neutral proteases or calpains. Such enzymes have been found in virtually every eukaryotic cell type examined and proposals for their function have included involvement in signal transduction, platelet activation, cell fusion, mitosis and cytoskeleton and contractile protein turnover (Pontremoli and Melloni, 1986, Johnson, 1990).

**Erythrocyte calpain** Erythrocyte calpain is subject to a very sophisticated regulatory mechanism. Activation by calcium produces conformational changes in the enzyme and the activated species then binds to the protein to be modulated. The enzyme is present in the erythrocyte cytosol as a heterodimeric proenzyme (procalpain) consisting of two subunits of 30kd and 80kd molecular weight, the larger of which contains the catalytic site (Melloni et al., 1982). Calpain activation is a two stage process involving initial dissociation of procalpain followed by the autoproteolysis of the 80kd fragment to release the active 75kd enzyme. At millimolar calcium concentrations both stages proceed in the cytosol. However, micromolar calcium induces the dissociation of procalpain in the cytosol but the active species is only released following association of the 80kd subunit with the cytoplasmic surface of the cell membrane (Pontremoli and Melloni, 1986). This binding results in the reduction of the calcium concentration required for autoproteolysis

(Pontremoli et al., 1985a). However the site of this association is still under dispute and may be either membrane phospholipids (Pontremoli et al., 1985) or cytoskeletal proteins (Inomata et al., 1990, Kuboki et al., 1990). In the presence of a digestible substrate the calcium requirement for full activation is reduced to more physiological levels (Melloni et al., 1984). ß-haemoglobin is one such substrate and indeed it has been shown that calpain plays a functional role in the degradation of haemoglobin (Pontremoli et al., 1984a) In all cases the resulting 75kd enzyme is fully active in the presence of micromolar concentrations of calcium. The intracellular regulation of activated calpain appears to be achieved by inactivation through self digestion (Grasso et al., 1986) and by the calcium induced interaction of calpain with the specific endogenous inhibitor; calpastatin (Murachi, 1983).

The presence of a calcium activated proteolytic system in erythrocytes has lead to suggestions that the enzymic cleavage of cytoskeletal proteins may be responsible for the echinocytic shape changes of erythrocytes induced by both calcium and metabolic depletion. Under the latter conditions a decrease in intracellular ATP may result in a reduced activity of the calcium ATP-ase leading indirectly to a rise in calcium concentration.

The treatment of erythrocytes with calcium and an ionophore does lead to the loss of cytosolic procalpain (Grasso et al., 1986), and in rat erythrocytes at least

induces the formation of the active enzyme (Croall, 1989). In addition the endopeptidases associated with the membrane are released into the cytosol, although the relevance of this is not known, since these enzymes would be inactive in the intracellular pH environment of the erythrocyte (Grasso et al., 1986). Purified erythrocyte calpain catalyzed the degradation of ankyrin, protein 4.1, band 3 and spectrin in ghost membranes in that order of sensitivity (Boivin et al., 1990). Several studies have examined protein modification in erythrocytes during calcium loading (Anderson et al., 1977, Allen and Cadman, 1979, Allan and Thomas, 1981, Siegel et al., 1980, Lorand et al., 1983, Pontremoli et al., 1984, Grasso et al., 1986) and it is generally accepted that such treatment eventually results in the degradation of most of the major structural proteins including spectrin, protein 2.1, band 3 and protein 4.1. However the majority of these studies were carried out either on erythrocyte ghosts or involved prolonged calcium exposure, and none attempted to correlate the rate of protein loss with the progression of shape change associated with calcium loading in intact cells.

More recently work in this laboratory did attempt this correlation (Tang, 1988) and the results indicated that the shape changes were accompanied by the proteolytic breakdown of protein 2.1, suggesting a role for this protein in echinocytosis. This supported earlier work by Jinbu and colleagues (1982) who demonstrated that the ability of

erythrocyte ghosts to change shape was closely correlated to the amount of ankyrin remaining after limited trypsin digestion. Calpain cleavage of ankyrin releases a 20kd terminal fragment which is involved in the association of the protein with band 3, and leads to an eight fold reduction in the affinity of ankyrin for the anion transporter (Hall and Bennett, 1987). It is possible that the activation of calpain may play a physiological role in detection and removal of senescent erythrocytes. However this loosening of a key membrane-skeletal link may also have some relevance during calcium induced shape changes.

Shape regulation by calmodulin

The relative abundance of calmodulin in the erythrocyte cytosol, and the observation that this protein interacts with the skeletal components spectrin (Anderson and Morrow, 1987), adducin (Gardner and Bennett, 1986) and protein 4.1 (Husain et al., 1985) has lead to suggestions that it may play a role the control of cell shape. However, so far the evidence for this has been inconclusive. The importance of calmodulin was suggested by Nelson and coworkers (1983), who observed a high correlation between the ability of a variety of compounds to both inhibit calmodulin function and to induce the loss of the discocyte morphology in intact erythrocytes. It was suggested that the inhibitors interfered with the maintenance of discoid shape by calmodulin, resulting in a

change in cell morphology. However, to date there is no evidence that calmodulin is responsible for resting erythrocyte shape; as previously stated, normal intracellular $Ca^{2+}$ concentrations are not even sufficient to activate the calmodulin regulation of cellular enzymes.

More recently, specific interactions between calmodulin and cytoskeletal proteins have been investigated. In <u>in vitro</u> assays, calmodulin binds with relatively low affinity to ß-spectrin in a calcium-dependent manner (Anderson and Morrow, 1987) at a site close to the amino terminus (Sears et al., 1986). This is the same region of spectrin that is involved with actin binding and indeed, calmodulin/spectrin binding in the presence of calcium inhibits the protein 4.1 stimulated interaction of spectrin with actin (Anderson and Morrow, 1987). Interestingly, an identical effect results from the calcium mediation of protein 4.1/calmodulin binding (Tanaka et al., 1991). Both of these calmodulin mediated effects have only been demonstrated under <u>in vitro</u> conditions. However, there is evidence that calcium and calmodulin induced alterations in erythrocyte ghosts have a profound effect on membrane stability (Takakuwa and Mohandas, 1988), and therefore some physiological role for these processes in cell shape control cannot be ruled out.

The possible role of a contractile system in the control of erythrocyte shape

The discovery of erythrocyte forms of actin, myosin tropomyosin and tropomodulin (see section 1.3) suggests the possibility of an erythrocyte actomyosin based contractile system. Fowler (1986), proposed a mechanism by which such a system may control cell shape. Tropomyosin-stabilized actin filaments play a key role in the molecular architecture of the erythrocyte cytoskeleton. If myosin filaments linked two sets of actin complexes at some distance from each other the unattached membrane in between would bulge out following myosin contraction and produce spicules such as those characteristically observed during echinocytosis. Since myosin contraction is both calcium regulated and ATP-dependent such a contractile system may mediate echinocytosis during cellular changes in both. However, this type of cytoskeletal regulation is only speculative and does not explain the progression of shape changes observed during echinocytosis.

## 1.11. The role of co-ordinated membrane and cytoskeletal changes in the control of erythrocyte shape.

In recent years, attempts to elucidate the molecular basis of erythrocyte shape control have been complicated by evidence indicating a closer interdependence between the plasma membrane and the skeletal complex than was previously imagined. It now seems likely that cell shape

is controlled by events involving both structural components (Elgsaeter et al., 1986, Steck, 1989). It would be expected that the major linkages between the bilayer and cytoskeleton would play an important role in these events and indeed in the absence of either the glycophorin C/ protein 4.1 or band 3/ankyrin association the mechanical integrity of the cell is reduced (Reid et al., 1987, Low et al., 1991)

Much of the evidence discussed in this section suggests that complex interactions between erythrocyte cytoskeletal proteins and membrane phosphoinositides are associated with the control of erythrocyte shape. This is supported by recent observations that these lipids influence cytoskeletal protein associations in other cells (Lassing and Lindberg, 1985, Goldschmidt-Clermont et al., 1990, Yonezawa et al., 1990).

In the erythrocyte, the phosphoinositides are subject to metabolic compartmentation. Functionally distinct pools of metabolically active or inert PtdIns(4,5)$P_2$, PtdIns4P and PtdIns coexist in the cytoplasmic leaflet of the plasma membrane with no free interchange between them (Muller et al., 1986, King et al., 1987, Gascard et al., 1989). The physical nature of this pooling is unknown, but the most reasonable explanation is the sequestration of a proportion of the lipids through interactions with specific proteins. Previous work from this laboratory has indicated that a functionally specific pool of membrane PtdIns(4,5)$P_2$ is

associated with erythrocyte morphology (Thompson et al., 1987).

Membrane levels of this lipid are known to influence the phosphorylation status of several skeletal proteins by modulating the activity of erythrocyte casein kinase I (Bazenet et al., 1990, Brockman and Anderson, 1991). In addition, PtdIns(4,5)$P_2$ membrane concentrations affect integral glycoprotein lateral diffusion (Sheetz et al., 1982) and, as discussed previously, also regulate the interaction of the integral protein glycophorin A with the skeletal component protein 4.1 (Anderson and Marchesi, 1985). Interestingly, the binding of antibodies or lectins to the external domain of glycophorin A alters the physical properties of the erythrocyte (Lovrien and Anderson, 1980, Anderson and Lovrien, 1981, Smith and Hochmuth, 1982, Evans and Leung, 1984, Chasis et al., 1985). It is thought that ligand binding stimulates transmembrane signal transduction via the integral protein and results in the rearrangement of the cytoplasmic skeletal network (Anderson and Lovrien, 1981, Chasis et al., 1985, Chasis et al., 1988). It has been suggested that changes in PtdIns(4,5)$P_2$ mediate this process, and indeed, the binding of erythrocytes to the immobilized lectin wheat germ agglutinin (WGA) does result in altered phospholipid metabolism (Dale and Suzuki, 1988). Alterations in cellular kinase activity are also observed in response to ligand binding (Danilov and Cohen, 1989). WGA interaction with glycophorin A modulates the protein

kinase C (PKC)-catalysed phosphorylation of several proteins. However, it is not yet clear whether the skeletal reorganisation associated with WGA binding is the result of such altered enzyme activity or the cause of it through changed accessibility of the substrate to the enzyme.

## 1.12. Summary

From this introduction it can be seen that, under normal conditions, the intracellular environment of the human erythrocyte is virtually calcium free and that an increase in cytosolic calcium concentration has profound morphological and biochemical effects. Increased calcium leads to the transformation of the erythrocyte from the biconcave discocyte to a spherical, crenated echinocyte. This gross morphological change is accompanied by the stimulation of a range of calcium-dependent cellular biochemical mechanisms, some of which have been described above as possible mediators of echinocytosis. However, insufficient information is available to establish a causative relationship between any one of these processes and the observed shape transitions.

Therefore, as mentioned previously, the major aims of the study described in this thesis were two fold: to further understand the physiological consequences of an abnormal calcium load, and to examine which events induced by calcium are involved in the echinocytic transition.

Following initial morphological studies, the relationship between the progression of echinocytic transformation and the stimulation of calcium induced intracellular biochemical changes has been examined, with particular attention to cytoskeletal modifications. A clearer understanding of the alterations of skeletal protein/protein associations during shape changes may provide information on the regulatory processes controlling cytoskeletal interactions.

In spite of the relative structural simplicity of the human erythrocyte there is growing evidence that the regulatory processes controlling cytoskeletal and cytoskeleton/membrane interactions of the red cell may have a relevance to these processes in more complex cells. As discussed in this introduction, not only have analogues of erythrocyte proteins been identified in more complex cell types, but in many cases these proteins perform a similar functional role in both erythroid and non-erythroid cells. In addition, the surface alterations noted in nucleated cells as an early consequence of cytotoxic cell injury may be the result of similar calcium-induced cytoskeletal perturbations as those leading to the appearance of membrane spicules during calcium induced echinocytosis of erythrocytes. Therefore, it appears that a greater understanding of the regulation of cytoskeletal associations and the pathophysiological effects of calcium on these interactions in the erythrocyte may provide a

useful insight into these processes in more complex cells.

# CHAPTER 2: EXPERIMENTAL MATERIALS AND METHODS

## 2.1. Source of experimental materials

**Materials obtained from Agar Scientific Ltd., Stanstead, Essex;** Copper SEM grids, glutaraldehyde (EM grade, 25% solution)

**Materials obtained from Amersham International Plc., Amersham Laboratories, White Lion Road, Amersham, Bucks.;** $^{45}Ca^{2+}$ as $CaCl_2$ in aqueous solution, hyperfilm-ECL, ECL Western Blotting Detection System, Hybond C nitrocellulose

**Materials obtained from BDH Chemicals Ltd., Poole, Dorset;** acetic acid (glacial), calcium chloride (1M solution), dimethyl sulfoxide, ethanol, methanol, N,N',methylene bisacrylamide (Electrophoresis grade), sodium dodecyl sulphate, sodium hydroxide, sodium dihydrogen orthophosphate

**Materials obtained from Becton Dickinson, Cowley, Oxford;** 19G hypodermic needles, syringes

**Materials obtained from Bio-Rad Laboratories Ltd., Watford, Herts.;** gel drying membranes, protein assay kit

**Materials obtained from Fisons Plc. (Scientific Equipment Division), Loughborough, Leics.;** acrylamide (ultrapure for electrophoresis), ethanol, methanol, perchloric acid

**Materials obtained from Peptide Institute Inc., (via Scientific Marketing, Barnet, Herts.)**; bestatin, leupeptin

**Materials obtained from LKB, Knowhill, Milton Keynes;** Hisafe III scintillation cocktail

**Materials obtained from Sigma Chemicals Co. Ltd., Poole, Dorset;** adenine, ammonium persulphate, anti-rabbit IgG (peroxidase conjugated), aprotinin, ATP assay kit (luciferin /luciferase), bovine serum albumin (dialysed), bromophenol blue, calcium chloride (20mM solution), calcium ionophore A23187, Coomassie brilliant blue, dextran (Mw 500,000), dithiothreitol, glucose, glycerol, glycine, hydrogen peroxide, inosine, iodoacetamide, ionomycin, luciferin/luciferase ATP assay kit,magnesiun chloride (4.9M solution), N-acetlyglucosamine, N,N,N',N'-tetramethyl ethylenediamine, phenylmethylsulphonylfluoride, potassium chloride, potassium hydroxide, sodium acetate, sodium chloride, sodium ethylenediaminetetraacetic acid, sodium ethyleneglycol-bis-(ß-aminoethylether) N,N,N',N', -tetraacetic acid, sodium gluconate, sodium pyruvate, sucrose, triethanolamine, Tris [(hydroxymethyl) aminoethane], trypsin, trypsin inhibitor (from soybean), wheat germ agglutinin (lectin from Triticum vulgaris)

## 2.2. Buffers

**Buffer A; glucose containing buffer for cell preparation**

| | |
|---|---|
| NaCl | 123mM |
| KCl | 10mM |
| Tris | 15mM |
| Na pyruvate | 5mM |
| Na gluconate | 2mM |
| Glucose | 10mM |
| Adenine | 1mM |
| Inosine | 1mM |
| $MgCl_2$ | 2mM |
| $NaH_2PO_4.H_2O$ | 1mM |
| Dextran-500 | 0.75%w/v |

Deionised $H_2O$

pH 7.6-7.8

0.002%w/v dialysed BSA added immediately before use

pH corrected to 7.4 at temperature required for experiment

**Buffer B; Tris buffer for cell preparation**

| | |
|---|---|
| NaCl | 130mM |
| KCl | 10mM |
| $MgCl_2$ | 2mM |
| Tris | 15mM |

Deionised $H_2O$

pH 7.6-7.8

pH corrected to 7.4 at temperature required for experiment

**Buffer C; glutaraldehyde buffer for cell fixation**

| | |
|---|---|
| Glutaraldehyde (EM grade) | 2%v/v |
| $NaH_2PO_4$ | 93mM |
| NaOH | 80mM |
| $dH_2O$ | |
| pH 7.3 | |

**Buffer D; washing buffer for SEM preparation**

| | |
|---|---|
| $NaH_2PO_4$ | 93mM |
| NaOH | 80mM |
| $dH_2O$ | |
| pH 7.3 | |

**Buffer E; lysing buffer for preparation of erythrocyte ghosts**

| | |
|---|---|
| EDTA | 1mM |
| NaCl | 7mM |
| Tris | 5mM |
| $dH_2O$ | |
| pH 8.0 | |

Add 50µg/ml phenylmethylsulphonylfluoride (PMSF) (dissolved at 10mg/ml in ethanol), 2µg/ml each of leupeptin, bestatin, aprotinin, 0.5mM iodoacetamide (dissolved in DMSO); all inhibitors of endogenous protease activity, to control post-sampling protein degradation.

These inhibitors are active against a broad spectrum of cell enzymes: PMSF against serine proteases; leupeptin

against trypsin and other serine proteases, aprotinin against trypsin and chymotrypsin; bestatin against leucine aminopeptidases and cell surface exopeptidases (Fairbanks et al., 1988).

**Buffer F; Western blotting transfer buffer**

| | |
|---|---|
| Tris | 6.06g |
| Glycine | 28.8g |
| Methanol | 400ml |
| $dH_2O$ | upto 1000ml |
| | De-gas before use |

**Buffer G; Phosphate buffered saline (PBS)**

| | |
|---|---|
| $Na_2HPO_4$ | 80mM |
| $NaH_2PO_4$ | 20mM |
| NaCl | 100mM |
| $dH_2O$ | upto 1000ml |
| pH 7.5 | |

## 2.3. Gel electrophoresis buffers

### Fairbanks gradient gel

**40% bis acrylamide stock**

| | |
|---|---|
| Acrylamide | 80g |
| Bis acrylamide | 3g |
| $dH_2O$ | upto 200ml |
| filter, store in dark at $4^oC$ | |

**0.5% TEMED stock**

| | |
|---|---|
| TEMED | 0.5ml |
| $dH_2O$ | upto 100ml |

**10X Tris buffer**

| | |
|---|---|
| 1M Tris | 400ml |
| 1M Na acetate | 200ml |
| 0.1M Na EDTA | 200ml |
| | pH 7.4 with acetic acid |
| $dH_2O$ | upto 1000ml |

**Running buffer**

| | |
|---|---|
| 10X Tris | 500ml |
| 10%w/v SDS | 100ml |
| $dH_2O$ | upto 5000ml |

**Gel composition for 1.5mm x 160mm x 160mm gradient gel**

| | **3.5%** | **17%** |
|---|---|---|
| 40% Bis/acryl. | 3.0ml | 3.4ml |
| 10X Tris buffer | 3.4ml | 0.8ml |
| 10%w/v SDS | 0.68ml | 0.16ml |
| $dH_2O$ | 26.9ml | 1.1 |
| Glycerol | 0.0 | 2.0ml |
| TEMED (undiluted) | 0.011ml | |
| (0.5%) | | 0.5ml |
| APS (16%w/v) | 0.25ml | 0.025ml |

## Laemmli gel system

### 30% bis acrylamide stock

| | |
|---|---|
| Acrylamide | 30g |
| Bis acrylamide | 0.8g |
| $dH_2O$ | upto 100ml |

filter, store in dark at $4^{\circ}C$

### Resolving gel buffer

| | |
|---|---|
| Tris | 19.2g |
| SDS | 0.4g |
| | pH 8.7 |
| $dH_2O$ | upto 100ml |

### Stacking gel buffer

| | |
|---|---|
| Tris | 6.06g |
| SDS | 0.4g |
| | pH 6.8 |
| $dH_2O$ | upto 100ml |

### Running buffer

| | |
|---|---|
| Tris | 3.03g |
| Glycine | 14.41g |
| SDS | 1.0g |
| | pH8.3 |
| $dH_2O$ | upto 1000ml |

| **Gel composition:** | **7% resolving gel** | **5% stacking gel** |
|---|---|---|
| 30% bis/acryl. | 7.0ml | 1.65ml |
| Running gel buffer | 7.5ml | |
| Stacking gel buffer | | 2.5ml |
| $dH_2O$ | 15.2ml | 5.75ml |
| APS (10%w/v) | 0.3ml | 0.1ml |
| TEMED | 0.020ml | 0.007ml |

| **Coomassie blue stain;** | **Stock** | **Working solution** |
|---|---|---|
| Coomassie brilliant blue | 24g | |
| Coomassie blue stock | | 50ml |
| Methanol | 300ml | 2000ml |
| Acetic acid | 60ml | 400ml |
| $dH_2O$ | to 600ml | to 4000ml |

| **Destain** | |
|---|---|
| Methanol | 150ml |
| Acetic acid | 100ml |
| $dH_2O$ | upto 1000ml |

| **Sample buffer** | **1X strength** | **2X strength** |
|---|---|---|
| 20%w/v SDS | 1.0ml | 1.0ml |
| 1M Tris-HCl, pH 7.0 | 0.5ml | 0.5ml |
| 60%w/v sucrose | 0.5ml | 0.5ml |
| $dH_2O$ | 8.0ml | 3.0ml |
| bromophenol blue concentrate | 4 drops | 2 drops |

25mg/ml DTT added immediately before use

## 2.4. Preparation of erythrocytes for experimentation

Human erythrocytes were collected to enable the examination of changes in membrane morphology induced by raising cytosolic calcium levels. For each experiment fresh venous blood was donated by a healthy, previously unmedicated volunteer and removed into tubes containing lithium heparin to prevent clotting. The whole blood was centrifuged at 1000g for 5 minutes at room temperature, the plasma removed and the cells washed twice with an equal volume of either buffer A or B (see section 2.2) warmed to the temperature at which the subsequent experiment was performed. Following each centrifugation the buffy coat of leucocytes was removed from the surface of the packed red cells to prevent contamination. The concentration of cells in the final suspension was determined using an improved Neubauer haemocytometer and the cells resuspended in either buffer A or B at the required concentration for experimental use. Since anaerobic glycolysis is the only source of metabolic energy (ATP) available to erythrocytes, the use of buffers A (containing metabolic substrates) and B (isotonic Tris buffer, without metabolic substrates) allowed the manipulation of cell metabolic status during experimental procedures.

## 2.5. Induction of morphological transitions by elevation of intracellular free calcium

### Using the calcium ionophore A23187 (A23187)

Calcium was added from stock solutions of either 20mM or 1M $CaCl_2$ to give the final required concentration in the cell suspension. After gentle mixing, A23187 was added from a 10mM stock in dimethylsulphoxide (DMSO) (stored at -20°C), to a final concentration of 5µM to initiate calcium entry and the cell suspension then incubated in a shaking waterbath at the required temperature. Final concentration of DMSO was 0.05%. This concentration of DMSO alone induced no apparent morphology change. Unless otherwise specified, all shape changes were induced by raising intracellular calcium levels by adding extracellular calcium and A23187.

### Using the calcium ionophore, ionomycin

The method was essentially that described above except that ionomycin was substituted for A23187. This ionophore was added from a 1mM stock in DMSO (stored +4°C) and used at a final concentration of 3µM. Final concentration of DMSO was 0.3%, which, in control experiments induced no apparent change in erythrocyte morphology.

## 2.6. Cell fixation and quantitation of cell morphologies

Duplicate samples of 0.25ml of cell suspension were removed and the cells in each fixed by the gentle addition of 5 volumes (1.25ml) of ice cold glutaraldehyde buffer (buffer C, section 2.2). The cells were left in the presence of the fixative for at least 60 minutes after which they were either allowed to pellet overnight, or were centrifuged at 1000g for 3 minutes. After removal of the supernatant the cells were resuspended in a small volume of $dH_2O$ for the quantitation of morphologies.

The fixed cells were mounted under a coverslip and examined at 400x magnification using Nomarski differential interference contrast (DIC) optics. At least 100 cells from several fields were scored for morphology as either discocytes, stage 1, 2, 3 echinocytes or sphereo-echinocytes as defined by Bessis et al. (1973). The distinguishing characteristics of each echinocyte stage as defined for the quantitation of morphology in this thesis are summarised below in figure 7 (See also figure 8).

When total echinocyte counts were performed on 10 separate samples removed from the same calcium treated cell population reproducibilty was found to be 63.35 ±1.97%. From 10 repeated counts on the same sample over a period of 2 days reproducibilty was found to be 61.4 ±1.89%

**FIGURE 7** A summary of the distinguishing characteristics of each echinocyte stage

| Echinocyte stage | Characteristics |
|---|---|
| Discocyte | Flat biconcave disc |
| Stage 1 | Flat disc with irregular edges |
| Stage 2 | Flat disc with vertical spicules |
| Stage 3 | Spherical cell, covered with spicules |
| Sphereo-echinocyte | Smooth spherical cell remaining after spicules have been shed |

## 2.7. Preparation of samples for scanning electron microscope (SEM)

Where appropriate scanning electron microscopy was used to obtain a more detailed examination of erythrocyte morphology than that routinely obtained by light microscopy. Following the required treatment with calcium and A23187, cell samples were fixed with 5 volumes of 2% glutaraldehyde buffer (buffer C, section 2.2) for between 60 to 120 minutes at $4^{o}C$. Following centrifugation at 1000g for 3 minutes the supernatant was discarded and the resulting pellet washed 4 times with buffer D (section 2.2), and then twice with $dH_2O$. The final pellet was resuspended in $dH_2O$ to give a concentration of approximately $10^8$ cells/ml. A drop of this suspension was allowed to air-dry overnight onto a formvar coated copper grid, which was then splutter coated with platinum prior to microscopy.

## 2.8. Examination of the effect of calcium concentration on the rate of echinocyte formation

Cells were prepared using buffer A (section 2.2) at 37°C as described in section 2.4 and resuspended at 2.5 x $10^8$ cells/ml. 5ml aliquots were prepared, and appropriate amounts of $CaCl_2$ was added to each to give a final calcium concentration of between 50 and 1000µM, followed by 5µM A23187. Each aliquot was incubated at 37°C for a further 5 minutes, after which samples were withdrawn for the scoring of morphology as described in section 2.6.

Control suspensions received only 5µM A23187 for 5 minutes; no added extracellular calcium. In general, such control treatments resulted in less than 10% total echinocytosis. On the rare occasions when control values exceeded this level the whole experiment was abandoned.

## 2.9. Examination of time-dependent echinocytosis

### Cells prepared in the presence of glycolytic substrates (buffer A)

Cells were prepared using buffer A (section 2.2) at 37°C and resuspended at 2.5 x $10^8$/ml. $CaCl_2$ was added to give a final calcium concentration of either 150µM or 1mM. After mixing, either 5µM A23187, or 3µM ionomycin was added and the cells incubated at 37°C for a maximum of 60 minutes. Samples were removed for fixation and scoring (section 2.6) after 0, 10, 20, 30, 40, 50 and 60 minutes. An additional control experiment carried out by incubating

cells for 60 minutes in the presence of extracellular calcium but in the absence of ionophore, indicated that extracellular calcium alone caused no morphological change.

Cells prepared in the absence of glycolytic substrates (Tris buffer B)

Cells were prepared using buffer B (section 2.2) at 37°C and resuspended at 2.5 x $10^8$/ml. The method was then continued as described for cells prepared in buffer A.

## 2.10. Reversal of calcium-induced echinocytosis

Reversal of calcium-induced shape change was attempted using a method based on that of Anderson and Lovrien (1981). Briefly, following the induction of echinocytosis by calcium and A23187 the inducing agents were removed by the addition of EGTA and bovine serum albumin (BSA) respectively. Shape reversal driven by metabolic energy was then facilitated by the incubation of the cells in the presence of glucose at 37°C.

A cell suspension of 2.5 x $10^8$ cells/ml was prepared from cells washed with buffer B (section 2.2) at 37°C. Two different calcium treatments were used:

either $CaCl_2$ was added to a final concentration of 150µM, followed by 5µM A23187 and the cell suspension then incubated for 10 minutes at 37°C,

or $CaCl_2$ was added to final concentration of 1mM, 5µM A23187 was added and the cells placed at 37°C for 15

minutes.

Previous experiments had indicated that the former treatment resulted in a cell population consisting predominantly of stage 1 echinocytes, whereas the latter treatment resulted almost exclusively in sphereo -echinocytes. Therefore these treatments allowed reversal of shape change to be examined in two different cell populations.

After calcium treatment samples were withdrawn for the quantitation of morphology (section 2.6). EGTA was then added to a final concentration of 10X that of the calcium to ensure complete chelation and BSA was added to a final concentration of 0.3%. After gentle mixing the cells were centrifuged at 1000g for 5 minutes. Following removal of the supernatant the pellet was resuspended to the original volume with buffer A and the cell suspension incubated at 37$^{o}$C for a maximum of 360 minutes. The progression of shape reversal was followed by the quantitation of cell morphologies at 0, 60, 120, 180, 240, 300 and 360 minutes.

For comparative purposes reversal was also examined after the calcium loading of cells in buffer A. The method was essentially that described above except that the cells were prepared and calcium loaded in buffer A.

In order to confirm the dependence of shape reversal on metabolic energy an experiment was also carried out in which restoration of the discocyte morphology was attempted in buffer B after the calcium loading of cells also in

buffer B.

For each of the above experiments control cells were treated identically but with the omission of A23187.

## 2.11. Density separation of erythrocytes into populations enriched in cells of different ages

Age separation of erythrocytes on a relatively large scale was achieved using a method based on that of Murphy (1973). Thus packed erythrocytes were centrifuged in a fixed angle rotor for 60 minutes at 30°C. This method separated erythrocytes on the basis of cell density which is related to cell age. Erythrocyte aging in the peripheral circulation is associated with a decrease in cell water and cation content, and therefore cell size; since haemoglobin synthesis is not continued in mature erythrocytes this volume loss is accompanied by an increase in cell specific density (Murphy, 1973).

40ml of anticoagulated whole blood was withdrawn and centrifuged at 2000g for 20 minutes at room temperature. The serum was removed and the buffy coat aspirated and discarded. The cells were resuspended in the serum and the centrifugation repeated. Following a second removal of the buffy coat, the packed erythrocytes were mixed and equally divided between two 10ml centrifuge tubes. To achieve age separation the cells were then spun for 60 minutes at 20,000g using a 10 x 10ml fixed angle rotor in an MSE Pegasus centrifuge pre-warmed to 30°C.

After spinning the small amount of serum was discarded. The top 10% of cells (young cells) was harvested by holding the tip of a Gilson pipette just below the surface of the cells and removing the sample by gentle aspiration while slowly moving the pipette around the edge of the tube. The mid portion of the cells were aspirated in a similar way and discarded. Finally, the bottom 10% (old cells) of the sample was collected.

The efficiency of the cell separation was assessed by comparing the mean cell volume (MCV) of the top and bottom collected fractions i.e. young and old cells. A difference of greater than 10% between the two fractions was taken as an indication of efficient density separation. On occasions when this degree of difference was not achieved the experiment was abandoned. MCV was calculated from measurements of cell count and haematocrit (Hct). For each cell sample, the former was estimated from two individual counts by haemocytometer. Hct values (x 2) were determined using an haematocrit centrifuge at room temperature after carefully resuspending an aliquot from each fraction in an equal volume of buffer B. The following calculation was then used to determine MCV:

$$\text{MCV (fl)} = \frac{\text{Hct (\%)}}{\text{count/ml}} \times 10^{12}$$

Following preparative separation, the cells were resuspended at $2.5 \times 10^8$/ml in buffer A and maintained at

37°C for a recovery period of 60 minutes before any further experimental manipulation.

## 2.12. Examination of time-dependent echinocytosis in erythrocyte populations enriched in young or old cells

Preparations enriched in either young or old erythrocytes were obtained as described in section 2.11. Following the recovery period the incubation buffer was replaced by centrifuging the cells at 1000g for 5 minutes and resuspending the pellet to the original volume in fresh buffer A (section 2.2) at 37°C. The progression of time-dependent echinocytosis during calcium loading with either 150μM or 1mM $CaCl_2$ was then examined for both separated fractions as described in section 2.9.

## 2.13. Examination of the reversal of calcium-induced echinocytosis in erythrocyte populations enriched in either young or old cells

Preparations enriched in either young or old erythrocytes were obtained as described in section 2.11. After the 60 minute recovery period the cell suspensions were spun at 1000g for 5 minutes, the supernatant discarded and the pellets resuspended to the original volume in either buffer A or buffer B (section 2.2). Prior to calcium loading the cells resuspended in buffer B were maintained at 37°C for 30 minutes in an attempt to reproduce the metabolic status of cells freshly prepared in

buffer B. Centrifugation and resuspension was then repeated. Calcium loading and shape reversal in both young and old cell populations were examined following the methods described in section 2.10.

## 2.14. Examination of the effect of incubation in buffer A at 37°C on subsequent calcium-induced morphological transitions

Cells were prepared using buffer A (section 2.2) at 37°C and resuspended at 2.5 x $10^8$/ml. The cell suspensions were incubated at 37°C in plastic universal containers in a gently shaking waterbath for a maximum of 360 minutes as specified in the figure legends. At 60 minute intervals the containers were gently inverted to maintain the cells in suspension. Following incubation the rate of either concentration-dependent or time-dependent echinocytosis was studied as described in sections 2.8 and 2.9.

The degree of cell lysis during long term incubations was monitored because of the possibility of misleading results due to the loss of a specific cell population in the course of the incubation. Cell lysis was estimated by examining haemoglobin release into the media in which the cells were incubated. At the end of each incubation a sample of cell suspension was removed, the cells pelleted by gentle centrifugation at 1500rpm for 5 minutes and the absorbance of haemoglobin in the media measured at 543nm wavelength. The number of cells lost through haemolysis

during the incubation was then estimated from a standard curve based on the absorbance at 543nm of the haemoglobin released from the lysis of known cell numbers. In all experiments cell loss was approximately 1-2% of the total over a 6 hour incubation.

Control experiments; cells washed after pre-incubation but prior to calcium loading

Control experiments were carried out in order to assess the effect of haemoglobin released through cell lysis on the progression of echinocytosis induced by calcium and ionophore. The method was essentially that described above. However, at the end of the incubation period the cells were pelleted at 1500rpm for 5 minutes and the supernatant removed and retained. Two treatments were then used; either cells were resuspended in fresh buffer A at 37°C to the original volume or, the cells were resuspended to the original volume in the retained supernatant at 37°C. The progression of time-dependent echinocytosis was then examined in each preparation as described above in section 2.9.

## 2.15. Uptake of $^{45}Ca^{2+}$ by erythrocytes in the presence of calcium ionophore

The rate of accumulation of calcium during the treatment of erythrocytes with the ion and ionophore was compared between cells treated either immediately after

preparation, or after incubation at 37°C for 360 minutes. To facilitate this, $^{45}Ca^{2+}$ was included in the extracellular medium during calcium loading and the cells were then analysed at various time intervals after the initiation of calcium entry for their content of the radioisotope.

Cells were prepared using buffer A (section 2.2) at 37°C and resuspended at 2.5 x $10^8$ cells/ml. Pre-incubation of cells for 360 minutes was carried out in either the presence or absence of extracellular calcium. Where it was included in the media the ion was added to a final concentration equal to that required for the subsequent calcium loading experiment. The number of cells lost through cell haemolysis during incubation of cells at 37°C for 360 minutes was estimated as described above in section 2.14.

$CaCl_2$ was added to give a final concentration of either 150µM or 1mM calcium depending on the experiment, and then $^{45}Ca^{2+}$ was added to give an activity of 20µCi/ml. 2 x 200µl samples were removed for estimation of the $^{45}Ca^{2+}$ retained on the cell surface. After mixing, either A23187 was added to a final concentration of 5µM, or ionomycin was added to a final concentration of 3µM. At specified time-points (see figure legends) 2 x 200ul samples of cell suspension were removed into 1ml of ice-cold buffer B in chilled 1.5ml microfuge tubes. At this temperature the activity of the $Ca^{2+}$-ATPase is blocked and the ionophore

-induced calcium permeability of the cells is greatly reduced. Previous reports have indicated insignificant loss of intracellular calcium from calcium-loaded cells kept on ice (Dagher and Lew, 1988). The cells were centrifuged at 13,000rpm for 30 seconds at 4°C in a microfuge and the pellets washed once more with 1ml of ice-cold buffer B. The final pellets were lysed with 200µl of distilled water and the lysates discoloured with 400µl of 30%v/v hydrogen peroxide ($H_2O_2$). The radioactivity was determined by liquid scintillation counting in the presence of 10ml of Optiphase Hisafe III in a Packard Tri-Carb Scintillation Counter. Preliminary experiments indicated that additional washes of cells prior to lysis did not significantly reduce the total radioisotope retained on the cells. Therefore, to keep post-sampling inaccuracies to a minimum all cells were washed only twice as described.

An identical incubation was performed in parallel but without the addition of $^{45}Ca^{2+}$ to allow the assessment of cell morphology changes during the experiment.

Control experiments in which cells were treated exactly as described above, but with the omission of the ionophore indicated no obvious influx of $^{45}Ca^{2+}$ in the absence of ionophore.

## 2.16. Preparation of erythrocyte ghosts to examine the effect of calcium on cytoskeletal proteins of intact cells

A parallel study was made of the rate of echinocytosis

and the changes to cytoskeletal integrity during calcium loading, in order to assess the relationship between the two. At appropriate time intervals during calcium loading erythrocyte ghost membranes were prepared by hypotonic lysis of cell samples and the proteins subsequently analysed by SDS-PAGE. Cell morphology from identical samples was also quantitated for comparison.

50ml of a suspension of 2.5 x $10^8$ cells/ml was prepared from cells washed with either buffer A or buffer B (section 2.2) at 37°C. An appropriate volume of $CaCl_2$ was added to give a final concentration of either 150µM or 1mM depending on the experiment and the cells placed at 37°C. For the 0 minute sample, aliquots of cell suspension were withdrawn for scoring of morphology (section 2.6), and 5ml of cell suspension was removed and immediately added to 40ml of ice cold lysis buffer (buffer E, section 2.2). To reduce protease mediated proteolysis of proteins during preparation, protease inhibitors were included in all buffers used, and all procedures were carried out on ice. A23187 was added to the remainder of the cells to a final concentration of 5µM and echinocytosis allowed to proceed for a maximum of 60 minutes. At 1, 3, 5, 10, 20, 30 and 60 minutes, samples were removed for ghost preparation and quantitation of morphologies (section 2.6).

For ghost preparation the cells in lysis buffer were left on ice for at least 10 minutes to ensure complete lysis. The cell lysates were then centrifuged for 20

minutes at 40,000g using an 8 x 50ml fixed angle rotor in an MSE Pegasus centrifuge cooled to 4°C. The supernatant was discarded and each tube tilted to slide away the membrane pellet and allow the removal of the dense white 'button' of leucocyte debris. The pellets were washed by resuspension in 50ml of ice cold lysis buffer and centrifugation was repeated as above. Following removal of the supernatant the resultant pellet was prepared for SDS-PAGE analysis. The protein samples were solubilised by the addition of 200µl of 2X sample buffer (section 2.3) and immediately heated in a boiling waterbath for 5 minutes. This treatment promoted the disruption of the membranes and allowed SDS binding to the proteins; thus facilitating efficient electrophoretic separation. The presence of DTT in the sample buffer ensured protein denaturation through the disruption of the intrinsic disulphide linkages within the proteins. Protein solubilisation and heating also induced the denaturation of proteases which may otherwise have caused post-sampling polypeptide degradation (Fairbanks et al., 1988). All samples were stored at -20°C until analysed.

## 2.17. Modulation of calcium-induced morphological transitions by wheat germ agglutinin (WGA)

Extracellular binding of the lectin, wheat germ agglutinin (WGA) has been reported to maintain the discocyte morphology of erythrocytes even when loaded with

calcium. A study was therefore made of the effects of pre-treatment with WGA on the pattern of proteolysis of cytoskeletal proteins during calcium treatment of cells. However, preliminary investigations to examine the modulation of morphology by WGA were initially carried out as described by Anderson and Lovrien (1981). A suspension of cells at 1 x $10^7$/ml was prepared from cells washed with buffer B (section 2.2) at 25°C. A cell concentration greater than this was found to induce cell aggregation leading to the distortion of surface morphology. WGA was added to the cells from a stock solution of 1mg/ml in PBS (pH 6.8) to give a final concentration of 2µg/ml. After mixing, calcium was added to a final concentration of 200µM (20mM stock), and A23187 was then added to give a 5µM final concentration. After 5 minutes incubation at either 25°C or 37°C, 30mM N-acetyl glucosamine (NAG) (1M stock) was added to the cells to remove WGA from the extracellular cell surface. The cell suspensions were then incubated for a further 30 seconds. At each stage a sample was removed for quantitation of morphologies as described in section 2.6.

For comparative purposes the above experiment was repeated at 37°C.

## 2.18. Examination of the effect of pre-treating cells with wheat germ agglutinin on calcium-induced cytoskeletal proteolysis

A comparison was made between the pattern of cytoskeletal proteolysis induced by calcium loading in erythrocytes either with or with out pre-treatment with WGA. 80ml of a suspension of cells at 1 x $10^7$ was prepared from cells washed with buffer B (section 2.2) at 25°C. WGA was added to the cells from a stock solution of 1mg/ml in PBS (pH 6.8) to give a final concentration of 2µg/ml, and after mixing, $CaCl_2$ was added from a 1M stock to give a final concentration of 1mM. 0.25ml aliquots were withdrawn for scoring of morphology (section 2.6) and 9.50ml was removed into 40ml of ice-cold lysis buffer for preparation of red cell membranes. A23187 was added to the remainder of the cells to a final concentration of 5µM and echinocytosis allowed to proceed at 25°C. At 1, 3, 5, 10, 20, 30, and 60 minute time-points samples were withdrawn for ghost preparation and quantitation of morphologies (section 2.6). The preparation of ghost membranes was then continued as described above in section 2.16. However the due to the use of fewer cells for this preparation the final membrane pellet was solubilised in only 25µl of 2 x sample buffer for subsequent SDS-PAGE analysis.

As a control for this experiment an identical membrane preparation was carried out in the absence of WGA.

## 2.19. Trypsin-mediated proteolysis of purified erythrocyte ghost proteins

The pattern of proteolysis obtained by the trypsin digestion of purified cytoskeletal proteins was examined and compared to the proteolytic events previously observed during the calcium loading of intact erythrocytes. Proteolytic digestion of purified erythrocyte proteins with trypsin was carried out using a method modified from Jinbu et al. (1982).

Membrane ghosts were prepared from previously untreated erythrocytes washed with buffer A (section 2.2) using the method described in section 2.16. However, no protease inhibitors were included in the lysis buffer because of their inhibitory effect on trypsin. The purified ghost protein was resuspended in lysis buffer at a concentration of 1.25mg/ml. Protein concentration was estimated as described below in section 2.20. Trypsin was added to equal aliquots of this protein to produce a final concentration of 12.5µg/ml. The aliquots were mixed gently and incubated on ice. At 0, 5, 10, 20, 40, 60, 90 and 120 second time-points trypsin inhibitor was added to a final concentration of 50µg/ml. An equal volume of 2x sample buffer (see section 2.3) was added and the sample heated in a boiling waterbath for 5 minutes before storage at -20$^{o}$C, and subsequent SDS-PAGE analysis.

## 2.20. Estimation of protein concentration

Where necessary protein concentration was quantified using a protein-dye binding method based on that of Bradford (1976). The reagents used were those supplied in the commercially available Bio-Rad protein assay kit, and the experimental procedure was followed as described in the instruction manual supplied with the kit. Briefly, an aliquot of the protein sample was mixed with 1ml of a 1 in 5 dilution of assay reagent, the absorbance measured at 595nM and the protein concentration calculated from a standard curve.

## 2.21. Sodium dodecyl sulphate polyacrylamide gel electrophoresis (SDS PAGE)

Two different types of slab gel electrophoresis system were used to separate and visualize erythrocyte ghost proteins: a continuous 3.5 - 17% gradient gel system using the buffers of Fairbanks et al (1971), and a discontinuous buffer system as described by Laemmli (1970). The relative advantages of these two systems are described in the results and discussion section.

### Fairbanks gradient gel system

**Gel pouring conditions**

A Bio-Rad Dual Protean II electrophoresis cell connected to a Bio-Rad power supply was used; final gel

size 160mm x 160mm x 1.5mm. Before use the gel plates were washed with detergent, thoroughly rinsed with distilled water and finally wiped with alcohol. Two acrylamide solutions of 3.5% and 17% were used and these were prepared as described in section 2.3. A 3.5-17% gradient slab gel was formed in the pre-assembled gel apparatus using a gradient maker and a Gilson peristaltic pump. After pouring, a 10 well comb was carefully inserted. Rapid polymerisation was encouraged by warming the gels with a lamp, and the process was then completed by overnight storage at 4°C before use.

**Running conditions**

All protein samples were heated to 100°C in a boiling waterbath immediately before loading to ensure complete denaturation and solubilisation of the proteins. The comb was removed from the slab gel and the wells washed with running buffer before loading with an equal amount of protein in each. Electrophoresis was performed initially at a constant voltage of 50V per gel. Once all of the tracker dye had entered the gel to a depth of approximately 5mm the voltage was increased to 80V/gel, and electrophoresis continued until the tracker dye reached the bottom of the gel.

Discontinuous buffer system using buffers of Laemmli

**Gel pouring conditions**

A Bio-Rad mini Protean II electrophoresis cell was used, connected to a Bio-Rad power supply; final gel size 80mm x 73mm x 0.75mm. Before use the gel plates were washed as described above. A 7% resolving gel solution was prepared as described in section 2.3 and carefully poured into the pre-assembled gel apparatus to a level about 2cm below the top of the shorter gel plate. Distilled water was slowly dripped on to the top of the gel solution to ensure a sharp interface. After polymerisation (approx 30 minutes), the water was drained off and the 5% stacking gel solution poured (section 2.3). A 10 well comb was carefully inserted and the gel allowed to completely polymerise.

**Running conditions**

Protein samples were heated to 100°C in a boiling water bath before loading. The comb was removed, the wells rinsed with running buffer, and an equal amount of protein then loaded into each well. Electrophoresis was carried out at 20V/gel until all of the dye had passed into the resolving gel, the voltage was then increased to 40V/gel and electrophoresis continued until the tracking dye reached the bottom of the gel.

Gel staining and destaining; both gel systems

On completion of electrophoresis, the polyacrylamide gel was carefully removed from the gel apparatus into Coomassie blue gel stain (section 2.3), and gently agitated for 60 - 120 minutes. After a brief rinse with water the gel was then immersed in destain (section 2.3) and destaining was continued until the background of the gel was clear.

Gel drying

Following the destain procedure the gels were dried between two layers of Bio-Rad drying membrane pre-soaked in water, and allowed to dry overnight in a fume hood.

Densitometric analysis of the intensity of protein bands on stained slab gels

Laser densitometry was carried out on dried slab gels using an LKB 2202 Ultrascan densitometer. The results obtained were analysed using Gelscan software, also from LKB.

## 2.22. Immunological detection of ankyrin by Western blotting

Proteins separated by SDS gel electrophoresis were transferred onto nitrocellulose using an electrophoretic method based on that of Towbin et al. (1979). Following antibody treatment the proteins of

interest were visualised using the Amersham Enhanced Chemiluminescence (ECL) Western Blotting detection system. The reagents supplied in the kit interact with a peroxidase conjugated second antibody to produce a luminescent product which is detected on X-ray film.

Electrophoretic transfer was performed in a Bio-Rad mini Protean II Western Blotting apparatus as described in the instructions supplied with the system. Briefly, following SDS gel electrophoresis the gels and nitrocellulose (Amersham Hybond C) were equilibrated in transfer buffer (buffer F, section 2.2) for 15 minutes with occasional agitation. The apparatus was then assembled and protein transfer was performed either overnight at 30V or for 60 minutes at 100V.

Following transfer the nitrocellulose blot was rinsed in phosphate buffered saline (PBS) and then non-specific binding sites were blocked by overnight incubation in a 5% w/v solution of 'Marvel' in PBS/0.1% Tween 20 at room temperature. After washing for 3 x 5 minutes in PBS/0.1% Tween 20 the blot was incubated with an anti-ankyrin antisera diluted 1/200 in PBS/0.1%Tween 20 with 1% Marvel, for 90 minutes at room temperature. The working dilution and time of incubation were recommended by Dr J Pinder who kindly donated the antibody. Washing was repeated as above before addition of the second antibody. Since the primary antisera was raised in rabbit a peroxidase conjugated anti-rabbit IgG was used as second antibody and the optimum

working dilution for this system was pre-determined by antibody titration. The blot was incubated for 60 minutes at room temperature with a 1/100,000 dilution of this antibody in PBS/0.1% Tween 20 with 1% Marvel. After washing for 5 x 5 minutes the proteins of interest were detected as described in the ECL kit instruction bulletin.

## 2.23. Extraction and quantitation of cellular ATP

### ATP extraction

Cellular levels of ATP were estimated in order to compare the effects of incubation in buffer A or B on cell metabolic status. In addition, an examination was made of the changes in cellular ATP levels during permeabilization of erythrocytes held in buffer A to calcium.

All ATP extraction procedures were carried out on ice to limit ATP breakdown. Cells were used at a concentration of $2.5 \times 10^8$ cells/ml. For each extraction 2 X 1.0ml samples of cell suspension were removed into pre-cooled 1.5ml microfuge tubes on ice and immediately spun in a microfuge at 1500rpm for 2 minutes to pellet the cells. For each tube, the supernatant was discarded and the cells washed in 1ml of ice cold phosphate buffered saline (PBS) (buffer G, section 2.2). Following a second spin, the pellet was resuspended in 500µl of ice cold PBS. 75µl of 12% perchloric acid (PCA) was added, the cells vortexed and then left on ice for 10 minutes. The resulting precipitate was pelleted by spinning in a microfuge at 13,000 rpm for 2

minutes, the supernatant was retained and the volume noted. The supernatant was then neutralised by adding a pre-determined volume of 2M potassium hydroxide (KOH)/0.5M triethanolamine and the sample vortexed again. After spinning at 13,000rpm for 2 minutes the supernatant was removed into a fresh microfuge tube and stored at -20°C until the ATP was assayed.

Quantitation of ATP

ATP levels of cell extracts were estimated using a luciferase/luciferin assay kit from Sigma. The assay was performed as described in the Sigma technical bulletin supplied with the assay kit. Briefly, ATP extracts were thawed, vortexed and spun at 13,000 rpm for 2 minutes in a microcentrifuge. 100µl of the ATP extract supernatant was transferred to a mini scintillation vial, then 100µl of a 1 in 300 diluted luciferase/luciferin mixture was added. After rapid mixing the luminescence was immediately measured using a Packard Tri-Carb Scintillation Counter set to bioluminescence mode. Each sample was measured in duplicate.

## 2.24. Examination of cellular adenosine triphosphate (ATP) levels in cells maintained in either buffer A or B at 37°C

Cells were prepared using either buffer A or buffer B (section 2.2) at 37°C and resuspended at 2.5 x $10^8$/ml. The cell suspensions were incubated for a maximum of 360

minutes and at 0, 120, 240 and 360 minute time-points, 0.25ml samples were withdrawn for the quantitation of cell morphology (see section 2.6) and 2 x 1ml samples were withdrawn into chilled microfuge tubes for ATP extraction. ATP extractions were continued as described above in section 2.23. The number of cells lost through haemolysis during incubation at 37°C for 360 minutes was monitored by estimation of haemoglobin release as described in section 2.14.

## 2.25. Estimation of cellular ATP levels during calcium loading of erythrocytes in buffer A containing metabolic substrates

Cells were prepared using buffer A (section 2.2) at 37°C and resuspended at 2.5 x $10^8$/ml. 5ml aliquots were prepared, and appropriate amounts of $CaCl_2$ was added to each to give a final calcium concentration of between 100 and 1000µM, followed by 5µM A23187. Each aliquot was incubated at 37°C for a further 5 minutes, after which 0.25ml was withdrawn for morphological scoring (section 2.6) and 2 x 1ml samples were withdrawn into chilled microfuge tubes for ATP extraction, which was then continued as described above (section 2.23).

Control values were determined on untreated samples after 5 minutes incubation at 37°C.

# CHAPTER 3: RESULTS AND DISCUSSION

## Section 3.1: An investigation into the progression of the calcium-induced morphological transitions of human erythrocytes and their relationship to both calcium concentration and the metabolic status of the cell.

### 3.1.1. Introduction; transitions of erythrocyte morphology induced by a rise in intracellular calcium

All experimental work described in this thesis was performed on intact normal human erythrocytes. It was designed in an attempt to understand the relationship between the molecular processes initiated in these cells during a rise in intracellular calcium and the observed parallel morphological transitions. In an *in vitro* environment, undisturbed normal human erythrocytes adopt the discocyte morphology (reviewed by Steck, 1989). Artificial manipulations resulting in an increase in cytosolic calcium are accompanied by a shape transition from the discoid to the crenated echinocyte form. In this study, the detailed examination of erythrocyte morphology during this shape transition, played an important role in determining the relevance of the concurrent biochemical changes occurring in the membrane and cytoskeleton.

The studies described in this section begin with a detailed classification of echinocyte morphologies and an investigation of the progression of the shape transition under a range of environmental conditions.

In all studies human erythrocytes were freshly

obtained from healthy volunteers and used immediately. For experimental purposes the echinocytic shape transition was induced by artificially raising intracellular calcium levels by the controlled addition of extracellular calcium and then an ionophore to facilitate calcium entry. The ionophore A23187 was used in most studies; it is a widely used tool in the manipulation of cell $Ca^{2+}$ levels because of its high selectivity for divalent over monovalent cations (Reed and Lardy, 1972, Pressman and Fahim, 1982). Upon addition to a cell suspension A23187 immediately partitions into the cells, and at least half of it remains in the membrane where it mediates a $M^{2+}:2H^{+}$ exchange with a turnover of 2-5 calcium ions/second/pair of ionophore molecules at 37°C (Lew and Simonsen, 1980).

Once initiated, the progression of echinocytosis was studied by cell sampling at timed intervals. Immediate sample fixation by glutaraldehyde allowed the subsequent microscopic examination of the cell population at each time-point. Since early echinocyte stages were difficult to detect using a simple light microscope, interference microscopy was employed which allowed a careful examination of erythrocyte surface architecture.

An increase in intracellular calcium is known to result in a progression of morphologies between the discocyte and the most extreme echinocyte form. The appearance of surface spicules is followed by the loss of discoid morphology as the cell becomes spherical.

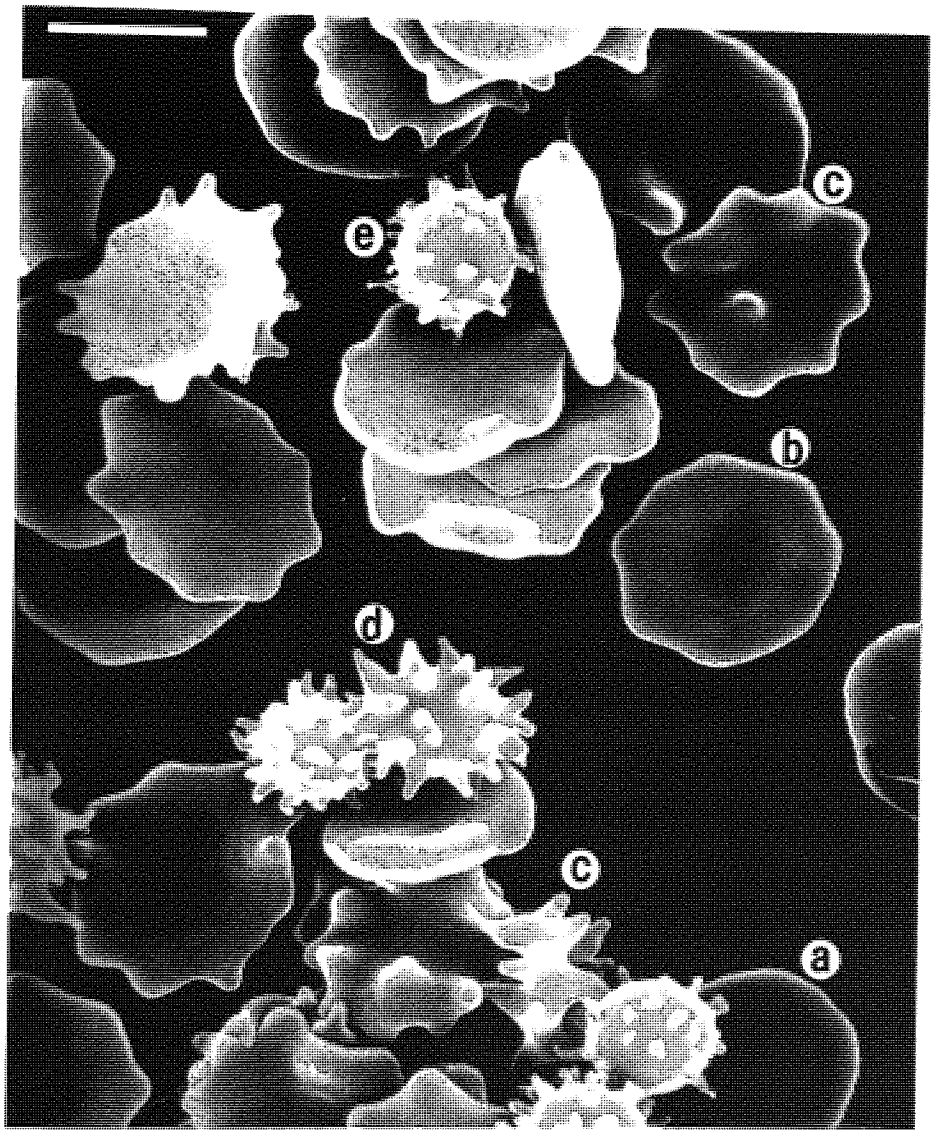


**FIGURE 8** The progression of echinocytosis, illustrating the morphological characteristics of each echinocyte stage.
Cells were treated with 150μM calcium and 5μM A23187 for 60 minutes, fixed and photographed using scanning electron microscopy. Calibration bar, 5μM.
a=discocyte, b=stage 1 echinocyte, c=stage 2 echinocyte, d=stage 3 echinocyte, e=sphereo-echinocyte.

Eventually, shedding of the spicules results in membrane loss and the formation of a smooth spherical cell. However, in most published investigations on erythrocytes involving an examination of the cellular consequences of a rise in intracellular calcium cell, morphologies, where noted, have been graded as either discs or echinocytes. This approach may mask any more subtle, possibly important stages of the shape transition. In the studies described here the echinocytic shape transition has been examined in greater detail and treated cells graded as stage 1, 2, 3, or sphereo-echinocytes depending on the morphology stage of the shape transition they represent. This classification is based on that described by Bessis (1973) and the morphological characteristics of each form are illustrated in figure 8.

The majority of studies described in this thesis were performed on erythrocytes prepared and maintained in a buffer containing metabolic substrates (buffer A). Previous work in this laboratory indicated that the use of this buffer ensured both low basal levels of non-discs in erythrocyte preparations and reproducible rates of echinocytosis during calcium treatment (Tang, 1988). Unless otherwise stated experiments were carried out in this buffer. However, for comparative purposes some studies were repeated in the absence of metabolic substrates using a simple isotonic Tris buffer (buffer B).

### 3.1.2. The progression of echinocytosis in a metabolically replete environment

In the presence of A23187, human erythrocytes were observed to undergo echinocytosis in a manner dependent on both $Ca^{2+}$ concentration and time of exposure. Figure 9 shows the morphological changes observed in cells treated with increasing calcium concentrations and 5μM A23187 for 5 minutes before fixation. Such treatment results in the loss of the discocyte morphology as calcium levels increase (figures 9A and B). A variety of echinocytic stages can be observed at lower calcium concentrations (<300μM), whereas after treatment with 400μM or more, the shape transitions occur rapidly, and most of the cells examined are either stage 3 or sphereo-echihocytes.

The time-dependent progression of echinocytosis during treatment of erythrocytes with 150μM calcium and 5μM A23187 over a 60 minute period is illustrated in figure 10. A steady increase in total echinocytes can be observed, reaching 100% after about 30 minutes (figure 10A). If the rate of formation of different stage echinocytes is examined, it can be noted that there is a progression towards more advanced stages during treatment (figure 10B). As the percentage of discocytes steadily decreases, the percentage of stage 1 echinocytes rises initially and then falls as these cells become stage 2 and eventually stage 3 echinocytes. No sphereo-echinocytes are observed in the population until after 30 minutes of calcium loading. It

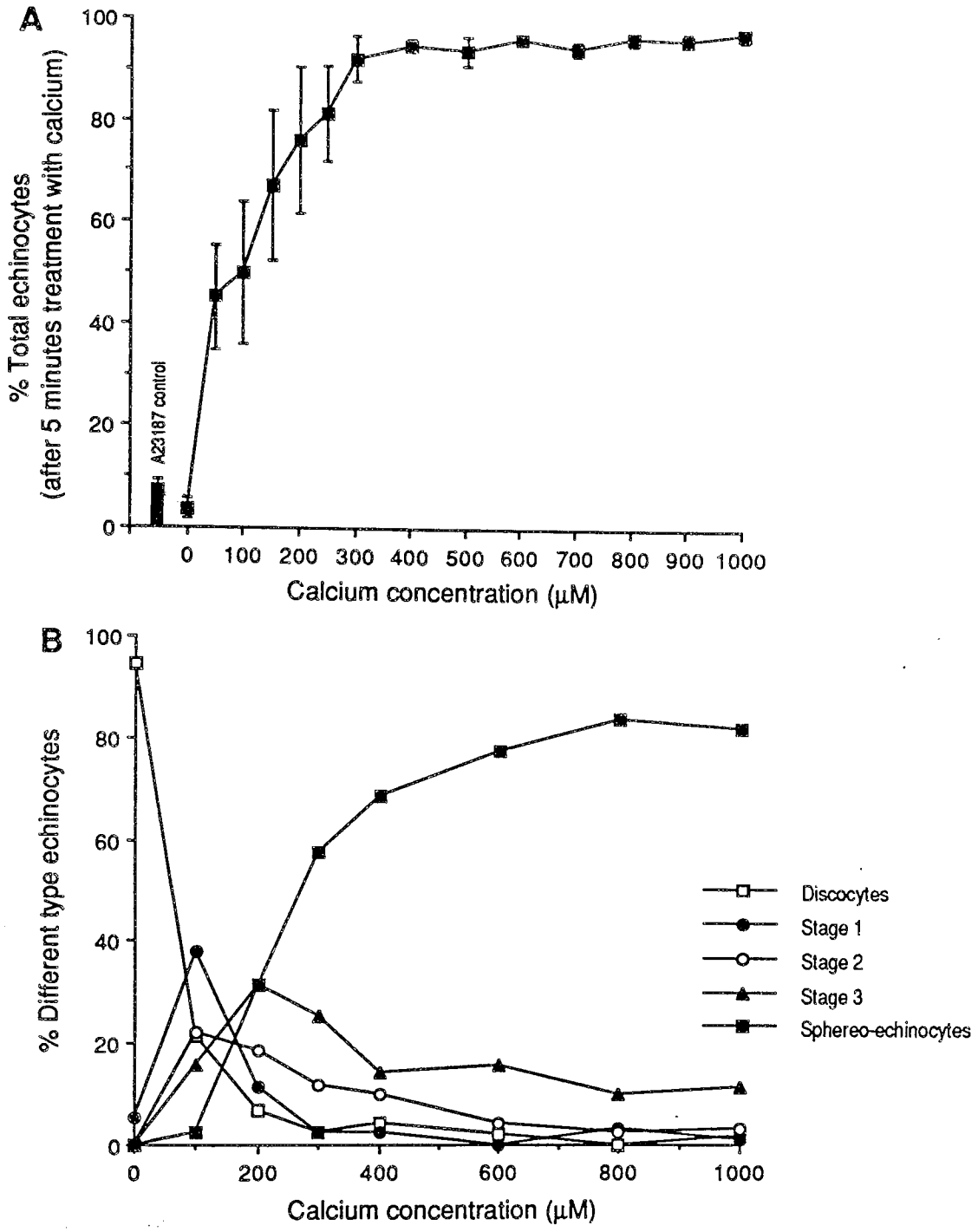


**FIGURE 9** The progression of echinocytosis induced by increasing calcium concentrations

Human erythrocytes held in buffer A were incubated with increasing concentrations of calcium (0-1mM) for 5 minutes in the presence of 5μM A23187.

**A** Quantitation of total echinocytes formed after 5 minutes exposure to each calcium concentration. Results are shown as mean ±SD, n=6.

**B** Analysis of the different stage echinocytes induced by 5 minutes exposure to each calcium concentration. Results shown are a representative graph from one experiment.

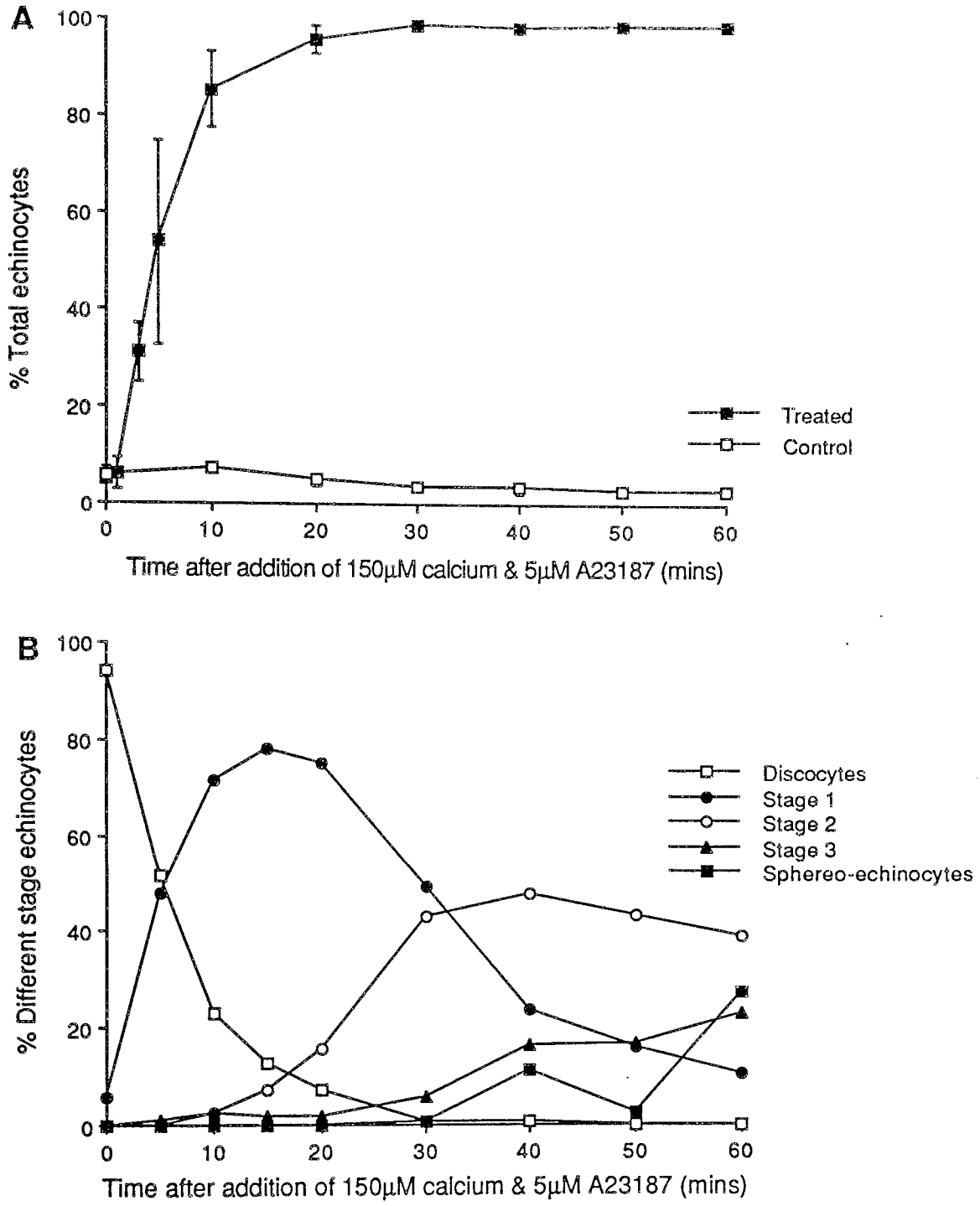


**FIGURE 10** The progression of time-dependent echinocytosis induced by 150µM calcium in erythrocytes held in buffer A
Human erythrocytes held in buffer A were incubated with 150µM calcium and 5µM A23187. Cell morphologies were quantitated at the time intervals specified. Control cells received only calcium.
**A** Time course for the formation of total echinocytes. Results are shown as mean ±SD, n=11.
**B** Analysis of the rate of formation of different stage echinocytes. Results shown are a representative graph from one experiment.

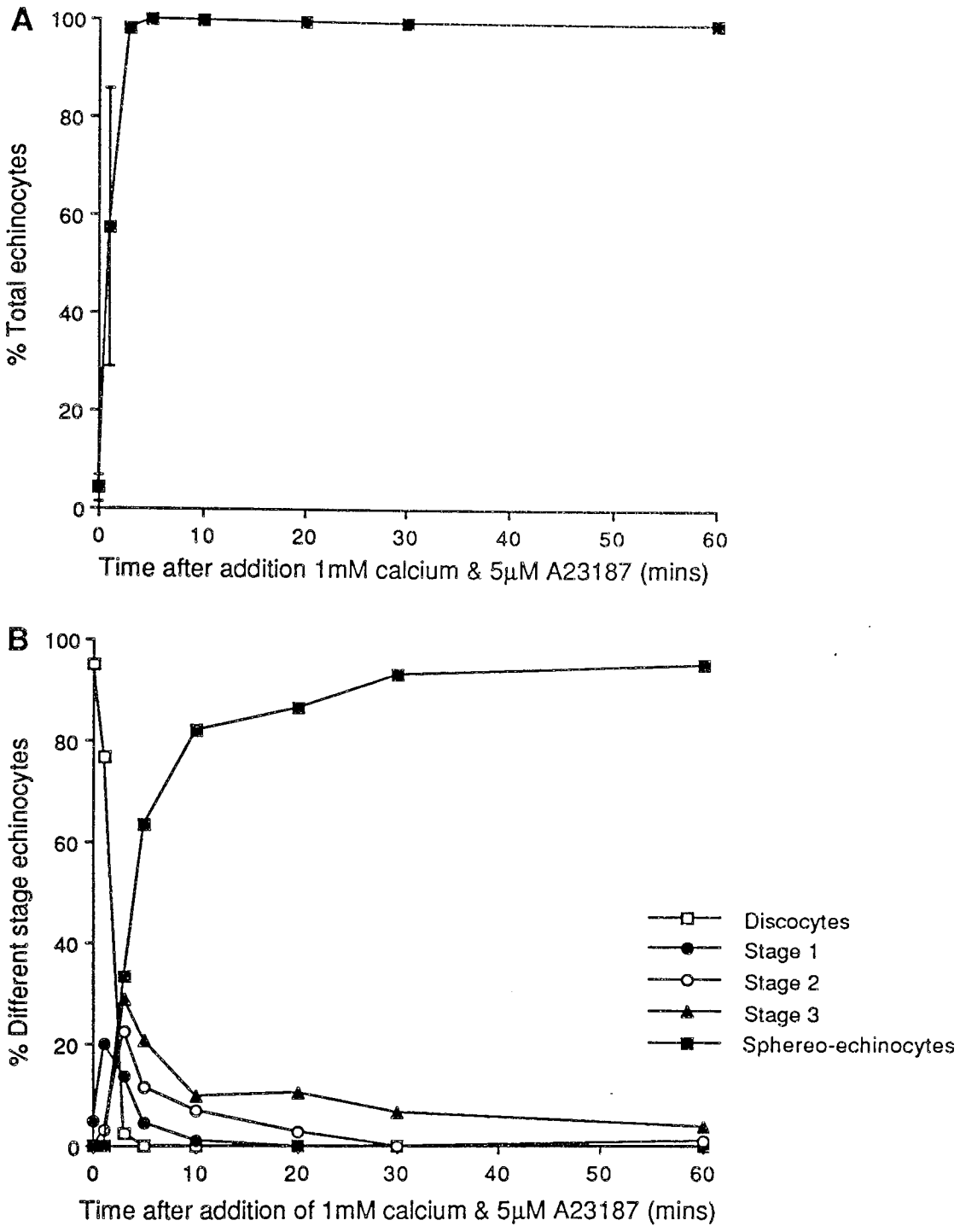


**FIGURE 11** The progression of time-dependent echinocytosis induced by 1mM calcium in erythrocytes held in buffer A
Human erythrocytes held in buffer A were incubated with 1mM calcium and 5µM A23187. Cell morphologies were quantitated the time intervals specified.
**A** Time course for the formation of total echinocytes. Results are shown as mean ± SD, n=10.
**B** Analysis of the rate of formation of different stage echinocytes. Results shown are a representative graph from one experiment.

appears that with continued calcium exposure each cell progresses through these defined stages of echinocyte formation, however not all of the cells pass through the same stage simultaneously; supporting the implication from figure 9 that the morphological response of a cell population to calcium permeabilization is heterogeneous.

For comparison, figure 11 shows the time-dependent morphological changes of erythrocytes treated with 1mM calcium and 5µM A23187. Under these conditions of greater calcium loading the echinocyte transformation occurred rapidly with complete loss of the discocyte morphology within 5 minutes. Progression of the cells through the defined echinocyte stages was also rapid with approximately 85% of the cells at the stage 3 or sphereo-echinocyte form within 5 minutes (figure 11B). Again the cells display a heterogeneous morphological response, although it is less obvious at this higher calcium concentration.

### 3.1.3. The progression of echinocytosis in erythrocyte populations enriched in either young or old cells

Since both A23187 ionophore distribution and induced calcium permeability have been reported to be uniform throughout the cells of a preparation (Simonsen et al., 1982, Garcia-Sancho and Lew, 1988), any heterogeneity must reflect variations in the response of individual cells to the handling of the calcium influx. One possible explanation for the heterogeneous morphological response to

calcium permeabilization is the presence of erythrocytes of varying ages in the original cell population. In the peripheral circulation a constant turnover of mature erythrocytes occurs; each cell surviving for approximately 120 days. The aging of circulating erythrocytes during this period is accompanied by many cellular modifications, and it is possible that some of these age-related changes may influence the morphological mechanisms initiated during calcium permeabilization. Changes related to cell age include a reduction in the activity of many erythrocyte enzymes, including protein kinases (Pfeffer and Swislocki, 1976), PLC and phosphatidylinositol-4-phosphate phosphatase (Palmer, 1985). Additionally the activity of the $Ca^{2+}$-ATPase has been reported to be reduced in older cells (Luthra and Kim, 1980), although this may be coincident with the age-related reduction in cell calmodulin content (Monzon et al., 1982). Changes in membrane phospholipid organisation also occur, with decreased total PtdIns content in older cells in comparison to that observed in younger erythrocytes (Jain, 1988). In addition, many age-related alterations to erythrocyte proteins have been reported; including a reduction in the number and affinity of ankyrin binding sites on the cytoplasmic surface of the membrane in older cells (Kay et al., 1988).

The possibility that the heterogeneity of erythrocyte age within a population contributes to the variation in the morphological response to calcium permeabilization was

examined. Populations of erythrocytes enriched with either young or old cells were loaded with 150µM calcium in the presence of 5µM A23187, and the rate of formation of different stages of echinocytes was compared in the two preparations. The results of these experiments are presented in figure 12. It can be seen that both cell populations still exhibit a heterogeneous morphological response to calcium loading. Also, there is no consistently significant difference in the rate of formation of any echinocyte stage between the young and old cells. It appears that erythrocyte aging is not responsible for the variable rates of echinocytic transformation observed in these experiments.

A non-uniform response of an erythrocyte population to A23187 permeabilization has also been noted by other workers (Feo and Mohandas, 1977, Garcia-Sancho and Lew, 1988, 1988a, 1988b, Almaraz et al, 1988). The more recent of these studies suggested that each cell behaves as if it has a defined threshold of $Ca^{2+}$ influx tolerance. If influx is below this threshold the cell can balance $Ca^{2+}$ entry by extrusion of the ion through the $Ca^{2+}$-ATPase, sustain normal ATP levels and maintain submicromolar steady-state calcium concentrations. If influx is above this threshold ATP production can not match pump-mediated hydrolysis, cell ATP levels fall, adenine nucleotides become irreversibly converted to inosine monophosphate (IMP), and cell $Ca^{2+}$ concentration approaches equilibrium

| Time (minutes) | Discocytes Top 10% | Discocytes Bottom 10% | Stage 1 Top 10% | Stage 1 Bottom 10% | Stage 2 Top 10% | Stage 2 Bottom 10% | Stage 3 Top 10% | Stage 3 Bottom 10% | Sphereo-echin Top 10% | Sphereo-echin Bottom 10% |
|---|---|---|---|---|---|---|---|---|---|---|
| 0 | 92.99 | 93.31 | 7.01 | 6.36 | | 0.33 | | | | |
| | 2.71 | 3.4 | 2.71 | 3.94 | | 0.57 | | | | |
| | N.S. | | N.S. | | | | | | | |
| 10 | 8.92 | 11.27 | 49.93 | 36.4 | 15.58 | 11.35 | 15.52 | 19.64 | 11.66 | 21.35 |
| | 2.15 | 6.05 | 12.47 | 5.59 | 6.1 | 6.04 | 6.13 | 3.42 | 10.36 | 6.71 |
| | N.S. | | N.S. | | N.S. | | N.S. | | N.S | |
| 20 | 3.14 | 0.48 | 33.43 | 20.75 | 30.5 | 20.55 | 18.36 | 27.16 | 14.58 | 31.03 |
| | 1.89 | 0.83 | 9.5 | 12.01 | 7.57 | 6.17 | 7.15 | 8.96 | 9.66 | 11.31 |
| | p=0.05 | | N.S. | | N.S. | | N.S. | | N.S | |
| 30 | 1.44 | 0.76 | 27.73 | 13.39 | 27.99 | 15.5 | 25.67 | 37.96 | 8.87 | 32.84 |
| | 1.73 | 0.15 | 7.3 | 5.53 | 8.56 | 5.88 | 7.29 | 5.32 | 10.74 | 16.28 |
| | N.S. | | P=0.05 | | N.S. | | P=0.05 | | N.S. | |
| 40 | 1.71 | 0.58 | 17.64 | 11.36 | 29.05 | 19.11 | 30.79 | 30.93 | 20.78 | 38.01 |
| | 0.98 | 1.01 | 10.07 | 5.09 | 8.31 | 7.99 | 4.63 | 3.49 | 12.39 | 15.25 |
| | N.S. | | N.S. | | N.S. | | N.S. | | N.S. | |
| 50 | 0.72 | 0.77 | 15.37 | 9.98 | 31.52 | 12.38 | 27.5 | 33.69 | 24.9 | 43.22 |
| | 0.65 | 1.33 | 9.75 | 8.26 | 8.46 | 1.54 | 2.15 | 12.6 | 15.83 | 13.21 |
| | N.S. | | N.S. | | P=0.05 | | N.S. | | N.S. | |
| 60 | 0.52 | 0.24 | 9.45 | 6.08 | 21.36 | 14.42 | 40.38 | 35.57 | 28.3 | 43.68 |
| | 0.47 | 0.41 | 3.16 | 4.73 | 11.3 | 6.72 | 4.58 | 12.29 | 14.94 | 17.93 |
| | N.S. | | N.S. | | N.S. | | N.S. | | N.S. | |

**FIGURE 12** A comparison of the levels of different echinocyte stages induced by 150µM calcium in populations of human erythrocytes enriched in either young or old cells Following density separation into populations enriched in either young or old cells, erythrocytes were treated with 150µM calcium and 5µM A23187. Cell morphologies were then quantitated at the time intervals specified. n=3, results are expressed as mean ±SD

with that the external medium (Garcia-Sancho and Lew, 1988 and 1988a, Almaraz et al, 1988). The mechanism of this heterogeneous cell response to calcium permeabilization is not known. Thresholds vary from cell to cell, however, the ultimate fate of each cell is determined by size of calcium influx since all cells become equilibrated if influx of the ion is great enough (Garcia-Sancho and Lew, 1988a). It is possible that these observed differences in the calcium handling capabilities between cells of a population may account for the heterogeneity in the morphological response of the cells to calcium permeabilization, however, since there is no morphological data provided in the above studies no such correlations can be safely made without further investigation.

### 3.1.4. The progression of echinocytosis in a Tris buffer containing no metabolic substrates

It is well documented that the metabolic depletion of erythrocytes is accompanied by loss of the discoid morphology in favour of the echinocytic form (Nakao et al., 1960, 1961), indicating that the metabolic state of an erythrocyte is important in determining cell morphology. To explore this observation further an examination was made of the importance of metabolic status on the shape transitions occurring during calcium loading. Since anaerobic glycolysis is the only source of metabolic energy (ATP) available to human erythrocytes, the metabolic status

of red cells during calcium loading can be manipulated by the availability of glycolytic substrates. The experiments described above in section 3.1.2. were carried out using buffer A (section 2.2) which contains glucose, adenine and inosine, all of which can be utilized by erythrocytes to provide ATP (Lew and Garcia, 1989, Kim, 1990). The metabolism of the latter produces ribose 1-phosphate which can then enter glycolysis through the pentose phosphate pathway. For comparison, morphological studies were carried out using cells prepared and treated in a Tris buffer with no available source of metabolic energy (buffer B, section 2.2).

Preliminary experiments were carried out to examine the influence of these two buffers on the metabolic status of suspended erythrocytes at 37$^{o}$C (figure 13A). It was observed that even after a 6 hour incubation, cells in buffer A containing glycolytic substrates remained metabolically replete and suffered no significant change in total cell ATP levels. However, the Tris buffer (buffer B) was unable to sustain the total ATP content of suspended cells and levels fell significantly by nearly 60% after only 2 hours. Cell morphologies were also monitored during these extended incubations and, as expected, were found to reflect the pattern of cell ATP changes (figure 13B). After 6 hours at 37$^{o}$C the cell sample incubated in buffer A contained discocyte levels comparable to those observed at 0 hours i.e. approximately 95%, confirming that at this

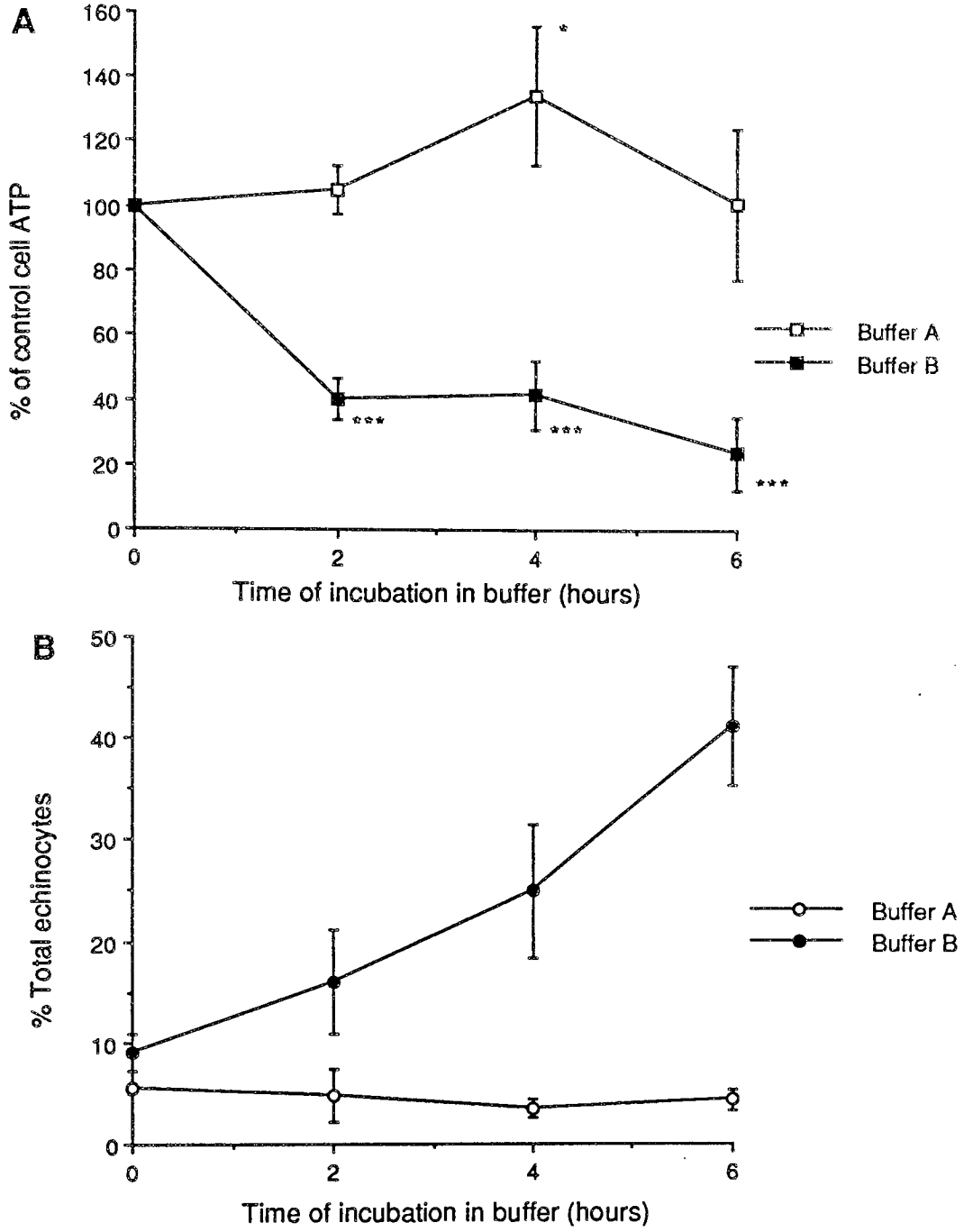


**FIGURE 13** The influence of the availability of metabolic substrates during prolonged incubation on erythrocyte morphology and metabolic status.
Human erythrocytes were incubated in either the presence (buffer A) or absence (buffer B) of glycolytic substrates for a maximum of 6 hours at 37°C. At the time intervals specified total cellular ATP was estimated and cell morphologies were quantitated.
**A** Changes in total cellular ATP levels. Results are shown as mean ±SD, (n=6). * = $P<0.05$, *** = $P<0.001$, when mean compared to 0 hours value by Student T test.
**B** Changes in levels of total echinocytes. Results are shown as mean ±SD, n=6.

temperature this buffer was able to maintain the discocyte morphology. However cells incubated in Tris buffer B slowly transformed into echinocytes with levels reaching approximately 40% after 6 hours, presumably because this buffer is incapable of meeting the metabolic demands of the cells.

The time-dependent shape transitions of erythrocytes loaded with 150uM calcium and 5μM A23187 in Tris buffer B are examined in figure 14. 100% transformation from the discocyte form occurs after approximately 30 minutes calcium loading. Interestingly, when this data is compared to that of cells treated identically in buffer A (figure 10), it can be observed that the rate of transition from the discocyte form is independent of the buffer in which the cells were suspended. In both media less than 10% discocytes remain after 20 minutes of loading with 150μM calcium. However, under conditions of metabolic depletion in the Tris buffer (buffer B) the progression of cells through the echinocyte stages following the loss of discocyte morphology is more rapid than in buffer A containing glycolytic substrates. In the former buffer over 75% of the cells have progressed to the sphereo-echinocyte form after 30 minutes treatment with 150μM calcium, compared to 0% after the same treatment in buffer A. A similar pattern is observed in cells treated with 1mM calcium and 5μM A23187 in buffer B (figure 15), with a rapid transition of cells to over 95% stage 3 or

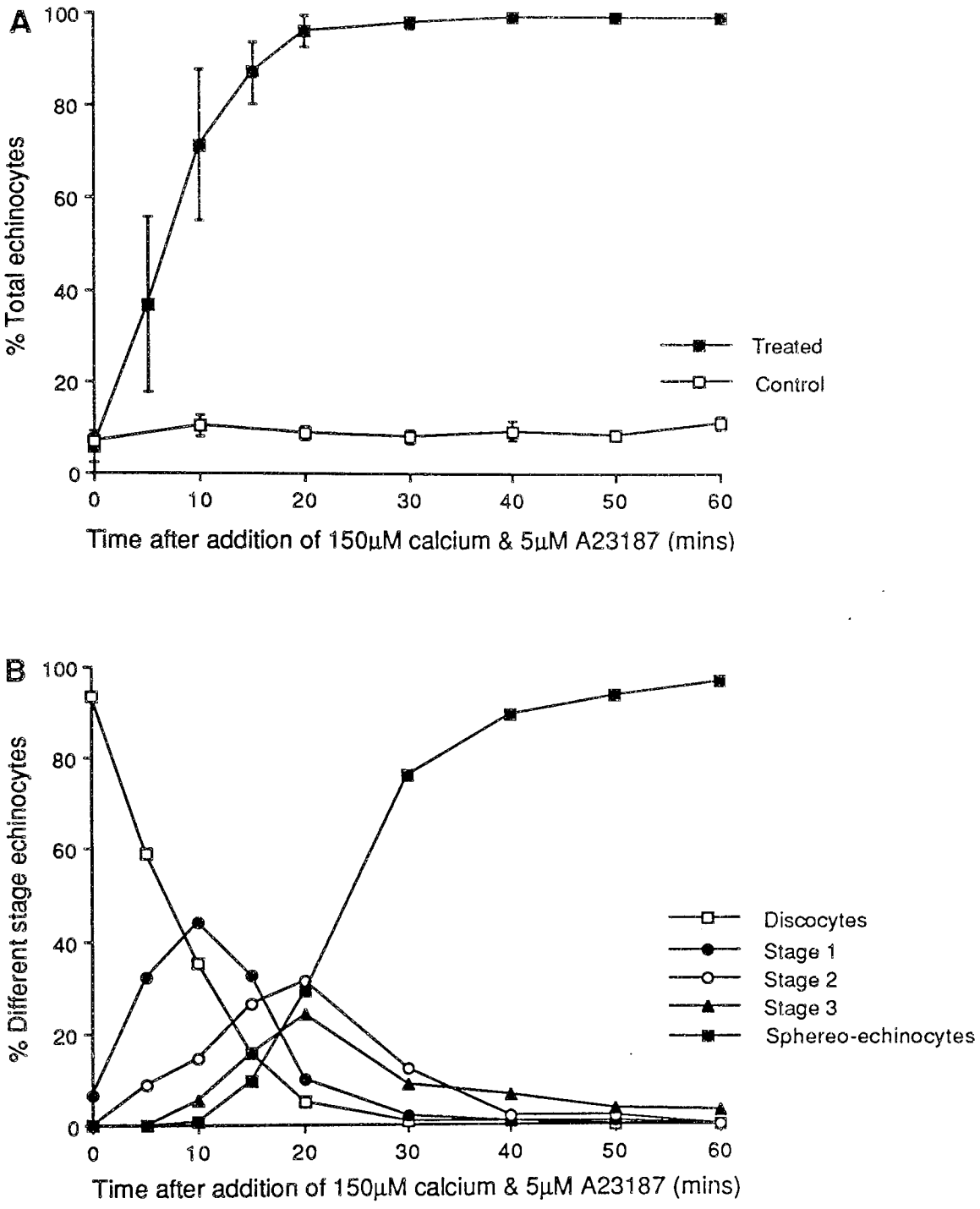


**FIGURE 14** The progression of time-dependent echinocytosis induced by 150µM calcium in erythrocytes held in buffer B
Human erythrocytes held in buffer B were incubated with 150µM calcium and 5µM A23187, and cell morphologies were quantitated at the time intervals specified.
**A** Time course for the formation of total echinocytes. Results are shown as mean ±SD, n=3.
**B** Analysis of the rate of formation of different stage echinocytes. Results from a representative experiment are shown.

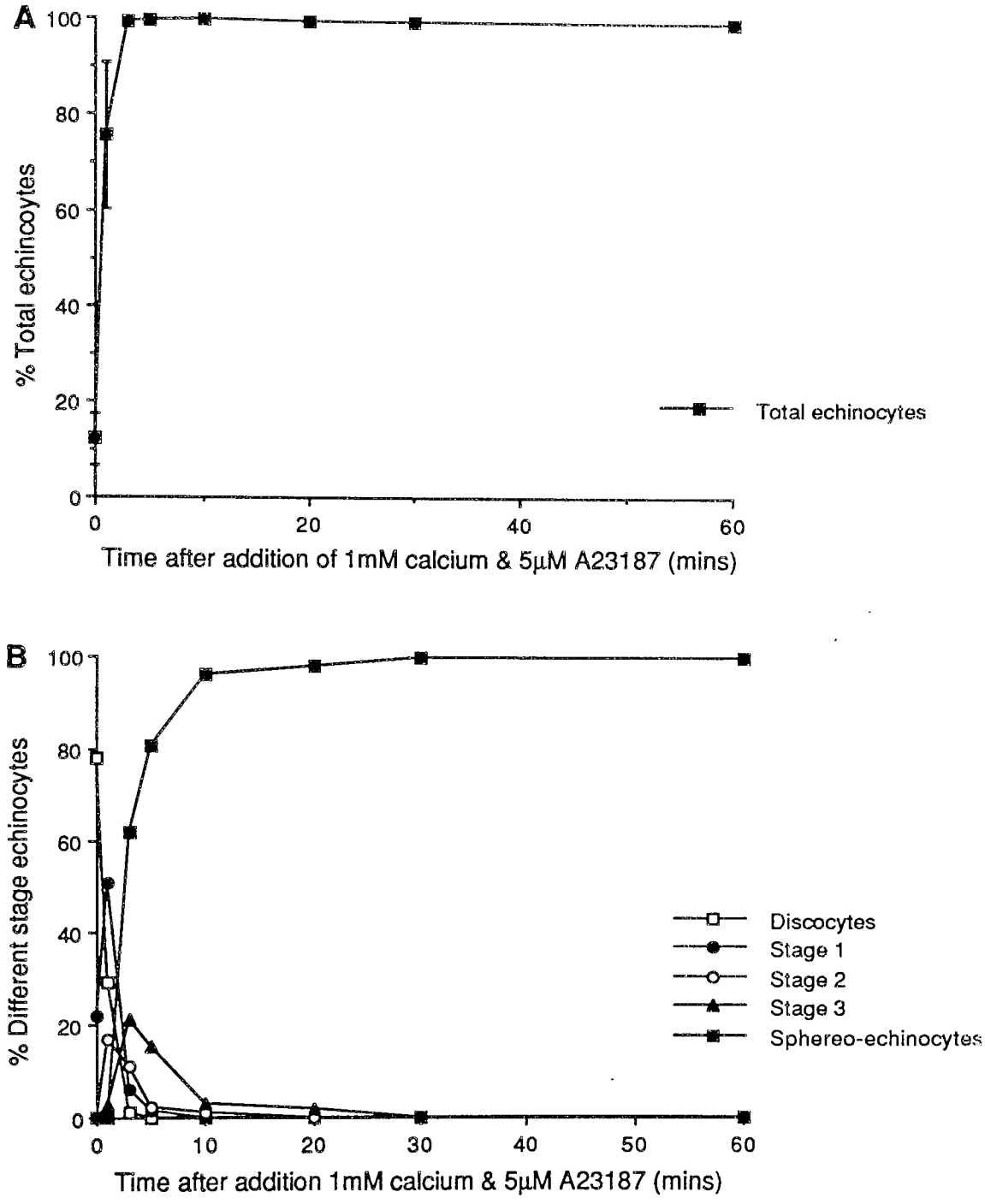


**FIGURE 15** The progression of time-dependent echinocytosis induced by 1mM calcium in erythrocytes held in buffer B
Human erythrocytes held in buffer B were incubated with 1mM calcium and 5µM A23187, and cell morphologies were quantitated at the time intervals specified.
**A** Time course for the formation of total echinocytes. Results are shown as mean ± SD, n=8.
**B** Analysis of the rate of formation of different stage echinocytes. Results from representative experiment are shown.

sphereo-echinocytes within 5 minutes of treatment (compare to figure 11).

### 3.1.5. Discussion

From these results it appears that the availability of glycolytic substrates in the buffer in which erythrocytes are treated does influence the rate of progression of morphological transitions induced by calcium. However, it is also clear from figure 16 that even ATP levels of 90% of those observed in undisturbed cells are not sufficient to maintain intracellular calcium below the threshold concentration for shape change (approximately 10-100μM, Sarkadi et al., 1976, Shimizu, 1988). Since intracellular calcium does influence ATP-dependent processes, the presence of metabolic substrates could have profound effects on cell ATP levels. Several previous studies have found that the A23187 permeabilization of erythrocytes to calcium in buffer without glycolytic substrates is accompanied by a large fall in cell ATP levels (Edmondson and Li, 1976, Taylor et al., 1977, Friederichs et al., 1989); presumably associated with the calcium activation of the membrane ATP-fuelled $Ca^{2+}$ pump (Taylor et al., 1977, Friederichs et al., 1989). The normal ATP content of erythrocytes is in the range 1.0-1.5mmol/L cells (Dagher and Lew, 1988, Lew and Garcia-Sancho, 1989). Since the saturated $Ca^{2+}$-ATPase can extrude $Ca^{2+}$ at rates of about 10-25mmol/L cells/hour and the pump operates with a

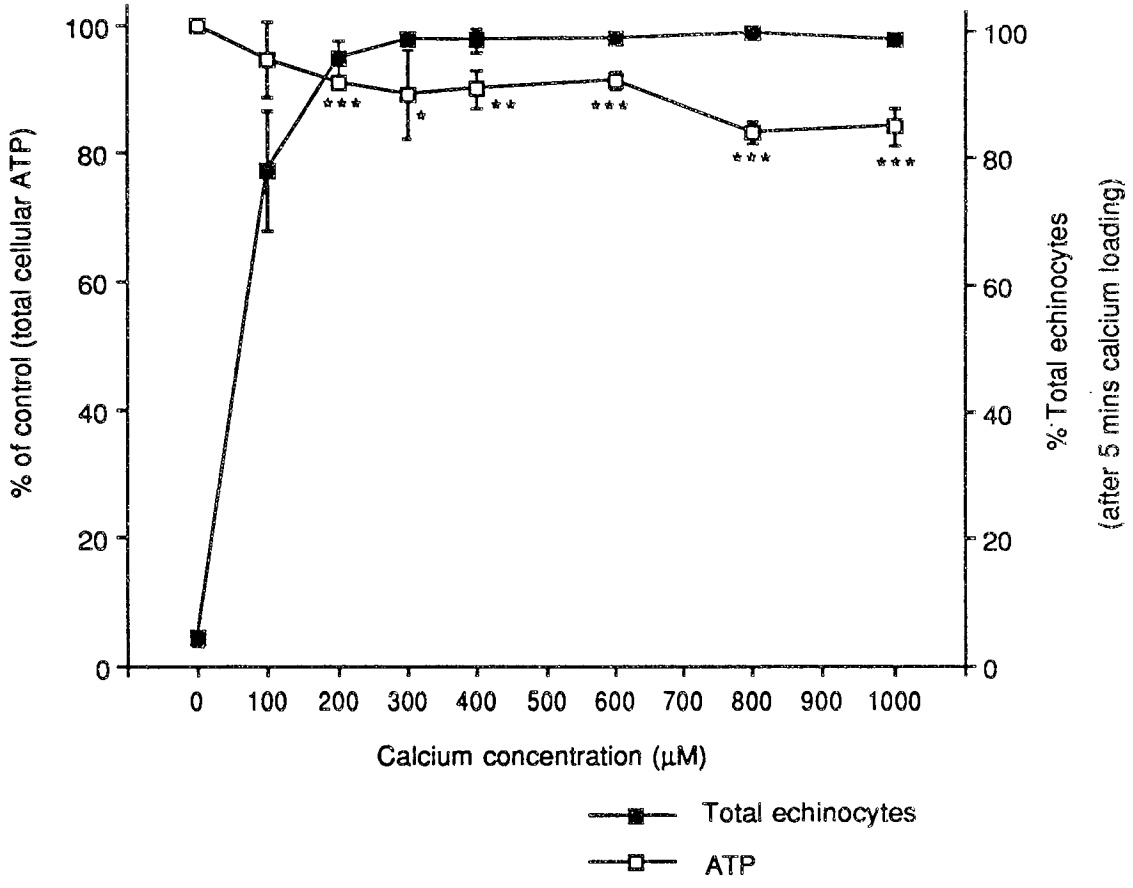


**FIGURE 16** The relationship between morphology transitions induced by calcium and cell ATP levels
Human erythrocytes held in buffer A were incubated with increasing concentrations of calcium (0-1mM) and 5uM A23187 for 5 minutes, after which total cellular ATP levels were estimated, and cell morphology was quantified. Results are shown as mean $\pm$ SD, n=4. P values calculated between mean values of control and treated samples using Student T Test, *=P<0.05, **=P<0.005, ***=P<0.001

$Ca^{2+}$:ATP stoichiometry of 1:1 (Dagher and Lew, 1988), calcium activation would be expected to rapidly deplete the cells of ATP in the absence of metabolic substrates.

In contrast, pump activation during calcium permeabilization in the presence of metabolic substrates would be expected to be associated with slower rates of ATP depletion. In the presence of available substrates, erythrocytes can produce ATP with a turnover in the range of 3-5 mmol/L cells/hour (Lew and Garcia-Sancho, 1989). In addition, internal calcium has been shown to stimulate glycolysis and therefore ATP production (Brown and Johnston, 1983). Indeed it can be seen that under the metabolically more replete conditions in buffer A, an almost 100% transition of erythrocytes to the echinocyte form was only accompanied by a 10% drop in cell ATP levels (figure 16), compared to the approximately 70% fall in cell ATP associated with a 40% echinocyte in buffer B (figure 13).

From the results presented here it appears that the physiological processes involved in the discocyte-stage 1 echinocyte morphological transition are not influenced by the availability of glycolytic substrates. This suggests that these processes are initiated by a rise in intracellular calcium independently of the cellular ATP concentration. However, the biochemical processes involved in the echinocytic transition after the calcium induced loss of the discocyte form do appear to be influenced in

some way by the ATP content of the cells. These results imply that the calcium induced discocyte to sphereo-echinocyte morphological transition is not a simple switch from one form to other but has discrete steps possibly involving different biochemical processes.

## Section 3.2: An investigation into the role of cytoskeletal proteolytic cleavage in the initiation of calcium-induced echinocytosis, and the importance of cytoskeletal integrity to the restoration of the discocyte form during shape reversal.

### 3.2.1. Introduction; calcium-induced proteolytic events

The transitions of erythrocytes into the echinocyte morphology induced by a rise in cytosolic calcium are accompanied by the activation of a range of biochemical processes. However, as discussed previously, the role of any one of these processes in the progression of the shape transitions is still not fully understood. Previous work carried out in this laboratory has focussed on the biochemical regulation of the erythrocyte cytoskeletal network and the possible changes in this regulation which may cause the onset of cell shape change (Tang, 1988). This work included an investigation into the possibility that any one proteolytic event induced by calcium in intact cells could lead to progressive shape change. Many previous reports have indicated that proteolytic activity is stimulated in erythrocytes by a rise in cytosolic calcium, however none have related these changes to cell shape (Anderson et al., 1977, Allen and Cadman, 1979, Siegel et al., 1980, Allan and Thomas, 1981, Lorand et al., 1983, Pontremoli et al., 1984, Grasso et al., 1986)). In his study Tang (1988) attempted to correlate the cellular

changes brought about by calcium stimulated proteolytic activity with the progression of echinocytosis. Through the examination of the pattern of cytoskeletal cleavage during calcium loading, a role for the ankyrin, protein 2.1 in the regulation of the shape transitions was suggested. Since this protein has binding sites for both spectrin (Tyler et al., 1979) and the cytoplasmic domain of the integral protein, band 3 (Bennett and Stenbuck, 1979), it provides sites of association between the erythrocyte membrane and cytoskeleton. However, in these studies the integrity of this protein was not studied directly but was estimated indirectly through the changes observed in proteins which were thought to be cleavage products of protein 2.1.

In the experiments described here the proteolytic events associated with echinocytosis induced by calcium in intact erythrocytes were examined in greater detail. Particular attention was given to the proteins which link the membrane and the cytoskeleton, notably the ankyrins and protein 4.1. These proteins may play a key role in the determination of erythrocyte shape. Proteolysis was examined in erythrocytes permeabilized to either 150uM or 1mM calcium under conditions of metabolic repletion (buffer A) so that lack of ATP would not be a complicating factor. Also, since the availability of glycolytic substrates has been shown to influence the progression of calcium-induced echinocytosis a comparative study was carried out to

examine the proteolytic events associated with the treatment of cells with 1mM calcium and ionophore in the absence of metabolic substrates (in buffer B). In all of these experiments it was important to relate the status of cytoskeletal proteins to that of cell morphology. Therefore, modifications to these proteins were analysed by SDS-PAGE at appropriate intervals during calcium loading and related to the progression of the morphological transformation examined by microscopy on the same samples. Two gel systems were used to facilitate the efficient separation and analysis of both high and low molecular weight cytoskeletal proteins; a 3.5-17% gradient gel system using the buffers of Fairbanks et al. (1971) and a 7% discontinuous system based on that of Laemmli (1970). The former system resolved the ankyrins, particularly band 2.1, (mw 215,000) from the spectrin ß chain which has a similar molecular weight (mw 225,000), and therefore allowed the integrity of this protein to be studied directly during calcium loading. However, protein 4.1 (approximate mw, 80,000) could not be reliably examined using a gradient gel, and therefore the discontinuous SDS-PAGE was used. This increased the resolution of the two subunits of band 4.1, and separated these polypeptides from others of a similar molecular weight, for example band 3 (mw 95,000). The pattern of proteins separated on these two electrophoresis systems is illustrated in figure 17.

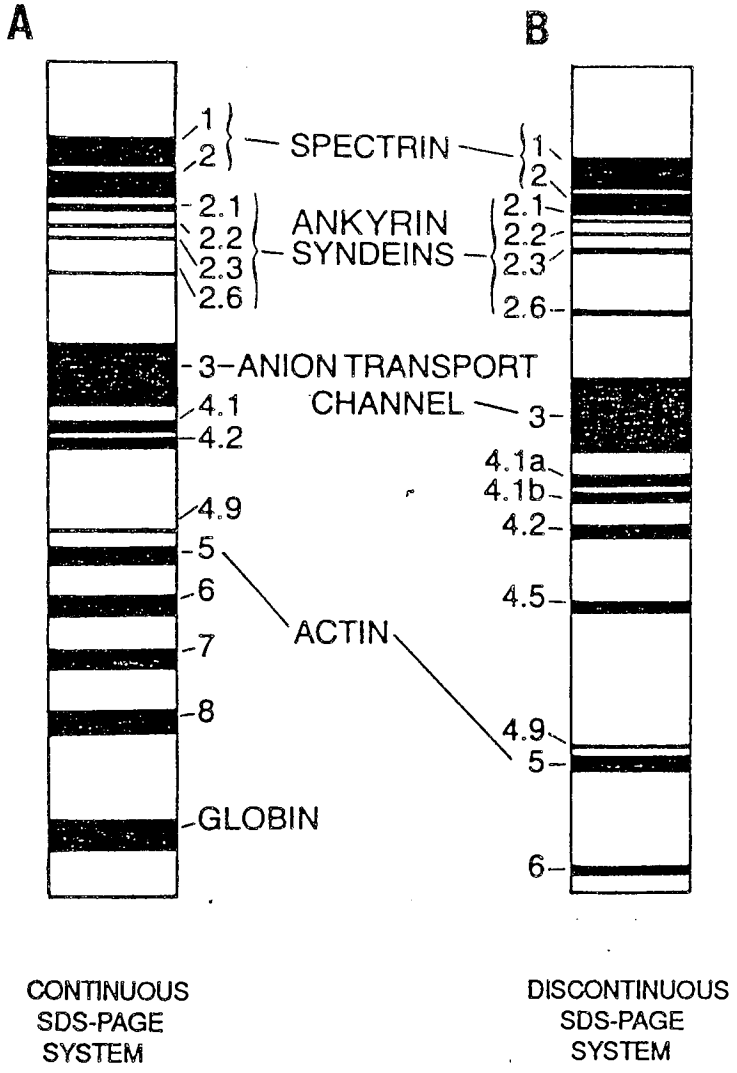


**FIGURE 17** The electrophoretic separation of erythrocyte ghost proteins by SDS-polyacrylamide gel electrophoresis
A comparison of the pattern of protein separation obtained using; **A** a continuous gradient SDS-PAGE system or **B** a discontinuous SDS-PAGE system.
(modified from Goodman and Zagon, 1986)

The degree of cytoskeletal proteolysis during calcium loading was quantified by laser densitometry of the Coomassie blue stained gels. Although densitometric measurements are subject to experimental variation (Fishbein, 1972), they have been shown to provide a useful estimation of the protein content of stained bands on acrylamide gels of the major erythrocyte proteins (Fairbanks et al., 1971, Fairbanks et al., 1988).

### 3.2.2. Proteolytic events associated with time-dependent echinocytosis in erythrocytes loaded with either 150µM or 1mM calcium in metabolically replete media

Following preparation in buffer A, human erythrocytes were treated with either 150µM or 1mM calcium plus 5µM A23187 for 0 to 60 minutes, at 37°C. At appropriate time intervals, samples of cells were removed for both the quantitation of morphology and the preparation of erythrocyte ghosts for the SDS-PAGE analysis of cytoskeletal proteins.

The results obtained with 150µM calcium are summarised in figure 18. From the morphological analysis it can be seen that the shape transformation to the echinocyte form proceeds gradually to reach 100% loss of the discocyte morphology within 30 minutes (figure 18C).

This level of calcium exposure induces one major alteration in the pattern of cytoskeletal proteins visualised by SDS-PAGE analysis (figure 18 A); after 5

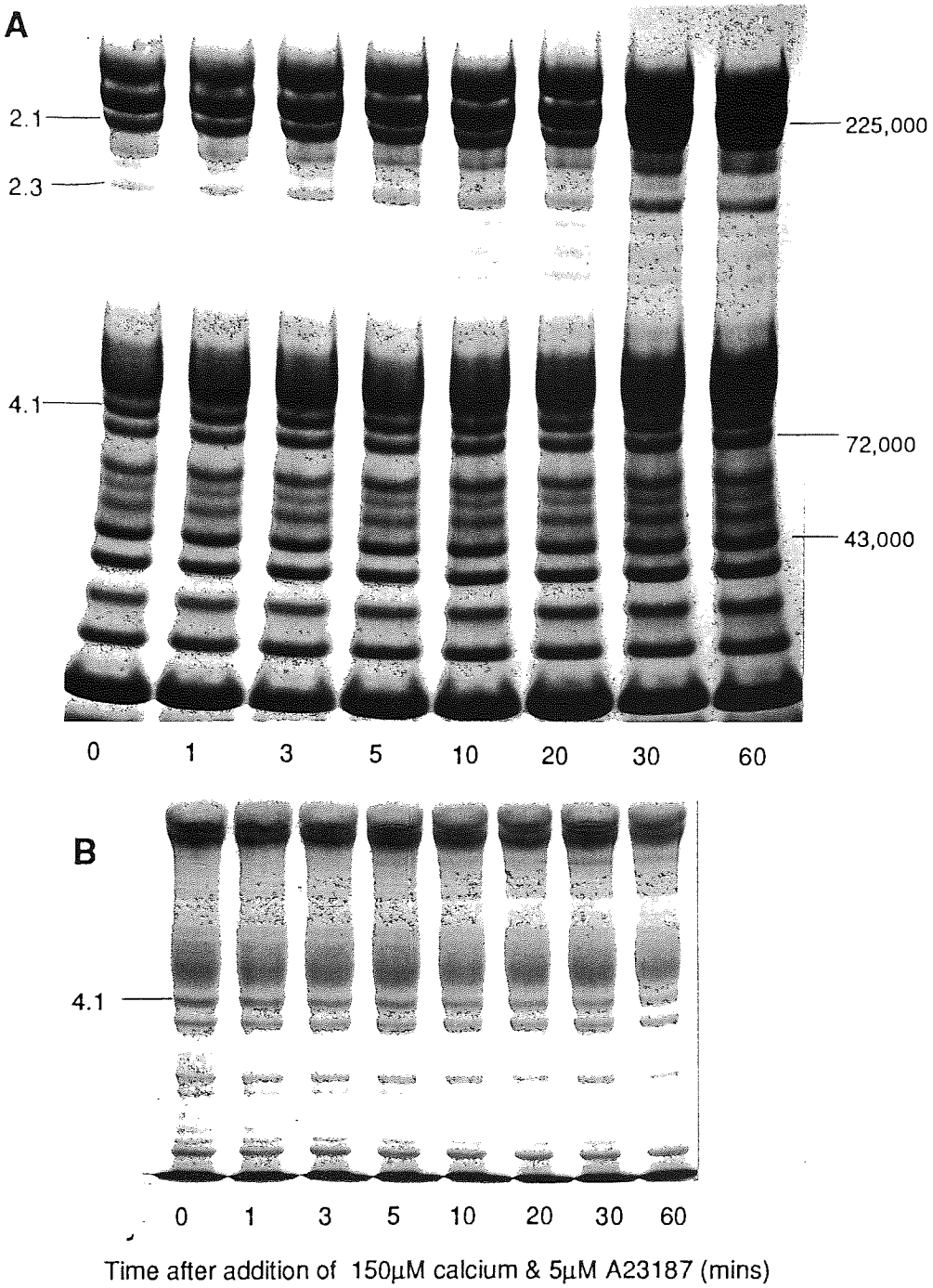


**FIGURE 18** Time-dependent proteolytic modification of cytoskeletal proteins in erythrocytes loaded with 150μM calcium

Intact human erythrocytes held in buffer A were treated with 150uM calcium and 5μM A23187 at 37°C. At the time intervals specified samples were removed for ghost preparation and the quantitation of cell morphology. The representative results from 6 analyses are shown.

**A** Coomassie blue stained pattern of ghost proteins separated by 3.5-17% gradient SDS-PAGE

**B** Proteins from (A) separated by 7% discontinuous SDS-PAGE

**C** Time-course of echinocytosis in the cell samples of A & B

**D** Densitometric analysis of proteins 2.1, 2.3 and 4.1

18 C

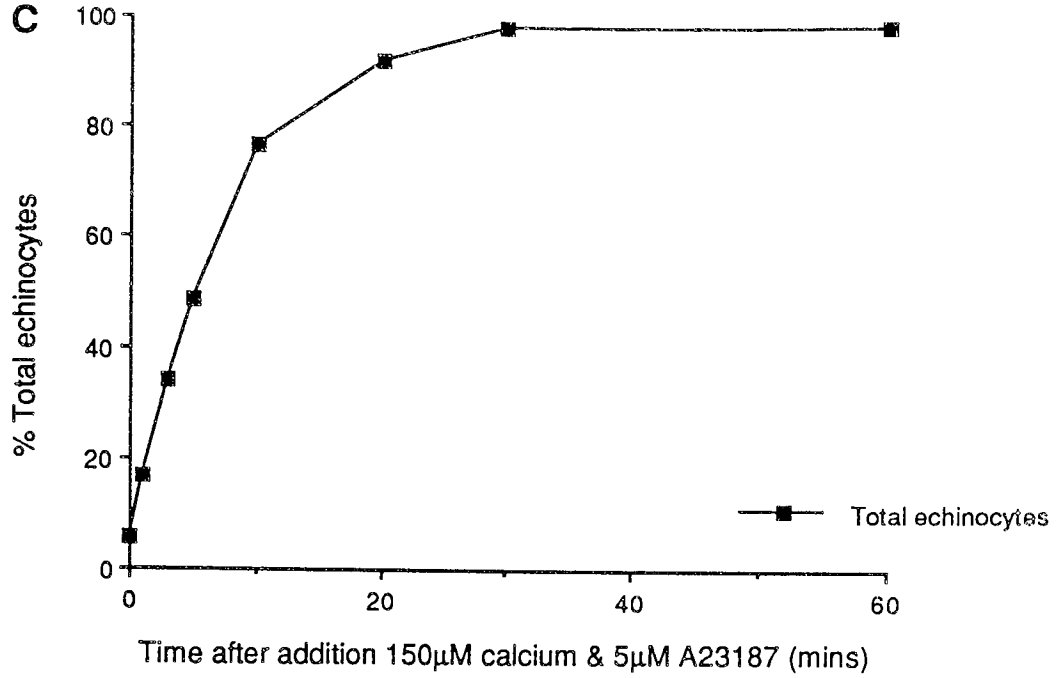
100
80
60
40
20
0
% Total echinocytes
0
20
40
60
Time after addition 150μM calcium & 5μM A23187 (mins)
Total echinocytes

18D

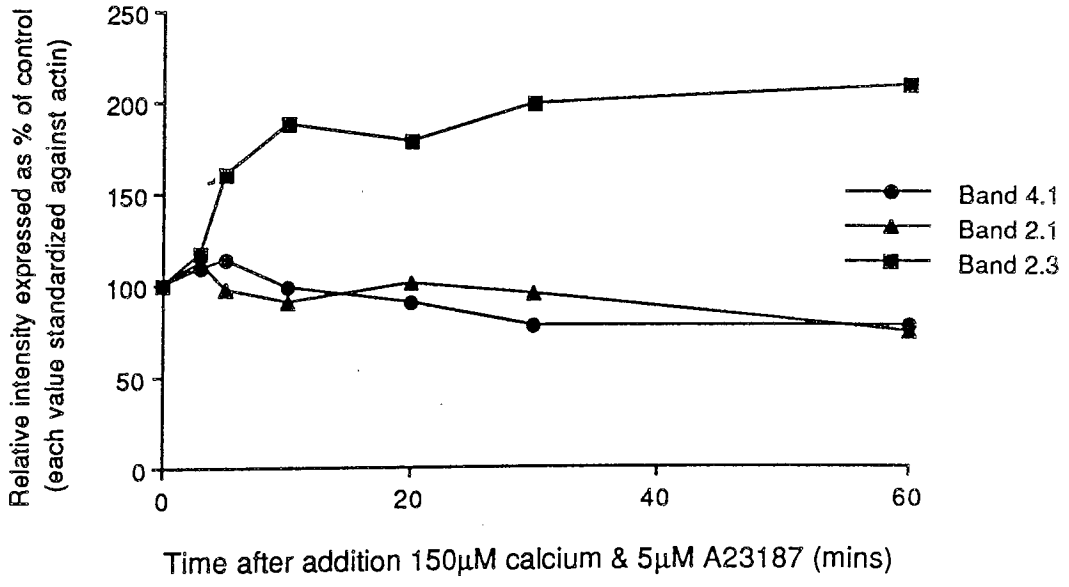
250
200
150
100
50
0
Relative intensity expressed as % of control
(each value standardized against actin)
0
20
40
60
Time after addition 150μM calcium & 5μM A23187 (mins)
Band 4.1
Band 2.1
Band 2.3

minutes there is an increase in the intensity of a stained band at approximately 179,000 molecular weight. This was confirmed by performing laser densitometry on the Coomassie blue stained gel (figure 18D). The size of this protein coincides with that reported for band 2.3 (see figure 2), which is thought to be a proteolytic cleavage product of protein 2.1 (Anderson et al., 1977, Siegel et al., 1980). Indeed previous studies have assumed increases in the intensity of band 2.3 on SDS-PAGE to be indicative of the degradation of band 2.1. (Tang, 1988). However, this is not supported by the results obtained here where both proteins are visualised, since the time-course of increase of 2.3 does not appear to be reflected by a simultaneous decrease in the intensity of band 2.1. These results differ from those reported by Allan and Thomas (1981), who found that the increase in intensity of band 2.3 associated with calcium loading was matched by a decrease in the staining of protein 2.1. However, in their experiments no protease inhibitors were included in the lysis and washing buffers during the preparation of ghost membranes for SDS-PAGE analysis. It is possible that the results these workers obtained for protein 2.1 integrity were complicated by the post-sampling loss of this protein, since it is known to be very sensitive to proteolysis (Agre and Bennett, 1988, Boivin et al., 1990). The increase in intensity of the 179,000 mw polypeptide described here may result from the accumulation of the cleavage products of

other high molecular weight proteins co-migrating with protein 2.3, since both the alpha and beta chains of spectrin have been shown to be susceptible to proteolysis induced by calcium (Allen and Cadman, 1980). However, this possibility could only be accurately examined by immunoblotting with specific antibodies.

A small decrease in the intensity of both protein 2.1 and band 4.1 can be observed after 60 minutes of calcium loading, suggesting that both proteins are subject to proteolytic degradation following prolonged exposure to this level of calcium. Six separate analyses were performed and this pattern of protein loss was found to be induced consistently at this level of calcium loading. Clearly the time-course of protein cleavage did not coincide with that of echinocytosis which was complete within 30 minutes, as estimated by the loss of the discocyte morphology.

Figure 19C shows the progression of the morphological transition of erythrocytes prepared in buffer A and then loaded with 1mM calcium in the presence of A23187. It can be seen that under these conditions echinocytosis is rapid and complete within 5 minutes, and the results obtained previously in section 3.1.2 indicated that over 80% of the cells were either stage 3 or sphereo-echinocytes by this time.

The SDS-PAGE analysis of the cytoskeletal proteins of these cells is shown in figures 19 A and B. Again it can be

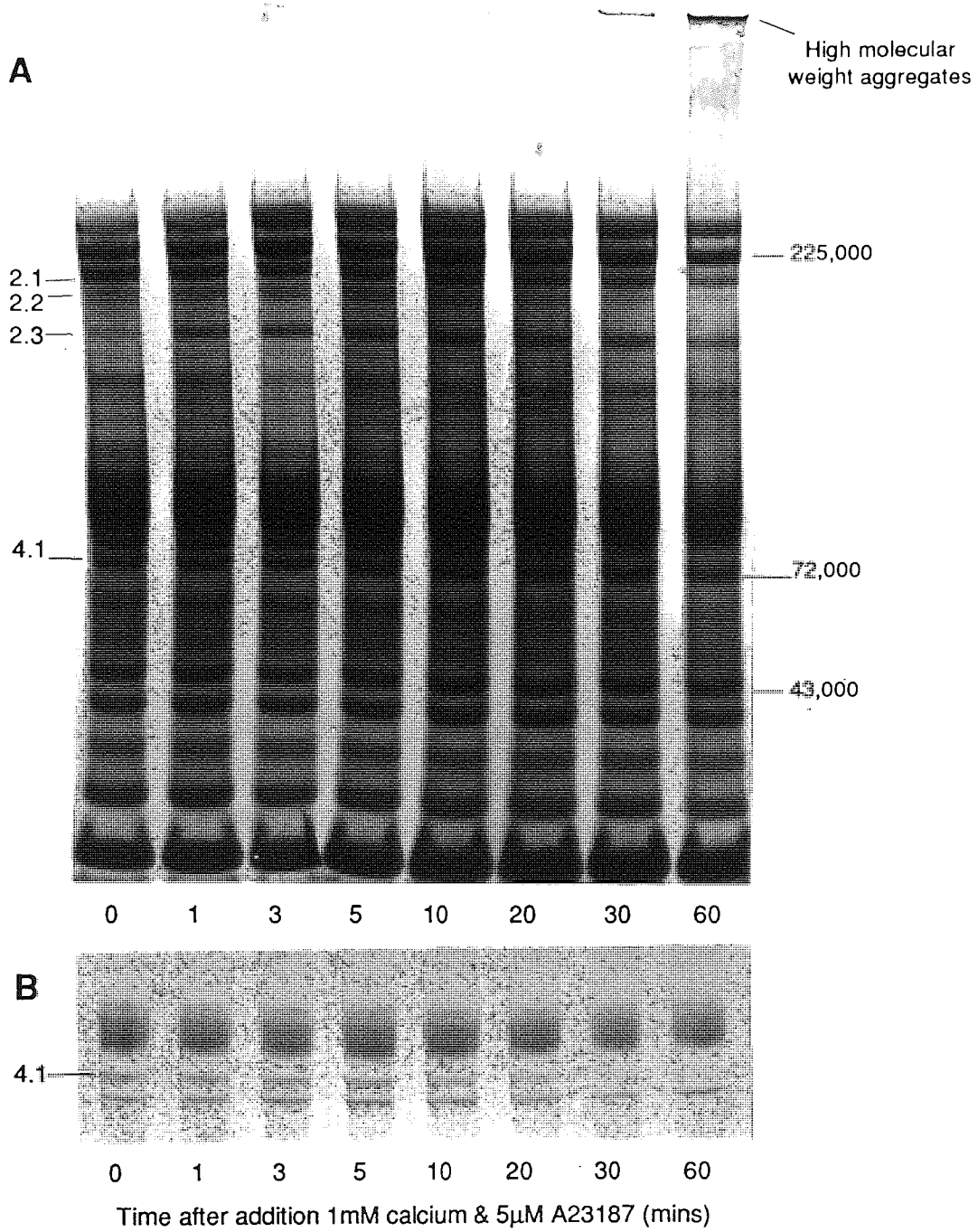


**FIGURE 19** Time-dependent proteolytic modification of cytoskeletal proteins in erythrocytes loaded with 1mM calcium in the presence of glycolytic substrates (buffer A)
Intact human erythrocytes held in buffer A were treated with 1mM calcium and 5µM A23187 at 37°C. At the time intervals specified samples were removed for ghost preparation and the quantitation of cell morphology. The representative results from 6 analyses are shown.
A Coomassie blue stained pattern of ghost proteins separated by 3.5-17% gradient SDS-PAGE
B Proteins from (A) separated by 7% discontinuous SDS-PAGE
C Time-course of echinocytosis in the cell samples of A & B

19C

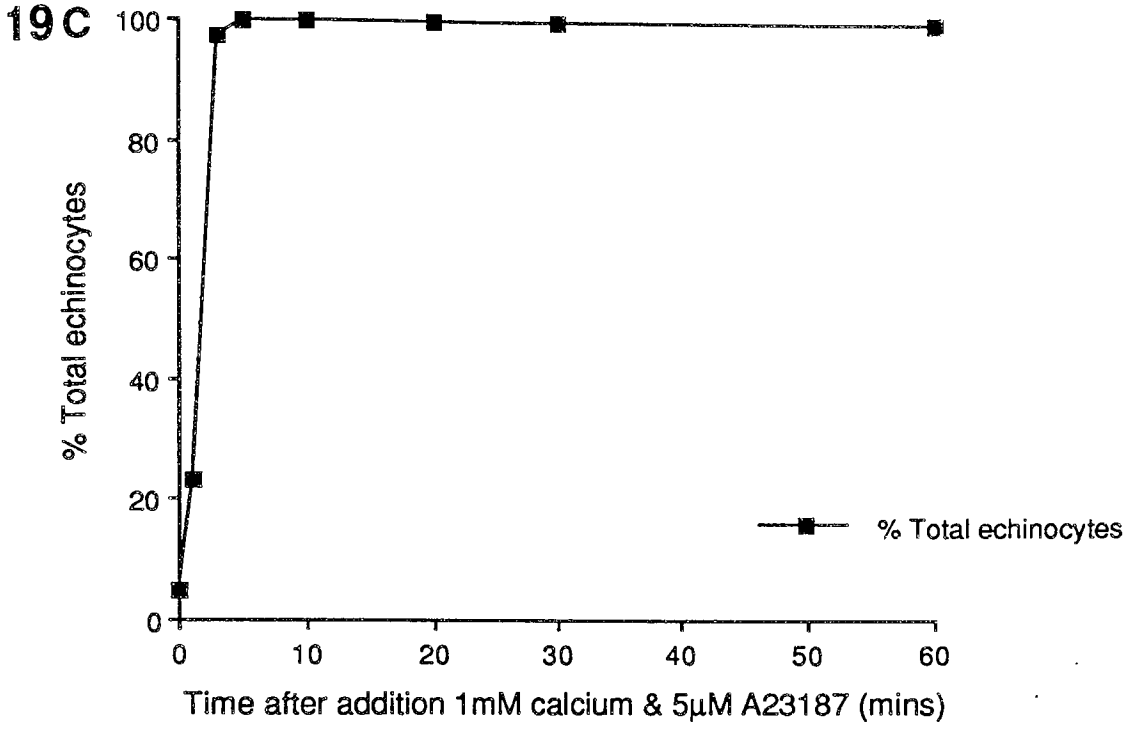
100
80
60
40
20
0
% Total echinocytes
0
10
20
30
40
50
60
Time after addition 1mM calcium & 5µM A23187 (mins)
% Total echinocytes

seen that calcium loading is associated with changes in the intensity of band 2.3. At this higher level of calcium loading the intensity of this band increases after only 1 minute, whereas with 150μM the intensity of this band did not increase until after 5 minutes of exposure to calcium. Densitometric analysis of the Coomassie blue stained gel confirmed this (figure 21C) and indicated an approximately 3 fold increase in the intensity of this protein after 10 minutes of calcium loading. However, following this initial rise the intensity of band 2.3 then decreases, suggesting that the proteolytic products forming this band are further degraded with increasing exposure to 1mM calcium. It is also possible that the some of the proteolytic products contributing to band 2.3 are utilized in the formation of crosslinked aggregates which is associated with high concentrations of calcium as discussed below (Gaffney, 1985). These results provide further evidence that the examination of band 2.3 is not a satisfactory indicator of the status of protein 2.1.

In addition to changes in band 2.3, permeabilization of erythrocytes to 1mM calcium results in the breakdown of protein 2.1, band 4.1, and a protein of mw approximately 188,000 (figures 19 and 21). The size of this latter protein coincides with that reported for protein 2.2 (Hall and Bennett, 1987, see also figure 2) which is an ankyrin related peptide of slightly smaller molecular weight present in human erythrocytes (Hall and Bennett, 1987).

This protein is known to be susceptible to calcium-induced proteolysis (Siegel et al., 1980) and it is possible that the cleavage products of this protein contribute to the increase observed in protein 2.3 noted above.

In contrast to cells loaded with a low concentration of calcium (150μM), a more rapid and greater degree of proteolysis of both protein 2.1 and band 4.1 is observed with 1mM calcium (compare figures 18A, B and D with figures 19 and 21). If the results for the former protein are examined it can be seen that although there is an approximately 40% decrease of this protein during 60 minutes of loading with 1mM calcium, this loss largely occurs after 20 minutes of calcium exposure (figure 21A). In comparison the shape change is very rapid and is complete within 5 minutes, by which time no proteolysis is evident. Several attempts were made to confirm the time-course of the breakdown of the ankyrins, including 2.1, under different calcium-loading conditions by the Western blotting of the protein using anti-ankyrin antibodies. However, after preliminary investigations to optimize the antibody dilutions needed for this technique, the antisera used were found to be non-specific for ankyrin and therefore the results were unreliable.

Protein 4.1 exists as doublet with an approximate Mw of 80,000. Analysis on a 7% discontinuous SDS-PAGE system increases the resolution of the a and b polypeptides of this protein (mw 80,000 and 78,000 respectively), and it

can be seen that the intensity of both components begins to decrease simultaneously after approximately 5-10 minutes of loading with 1mM calcium (figure 19B). Densitometry estimates the total intensity of both polypeptides and it can be seen that there is an approximately 80% loss of these proteins by 60 minutes of calcium treatment (figure 21). Again no correlation is observed between the rate of proteolytic cleavage and the time-course of echinocytosis.

In addition to these proteolytic events, the calcium loading of intact cells with 1mM calcium for time periods of 30 minutes or longer resulted in the appearance of a strongly staining band at the top of the gels. Previous workers have also noted similar staining (Anderson et al., 1977), and it has been attributed to the cross-linking of various proteins by calcium sensitive transglutaminase enzymes (Anderson et al., 1977, Gaffney, 1985). This produces high molecular weight aggregates too large to enter the gels during electrophoresis.

The findings obtained in these experiments are consistent with previous reports that proteolytic activity directed against cytoskeletal proteins is stimulated in intact erythrocytes by an increase in cytosolic calcium, presumably through the activation of calcium-activated cellular proteases such as calpain. Interestingly, the proteins most sensitive to proteolytic degradation are the key membrane and cytoskeleton linkage proteins; 2.1 and 4.1. However, when the time-course of the changes in these

proteins is compared to the rate of progression of the morphological transitions it is evident that no clear correlation exists; at both calcium concentrations examined the appearance of the echinocyte morphology is complete before the detectable proteolytic loss of any cytoskeletal protein. These results strongly suggest that the onset of the shape transitions is not directly related to cytoskeletal cleavage mediated by calcium-activated proteases. Similarly, the delay in onset of the transglutamination processes indicates that a role for these enzymes in erythrocyte shape transitions is unlikely.

However, it should be noted that these results do not rule out the possibility that proteolytic events too insignificant to be detected by the SDS-PAGE and densitometric analyses presented here could contribute to the control of erythrocyte shape.

### 3.2.3. Proteolytic events associated with time-dependent echinocytosis in erythrocytes loaded with 1mM calcium in the absence of metabolic substrates (buffer B).

The influence of the metabolic status of the cell on the pattern of cytoskeletal protein cleavage was examined by comparing the above results with those obtained from similar experiments performed on cells prepared and permeabilized to 1mM calcium in the absence of metabolic substrates (Tris buffer B). The results of these latter

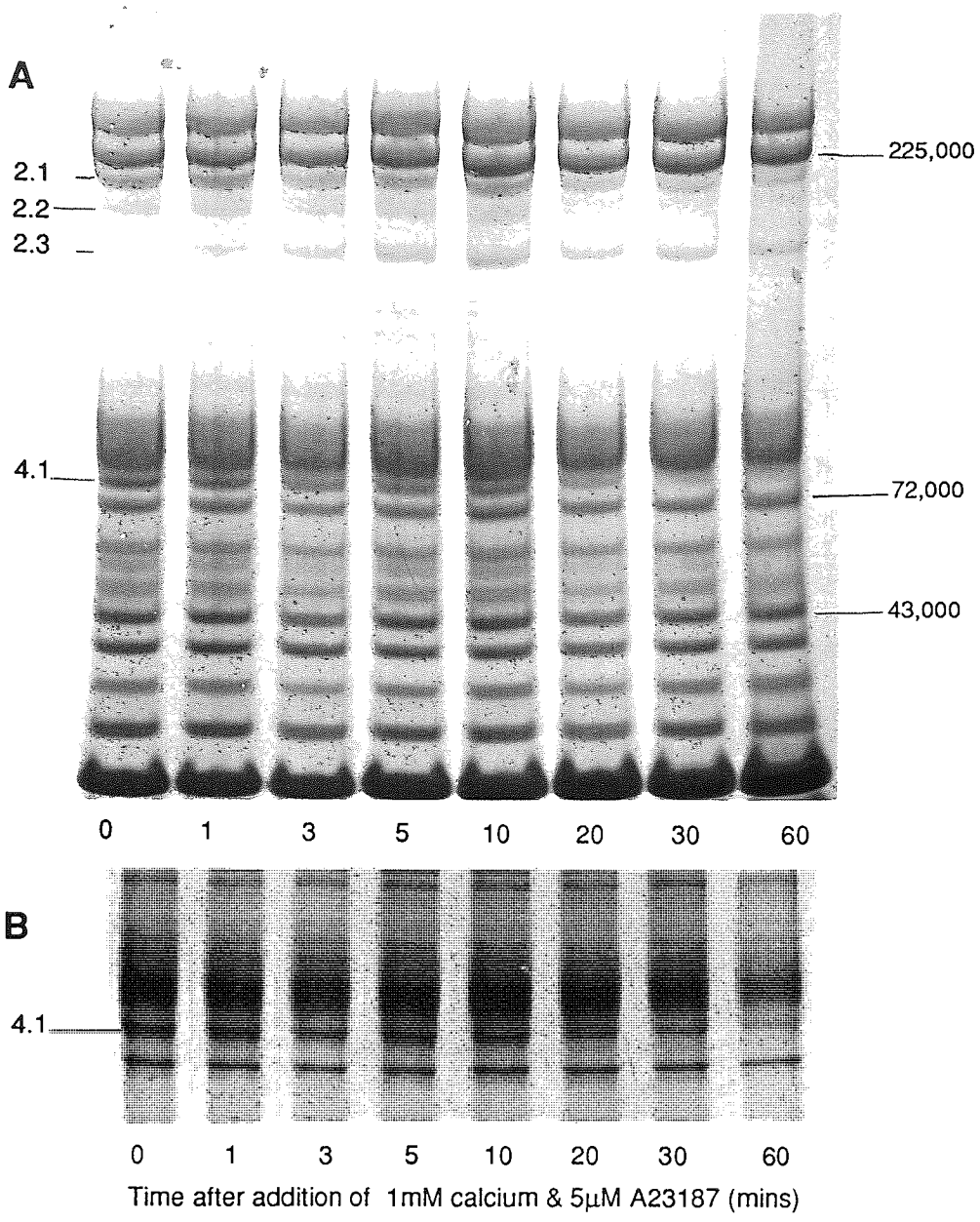


**FIGURE 20** Time-dependent proteolytic modification of cytoskeletal proteins in erythrocytes loaded with 1mM calcium in the absence of glycolytic substrates (buffer B)
Intact human erythrocytes held in buffer B were treated with 1mM calcium and 5μM A23187 at 37°C. At the time intervals specified samples were removed for ghost preparation and the quantitation of cell morphology. The representative results from 6 analyses are shown.
**A** Coomassie blue stained pattern of ghost proteins separated by 3.5-17% gradient SDS-PAGE
**B** Proteins from (A) separated by 7% discontinuous SDS-PAGE

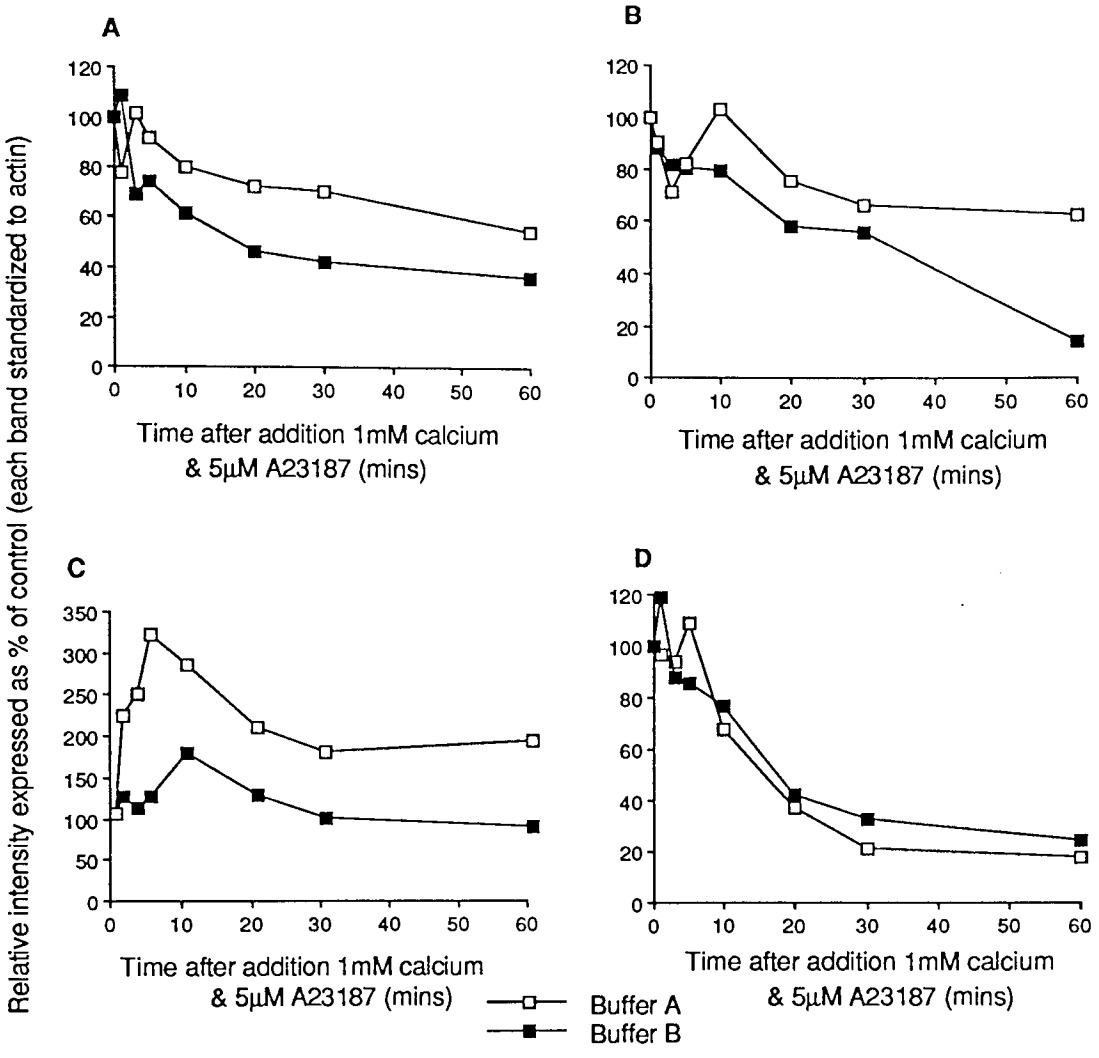


**FIGURE 21** Densitometric analysis of protein cleavage in erythrocytes loaded with 1mM calcium in either the presence (buffer A) or absence (buffer B) of glycolytic substrates. Comparison of the rate and extent of proteolysis of proteins 2.1 (**A**), 2.2 (**B**), 2.3 (**C**) and 4.1 (**D**) from SDS-PAGE analyses such as those shown in figures 19 and 20

experiments are presented in figure 20. It can be seen that the general pattern of proteolytic cleavage induced by 1mM calcium is independent of the buffer system used; treatment of cells in Tris buffer also results in a decrease in the intensity of both protein 2.1 and 4.1, and an increase in the intensity of protein 2.3. In addition, the results obtained from cells treated in Tris buffer also show no correlation between the onset of shape change, which is complete within 3 minutes, and the detectable loss of any cytoskeletal protein. However, there do appear to be differences in the proteolytic sensitivity of the cytoskeleton according to the metabolic state of the cells (figure 21). The accumulation of protein 2.3 as estimated by densitometry, was more modest in cells treated in Tris buffer (<200%), compared to the large increase observed in cells prepared in the presence of metabolic substrates (>300%). Also, the loss of proteins 2.1 and 2.2 does appear to be more extreme in cells loaded with 1mM calcium in Tris buffer, compared to those treated in the presence of metabolic substrates. Each analysis was performed at least 6 separate times, and the differences in proteolytic susceptibility of these proteins found to be consistent. Interestingly, the rate of cleavage of protein 4.1, as estimated by densitometry, is similar in both media. However, this technique is unable to distinguish the 4.1a and 4.1b polypeptides; if the SDS-PAGE gels are compared directly (compare figures 19B and 20B) it can be observed

that in contrast to the results obtained above for cells treated in buffer A, permeabilization to 1mM calcium in Tris buffer appears to result in the preferential loss of the lower molecular weight 4.1b component (mw 78,000).

These results indicate that the susceptibility of erythrocyte proteins to $Ca^{2+}$-activated proteolytic events is affected by the availability of metabolic substrates during treatment. It is possible that the conformation of cytoskeletal proteins is influenced in some way by the metabolic state of the cells so as to modify the interaction of proteases with enzyme susceptible sites. Such effects could be mediated through the influence of cell ATP levels on the phosphorylation status of cytoskeletal proteins; either through changes in individual proteins, or possibly through alterations in the relative strength of protein-protein interactions such as ankyrin:band 3 or 4.1:spectrin:actin, both of which are known to be influenced by protein phosphorylation levels (Eder et al., 1986, Ling et al., 1987, Soong et al., 1987). Alternatively, alterations in the phosphorylation status of membrane lipids may modify protein associations, leading to changes in the conformational state of proteins. For instance, the association between protein 4.1 and the integral protein glycophorin A is modulated by the lipid PtdIns(4,5)$P_2$ (Anderson and Marchesi, 1985), the membrane pools of which are in turn regulated by the ATP-dependent futile cycle (Berridge, 1984).

### 3.2.4. Proteolytic events associated with the trypsin digestion of purified cytoskeletal proteins.

The results discussed above conflict with previous reports which have suggested that alterations in the levels of intact ankyrin in the cytoskeleton are pivotal to the control of erythrocyte shape (Jinbu et al., 1982, 1984a). However, the studies carried out by these workers involved the digestion of erythrocyte ghost proteins with trypsin. To examine the relevance of these studies to cellular processes, the pattern of cytoskeletal cleavage induced in erythrocyte ghosts by trypsin digestion was studied, for comparison with the cleavage patterns obtained above in intact cells. These experiments were carried out using a method based on that described by Jinbu (1982). Erythrocyte ghost proteins were digested with trypsin for time intervals between 0 and 60 seconds before the termination of digestion by the addition of trypsin inhibitor, the proteins were then examined by SDS-PAGE analysis. The results are shown in figure 22. As in the previous experiments on intact cells, the proteins most sensitive to proteolysis include 2.1 and 4.1, although the analysis of the loss of the former protein is complicated by the appearance of two polypeptides in this region of the gel. Cleavage of protein 2.1 during trypsin digestion could be more accurately studied by immunoblotting with a specific antibody. However, other proteolytic events also

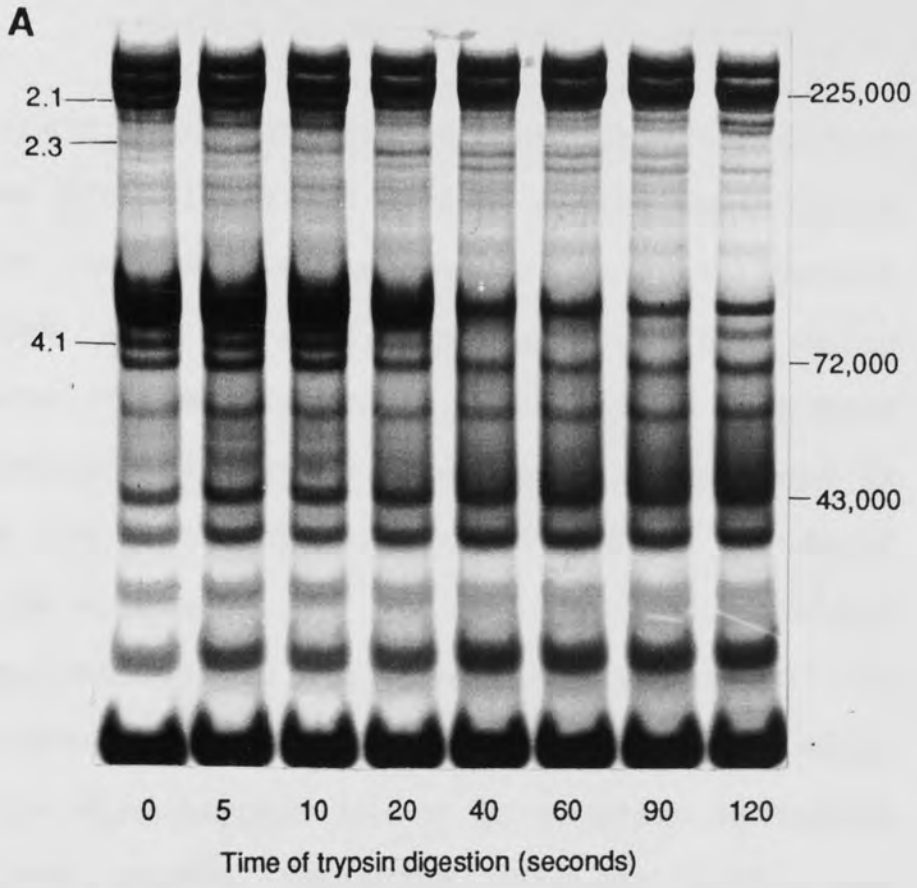


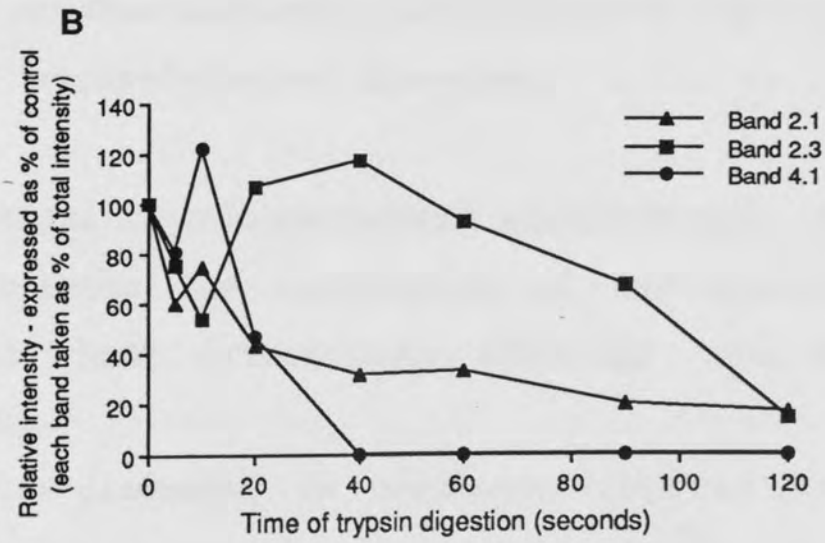


**FIGURE 22** The proteolysis of erythrocyte ghost proteins during digestion with trypsin
Purified erythrocyte ghosts prepared from previously untreated cells were digested with trypsin for the time intervals specified.
**A** Coomassie blue stained pattern of ghost proteins separated by 3.5-17% gradient SDS-PAGE
**B** Densitometric analysis of protein cleavage during trypsin digestion

result from trypsin treatment which are not observed during calcium induced proteolysis in intact cells; there is a decrease in the intensity of a protein at approximately 89,000 mw which is the size reported for the anion transporter, band 3 (see figure 2), suggesting that this protein is sensitive to trypsin digestion. Also there is an increase in the intensity of stained protein bands of molecular weight approximately 200,000, 191,000, 162,000 and 43,000, presumably due to the accumulation of the degradation products of higher molecular weight proteins. Clearly digestion with trypsin is not an accurate indicator of the proteolytic events occurring in intact cells, and the results of studies involving such treatment may not be fully relevant to physiological processes

3.2.5. The reversal of calcium-induced echinocytosis; the relationship between the restoration of the discocyte morphology and both cytoskeletal integrity and cell metabolic status

The results discussed in sections 4.2.2 and 4.2.3 appear to rule out a role for proteolytic events in the progression of echinocytosis. It was noted that although the prolonged exposure of erythrocytes to calcium was associated with the loss of both protein 2.1 and 4.1, neither event reflected the rate of shape change. In this section the importance of cytoskeletal cleavage to the control of cell shape was examined further, by

investigating the influence of cytoskeletal integrity on the ability of erythrocytes to undergo shape reversal from the echinocyte to the discocyte form. Previous studies have indicated that the reversal of the echinocyte morphology can be facilitated by the removal of the agent used to induce echinocytosis and the incubation of erythrocytes in the presence of glucose (Feo and Mohandas, 1977, Palek and Liu, 1978, Anderson and Lovrien, 1981). Since a proteolytic event would be expected to be an irreversible one with respect to cell shape, reversal from the echinocyte form would be expected to be impossible in cells in which cytoskeletal damage had occurred to proteins instrumental to the control of cell shape.

Shape reversal was attempted using a method based on that of Anderson and Lovrien (1981). Following the addition of EGTA and BSA to chelate the calcium and A23187 respectively, the cells were washed and allowed to recover at 37$^{o}$C in fresh buffer containing metabolic substrates (buffer A). Samples were removed for the quantitation of morphologies at appropriate time intervals for a maximum of 360 minutes in order to assess the progression of shape reversal.

In the experiments described here the possible restoration of the discocyte morphology from two different echinocyte populations was examined. Cells were loaded with either 1mM calcium for 15 minutes or 150μM calcium for 10 minutes in the presence of 5uM A23187; treatments which

resulted in populations which were predominantly sphereo-echinocytes (former treatment), or stage 1 echinocytes (latter treatment). It has been previously reported that shape reversal becomes impossible in cells treated with greater than 500μM calcium for 15 minutes (Anderson and Lovrien, 1981). To examine the influence of cell metabolic status on the control of erythrocyte morphological transitions, shape reversal from the echinocyte morphology was compared in cells loaded with calcium in both the presence and absence of glycolytic substrates. An additional, control experiment was also carried out in which reversal was attempted in Tris buffer to establish the importance of the availability of glycolytic substrates for shape recovery.

Figure 23 shows the morphological transitions of cells permeabilized to calcium in the absence of metabolic substrates (Tris buffer B) prior to attempted shape reversal in replete media (buffer A). Almost 100% transformation to the echinocyte form is induced by both calcium treatments (figure 23A). Approximately 60% of stage 1 echinocytes are able to revert to the normal discocyte morphology when resuspended in buffer A. In contrast sphereo-echinocytes (induced by 15 minutes exposure to 1mM calcium and 5μM A23187) show no restoration of the discocyte morphology even after 360 minutes incubation in the presence of metabolic substrates. However, these cells do undergo partial reversal from the

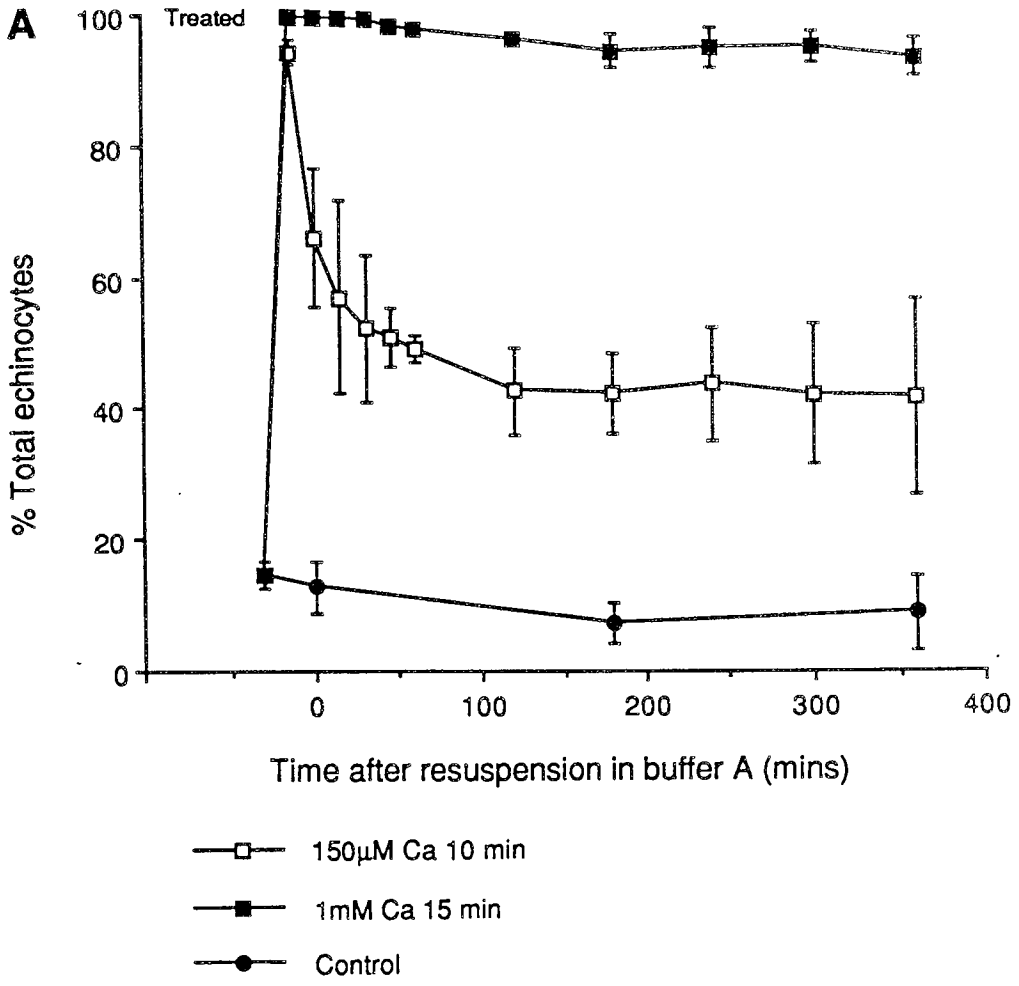


**FIGURE 23** The quantitation of cell morphologies during shape reversal from echinocytosis induced in the absence of glycolytic substrates (buffer B); shape recovery attempted in the presence of metabolic substrates (buffer A)
Human erythrocytes held in buffer B were loaded with either 150µM calcium for 10 minutes or 1mM calcium for 15 minutes. After removal of the calcium and A23187, cells were resuspended in buffer A and shape recovery examined by the quantitation of morphology at the time intervals specified.
**A** Total echinocyte levels. Results expressed as mean ±SD (n=3)
**B** Analysis of the changes in the levels of different stage echinocytes in cells initially loaded with 150µM calcium. Results are expressed as mean of n=3.
**C** Analysis of the changes in the levels of different stage echinocytes in cells initially loaded with 1mM calcium. Results are expressed as mean of n=3.

23B

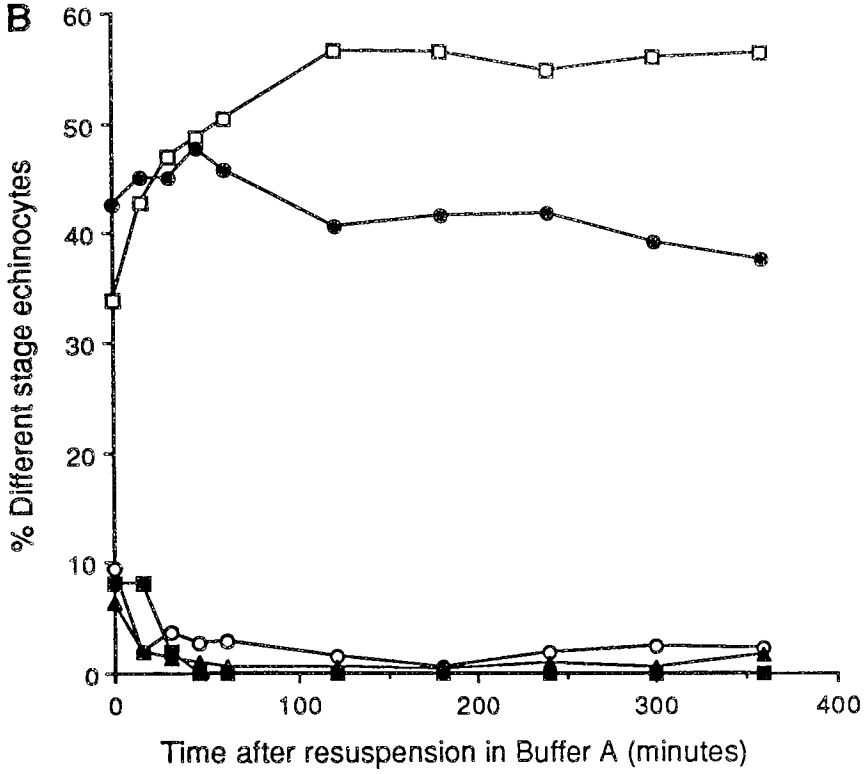
% Different stage echinocytes
60
50
40
30
20
10
0
0
100
200
300
400
Time after resuspension in Buffer A (minutes)

23C

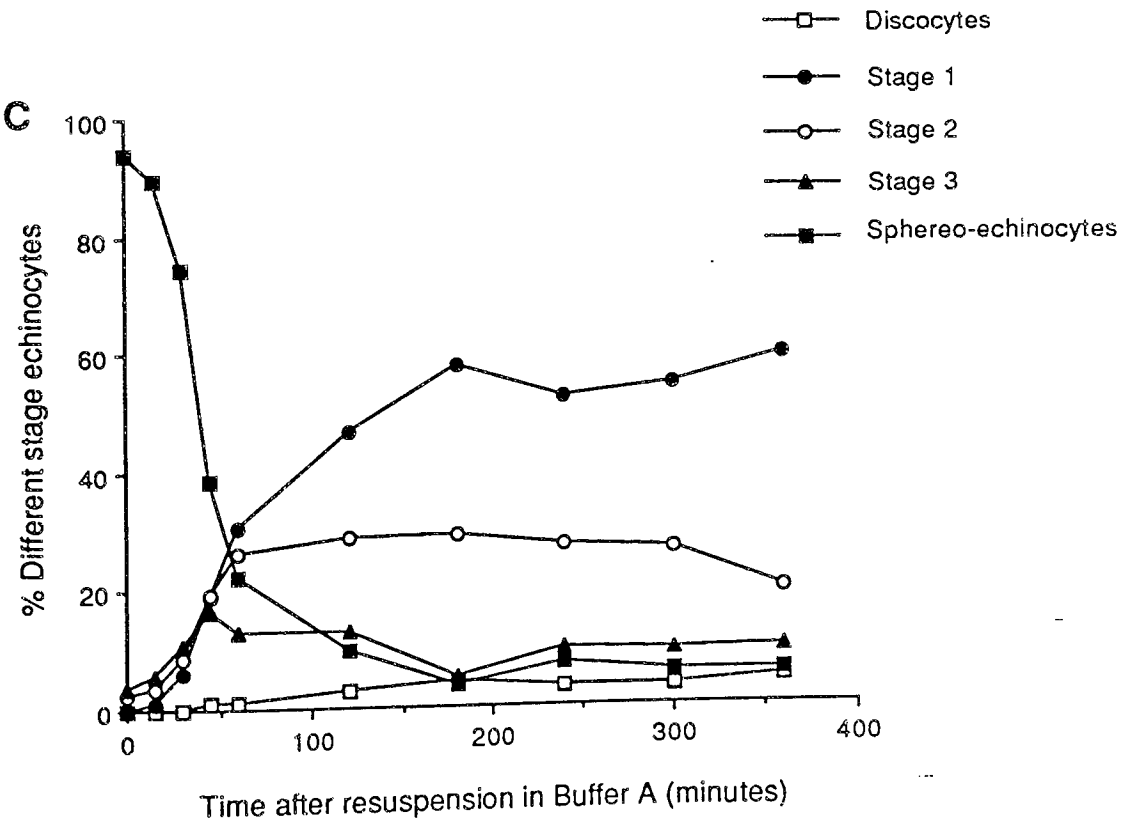
Discocytes
Stage 1
Stage 2
Stage 3
Sphereo-echinocytes
% Different stage echinocytes
100
80
60
40
20
0
0
100
200
300
400
Time after resuspension in Buffer A (minutes)

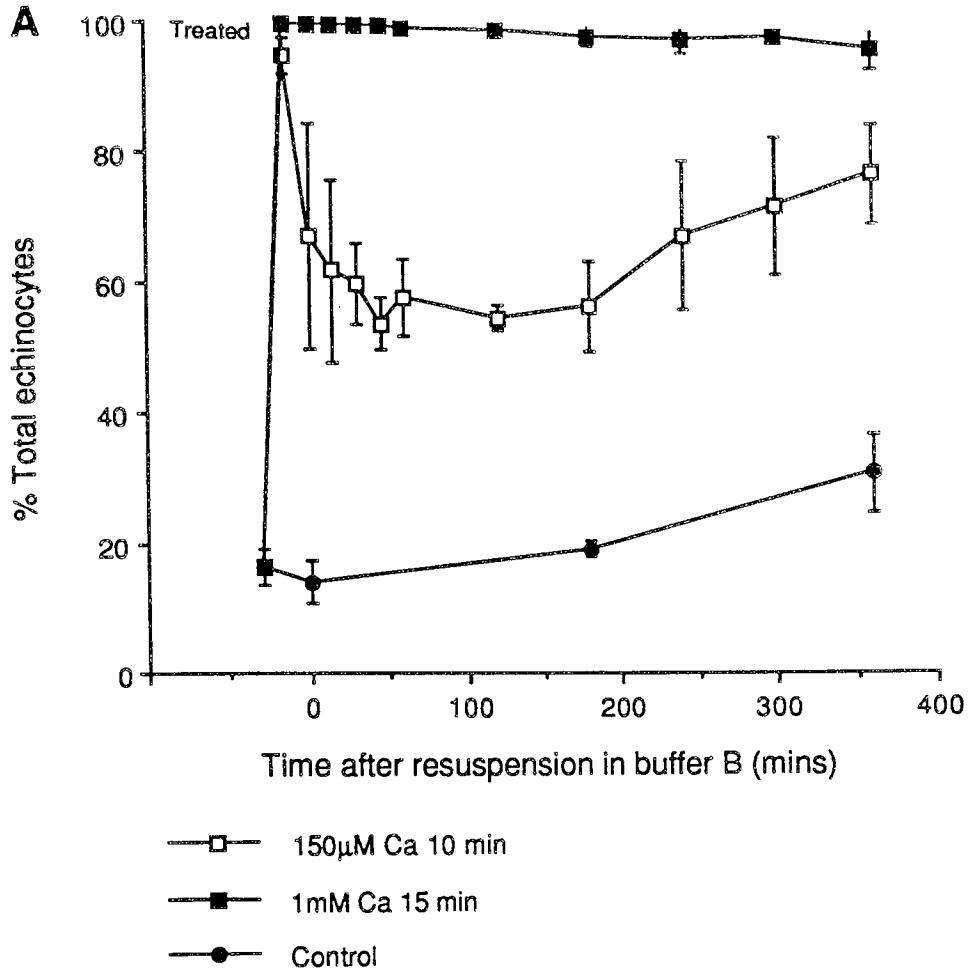


**FIGURE 24** The quantitation of cell morphologies during shape reversal from echinocytosis induced in the absence of glycolytic substrates (buffer B); shape recovery also attempted in buffer B

Human erythrocytes held in buffer B were loaded with either 150µM calcium for 10 minutes or 1mM calcium for 15 minutes. After removal of the calcium and A23187, cells were resuspended in buffer B and shape recovery examined by the quantitation of morphology at the time intervals specified.

**A** Total echinocyte levels. Results expressed as mean ± SD (n=3).

**B** Analysis of the changes in the levels of different stage echinocytes in cells initially loaded with 150µM calcium. Results are expressed as mean of n=3.

**C** Analysis of the changes in the levels of different stage echinocytes in cells initially loaded with 1mM calcium. Results are expressed as mean of n=3.

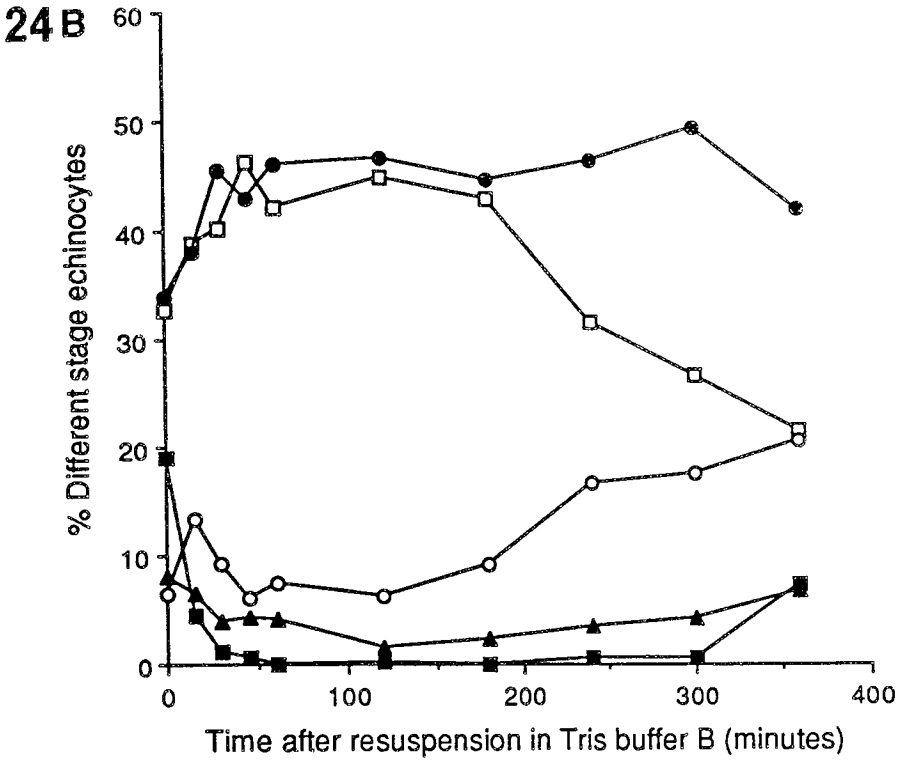
24B
% Different stage echinocytes
Time after resuspension in Tris buffer B (minutes)
0
10
20
30
40
50
60
0
100
200
300
400

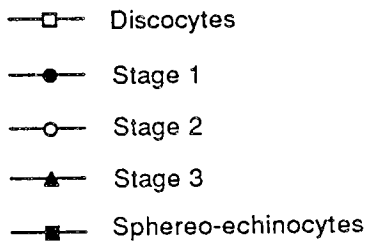
Discocytes
Stage 1
Stage 2
Stage 3
Sphereo-echinocytes

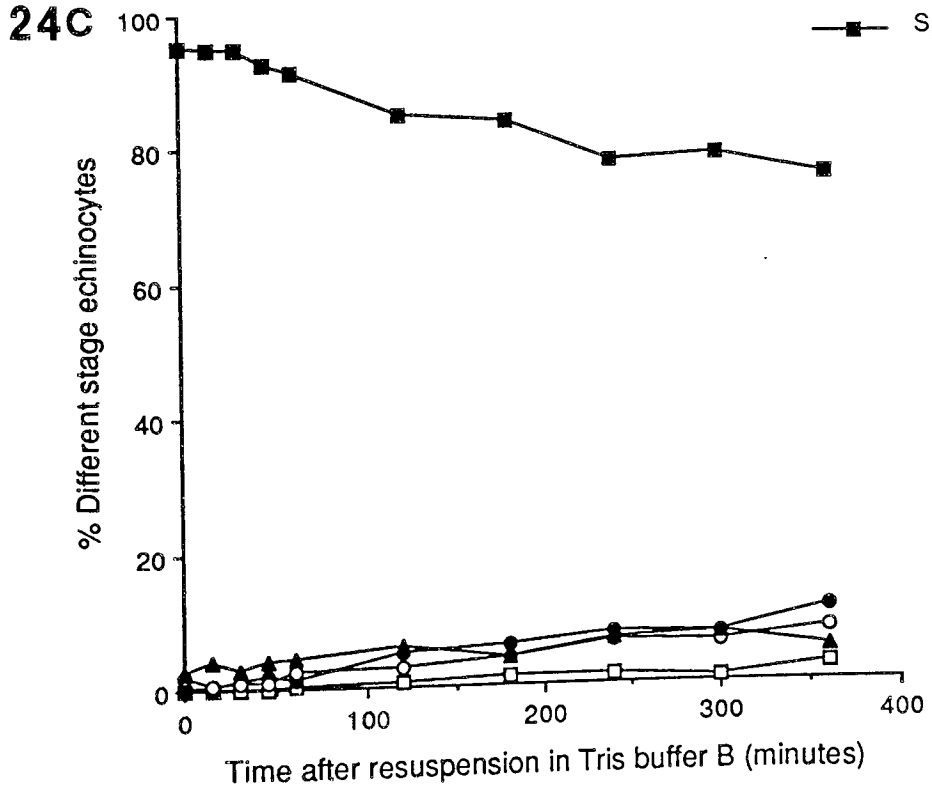
24C
% Different stage echinocytes
Time after resuspension in Tris buffer B (minutes)
0
20
40
60
80
100
0
100
200
300
400

sphereo-echinocyte form to less extreme forms of echinocytes; after 360 minutes incubation only 5%sphereo-echinocytes are observed compared to nearly 100% immediately after calcium treatment (figure 23C).

In comparison when recovery was attempted in Tris buffer B rather than the metabolically enriched buffer A, shape reversal was compromised (figure 24). Cells loaded with 150μM for 15 minutes initially undergo a rapid partial shape reversal to the discocyte form with approximately 45% of the cells reverting to discs within 40 minutes, but after this time the level of discocytes falls again. Cells loaded with 1mM calcium for 15 minutes do not undergo any significant reversal from the sphereo-echinocyte morphology to either the discoid form or to less extreme forms of echinocyte. It appears that sustained recovery to the discocyte or less extreme echinocyte forms is dependent on the availability of metabolic substrates; presumably as a result of a process involving ATP.

In contrast to the above results, approximately 50-60% of cells exposed to both high and low calcium loading regimes in the presence of metabolic substrates (buffer A) were able to reestablish the normal discocyte morphology after the removal of the ionophore and excess calcium (figure 25). It appears that even cells transformed to the sphereo-echinocyte morphology (treated with 1mM calcium and 5μM A23187 for 15 minutes) are capable of regaining the discocyte form. Interestingly, when these results are

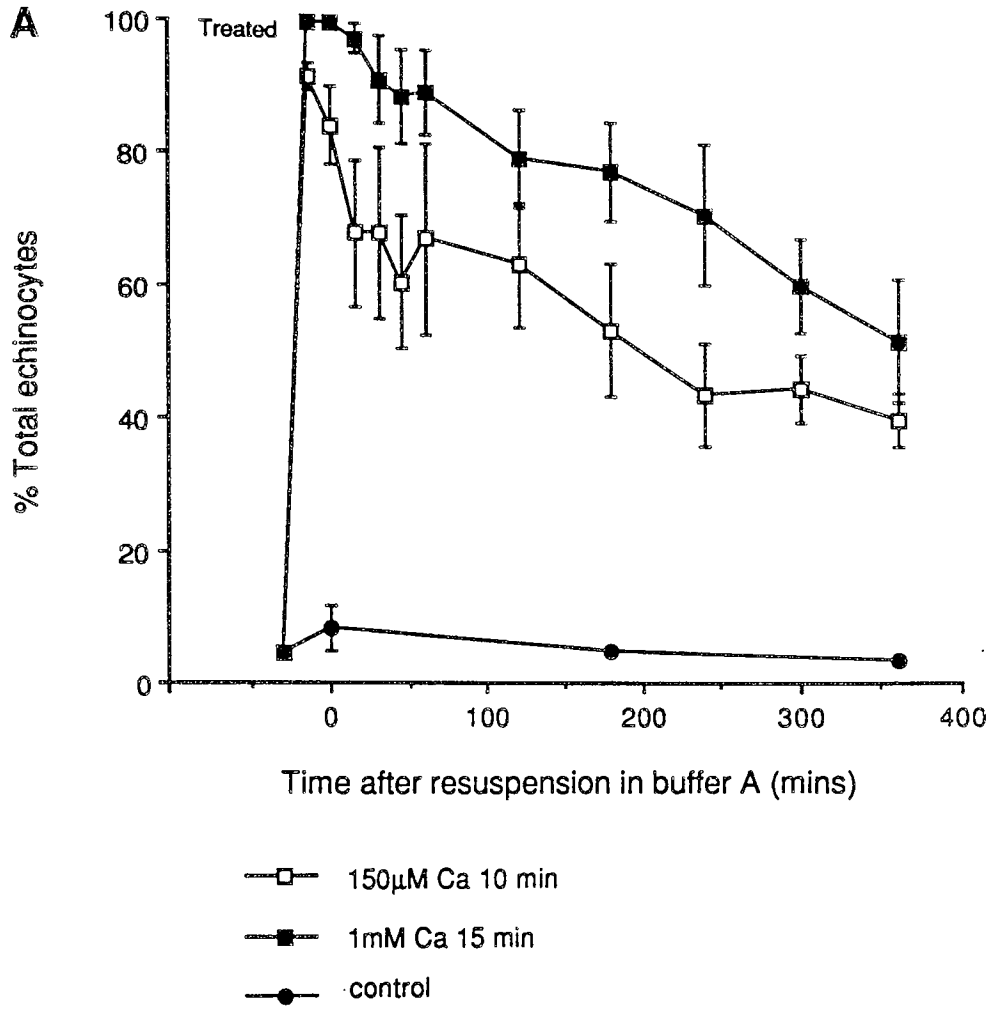


**FIGURE 25** The quantitation of cell morphologies during shape reversal from echinocytosis induced in the presence of glycolytic substrates (buffer A); shape recovery also attempted in buffer A

Human erythrocytes held in buffer A were loaded with either 150µM calcium for 10 minutes or 1mM calcium for 15 minutes. After removal of the calcium and A23187, cells were resuspended in buffer A and shape recovery examined by the quantitation of morphology at the time intervals specified (n=3).

**A** Total echinocyte levels. Results expressed as mean ± SD.

**B** Analysis of the changes in the levels of different stage echinocytes in cells initially loaded with 150µM calcium. Results expressed as mean of n=3.

**C** Analysis of the changes in the levels of different stage echinocytes in cells initially loaded with 1mM calcium. Results expressed as mean of n=3.

25B

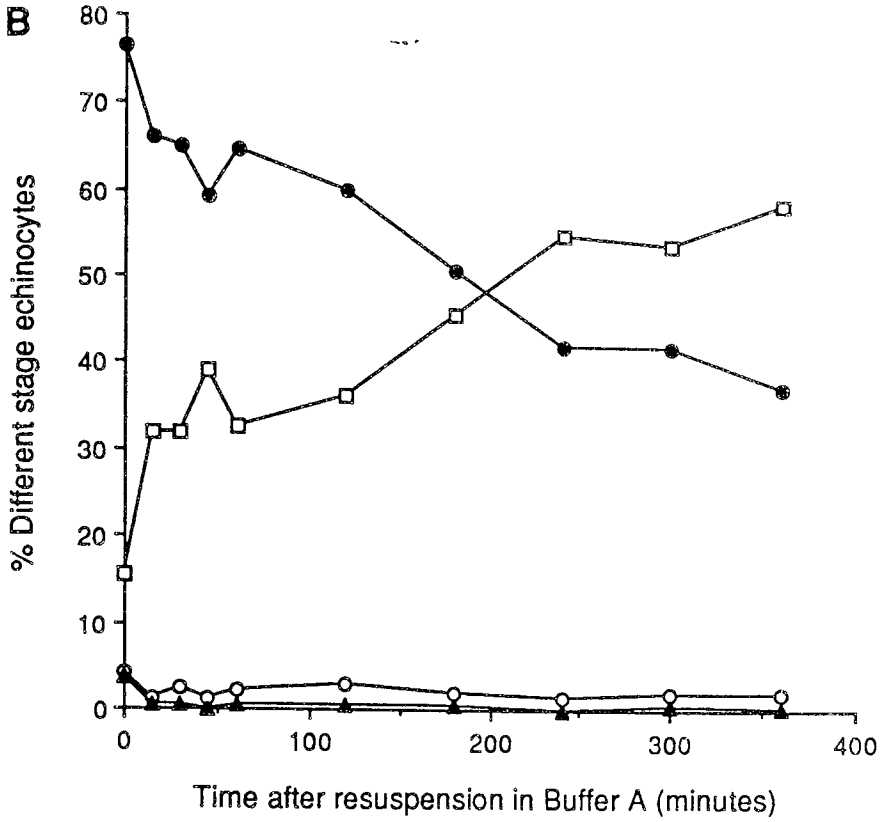
% Different stage echinocytes
0
10
20
30
40
50
60
70
80
0
100
200
300
400
Time after resuspension in Buffer A (minutes)

25C

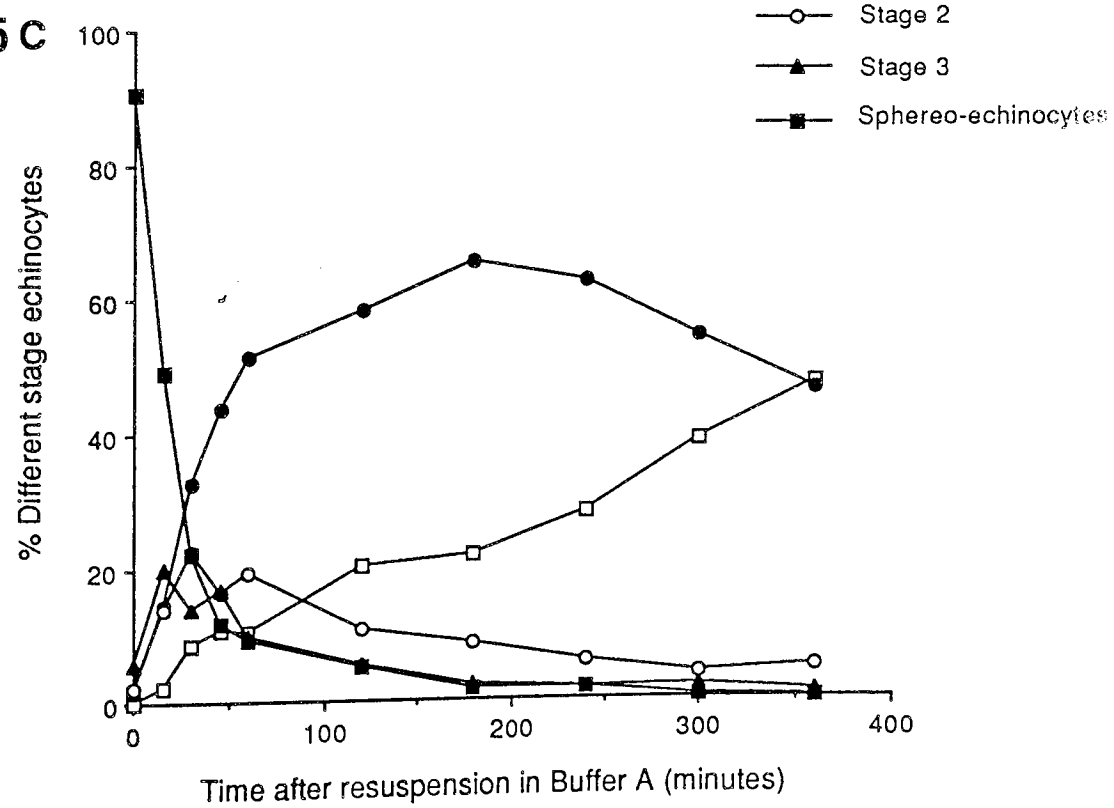
Discocytes
Stage 1
Stage 2
Stage 3
Sphereo-echinocytes
% Different stage echinocytes
0
20
40
60
80
100
0
100
200
300
400
Time after resuspension in Buffer A (minutes)

compared to those obtained above for cells loaded with calcium in Tris buffer it can be seen that the availability of glycolytic substrates during both the induction and recovery phase does appear to influence the degree of restoration of the discocyte form. The degree of shape reversal observed in cells loaded with 150μM calcium for 10 minutes in buffer A is similar to that described above for cells loaded with 150μM calcium in Tris buffer. This suggests that the degree of shape reversal in cells treated at this calcium concentration is not influenced by the metabolic status of the cells during treatment.

The influence of the metabolic status of the cells on the ability to achieve shape reversal from a high calcium load (1mM for 15 minutes) does not appear to be related the differences in the proteolytic sensitivity of the cytoskeleton according to the metabolic state of the cells. When the integrity of the cytoskeleton in the two cell populations following exposure to calcium is compared from the previous SDS-PAGE and densitometric analyses ( figures 19, 20, 21), it can be seen that the loading of cells with 1mM calcium for 15 minutes in both the presence and absence of metabolic substrates results in the significant loss of protein 2.1; approximately 30% under the former conditions and 45% under the latter. It can also be seen that both cell populations lose approximately 50% of intact protein 4.1 during calcium treatment. Clearly despite the loss of cytoskeletal proteins erythrocytes are still capable of

regaining the discocyte morphology, although this recovery is also dependent on the availability of metabolic energy.

It is more likely that since shape reversal from the sphereo-echinocyte form is ATP-dependent the media in which cells are treated alters their subsequent ability to synthesise ATP. Previous reports have indicated that erythrocytes permeabilized to calcium in the presence of A23187 eventually become irreversibly ATP-depleted as the adenine nucleotide becomes trapped as inosine monophosphate (IMP) (Almarez et al., 1988). High ATP consumption within the cells leads to the increased production of adenine monophosphate (AMP) which is irreversibly converted to IMP through the activation of AMP deaminase. As discussed in section 3.1 cells loaded with calcium in Tris buffer B have a greater rate of ATP depletion and therefore presumably AMP production, than those in buffer A. Therefore, it is possible that shape reversal may be impeded in the former cells because a larger fraction of the adenine pool is trapped as IMP and ATP levels cannot be restored during reversal.

In an attempt to further investigate the importance of intact proteins 2.1 and 4.1 to the ability of cells to recover the discocyte form, shape reversal was attempted in cells loaded with 1mM calcium for 60 minutes in the presence of metabolic substrates (figure 26). It can be seen that this treatment induces the loss of approximately 80% of intact protein 4.1 and 40% of the ankyrin, protein

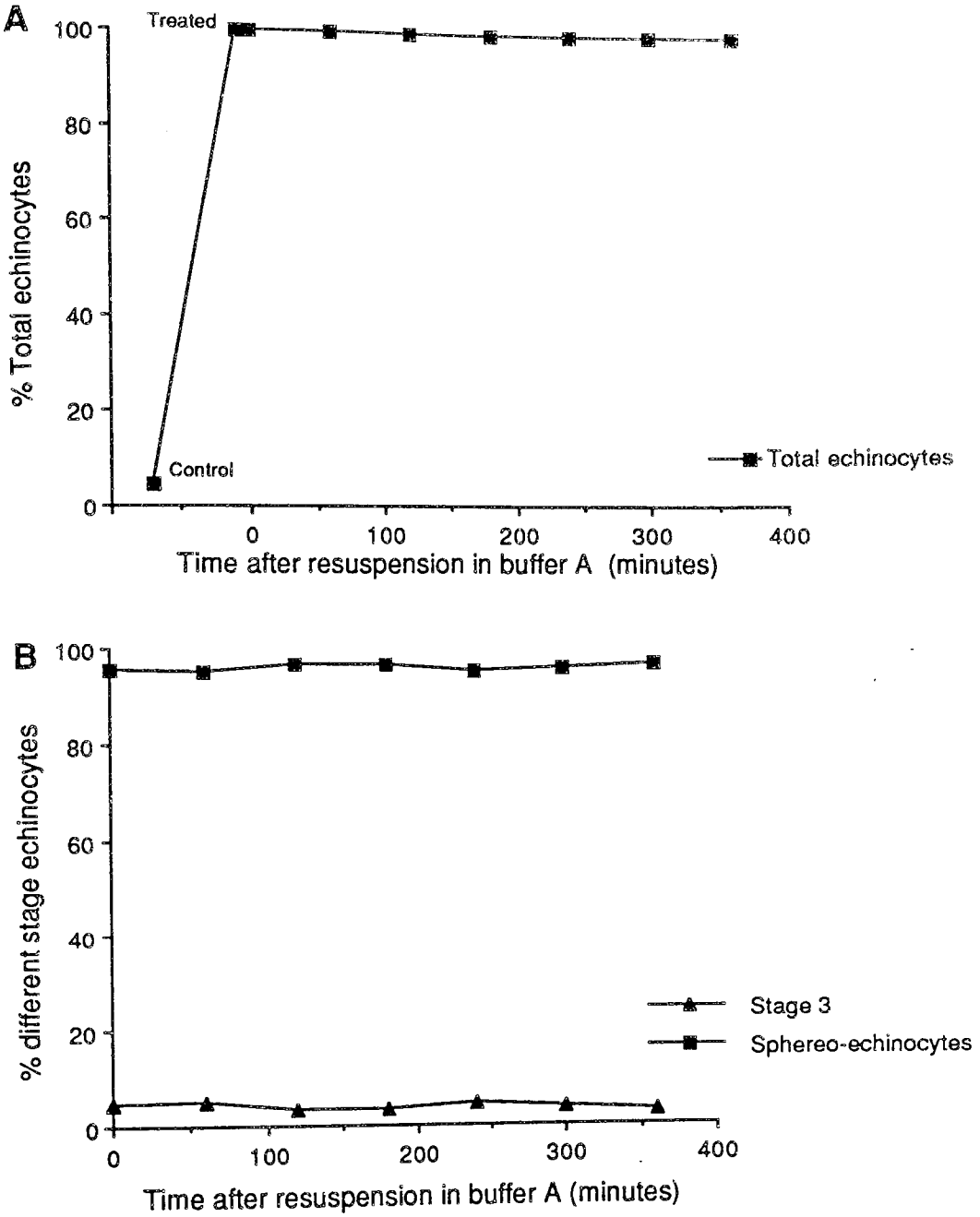


**FIGURE 26** The quantitation of cell morphologies during the attempted shape reversal of erythrocytes previously loaded with 1mM calcium for 60 minutes

Human erythrocytes held in buffer A were loaded with 1mM calcium for 60 minutes. After removal of the calcium and A23187, cells were resuspended in buffer A and shape recovery examined by the quantitation of morphology at the time intervals specified.

A Total echinocyte levels. Results expressed as mean ±SD (n=3).

B Analysis of changes in the levels of different stage echinocytes. Results expressed as mean of n=3

2.1. It is impossible to know whether these results represent an equal loss of the proteins throughout all the cells in a population or whether the decrease is unequally distributed. However, the observation that all of the cells are irreversibly committed to the sphereo-echinocyte form suggests that the former possibility is more likely. It is clear that even cells retaining significant amounts of intact protein 2.1 are incapable of regaining the discocyte morphology. These results conflict with previous conclusions, reached through the trypsin digestion of erythrocyte ghosts, that the presence of intact ankyrin in the erythrocyte cytoskeleton is the pivotal factor determining the ability of erythrocytes to undergo reversal of echinocytosis (Jinbu et al., 1982, 1984a). However, the relevance of these findings to intact cells is not clear since evidence described previously in section 4.2.4 indicates that trypsin digestion is not an accurate model for the proteolytic events initiated during calcium loading.

3.2.6. Reversal of calcium-induced echinocytosis in populations of erythrocytes enriched in either young or old cells.

The ability of erythrocytes within a population to recover the discoid form following a disturbance in calcium homeostasis appears to be heterogeneous (section 3.2.4). Ionophore distribution and calcium permeabilization however

are equal throughout the cells of a population (Simonsen et al., 1982, Garcia-Sancho and Lew, 1988), implying that the inherent differences in recovery capabilities is linked to the ability of different cells within a population to deal with a rise in cytosolic calcium. The biochemical basis of these differences may be related to the size of the adenine nucleotide pool irreversibly converted to IMP after high calcium loading (Almaraz et al., 1988). However, this mechanism is unlikely to play a role following loading with low calcium concentrations such as 150μM, since under these conditions it has been shown that the degree of shape reversal is independent of the metabolic status of the cell. Another possible biochemical mechanism for the heterogeneous pattern of shape reversal could be variation in the amount of the membrane lipid PtdIns(4,5)$P_2$ remaining after calcium loading. Thompson et al., (1987), have suggested that a discrete membrane pool of this lipid may be responsible for the maintenance of the discocyte morphology. Calcium stimulation of PLC leads to the cleavage of PtdIns(4,5)$P_2$ (Downes and Michell, 1981), and since erythrocytes are incapable of the <u>de novo</u> synthesis of the phosphoinositides (Percy et al., 1973) it is possible that the irreversible loss of this lipid from the membrane results in the inability of cells to regain the discocyte form.

Heterogeneity in the morphological response of an erythrocyte population to uniform calcium permeabilization

has also been previously noted in section in 4.1. However, the differential ability of cells to recover the discocyte morphology does not appear to be simply related to the severity of the initial echinocytic transition, since approximately 40% of cells induced to sphereo-echinocytosis are capable of the reverse transformation. Heterogeneity within an erythrocyte population can result from the presence of cells of different ages. Although the loss of the discocyte form during calcium loading was found to be independent of cell age, it is possible that age does influence the biochemical mechanisms which control the ability of cells to recover and maintain the discoid form following calcium-induced echinocytosis.

To examine this possibility erythrocytes were separated into populations enriched in either young or old cells. Shape reversal studies similar to those described above in section 3.2.4. were then carried out.

The results obtained from these studies are shown in Appendix 1 and indicate that the ability of erythrocytes to undergo shape recovery from the echinocyte to the discocyte morphology is also independent of cell age. In the experiments performed, both shape reversal to the discocyte and to less extreme forms of echinocyte was almost identical in populations enriched with either young or old cells.

### 3.2.7. Electron micrographic examination of erythrocyte shape reversal.

Surprisingly, the data presented here indicates that erythrocytes permeabilized to calcium in replete media are capable of recovering the discoid form even after the severe shape changes involved in sphereo-echinocytosis. However, in all of these studies cell morphology has been quantified using light microscopy. In order to study cell surface architecture during the echinocyte to discocyte transition in greater detail the morphological examination of the shape reversal of erythrocytes permeabilized to both 150μM and 1mM calcium in replete media was repeated using scanning electron microscopy. The results are presented in figures 27 and 28. It can be seen that cells treated with 150μM calcium for 10 minutes recover from stage 1 echinocytes to `normal' looking discocytes. However, those cells which recover the discocyte morphology from the sphereo-echinocyte form induced by 1mM calcium for 15 minutes have a `mottled' membrane surface, apparently as a result of the release of membrane vesicles (Lutz et al., 1977, Rumsby et al., 1977, Allan and Thomas, 1981, Liu et al., 1989).

### 3.2.8. Discussion

The results presented here suggest that loss of the erythrocyte discoid morphology during calcium loading is not directly related to cytoskeletal cleavage mediated by

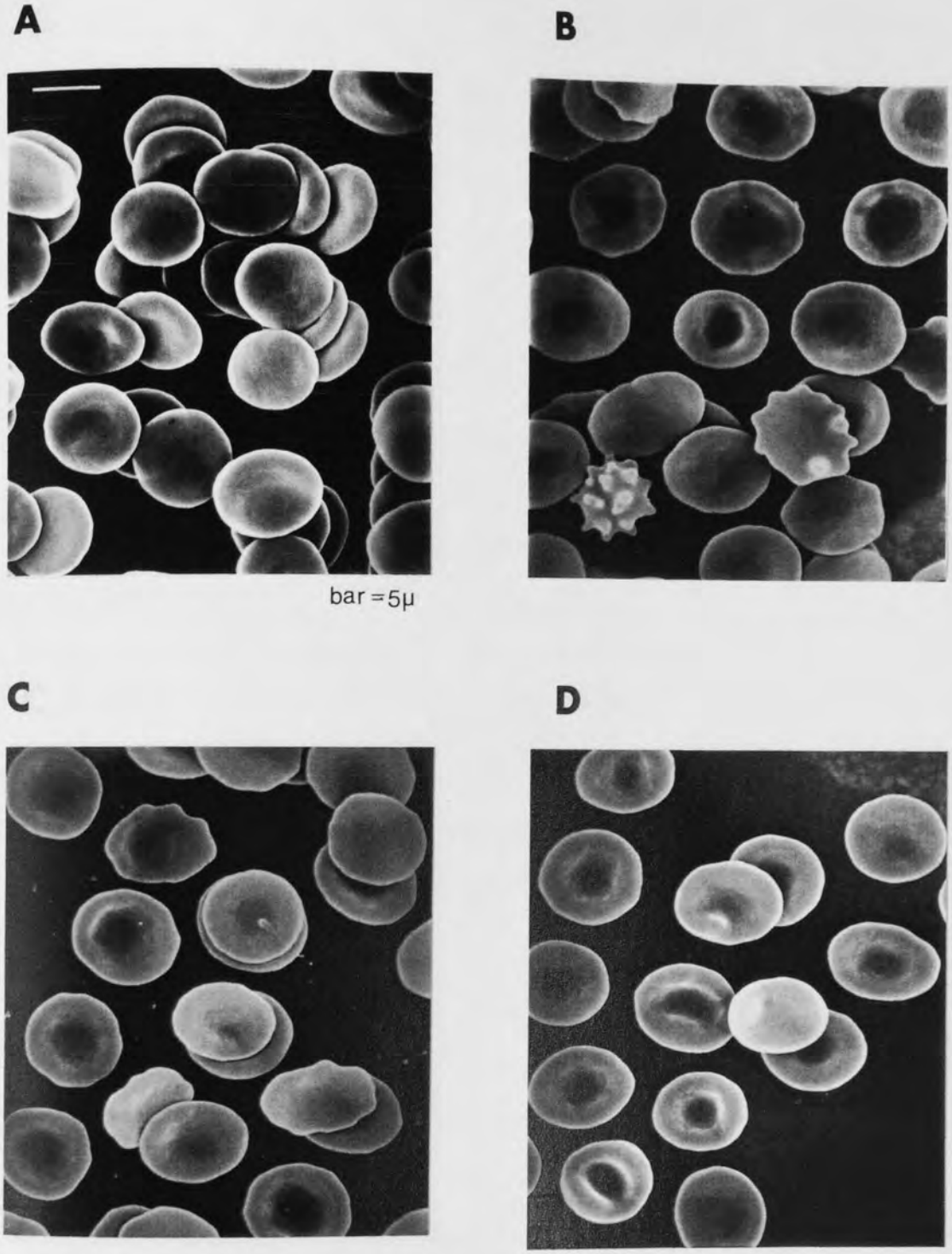


**FIGURE 27** SEM analysis of shape reversal from echinocytosis induced by loading cells held in buffer A with 150μM calcium for 10 minutes; shape recovery also attempted in buffer A
This analysis complements the morphology data presented in figure 21
**A** Control cells
**B** Erythrocytes loaded with 150μM calcium for 10 minutes
**C** Cell morphologies after 30 minutes attempted shape reversal
**D** Cell morphologies after 360 minutes attempted shape reversal

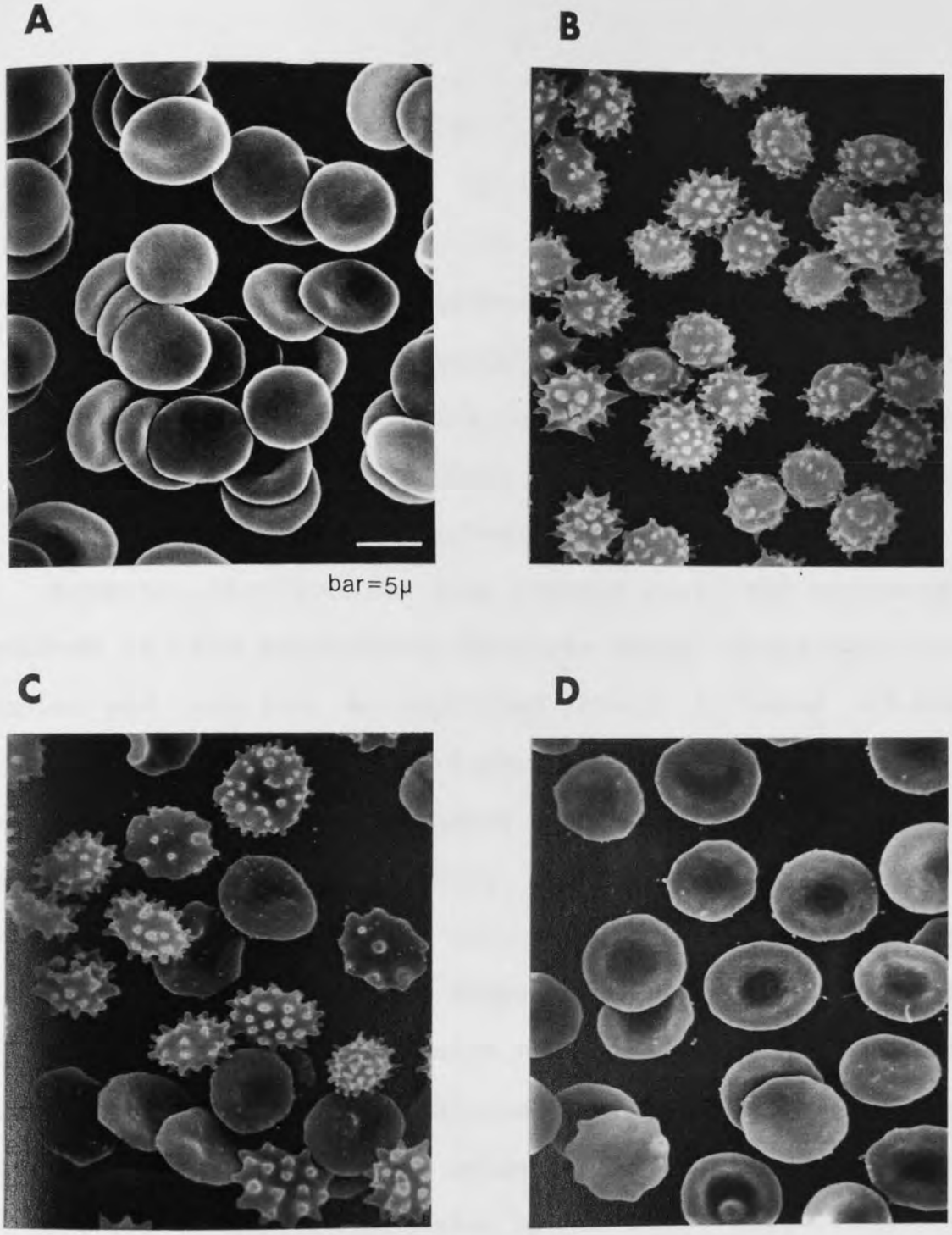


**FIGURE 28** SEM analysis of shape reversal from echinocytosis induced by loading cells held in buffer A with 1mM calcium for 15 minutes; shape recovery also attempted in buffer A
This analysis complements the morphology data presented in figure 21
A Control cells
B Erythrocytes loaded with 1mM calcium for 15 minutes
C Cell morphologies after 30 minutes attempted shape reversal
D Cell morphologies after 360 minutes attempted shape reversal

calcium-activated proteases. However, cytoskeletal integrity may contribute to the maintenance of the discocyte morphology since the degree of calcium-induced cytoskeletal alterations appears to influence the ability of cells to fully recover the discocyte morphology from the echinocyte form. Cells which had lost of 80% of intact protein 4.1 and 40% protein 2.1 were committed to irreversible sphereo-echinocytosis.

However, the results also suggest that the processes involved in the echinocyte-discocyte shape transition are complex and can not be explained solely in terms of the integrity of any cytoskeletal protein. Cells permeabilized to 1mM calcium for 15 minutes in both the presence and absence of metabolic substrates retain intact protein 4.1, but only the former cells are capable of recovery to the discocyte form. Therefore, shape recovery also appears to be dependent on the metabolic state of the cells during calcium loading, which as discussed earlier may influence the subsequent ability of cells to synthesize ATP. The results are further complicated by the observation that the degree of shape reversal in cells loaded with 150uM calcium is not altered by the metabolic status of the cells and yet 100% restoration of the discocyte morphology is not achieved in spite of no detectable loss in cytoskeletal integrity. This suggests that shape reversal involves additional physiological processes either too subtle to detect or alternatively not fully examined using the

experimental methods employed here.

Interestingly, where reversal of cells from the sphereo-echinocyte to the discocyte form occurs a discontinuous pattern of shape recovery is observed; restoration to stage 1 echinocytes is rapid, but the recovery of the discocyte morphology is much slower, providing the rate-limiting step of the reversal process. This provides further evidence that the erythrocyte morphology transition induced by a rise in cytosolic calcium maybe a discontinuous process which proceeds through discrete morphological steps, possibly brought about by different biochemical processes.

## 3.3. The modulating effects of lectin binding on cell shape and cytoskeletal integrity during the loading of erythrocytes with calcium

### 3.3.1. Introduction; the effects of extracellular ligand binding on erythrocyte properties.

The results presented in section 3.2. suggested that the presence of a threshold level of intact protein erythrocyte 4.1 may contribute to cytoskeletal integrity, as measured by the ability of erythrocytes to undergo the reversal of calcium-induced echinocytosis, although it is clearly not the sole determinant of the ability of cells to undergo morphology transitions. As discussed previously, protein 4.1 interacts with both spectrin and the cytoplasmic domain of an integral membrane protein, and therefore contributes to the close association between the cell plasma membrane and cytoskeleton.

Previous reports have indicated that one of the membrane binding sites of protein 4.1 is the cytoplasmic portion of glycophorin A (Anderson and Lovrien, 1984), and that the association between these two proteins is regulated by the membrane lipid PtdIns(4,5)$P_2$ (Anderson and Marchesi, 1985). It has also been reported that the binding of the lectin, wheat germ agglutinin (WGA) to the extracellular surface of erythrocytes alters the physical properties of the cell by causing membrane rigidification (Lovrien and Anderson, 1980, Anderson and Lovrien, 1981,

Smith and Hochmuth, 1982, Evans and Leung, 1984, Chasis et al., 1985). Since the receptor for WGA is the extracellular domain of glycophorin (Adair and Kornfeld, 1974), it has been suggested that WGA binding stimulates transmembrane signal transduction via the integral protein resulting in the rearrangement of the cytoplasmic cytoskeletal network (Anderson and Lovrien, 1981, Chasis et al., 1985, Chasis et al., 1988). These changes could be mediated through receptor coupled alterations in PtdIns(4,5)$P_2$, leading to changes in the membrane and cytoskeletal associations maintained by protein 4.1.

In the studies described in this section, the importance of intact protein 4.1 to erythrocyte shape has been investigated using a different approach, through the utilization of WGA to modulate cell shape. Anderson and Lovrien (1981) have reported that erythrocytes pre-treated with this lectin maintain the discocyte morphology even during a rise in cytosolic calcium; presumably as a result of the increased membrane rigidity. Since the extracellular binding of WGA may result in cytoskeletal rearrangements involving protein 4.1 a study was carried out to examine whether the preservation of the discoid form by WGA is associated with the maintenance of intact protein 4.1 in the cytoskeleton.

The experiments presented here involve an initial preliminary investigation into the modulating effects of WGA on erythrocyte shape. The effects of WGA on the

integrity of protein 4.1 during calcium loading was then examined by comparing the pattern of cytoskeletal cleavage of erythrocytes permeabilized to calcium with or without pre-treatment with the lectin.

4.3.2. Modulation of the calcium-induced shape transitions of human erythrocytes by the extracellular binding of wheat germ agglutinin (WGA)

An examination of the effects of WGA on erythrocyte morphology during calcium loading was carried out using the method of Anderson and Lovrien, (1981). Erythrocytes prepared in Tris buffer B and resuspended at 1 x $10^7$/ml, were pre-treated with 2µg/ml of WGA for 1 minute, prior to treatment with 200µM calcium and 5µM A23187. Preliminary investigations were carried out using cells at a concentration consistent with previously described investigations into the progression of calcium-induced echinocytosis (section 3.1.2). It was found, in agreement with previous reports (Lovrien and Anderson, 1980), that at cell concentrations greater than 1 x $10^7$/ml, the lectin induced severe cell aggregation; causing a distortion of cell morphology. After 5 minutes incubation at 25$^{o}$C, the lectin was displaced from the extracellular surface of the cells by the excess addition of the sugar, N-acetylglucosamine (NAG) (30mM) which competitively binds the lectin. This concentration of NAG has been reported to displace all WGA from the cell surface within 30 seconds of

addition (Anderson and Lovrien, 1981). This experiment was performed at 25°C in order to be consistent with published investigations involving the modulation of the discocyte-echinocyte transformation by WGA (Lovrien and Anderson, 1980, Anderson and Lovrien, 1981). However, for comparison with the above experiment, and to be consistent with the other studies in this thesis the experiment was repeated at 37°C.

The results of these studies are illustrated in figure 29. It can be seen that WGA binding slightly reduces the basal level of echinocytes in a cell population, but microscopic studies indicate that the lectin does not induce any other modification of erythrocyte morphology at this cell concentration. At 25°C over 95% of the cells maintain the discocyte morphology even after 5 minutes calcium loading, confirming previous reports that lectin inhibits the echinocytic shape transition. It is known that WGA binding to the extracellular surface of cells does not interfere with calcium entry mediated by the ionophore (Anderson and Lovrien, 1981), indicating that the lectin does not simply prevent a rise in cytosolic calcium. The removal of WGA by the addition of NAG immediately abolishes the effects of the lectin and results in the rapid (<30 seconds) transformation of the cells to over 95% echinocytes. These results suggest that the calcium-activated processes responsible for the initiation of echinocytosis are stimulated in WGA treated cells, but

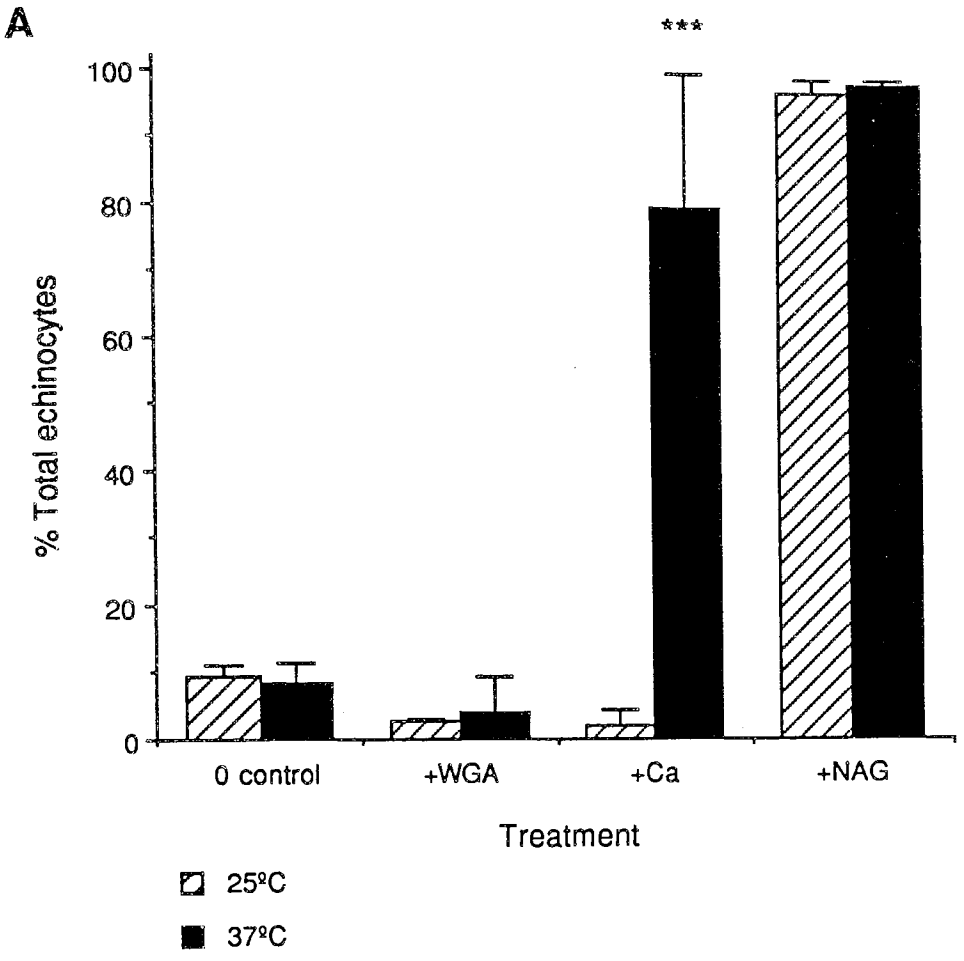


**FIGURE 29** A comparison of the extent of erythrocyte shape modulation by WGA at 25°C and 37°C
Human erythrocytes held at either 25°C or 37°C were pre-treated with 2µg/ml of WGA prior to treatment with 200µM calcium in the presence of 5µM A23187. After 5 minutes, N-acetylglucosamine (NAG) was added to 200mM and the cell suspension incubated for a further 30 seconds. Cell morphologies were quantitated at each stage.
Key to treatments; 0 control=untreated cells, +WGA=cells pre-treated with WGA, +Ca=cells loaded with calcium for 5 minutes, +NAG=cells treated with NAG for 30 seconds
A Comparison of total echinocyte levels. Results expressed as mean ±SD
*** P=<0.001 when mean values at 25°C and 37°C compared using Student T test (n=4)
B Quantitation of the formation of different stage echinocytes

Figure 29B

| Treatment | % different type echinocytes | | | | |
|---|---|---|---|---|---|
| | Discs | Stage 1 | Stage 2 | Stage 3 | Sphereo-echinocyte |
| 25°C | | | | | |
| Control | 88.68 | 10.31 | 0.94 | | |
| +WGA | 97.27 | 2.73 | | | |
| +Ca | 99.07 | 0.93 | | | |
| +NAG | 4.8 | 15.2 | 6.4 | 23.2 | 50.4 |
| 37°C | | | | | |
| Control | 89.66 | 10.34 | | | |
| +WGA | 96.06 | 3.94 | | | |
| +Ca | 3.96 | 25.74 | 19.8 | 26.73 | 23.76 |
| +NAG | 0 | 1.54 | 0.77 | 3.85 | 93.85 |

Results shown are from one representative experiment

the presence of the lectin alters the physical properties of the cell, therefore preventing shape change.

In contrast, erythrocytes pre-treated with WGA and calcium-loaded at 37°C do not maintain the discocyte morphology. Almost 80% of the cells are transformed to the echinocyte form after 5 minutes exposure to 200μM calcium; a significantly different result to that obtained at 25°C. It appears that the ability of WGA to maintain the discocyte morphology during calcium loading is temperature dependent.

It is possible that the lectin simply does not bind to the extracellular domain of glycophorin at the higher temperature. However, the finding that the basal level of echinocytes is reduced by WGA at this temperature in a similar manner to that observed at 25°C indicates that this is unlikely. Additionally, at higher cell concentrations agglutination was still observed at 37°C. Therefore, it appears that either lectin binding does not induce alterations in erythrocyte physical properties to the same extent at 37°C, or that at the higher, more physiological temperature a greater stimulation of the calcium-activated cellular processes responsible for echinocytosis opposes the alterations in the physical properties of the cells resulting from lectin binding. The latter possibility may indeed contribute to the observed results. Although displacement of the WGA after 5 minutes calcium loading results in similar levels of total echinocytes at both

temperatures, the quantitation of different stage echinocytes illustrated in figure 29B indicates that cells at 25°C adopt a range of echinocyte stages, whereas the cells at 37°C are almost exclusively transformed to sphereo-echinocytes. However, these results do not provide sufficient information to allow firm conclusions to be reached on the effect of temperature on the WGA control of erythrocyte shape during calcium loading. Ideally, further experimental investigations need to be carried out to examine WGA effects on membrane rigidity at 37°C.

### 3.3.3. The effect of extracellular WGA binding on the proteolytic cleavage of protein 4.1 resulting from the calcium loading of erythrocytes

An investigation was carried out to examine whether the maintenance of the discocyte morphology by WGA during calcium loading at 25°C is associated with the presence of intact protein 4.1 in the erythrocyte cytoskeleton. Therefore, the pattern of proteolytic cleavage of protein 4.1 during the loading of intact erythrocytes with calcium was examined in cells pre-treated with WGA and compared to cells treated similarly but without WGA, using a similar method to that described in section 3.2.2.

Erythrocytes prepared in Tris buffer and resuspended at a cell concentration of 1 x $10^7$/ml were pre-treated with 2µg/ml of WGA for 1 minute. The cells were loaded with 1mM calcium and 5µM A23187 for a maximum of 60 minutes.

preliminary investigations indicated that lectin binding could maintain the discocyte morphology under these conditions. After 60 minutes the WGA was displaced by the addition of NAG. At appropriate time intervals, samples were removed for both the quantitation of morphology and the preparation of erythrocyte ghosts for SDS-PAGE analysis on 7% discontinuous gels. An comparative study was carried out using cells treated with neither WGA or NAG.

The results of the latter study are illustrated in figure 30. The morphological data indicates that increasing exposure to calcium induces echinocytosis which reaches completion after 5 minutes. Under these conditions of calcium loading the proteolytic cleavage of protein 4.1 as analysed by SDS-PAGE also occurs. This is supported by densitometric analysis of the Coomassie blue stained gel which indicates that the intensity of protein 4.1 falls by approximately 50% over 60 minutes (figure 32).

In contrast it can be seen that as described above cells pre-treated with WGA retain the discocyte morphology even after 60 minutes treatment with 1mM calcium. Displacement of the lectin results in the transformation of the cells to over 95% echinocytes. Interestingly, from the SDS-PAGE analysis of these cells illustrated in figure 31 it can be seen that the calcium loading of WGA treated cells is associated with the proteolytic cleavage of protein 4.1. Indeed from the densitometric analysis it can be seen that the rate of loss in intensity of this protein

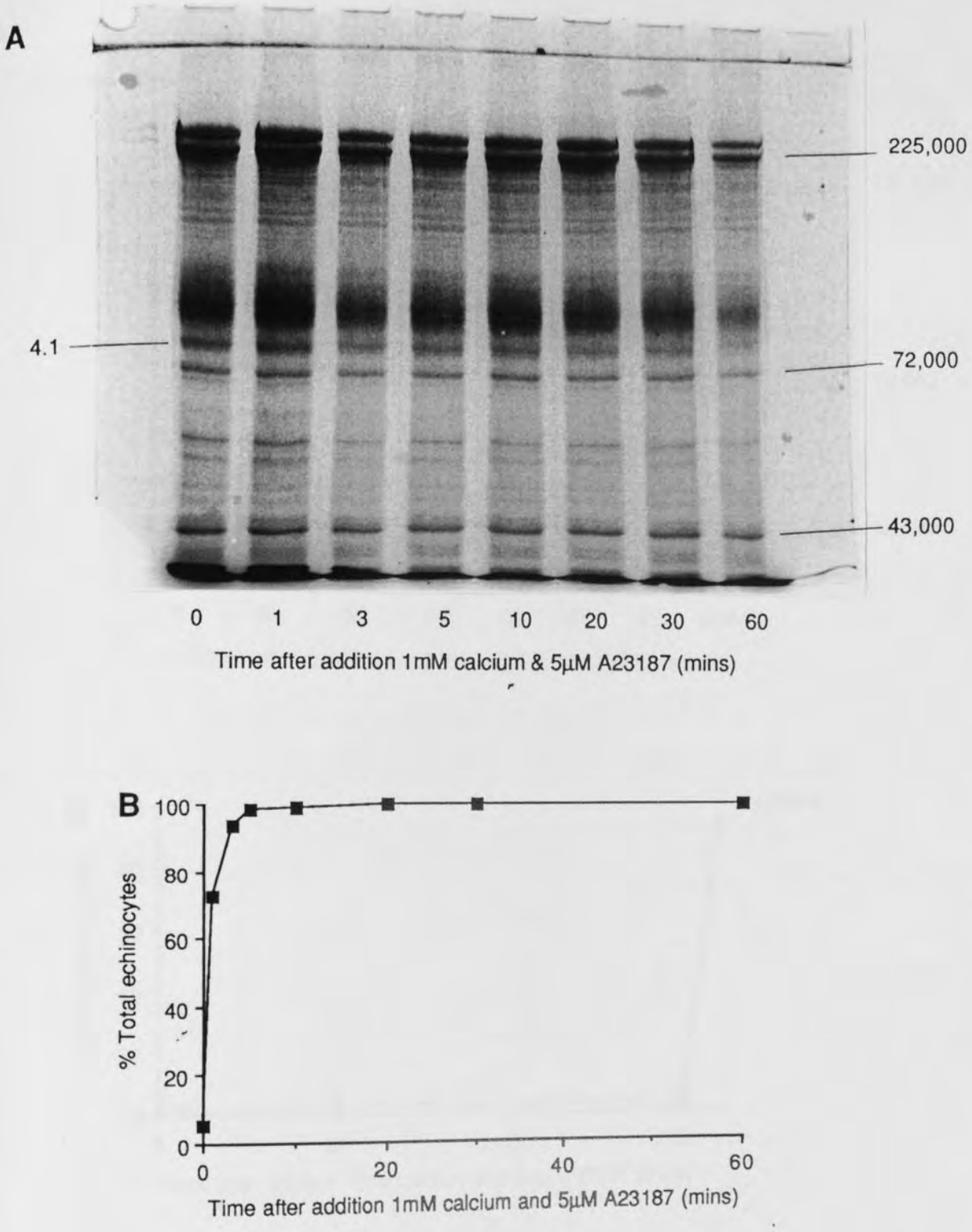


**FIGURE 30** Time-dependent proteolytic modification of human erythrocyte cytoskeletal proteins in intact cells loaded with 1mM calcium at 25°C

Human erythrocytes held in buffer B at $10^7$/ml were treated with 1mM calcium and 5μM A23187 at 25°C. Samples were removed at the time intervals specified for the preparation of erythrocyte ghosts and the quantitation of morphology

**A** Coomassie blue stained pattern of ghost proteins analysed on a 7% discontinuous SDS-PAGE

**B** Morphological state of cells from the same samples as those analysed in (A)

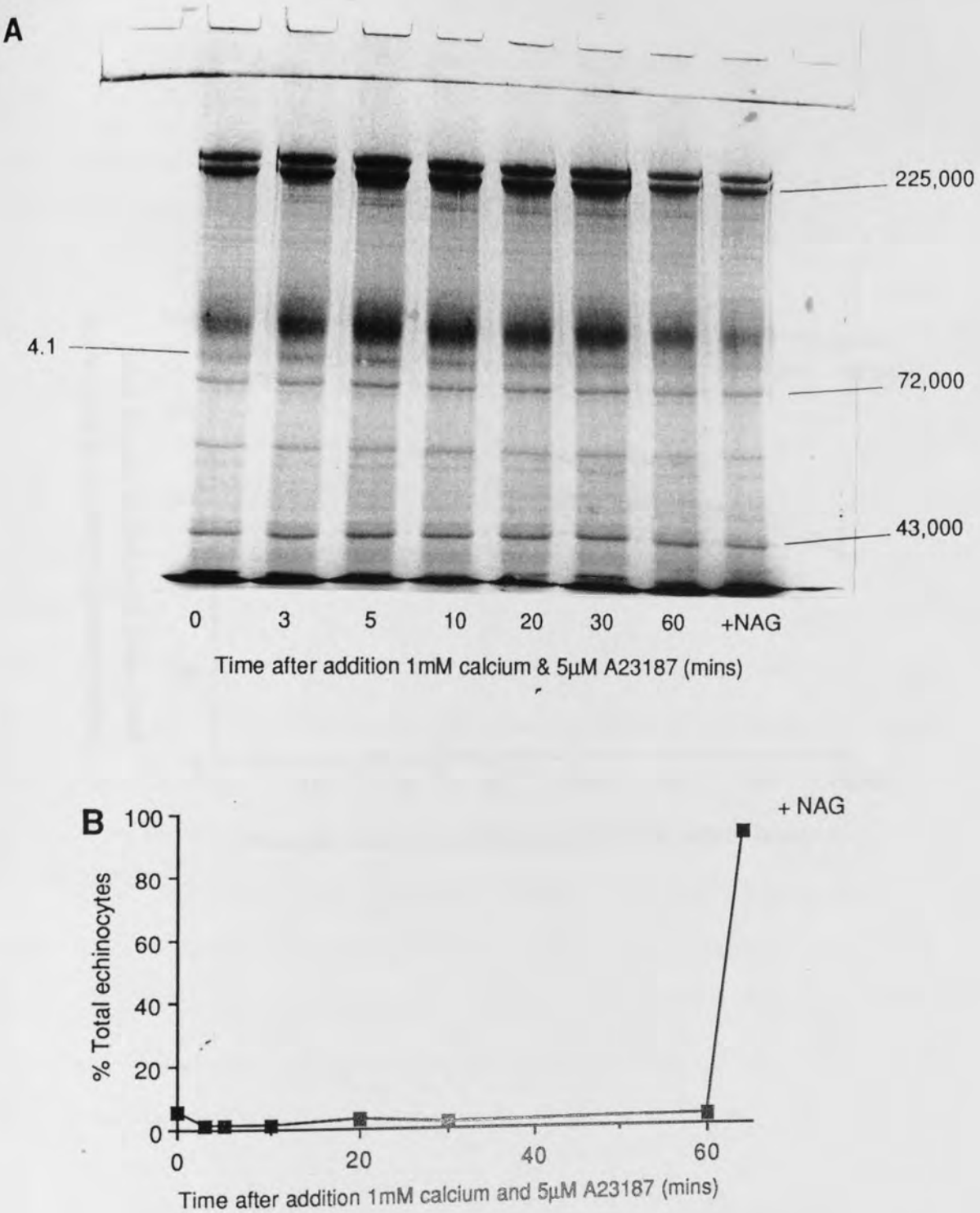


**FIGURE 31** Time-dependent proteolytic modification of human erythrocyte cytoskeletal proteins in intact cells loaded with 1mM calcium at 25°C after pre-treatment with WGA
Erythrocytes held in buffer B at $10^7$/ml were pre-treated with WGA at 25°C, prior to treatment with 1mM calcium and 5µM A23187. After 60 minutes, NAG was added for 30 seconds. At the time intervals specified erythrocyte ghosts were prepared and cell morphology quantitated.
**A** Coomassie blue stained 7% SDS-PAGE of ghost proteins
**B** Morphological state of cells from the same samples as those analysed in (A)

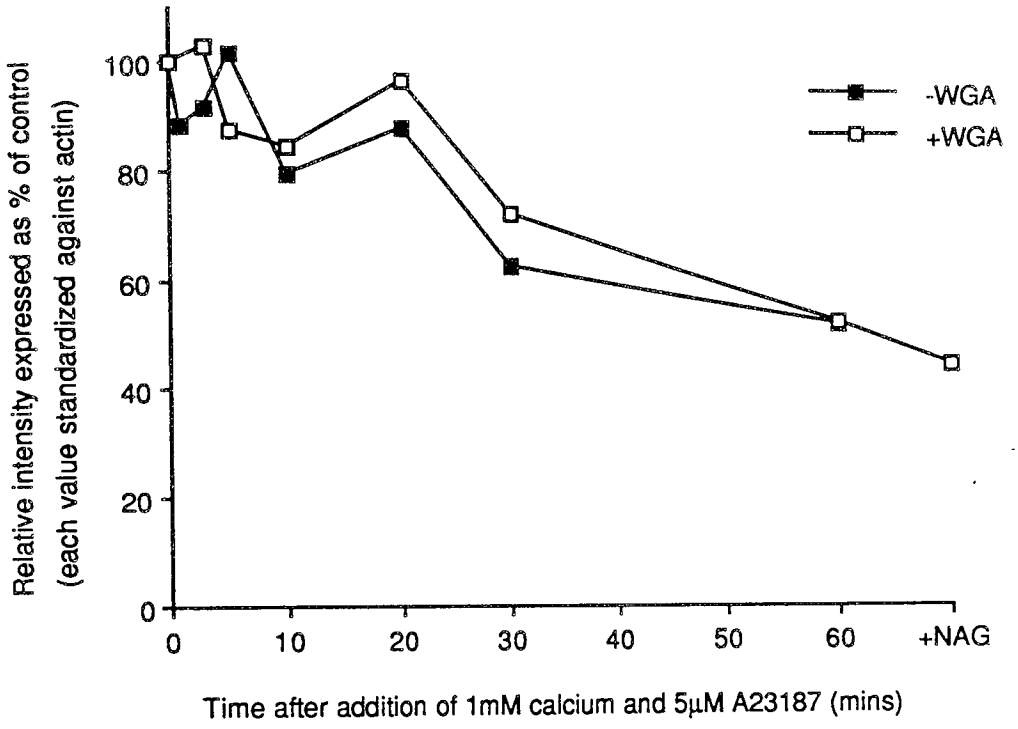


**FIGURE 32** Densitometric quantitation of the rate and extent of the cleavage of protein 4.1 in erythrocytes loaded with 1mM calcium with (+WGA) or without (-WGA) prior treatment with WGA

Densitometric analysis of protein 4.1 cleavage illustrated in figures 29A and 30A

with increased exposure to calcium is very similar to that obtained above in the absence of WGA at all time intervals (figure 32). In addition, the severe alteration in cell morphology associated with removal of the WGA does not induce any change in the intensity of protein 4.1.

The proteolytic loss of intact band 4.1 associated with a rise in cytosolic calcium occurs regardless of whether or not the cells undergo the echinocytic shape transformation; cell populations of both 100% echinocytes and >95% discocytes retain only 50% intact protein 4.1 after 60 minutes loading with 1mM calcium. These results indicate that the maintenance of the discocyte form by WGA is not associated with the presence of intact protein 4.1 in the erythrocyte cytoskeleton. These experimental results support those obtained in the previous section (3.2), further indicating that no obvious relationship exists between proteolytic cleavage and the onset of erythrocyte shape transformation.

## Section 3.4: Effects of long term incubation in replete media on the progression of erythrocyte shape changes induced by calcium

### 3.4.1 Introduction

During the course of the studies described so far, it was noticed that the A23187 permeabilization of erythrocytes to calcium after the cells had been held in replete media (buffer A, section 2.2) at 37°C, appeared to result in lower levels of echinocyte formation than expected from control values obtained under identical conditions of calcium treatment immediately after cell preparation. This suggested that the progression of the morphological transition of erythrocytes loaded with calcium is in some way modified by the incubation of the cells in the presence of glycolytic substrates. For the reasons itemised below, it was decided to carry out preliminary morphological studies to further examine the effects of such pre-incubation on echinocytosis induced by calcium and ionophore.

(i) If incubation in replete media does modify the response of an erythrocyte population to a calcium load then the results of studies incorporating such incubations, for instance those involving metabolic labelling, may be misleading if the biochemical effects of calcium after incubation are assumed to be identical to those before.

(ii) If the different responses of incubated and non-incubated cells were the result of intracellular

biochemical modifications occurring during incubation, a greater understanding of these processes could prove useful for further investigations into the factors controlling erythrocyte shape transitions. The biochemical effects of identical calcium loading could be examined in the same original cell population, under conditions in which echinocytosis does or does not take place.

Preliminary morphological experiments were carried out to examine the effects of pre-incubation of erythrocytes on both calcium concentration-dependent and time-dependent echinocytosis.

### 3.4.2. The effects of pre-incubation in replete media on echinocytosis induced by increasing calcium concentrations

A comparison was made of the rate of total echinocyte formation in cells loaded with calcium in a concentration -dependent manner before and after the incubation of cells in buffer A for a maximum of 360 minutes. It has already been demonstrated that the discocyte morphology is maintained under such conditions (section 3.1.4) and therefore, the morphological characteristics of the cell population were similar before and after incubation.

Following incubation of erythrocytes in buffer A at 37$^{o}$C for a maximum of 360 minutes, cells were loaded with increasing calcium concentrations in the presence of 5µM A23187 and total echinocyte levels examined after 5 minutes treatment. The results are shown in figure 33. A direct

relationship appears to exist between the length of time of pre-incubation and the degree of inhibition of the shape transition. Six hours of pre-incubation significantly reduces total echinocytosis compared to the 0 minute values at all calcium concentrations studied; indeed at low levels of calcium loading (<300μM) echinocytosis is apparently blocked (figure 33A). Therefore this length of pre-incubation was used in all further investigations.

One possible explanation for the reduced morphological response of erythrocytes to calcium permeabilization after pre-incubation is the loss of a calcium sensitive sub-population of erythrocytes through haemolysis during this time period. As a control for this possibility the proportion of cells lost during the pre-incubation period through haemolysis was estimated. It was found that approximately 1.5-2% of the erythrocytes in a preparation

**FIGURE 33** Total echinocytosis induced by increasing calcium concentrations in erythrocytes incubated in buffer A at 37°C prior to calcium loading
Human erythrocytes held in buffer A were incubated at 37°C for the time periods specified prior to loading with increasing calcium concentrations. After 5 minutes samples were removed for the quantitation of morphologies. All results expressed as mean ± SD, P values calculated by comparison of 0 minutes mean values with mean values after incubation using Student T test, n=6 or 8
**A** Low calcium concentrations (0-250uM).
**B** High calcium concentrations (100-1000uM).

a=P<0.001 180 and 360 mins, b=P<0.005 30 mins, P<0.001, 180 and 360 mins, d=P<0.001 360 and 360 mins, c=P<0.001 30, 180 and 360 mins, f=P<0.05 30 mins, e=P<0.05 30 mins, P< 0.001 360 mins, h=P<0.05 mins, P<0.005 360 mins, g=P<0.05 30 and 360 mins, 360 mins

**33A**

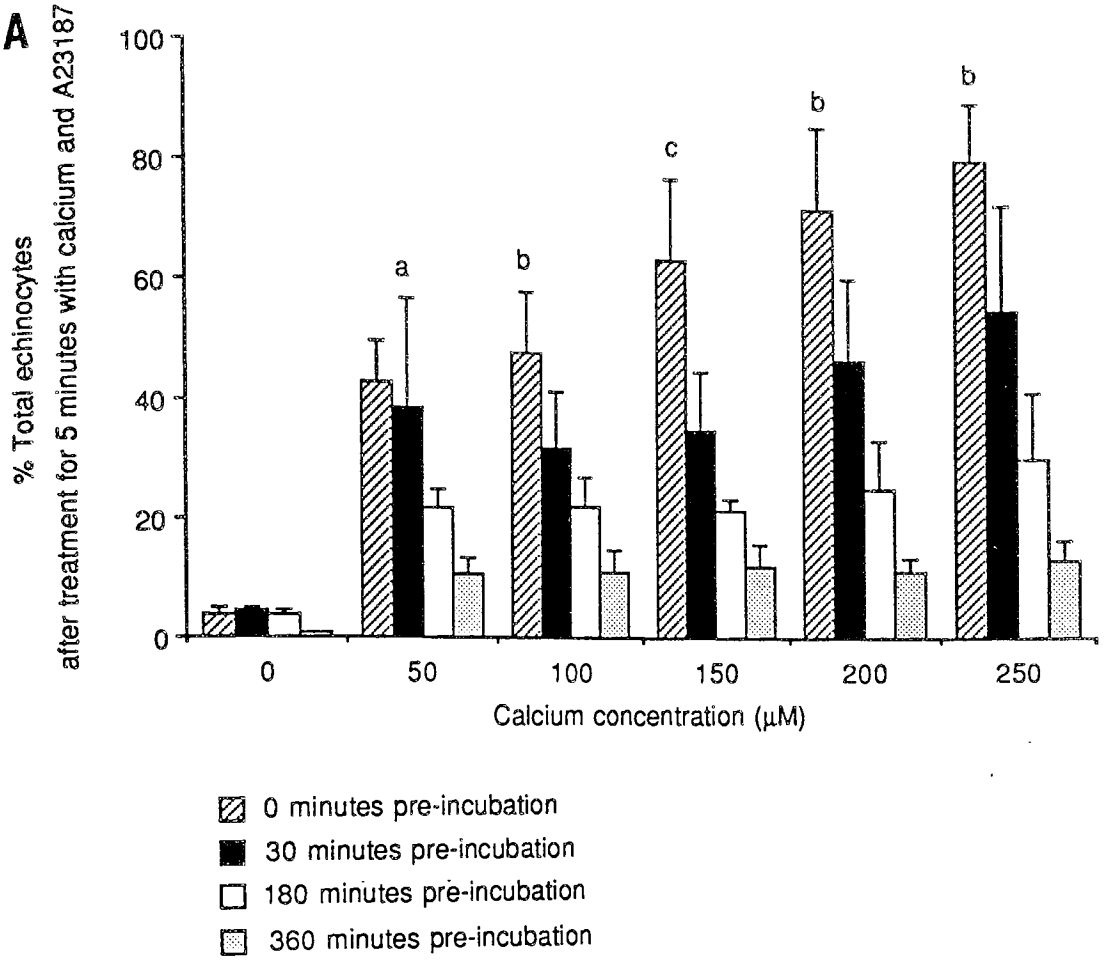
% Total echinocytes
after treatment for 5 minutes with calcium and A23187
100
80
60
40
20
0
a
b
c
b
b
0
50
100
150
200
250
Calcium concentration (μM)
0 minutes pre-incubation
30 minutes pre-incubation
180 minutes pre-incubation
360 minutes pre-incubation

**33B**

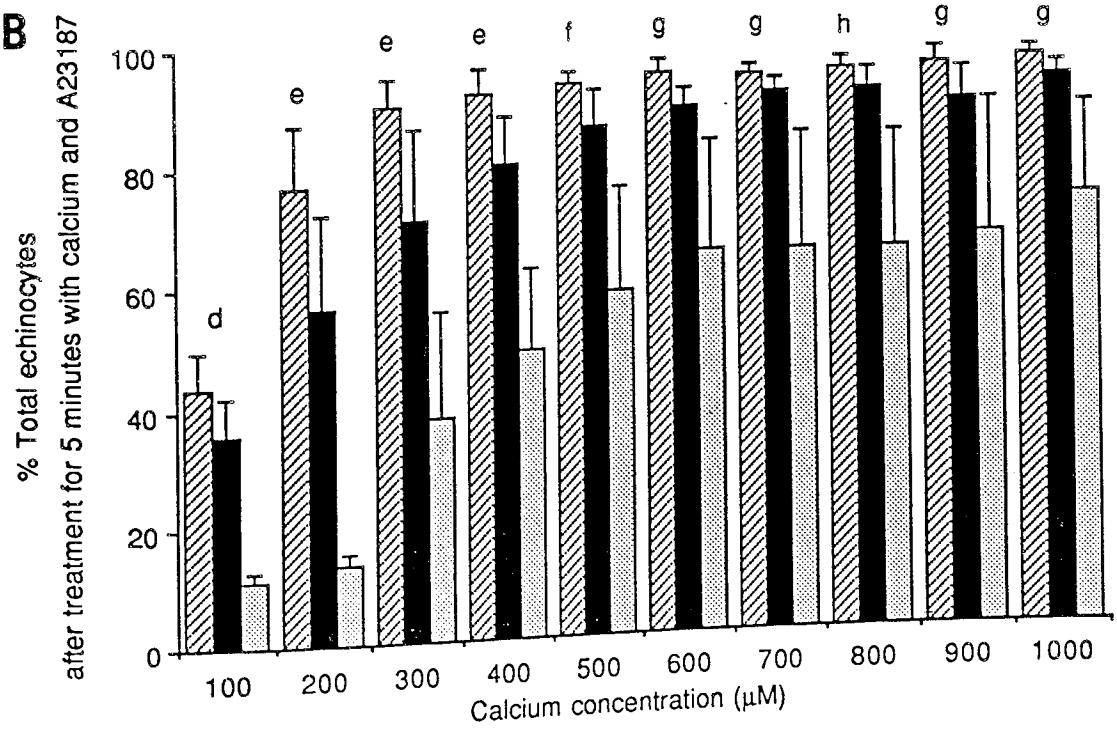
% Total echinocytes
after treatment for 5 minutes with calcium and A23187
100
80
60
40
20
0
d
e
e
e
f
g
g
h
g
g
100
200
300
400
500
600
700
800
900
1000
Calcium concentration (μM)

lyse during a 6 hour incubation at 37°C in replete media; a value which is comparable to previously reported *in vitro* rates of spontaneous haemolysis for red cells washed and resuspended in balanced electrolyte solutions (Lew, 1990). This low level of cell loss would not be sufficient to account for the reduced proportion of erythrocytes undergoing echinocytosis after a 6 hour pre-incubation.

### 3.4.3. The effects of pre-incubation in replete media on time-dependent echinocytosis

Figure 34 shows the effects of the pre-incubation of erythrocytes on time-dependent echinocytosis. After initial preparation, cells were incubated for either 0 minutes or 6 hours at 37°C in buffer A and the progression of total echinocytosis induced by 150µM or 1mM calcium in the presence of 5µM A23187 was then examined. At both calcium concentrations the rate of total echinocyte formation is significantly reduced by the incubation of the cells for 6 hours before permeabilization to the ion.

Interestingly, if the rate of formation of different stage echinocytes during 60 minute treatment with 150uM calcium and 5µM A23187 is examined it can be seen that a very different pattern is observed before and after 6 hour pre-incubation (compare figure 35 with figure 10). As described in section 3.1.2, under the former conditions there is a predominance of stage 2, 3 and sphereo-echinocytes after 60 minutes treatment. In

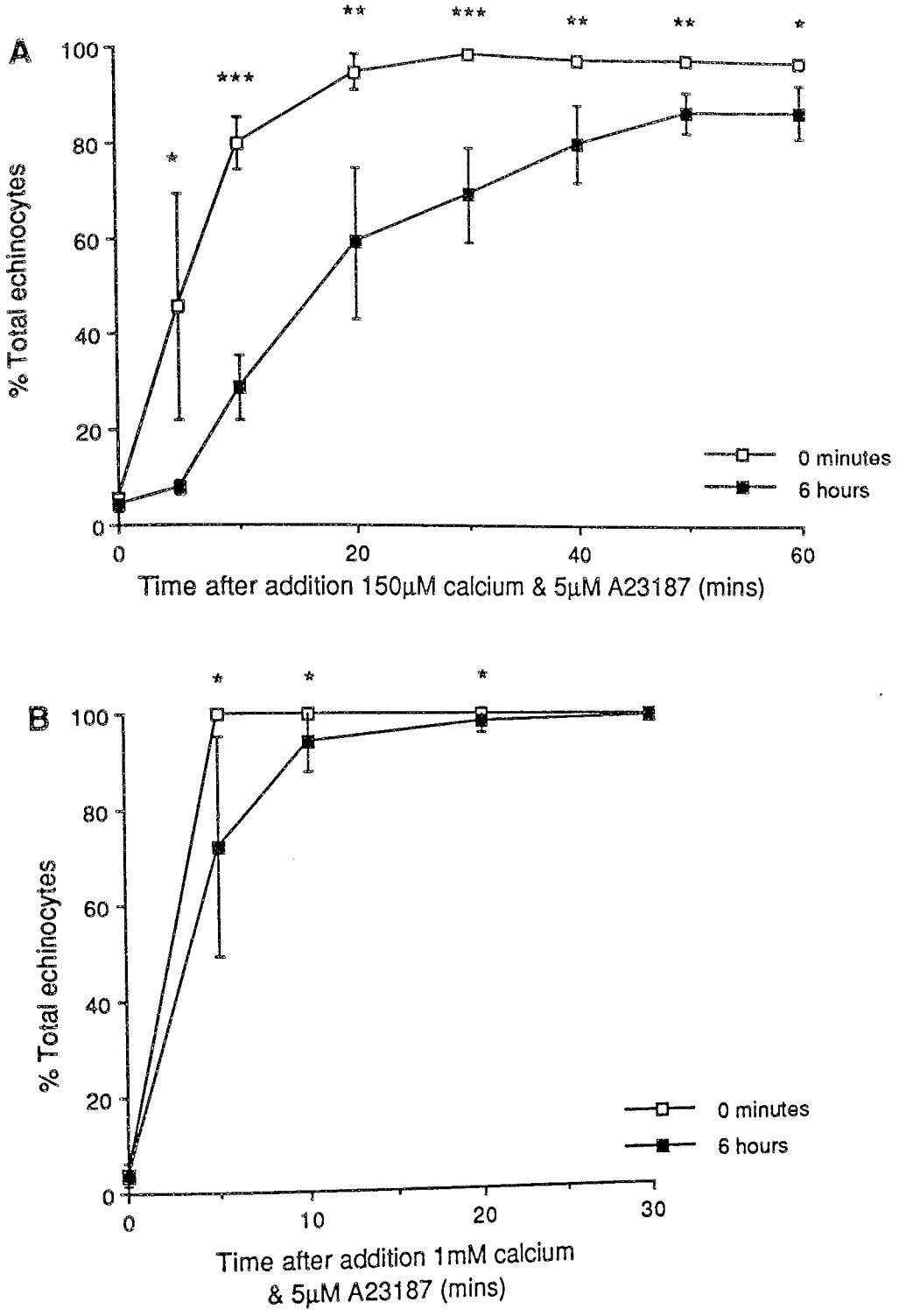


**FIGURE 34** Comparison of the time-course of echinocytosis before and after 6 hours incubation in buffer A when A23187 is used to initiate calcium entry

Human erythrocytes held in buffer A were treated with calcium and 5µM A23187 either immediately after preparation or after 6 hours incubation at 37°C.

A 150µM calcium. Results expressed as mean ± SD, n=6

B 1mM calcium. Results expressed as mean ± SD, n=6

*=P<0.05, **=P<0.005, ***=P<0.001 when mean values at 0 minutes and 6 hours compared using Student T test.

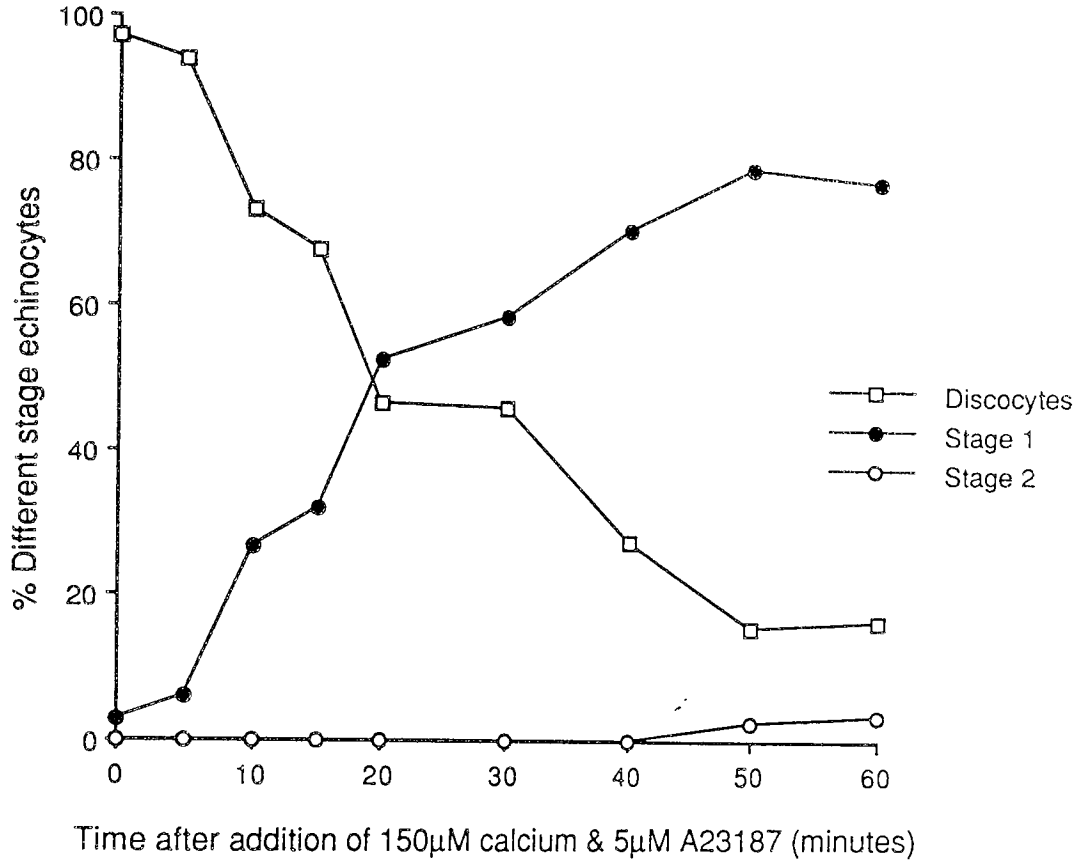


**FIGURE 35** The time-course of formation of different stage echinocytes in erythrocytes treated with 150µM calcium and 5µM A23187 after 6 hours incubation in buffer A at 37°C
The results are shown for a representative experiment (n=6)

contrast, in erythrocytes loaded with 150μM calcium after a 6 hour incubation the shape transition induced is almost exclusively to stage 1 echinocytes (figure 35).

From these preliminary studies it appears that incubation slows the progression of cells through the sequential stages of echinocytosis, reducing the number of cells passing through the discocyte-echinocyte transition and therefore reducing the observed levels of total echinocytes compared to those observed under identical calcium loading conditions immediately after cell preparation.

The physiological mechanisms involved in the reduced response to calcium loading following incubation were examined. Several hypotheses for the effects of incubation were thought to be possible:

(i) Incubated cells have reduced ionophore-mediated calcium influx, resulting in lower cytosolic calcium levels than those achieved in cells treated at 0 minutes and therefore less extreme shape transformations. Reduced calcium influx could result from less ionophore partitioning into the cell membranes, possibly through membrane alterations occurring during incubation.

(ii) Incubated cells have a similar rate of calcium entry to non-incubated cells but extrusion is equal to influx, preventing prolonged increases in cytosolic concentrations of the ion. Increased extrusion of the ion after incubation could only result from the increased

activity of the $Ca^{2+}$-ATP-ase. Since cells incubated in buffer A at 37°C maintain constant ATP levels over a 6 hour period, pump activity is not enhanced by increased availability of metabolic fuel. Pump activity is saturable (Schatzmann, 1983, Dagher and Lew, 1988), therefore increased extrusion after incubation could occur if the membrane pumps were not saturated at 0 minutes. Alternatively, incubation could alter the affinity of the pump for the ion, or lead to changes in the conformation of enzyme, resulting in a greater number of pumps being activated by a rise in cytosolic calcium.

(iii) Incubated cells have a similar rate of calcium influx to non incubated cells, but the physiological mechanisms involved in the morphological transitions have reduced sensitivity to the ion. Such effects could be observed if incubated cells had altered accessibility of intracellular substrates to the enzymes responsible for initiating the shape changes.

### 3.4.4. The effects of pre-incubation in replete media on the rate of accumulation of $^{45}Ca^{2+}$ following permeabilization of erythrocytes with A23187

Calcium uptake experiments were performed using a radioisotope of calcium to compare the rates of calcium accumulation in cells before and after incubation in buffer A. Tracer amounts of $^{45}Ca^{2+}$ were included in the media in which the cells were resuspended during calcium loading,

and, following addition of 5uM A23187 to initiate entry, the cells were analysed at various time intervals for their content of the radioisotope. Post-sampling inaccuracies resulting from the extrusion of calcium by the $Ca^{2+}$-ATPase were reduced by performing all procedures on ice (Garcia-Sancho and Lew, 1988, Dagher and Lew, 1988). Since the total calcium content of erythrocytes at any one time is dependent on both the rate of influx and extrusion this technique would only accurately measure rates of calcium influx if the action of the calcium pump was inhibited. However, it does provide information on the rate of accumulation of $^{45}Ca^{2+}$ and therefore total intracellular calcium during treatment with calcium and ionophore, and therefore allows a comparison of this rate between cells permeabilized to calcium before and after incubation in buffer A.

Figure 36 shows the rate of accumulation of $^{45}Ca^{2+}$ in erythrocytes treated with 150μM calcium and 5μM A23187 at 0 minutes and after 6 hours incubation at 37°C in the presence or absence of calcium. Since buffer A contains no calcium, duplicate experiments were performed with added calcium present in the incubating media to determine whether the availability of extracellular calcium during incubation affects the rate of subsequent calcium uptake. It can be seen that cells treated immediately after preparation rapidly accumulate $^{45}Ca^{2+}$ after the addition of A23187 to initiate calcium loading. However, 6 hours

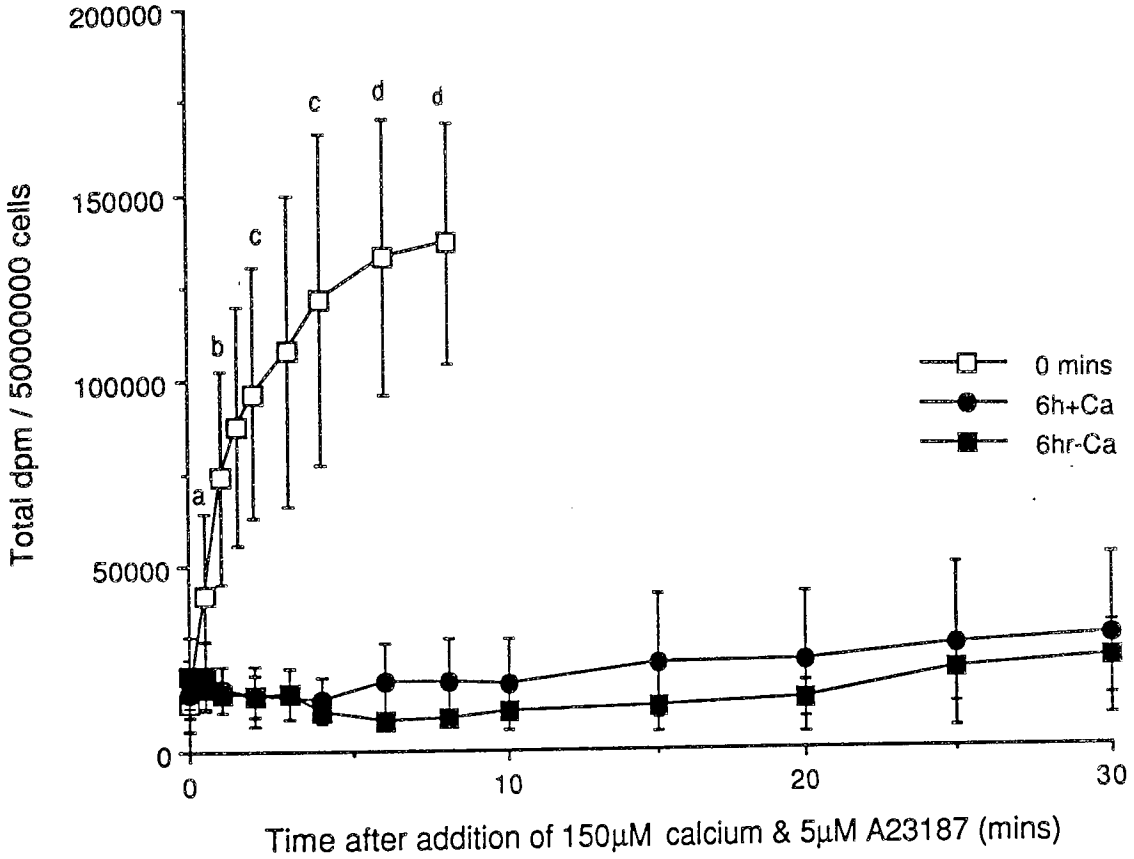


**FIGURE 36** Comparison of the rate of accumulation of $^{45}Ca^{2+}$ during the treatment of erythrocytes with 150µM calcium and A23187 before and after 6 hours incubation in buffer A

Human erythrocytes held in buffer A were permeabilized to 150µM calcium by 5µM A23187 in the presence of $^{45}Ca^{2+}$. At the time intervals specified samples were analysed for their content of the radioisotope. Isotope accumulation was compared in cells immediately after preparation, and after 6 hours incubation at 37°C in the presence or absence of extracellular calcium. Results expressed as mean ±SD, n=4 or 6. All P values calculated by comparison of the mean value at 0 minutes with the mean value of incubated cells with using Student T test

a $P<0.05$ 6hr +Ca
b $P<0.001$ 6hr +Ca, $<0.05$ 6hr -Ca
c $P<0.001$ 6hr +Ca, $<0.005$ 6hr -Ca
d $P<0.001$ 6hr + & - Ca

pre-incubation in buffer A with and without added calcium significantly reduces the rate of calcium accumulation compared to 0 minute values. Indeed, in cells treated after pre-incubation there is no apparent accumulation of $^{45}Ca^{2+}$ during permeabilization: the results obtained are similar to those observed in the control experiments examining $^{45}Ca^{2+}$ accumulation in the absence of A23187 (figure 38).

Cells loaded with 1mM calcium immediately after preparation also rapidly accumulate $^{45}Ca^{2+}$ following permeabilization with 5μM A23187. These results are shown in figure 37. At this higher calcium concentration the incubation of cells for 6 hours at 37°C does not eliminate $^{45}Ca^{2+}$ accumulation, but again it does significantly reduce the rate of uptake of the ion compared to the rate observed at 0 minutes regardless of whether or not calcium is present in the incubation media. Interestingly, cells loaded with 1mM calcium at 0 minutes do not reach a steady-state equilibrium within the 30 minutes studied. Steady-state kinetics would be obtained when the ionophore induced influx of $^{45}Ca^{2+}$ is equalled by the calcium pump mediated efflux, either before or after the intracellular concentration of the ion reaches that of the extracellular environment. Since such a situation is not observed during the course of the experiment, this suggests that the activity of the $Ca^{2+}$-ATPase is saturated during the permeabilization of non-incubated erythrocytes to 1mM

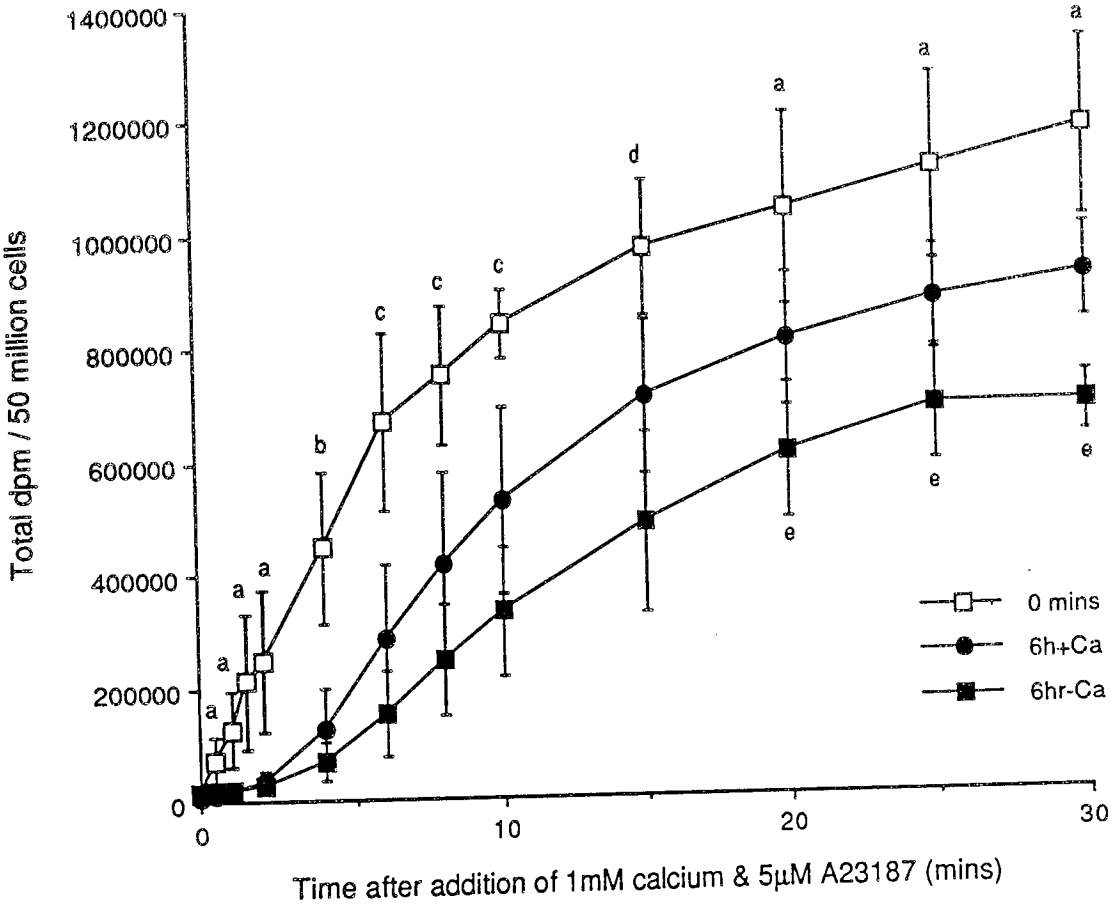


**FIGURE 37** The rate of accumulation of $^{45}Ca^{2+}$ during the treatment of erythrocytes with 1mM calcium and A23187 before and after 6 hours incubation in buffer A

Human erythrocytes held in buffer A were permeabilized to 150µM calcium by 5µM A23187 in the presence of $^{45}Ca^{2+}$. At the time intervals specified samples were analysed for their content of the radioisotope. Isotope accumulation was compared in cells immediately after preparation, and after 6 hours incubation at 37°C in the presence or absence of extracellular calcium. Results expressed as mean ±SD, n=4 or 6.

P values calculated by comparison of mean value at 0 minutes with the mean value of incubated cell using Student T test

a P<0.005 6hr + & - Ca b P<0.001 6hr + & -Ca

c P<0.005 6hr +Ca,<0.001 6hr -Ca d P<0.05 6hr +Ca, <0.005 6hr -Ca

P values calculated by comparison of mean value of cells incubated in the presence and absence of calcium

e P<0.05

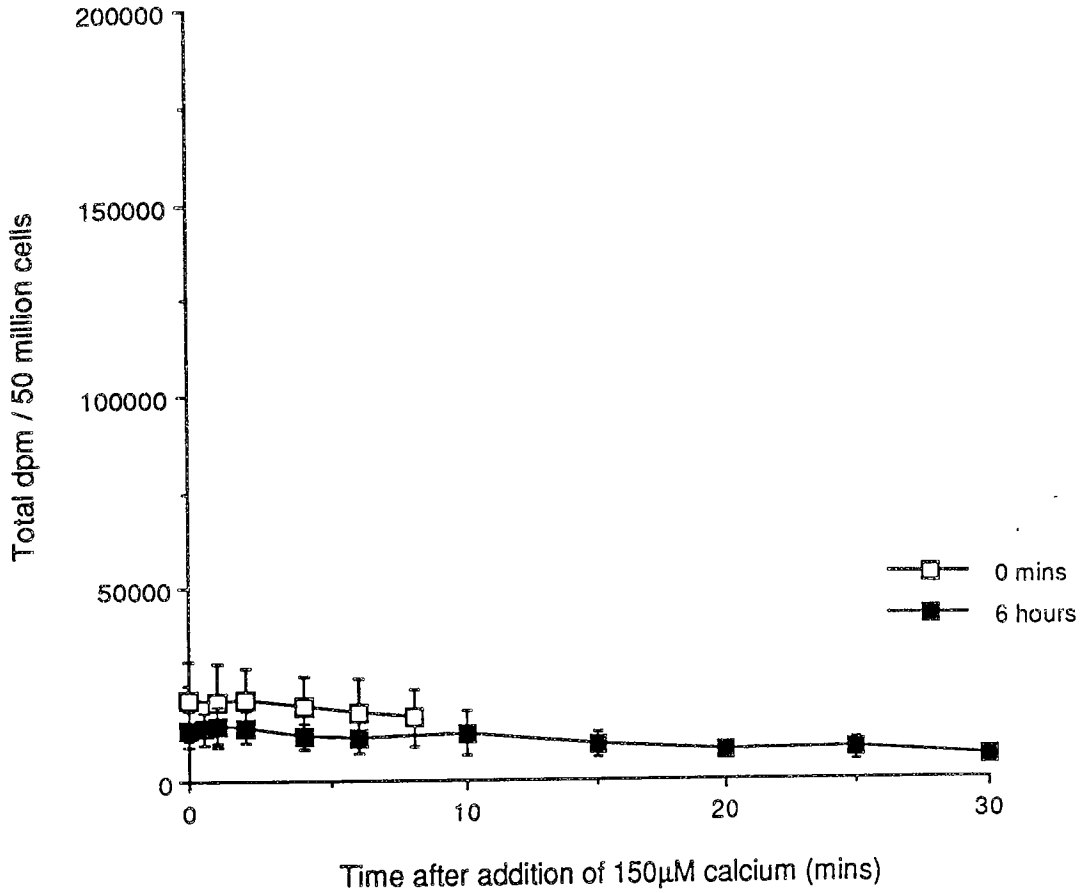


**FIGURE 38** The rate of accumulation of $^{45}Ca^{2+}$ during the treatment of erythrocytes with 150µM calcium in the absence of ionophore

Human erythrocytes held in buffer A were treated with 150µM calcium and $^{45}Ca^{2+}$ before and after 6 hours incubation at $37^{o}C$. At the time intervals specified samples were analysed for their content of the radioisotope. Results are expressed as mean ±SD, n=4

calcium, with cellular levels of the radioisotope increasing as calcium continues to enter the cells down the concentration gradient existing between the internal and external environments. If $Ca^{2+}$-ATPase activity is saturated in cells treated immediately after preparation it appears that the reduced rate of calcium accumulation in incubated cells is not the result of spare pump capacity, as suggested in possibility (ii) above.

The results of the above studies indicate that the pre-incubation of erythrocytes at 37°C for 6 hours in a replete media significantly reduces the rate at which they accumulate calcium during subsequent permeabilization with A23187, compared to the rates observed at 0 minutes. Thus lower levels of cytosolic calcium are reached during calcium loading after pre-incubation, presumably explaining the reduction in the rate of echinocytic morphological transition observed in cells which have been pre-incubated. From the experiments performed it appears that this reduced rate of calcium accumulation is the result of a lowered rate of calcium entry into the cells. Since calcium entry is facilitated in these experiments by A23187, it appears that the ionophore has a reduced ability to permeabilize cells to calcium if they have been held in replete media for 6 hours at 37°C.

At both calcium concentrations examined the rate of uptake of $^{45}Ca^{2+}$ after incubation was significantly reduced by the incubation of erythrocytes in both the presence and

absence of extracellular calcium; suggesting that the permeabilization of erythrocytes to calcium is independent of the previous availability of the ion. Therefore, the absence of calcium in the incubation buffer during the preliminary morphological studies was not the cause of the reduced rate of morphological transition observed in incubated cells during calcium loading. However, it is interesting to note that cells incubated in the presence of calcium and then treated with 1mM calcium and 5μM A23187 do have a greater rate of $^{45}Ca^{2+}$ accumulation than those incubated in the absence of the ion (figure 37), and the probable reason for this will be explained later in this section.

### 3.4.5. The effects of pre-incubation in replete media on the rate of accumulation of $^{45}Ca^{2+}$ following permeabilization of erythrocytes with ionomycin

The divalent cation ionophore A23187 is an antibiotic which partitions into cell membranes and facilitates the exchange of $H^+$ and $Ca^{2+}$ with an ionophore:cation mole ratio of 2:1 (Reed and Lardy, 1972, Pressman, 1976). It is possible that the reduced A23187-mediated $Ca^{2+}$ flux observed in incubated erythrocytes is the result of the ionophore becoming less effective as an ion carrier in these cells. To examine whether this effect of pre-incubation reflects a particular molecular property of A23187, morphological and $^{45}Ca^{2+}$

influx experiments were carried out using another calcium ionophore; ionomycin. This is also an ionophorous antibiotic with a preference for binding divalent cations, especially $Ca^{2+}$ (Liu and Hermann, 1978). However, in contrast to A23187, ionomycin transports calcium ions with an ionophore:cation mole ratio of 1:1, and therefore possesses different molecular properties (Liu and Hermann, 1978).

Figure 39 shows a comparison of the rate of total echinocytosis between cells treated with 150µM calcium and 3µM ionomycin immediately after cell preparation and after 6 hours incubation in buffer A at 37°C. There is no consistent significant difference between the rate of total echinocytosis under these two conditions. In addition when the rate of formation of different echinocyte stages was examined a very similar pattern was observed in cells loaded with calcium before and after incubation. It appears that pre-incubation does not significantly slow the progression of the calcium induced morphological transition when ionomycin rather than A23187 is used to facilitate calcium entry. Because of this it is unlikely that the maintenance of erythrocytes in replete media at 37°C causes a general reduction in the calcium-sensitivity of the physiological processes initiated during echinocytosis, as suggested in hypothesis (iii) above.

Interestingly, further investigations shown in figure 40, comparing the rate of accumulation of $^{45}Ca^{2+}$ in

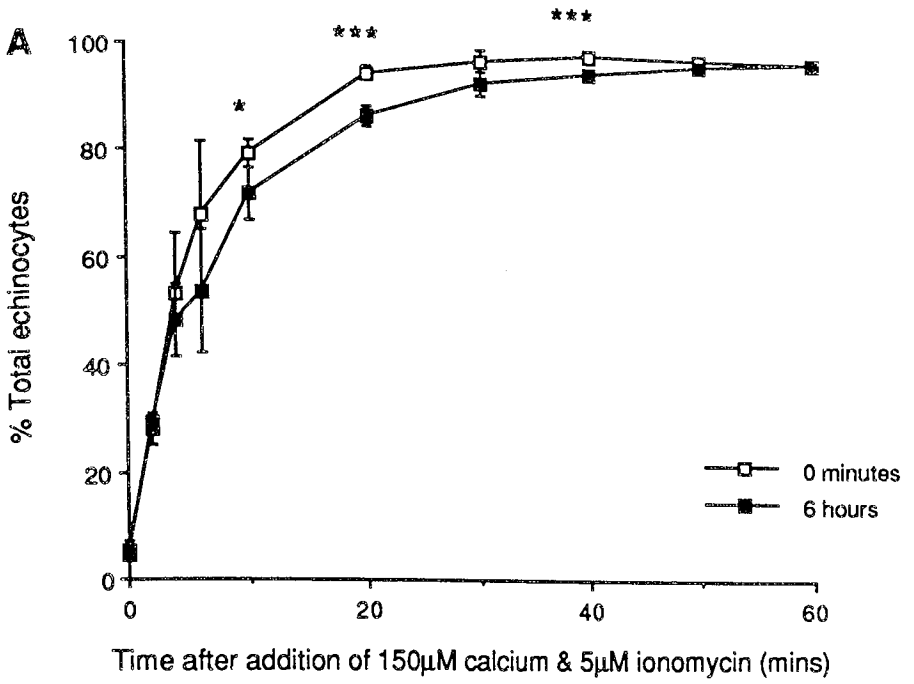


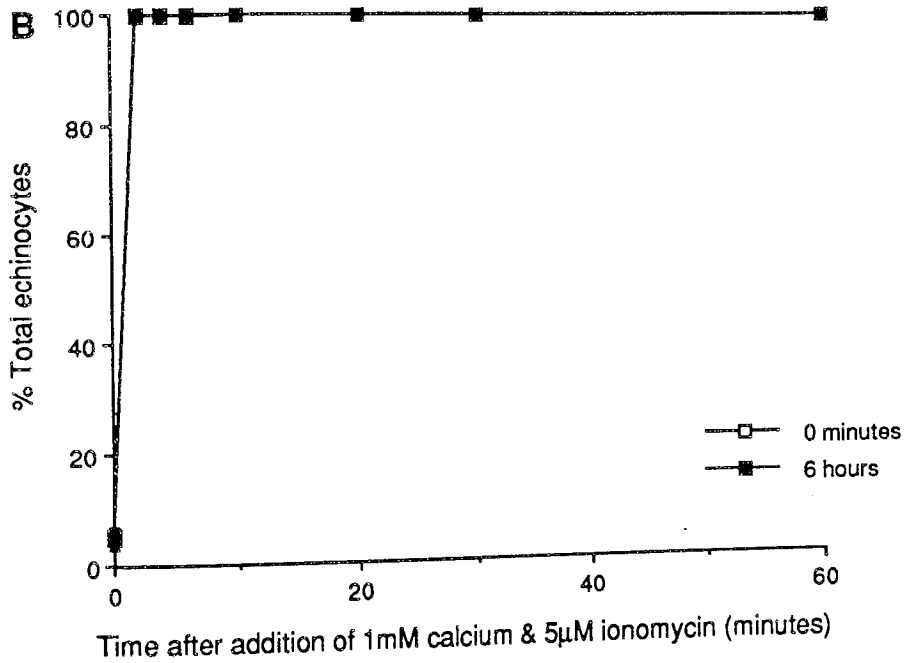


**FIGURE 39** Comparison of the time-course of echinocytosis before and after 6 hours incubation in buffer A when ionomycin is used to initiate calcium entry

Human erythrocytes held in buffer A were treated with calcium and 5µM A23187 either immediately after preparation or after 6 hours incubation at 37°C.

A 150µM calcium. Results expressed as mean ±SD, n=6

B 1mM calcium. Results expressed as mean ±SD, n=6

*=P<0.05, ***=P<0.001 when mean values at 0 minutes and 6 hours compared using Student T test.

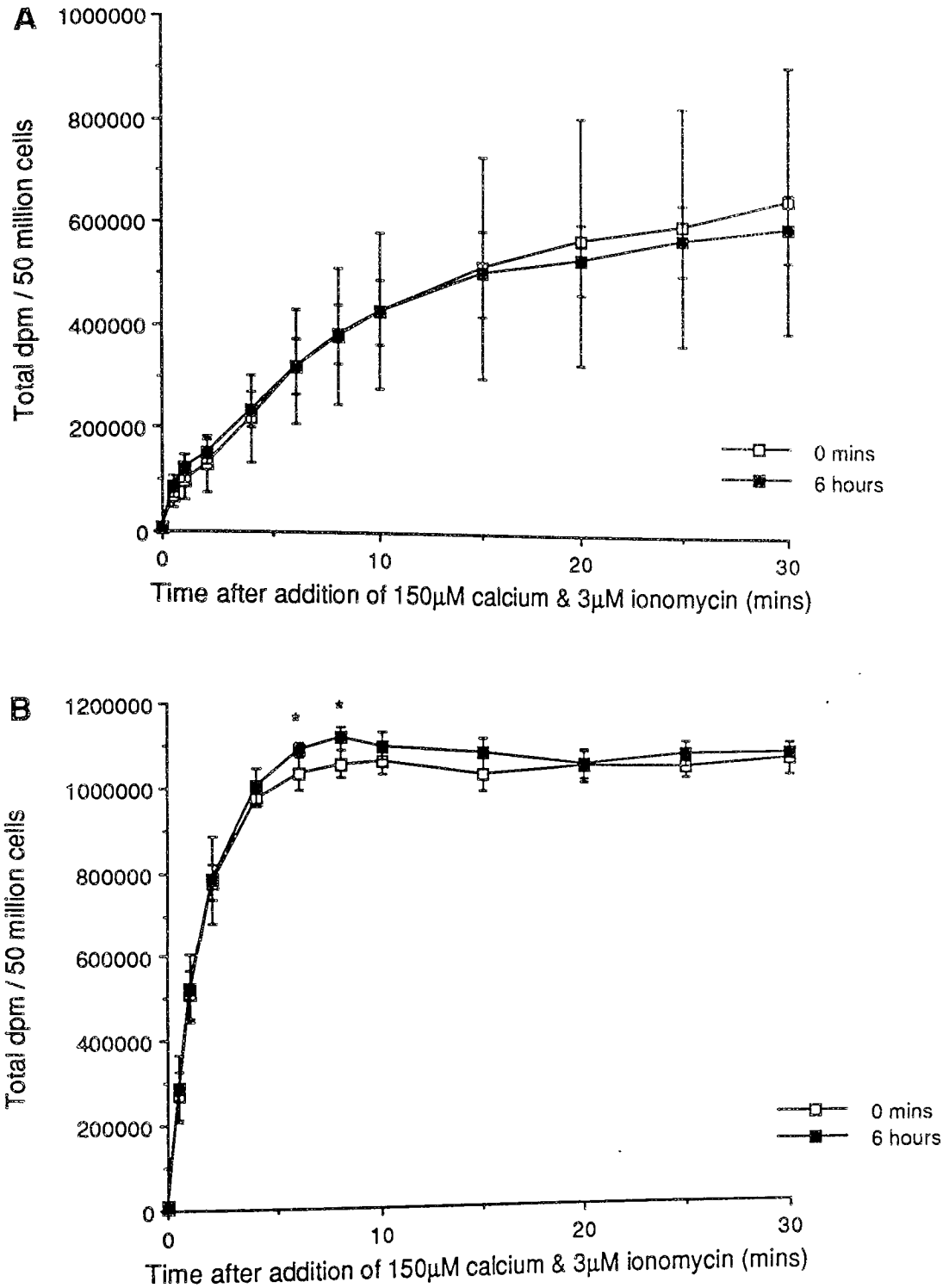


**FIGURE 40** The rate of accumulation of $^{45}Ca^{2+}$ during the treatment of erythrocytes with calcium and ionomycin before and after 6 hours incubation in buffer A

Human erythrocytes held in buffer A were permeabilized to either 150µM calcium or 1mM by 3µM ionomycin in the presence of $^{45}Ca^{2+}$. At the time intervals specified samples were analysed for their content of the radioisotope. Isotope accumulation was compared in cells immediately after preparation, and after 6 hours incubation at 37°C. Results expressed as mean ± SD, n= 6. All P values calculated by comparison of mean values using Student T test, *=P<0.05 mins
A 150µM calcium B 1mM calcium

in ionomycin permeabilized cells before and after pre-incubation complemented these results. The rate of accumulation of the radioisotope during calcium loading with both 150μM and 1mM in the presence of 3μM ionomycin was almost identical in cells treated immediately after preparation and cells treated after a 6 hour incubation in buffer A at 37°C.

It appears that the reduced rate of calcium accumulation resulting from the incubation of erythrocytes in replete media is dependent on the ionophore used to initiate calcium entry. Incubation has no significant effect on the ionophorous properties of ionomycin, suggesting that the differences observed with A23187 are related to the properties of this ionophore. A23187-induced permeability is known to be strongly dependent on both temperature and pH (Liu and Hermann, 1978, Lew, 1990), however, after testing, both of these environmental factors were found to be unchanged throughout the course of the experiments described. Since $Ca^{2+}$ permeability is dependent on ionophore concentration (Lew and Simonsen, 1980), another possible reason for the reduced ion fluxes observed in incubated erythrocytes was that fewer A23187 molecules become incorporated into the membranes of these cells. When added to intact fresh human red cells, A23187 accumulates in the cells with a partition ratio of about 60 to 1 (Lew and Simonsen, 1980), a reduction in this following incubation would lower the

number of molecules available for calcium transport. Because A23187 is known to bind to the protein albumin (Simonsen, 1981), it was thought possible that it may also bind to the haemoglobin released from the cells disrupted during the incubation period. Although it has been shown that the number of cells lost through haemolysis is insignificant to the results of the morphological studies described, it is possible that the cell proteins released are in sufficient concentration to bind a proportion of the ionophore. To test this hypothesis a comparison was made between the rate of total echinocyte formation in cells held in buffer A and then treated with calcium and A23187 in either fresh media or the media in which they were incubated.

For the experiment shown in figure 41 duplicate preparations of erythrocytes were maintained in buffer A at 37$^{o}$C for 6 hours and, after centrifugation and removal of the supernatant the cells were either resuspended back into the media which had just been removed or into fresh buffer A at 37$^{o}$C. The progression of total time-dependent echinocytosis induced by 150uM calcium in the presence of 5μM A23187 was then examined. In incubated cells loaded with 150μM calcium in fresh buffer the rate of echinocytosis is not significantly different to that observed in cells treated with 150μM calcium and 5μM A23187 immediately after preparation. In addition, when the rate of formation of different stage echinocytes was examined

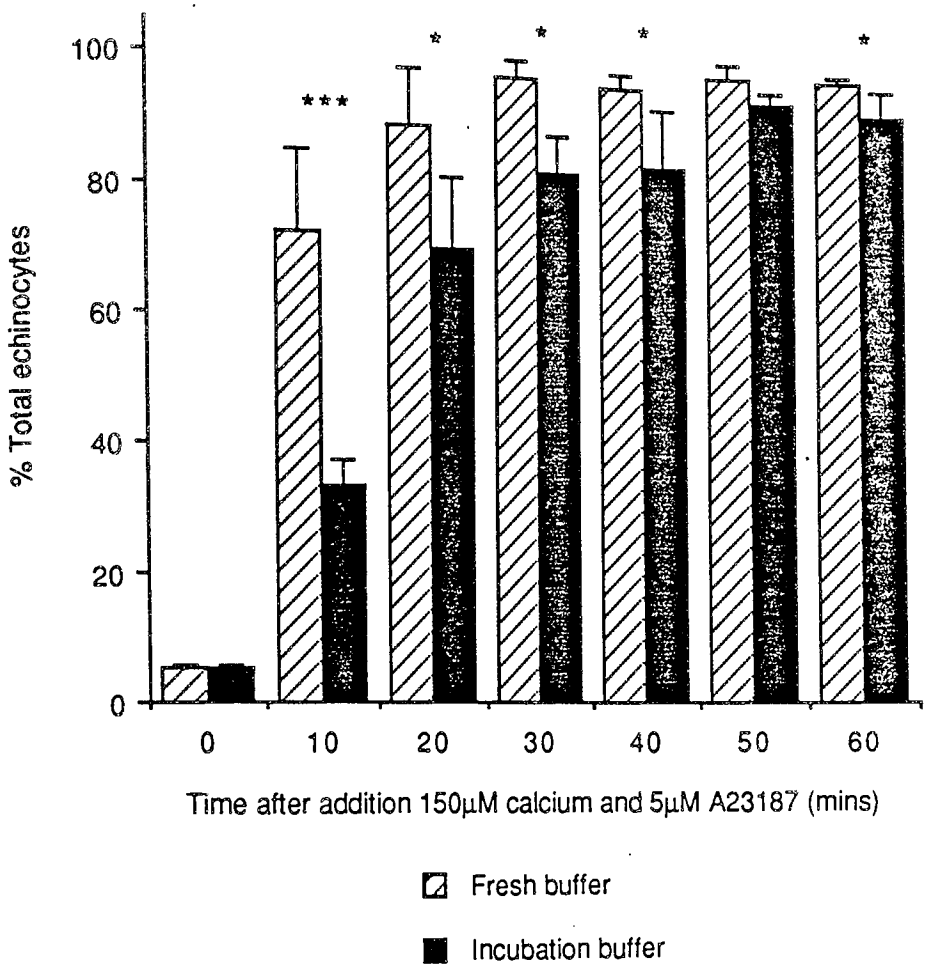


**FIGURE 41** Comparison of the time-course of echinocytosis in erythrocytes incubated in buffer A for 6 hours at 37°C and then resuspended in either fresh buffer or the buffer used for incubation, before treatment with 150µM calcium.
Human erythrocytes were held in buffer A for 6 hours at 37°C. After centrifugation the cells were either resuspended in fresh buffer or alternatively replaced into the buffer sample in which the incubation was performed. Both cell populations were then treated with 150uM calcium and 5uM A23187. Results expressed as mean ± SD, n=4. P values calculated by comparison of the mean values using Student T test, *=P<0.05, ***=P<0.005

(data not shown) a very similar progression was observed in cells treated with 150μM calcium and 5μM A23187 under these two conditions. However, at each time point studied the percentage of total echinocytes is significantly lower in cells treated with 150μM calcium and 5uM A23187 in incubation buffer compared to those treated in fresh buffer. An examination of the rate of formation of echinocyte stages under the former conditions indicates that the shape transition induced is almost exclusively to stage 1 echinocytes: a pattern comparable to that induced by identical calcium loading conditions in cells incubated for 6 hours in replete media (figure 35).

### 3.4.6. Discussion

It appears that the significant reduction in the rate of calcium-induced echinocytosis observed in erythrocytes held in replete media for 6 hours at 37°C is the result of an experimental artifact. Although only 1.5-2% of the cells in a preparation are lost through haemolysis during a 6 hour incubation it is likely that the cell protein released is in sufficient concentration to bind to a proportion of the A23187 added to facilitate calcium permeabilization. Therefore cells loaded with calcium in the same buffer in which they were incubated are less permeable to calcium than cells in fresh buffer and the reduced rate of calcium influx leads to a reduced rate of morphological transition. Interestingly, in the $^{45}Ca^{2+}$

influx experiments, cells incubated with extracellular calcium had a greater rate of calcium accumulation than those without, suggesting that the presence of calcium reduces the rate of spontaneous haemolysis.

The results obtained in this section do indicate the experimental problems that can be associated with the long term incubation of erythrocytes in replete media. In studies where incubation is followed by an examination of the physiological effects of calcium loading cells must be carefully washed free of protein or the choice of ionophore must be considered.

# CHAPTER FOUR: CONCLUSIONS

The control of the morphology of the human erythrocyte both at rest and during transient or permanent shape alterations is thought to be conferred jointly by the plasma membrane and the associated cytoskeleton (Elgsaeter et al., 1986, Steck, 1989), although the molecular basis of shape control is still unclear. The study presented here involved a detailed in vitro investigation of the underlying mechanisms associated with the morphological transition of erythrocytes from the resting discocyte to the crenated echinocyte form. Echinocytosis was initiated by a rise in intracellular calcium which is known to stimulate a range of biochemical processes in human erythrocytes. The results of the experimental studies were presented and discussed in relation to the biochemical mechanisms which may be involved in the loss of the discocyte morphology and the progression of echinocytosis induced by the elevation of intracellular calcium.

One such biochemical consequence of a rise in cytosolic calcium is known to be the cleavage of erythrocyte cytoskeletal components (Anderson et al., 1977, Allen and Cadman, 1979, Siegel et al., 1980, Allan and Thomas, 1981, Lorand et al., 1983, Pontremoli et al., 1984, Grasso et al., 1986). Previously the possible relevance of these changes to alterations in cell morphology has not been fully investigated. However, the studies described in chapter 3 were planned to examine this possibility. The findings were consistent with the reports

mentioned above in that the loading of erythrocytes with calcium did stimulate proteolytic activity directed against cytoskeletal proteins, notably 2.1, 2.2 and 4.1. However, it was clear that at calcium loads of both 150μM and 1mM the rate of loss these cytoskeletal elements was independent of the rate of accompanying echinocytosis as estimated by the complete loss of the discoid morphology. A direct role for cytoskeletal proteolysis in the induction of calcium-induced echinocytosis therefore seemed unlikely.

This conclusion was further supported by the results of studies examining shape reversal from the echinocyte back to the discocyte morphology. Erythrocytes which had lost upto 50% of intact protein 4.1 and 30% of intact protein 2.1 were still capable of reverting from the sphereo-echinocyte to the discocyte morphology. Evidently the loss of considerable cytoskeletal integrity is not necessarily associated with the echinocyte morphology. Additionally studies involving the modulation of erythrocyte shape with wheat germ agglutinin indicated that pre-treatment with the lectin preserved the discocyte morphology despite continued cytoskeletal proteolysis.

In contrast, the loss of cytoskeletal integrity below a threshold level did appear to contribute to the inability of cells to undergo shape reversal. The loss of 80% of intact protein 4.1, 60% protein 2.1 and 30% protein 2.2 was associated with irreversible sphereo-echinocytosis. Interestingly, all three proteins provide linkages between

erythrocyte membrane and cytoskeletal network. Protein 4.1 associates with both the skeletal component spectrin (Ungewickell et al., 1979) and the cytoplasmic domain of several integral proteins (Anderson and Lovrien, 1984, Pasternack et al., 1985, Reid et al, 1990). Protein 2.2 is closely related to 2.1 (Luna et al., 1979, Yu and Goodman, 1979) and both are members of the family of ankyrins which link spectrin with the integral protein band 3 (Tyler etal., 1979, Bennett and Stenbuck, 1979). Protein 2.2 is reported to be an activated form of protein 2.1, presumably formed by site directed post-translational proteolysis or alternative mRNA splicing (Hall and Bennett, 1987). It has an increased affinity for spectrin compared to protein 2.1, and is capable of interacting with twice as many high affinity binding sites on anykrin-depleted inside-out membrane vesicles (Hall and Bennett, 1987).

The most likely explanation for the above results is that proteolysis is not itself instrumental in causing the echinocyte transition, but that the essentially irreversible cleavage of the critical bridging proteins 2.1, 2.2 and 4.1 does have profound effects on the ability of erythrocytes to undergo shape transformations. Irreversible shape changes may not associated with the cleavage of any one protein but with the cumulative loss of sites of membrane-cytoskeleton coupling below a threshold level. Severe echinocytosis is accompanied by the shedding of protein-free lipid vesicles, usually originating at the

tips of the spicules (Lutz et al., 1977, Allan and Thomas, 1980, Wagner et al., 1986, Liu et al., 1989). Electron microscope studies have indicated that vesicle formation in echinocytic erythrocyte ghosts is the result of the physical separation of the lipid membrane from the cytoskeleton at the base of the spicules (Liu et al., 1989). Thus it is clear that advanced echinocytosis is indeed accompanied by the dissociation of the membrane and cytoskeletal components.

It is evident that the loss of cytoskeletal integrity is not the only factor contributing to the inability of erythrocytes to undergo shape reversal from the sphereo-echinocyte form. Both the metabolic status of the cells during treatment with calcium and the availability of metabolic substrates during shape reversal also influenced the progression of shape reversal, clearly indicating that the ability of cells to resynthesize ATP was essential to their ability to regain the discoid form. It is possible that the extent of shape reversal was related to the amount of the cell adenine nucleotide pool irreversibly converted to IMP under conditions of ATP depletion, thus affecting the availability of adenine for the resynthesis of ATP (Almaraz et al., 1988).

The metabolic state of erythrocytes during loading with calcium was also found to influence the rate of progression of the cells through the morphology stages associated with echinocytosis, giving further support for

the role of processes dependent on metabolic energy in the control of cell morphology. Indeed, the importance of ATP in the control of erythrocyte shape has been discussed ever since a relationship between the two was first reported n the 1960's, (Nakao et al., 1960, 1961, Weed, 1969). In the results presented here a direct relationship between cell ATP levels and the degree of echinocytosis during calcium loading was not observed. A comparison of figures 13 and 16 illustrates that at the same cellular concentrations of ATP, cell populations with different morphological profiles were obtained. Similar conclusions have also been reached by other workers (Feo and Mohandas, 1977, Shimizu, 1988). Presumably although ATP concentration does not directly control cell shape, it is necessary for maintaining the integrity of energy-dependent cellular processes which are involved in the control of erythrocyte morphology.

One of the most interesting observations from these studies is that the shape transformation from the discocyte to the sphereo-echinocyte form may not be a simple switch from one to the other. Evidence suggests that the shape transition progresses through at least two distinct steps brought about through different biochemical mechanisms. It appears that the discocyte to stage 1 echinocyte transition is independent of the metabolic status of the cell, suggesting the involvement of processes which do not consume metabolic energy. Interestingly, the extent of the reverse shape transformation from the stage 1 echinocyte to

the discocyte form is also independent of metabolic status. In contrast, as indicated above the rate of progression of cells through the subsequent echinocyte stages is determined by their metabolic state; implying that ATP-dependent mechanisms are important for the transformation of essentially discoid stage 1 echinocytes to spherical cells. Previous workers have detailed ATP-dependent reversible shape changes in isolated erythrocyte cytoskeletons (Jinbu et al., 1984, 1984b). If these results are applicable to intact cells this would suggest that the ATP-dependent `rounding up' of erythrocytes from stage 1 echinocytes through stages 2, 3, and sphereo-echinocytes is mediated by energy-consuming modifications to the cytoskeletal network. Finally the possibility exists that membrane loss through microvesiculation observed during the final stages of sphereo-echinocyte formation is brought about by yet another biochemical process; physical separation of the membrane and cytoskeleton through the loss of sites of association, proteolysis may not necessarily cause this, but may compound it.

Discontinuity of the echinocytic shape transformation has also been noted in separate studies carried out in this laboratory, in which the shape transition was induced by the treatment of the cells with sodium fluoride (NaF) (Thompson, Whatmore and Hickman, personal communication.) The mechanisms by which this agent induces echinocytosis

echinocytosis are not fully understood. However, again the ATP requirement of the processes inducing the transformation of cells from the stage 1 echinocyte to a more spherical form differed from those inducing the loss of the discocyte morphology. This raises the possibilty that this step wise transition is common to echinocytosis induced by many agents, but is not distinguished by less subtle morphological studies.

Studies involving the mathematical and physical modelling of the erythrocyte membrane have indicated that the type of crenations observed in stage 1 echinocytes arise readily from a membrane with a negative intrinsic precurvature (Aldana et al., 1989). If the closely associated lipid bilayer and cytoskeleton forming the membrane of the intact erythrocyte have such intrinsic precurvature, as has been suggested by Elgsaeter et al. (1986) membrane crenation would also readily occur in the intact cell. Therefore during echinocytosis it is possible that any number of factors causing a disturbance in the intracellular homeostasis of discocytes could non-specifically result in membrane morphology changes leading to the formation of a stage 1 echinocyte. Following this, the more severe morphology changes associated with the transformation of cells to stages 2, 3, and sphereo-echinocytes could then be mediated by the activation of biochemical mechanisms inducing changes in the cytoskeletal network.

**Relevance of these findings to processes occurring in other cell types** Analogues of many erythrocyte cytoskeletal components have been discovered in non-erythroid cells (reviewed by Coleman et al., 1989). The similarity in spatial organisation of these proteins in both cell types does suggest that a greater understanding of the factors controlling erythrocyte shape may have some general relevance in cell biology.

However, it is difficult to imagine that the biochemical processes involved in shape change induced by the elevation cytosolic calcium in erythrocytes could play a role in non-erythroid cells under normal physiological conditions. Cytosolic free calcium levels in a range of nucleated cells has been estimated to be approximately 100-300nM (reviewed by Rasmussen and Waisman, 1983). Transient increases to approximately 1.0μM are associated with calcium fluxes during signal transduction (Rasmussen and Waisman, 1983). These levels are at least 10 fold lower than those required to induce shape changes in erythrocytes; 10-100μM (Sarkadi et al., 1976, Shimizu, 1988).

However, it is possible that the underlying biochemical processes inducing echinocytosis are related to those induced during the toxic injury to non-erythroid cells. In many nucleated cells an early consequence of toxic injury is an increase in cytosolic free calcium (Schanne et al., 1979, Jewell, et al., 1982). In some

cells this has been linked to the onset of cell surface morphology changes resulting in membrane `blebbing', which occurs in advance of cell death (Jewell et al., 1982, Lemasters, 1983). Orrenius and colleagues (1989), identified several possible biochemical mechanisms which were influenced by calcium and had the potential to induce surface blebbing. These included cytoskeleton weakening by calcium-activated proteases including the dissociation of membrane/cytoskeleton linkages, and also the calcium-activated attack of phospholipases on membrane lipids. All of these biochemical mechanisms have been suggested as contributing to the control of echinocytosis induced by calcium. Therefore, it is possible that a greater understanding of the principles governing the formation of spicules during echinocytosis in erythrocytes may clarify the events leading surface to `blebbing' associated with elevated calcium during the toxic cell death of some nucleated cells.

**Suggestions for future work** Evidently the results presented here do not provide conclusive information into the causative role of any one biochemical process in the progression of echinocytosis induced by calcium in human erythrocytes. However, the basic experimental design, relating the biochemical changes to the morphological transitions during shape change may provide a useful basis for future work. Athough specific information on

erythrocyte biochemical processes obtained from *in vitro* studies and the examination of erythrocytes ghosts is growing, the relevance of these findings to the intact cell is still not known. Until such a time, studies such as those described here on intact cells probably provide the most relevant insights into the changes occurring in the erythrocyte during echinocytosis.

One area for future work could be an examination of the role of the membrane inositol phospholipids in erythrocyte shape. A specific functional pool of PtdIns(4,5)$P_2$ in the inner surface of the plasma membrane may be important in the control of erythrocyte morphology (Thompson et al., 1987). Membrane levels of PtdIns(4,5)$P_2$ are also known to modulate the activity of the erythrocyte enzyme, casein kinase I (Bazenet et al., 1990, Brockman and Anderson, 1991). In addition both the association of protein 4.1 with glycophorin A (Anderson and Marchesi, 1985) and the rates of lateral diffusion of integral proteins (Sheetz et al., 1982) are influenced by PtdIns(4,5)$P_2$.

The loading of erythrocytes with calcium induces the cleavage of certain pools of PtdIns(4,5)$P_2$ by PLC (Downes and Michell, 1981). Since erythrocytes are unable to resynthesize this lipid following cleavage (Percy et al., 1973) a calcium load would be expected to irreversibly deplete the cells of a proportion of total PtdIns(4,5)$P_2$. Additionally, the metabolic status of the cell influences

membrane levels of the lipid since it is subject to continual cycles of phosphorylation and dephosphorylation (Berridge 1982). It should be possible to subject cells to repeated cycles of echinocytosis induced by calcium followed by shape reversal, measuring the membrane levels of the lipid after each shape transformation. If PtdIns(4,5)$P_2$ is indeed pivotal to the ability of erythrocytes to change shape the eventual depletion of this lipid would be expected to be associated with the inability of erythrocytes to undergo shape transformations.

The possibility also exists that critical phosphorylation/dephosphorylation reactions involving either cytoskeletal proteins or membrane lipids are responsible for the control of erythrocyte shape, although to date no such evidence has been found. A detailed examination of phosphorylation patterns during cycles of discocyte - echinocyte transformation may also provide a basis for further study.

Finally, although the biochemical effects of WGA binding on the modulation of the echinocytic shape transformation are not fully understood it is possible that binding of the lectin does affect a critical biochemical step in the induction of the morphology change. Further investigations into possible biochemical changes induced in erythrocytes treated with WGA, loaded with calcium, and then examined before and after the addition of NAG, may prove useful.

# CHAPTER FIVE: REFERENCES

ADAIR, W. L., and KORNFELD, S. (1974) Isolation of the receptors for wheat germ agglutinin and the Ricinus communis lectins from human erythrocytes using affinity chromatography. J. Biol. Chem. **249**, 4696-4704.

AGRE, P., and BENNETT, V. (1988) Quantitative and functional analyses of spectrin, ankyrin, band 3, and calmodulin in human red cell membranes. In: Red Cell Membranes. Shohet, S. B., and Mohandas, N, (Eds) Churchill Livingstone, pp95-133.

ALDANA, D. H., BRAILSFORD, J. D., and BULL, B. S. (1989) Red cell membrane crenation: A macromodel of the echinocyte 1. J. Theor. Biol. **140**, 185-192.

AL-JOBORE, A., MINOCHERHOMJEE, A. M., VILLALOBO, A., and ROUFOGALIS, B. D. (1984) Active calcium transport in normal and abnormal human erythrocytes. In: Erythrocyte Membranes 3: Recent Clinical and Experimental Advances. Alan R. Liss, Inc., New York, pp243-292.

ALLAN, D., and MICHELL, R. H. (1975) Accumulation of 1,2-diacylglycerol in the plasma membrane may lead to echinocyte transformation of erythrocytes. Nature **258**, 348-349.

ALLAN, D., and THOMAS, P. (1981) $Ca^{2+}$-induced biochemical changes in human erythrocytes and their relation to microvesiculation. Biochem J. **198**, 433-440.

ALLAN, D., THOMAS, P., and MICHELL, R. H. (1978) Rapid transbilayer diffusion of 1,2-diacylglycerol and its relevance to control of membrane curvature. Nature **276**, 289-290.

ALLEN, D. W., and CADMAN, S. (1979) Calcium-induced erythrocyte membrane changes. The role of adsorption of cytosol proteins and proteases. Biochim. Biophys. Acta **551**, 1-9.

ALMARAZ, L., GARCIA-SANCHO, J., and LEW, V. L. (1988) Calcium-induced conversion of adenine nucleotides to inosine monophosphate in human red cells. J. Physiol. **407**, 557-567.

ANDERSON, D. R., DAVIS, J. L., and CARRAWAY, K. L. (1977) Calcium-promoted changes of the human erythrocyte membrane. J. Biol. Chem. **252**, 6617-6623.

ANDERSON, J. M., and TYLER, J. M. (1980) State of spectrin phosphorylation does not affect erythrocyte shape or spectrin binding to erythrocyte membranes. J. Biol. Chem. **255**, 1259-1265.

ANDERSON, J. P., and MORROW, J. S. (1987) The interaction of calmodulin with human erythrocyte spectrin. J. Biol. Chem. **262**, 6365-6372.

ANDERSON, R. A., and LOVRIEN, R. E. (1981) Erythrocyte membrane sidedness in lectin control of the $Ca^{2+}$-A23187-mediated discocyte=echinocyte conversion. Nature **292**, 158-161.

ANDERSON, R. A., and LOVRIEN, R. E. (1984) Glycophorin is linked by band 4.1 protein to the human erythrocyte membrane skeleton. Nature **307**, 655-658.

ANDERSON, R. A., and MARCHESI, V. T. (1985) Regulation of the association of membrane skeletal protein 4.1 with glycophorin by a polyphosphoinositide. Nature **318**, 295-298.

ASTER, J. C., BREWER, G. J., MAISEL, H. (1986) The 4.1-like proteins of the bovine lens: Spectrin-binding proteins closely related in structure to red blood cell protein 4.1. J. Cell Biol. **103**, 115-122.

BACKMAN, L. (1986) Shape control in the human red cell. J. Cell Sci. **80**, 281-298.

BACKMAN, L. (1988) Functional or futile phosphorus? Nature **334**, 653-654.

BAZENET, C. E., BROCKMAN, J. L., LEWIS, D., CHAN, C., and ANDERSON, R. A. (1990) Erythroid membrane-bound protein kinase binds to a membrane component and is regulated by phosphatidylinositol 4,5-bisphosphate. J. Biol. Chem. **265**, 7369-7376.

BENNETT, V. (1979) Immunoreactive forms of human erythrocyte ankyrin are present in diverse cells and tissues. Nature **281**, 597-599.

BENNETT, V. (1985) The membrane skeleton of human erythrocytes and its implications for more complex cells. Ann. Rev. Biochem. **54**, 273-304.

BENNETT, V. (1989) The spectrin-actin junction of erythrocyte membrane skeletons. Biochim. Biophys. Acta **988**, 107-121.

BENNETT, V., DAVIS, J., and FOWLER, W. E. (1982) Brain spectrin, a membrane-associated protein related in structure and function to erythrocyte spectrin. Nature **299**, 126-131.

BENNETT, V., GARDNER, K., and STEINER, J. P. (1988) Brain adducin: A protein kinase C substrate that may mediate

site-directed assembly at the spectrin-actin junction. J. Biol. Chem. **263**, 5860-5869.

BENNETT, V., and STENBUCK, P.J. (1979) The membrane attachment protein for spectrin is associated with band 3 in human erythrocyte membranes. Nature **280**, 468-473.

BENNETT, V., and STENBUCK, P. J. (1980) Association between ankyrin and the cytoplasmic domain of band 3 isolated from the human erythrocyte membrane. J. Biol. Chem. **255**, 6424-6432.

BERRIDGE, M. J. (1984) Inositol trisphosphate and diacylglycerol as second messengers. Biochem. J. **220**, 345-360.

BERRIDGE, M. J. (1987) Inositol trisphosphate and diacylglycerol: Two interacting second messengers. Ann. Rev. Biochem. **56**, 159-193.

BESSIS, M. (1973) Living blood cells and their ultrastructure. Springer-Verlag, New York.

BIRCHMEIER, W., and SINGER, S. J. (1977) On the mechanism of ATP-induced shape changes in human erythrocyte membranes. II. The role of ATP. J. Cell Biol. **73**, 647-659.

BOIVIN, P. (1988) Role of the phosphorylation of red blood cell membrane proteins. Biochem. J. **256**, 689-695.

BOIVIN, P., GALAND, C., and DHERMY, D. (1990) In vitro digestion of spectrin, protein 4.1 and ankyrin by erythrocyte calcium dependent neutral protease (calpain I). Int. J. Biochem. **22**, 1479-1489.

BRADFORD, M. M. (1976) A rapid and sensitive method for the quantitation of microgram quantities of protein utilizing the principle of protein-dye binding. Anal. Biochem. **72**, 248-245.

BROCKMAN, J. L. and ANDERSON, R. A. (1991) Casein kinase I is regulated by phosphatidylinositol 4,5-bisphosphate in native membranes. J. Biol. Chem. **266**, 2508-2512.

BROWN, A. M., and JOHNSTON, M. J. (1983) Stimulation of lactate production by Ca + ionophore A23187 in inosine-fed human red cells. J. Physiol. **341**, 63P.

BROWN, A. M., and LEW, V. L. (1983) The effect of intracellular calcium on the sodium pump of human red cells. J. Physiol. **343**, 455-493.

BURRIDGE, K., KELLY, T., and MANGEAT, P. (1982)

Nonerythrocyte spectrins: Actin-membrane attachment proteins occurring in many cell types. J. Cell Biol. **95**, 478-486.

BUTIKOFER, P., LIN, Z. W., CHIU, D. T.-Y., LUBIN, B., and KUYPERS, F. A. (1990) Transbilayer distribution and mobility of phosphatidylinositol in human red blood cells. J. Biol. Chem. **265**, 16035-16038.

BYERS, T. J., DUBREUIL, R., BRANTON, D., KIEHART, D. P., and GOLDSTEIN, L. S. B. (1987) Drosophila spectrin. II. Conserved features of the alpha-subunit are revealed by analysis of cDNA clones and fusion proteins. J. Cell Biol. **105**, 2103-2110.

CARAFOLI, E. (1987) Intracellular calcium homeostasis. Ann. Rev. Biochem. **56**, 395-433.

CARAFOLI, E., ZURINI, M., NIGGLI, V., and KREBS, J. (1982) The calcium-transporting ATPase of erythrocytes. Annals of N.Y. Acad. Sci. **402**, 305-326.

CHASIS, J. A., MOHANDAS, N., and SHOHET, S. B. (1985) Erythrocyte membrane rigidity induced by glycophorin A-ligand interaction. J. Clin. Invest. **75**, 1919-1926.

CHASIS, J. A., REID, M. E., JENSEN, R. H., and MOHANDAS, N. (1988) Signal transduction by glycophorin A: Role of extracellular and cytoplasmic domains in a modulatable process. J. Cell Biol. **107**, 1351-1357.

CHEUNG, W. Y. (1982) Calmodulin. Scientific American **246**, 62-70.

CHOQUETTE, D., HAKIM, G., FILOTEO, A. G., PLISHKER, G. A., BOSTWICK, J. R., and PENNISTON, J. T. (1984) Regulation of plasma membrane $Ca^{2+}$ ATPases by lipids of the phosphatidylinositol cycle. Biochem. Biophys. Res. Commun. **28**, 908-915.

COHEN, C. M., FOLEY, S. F., and KORSGREN, C. (1982) A protein immunologically related to erythrocyte band 4.1 is found on stress fibres of non-erythroid cells. Nature, **299**, 648-650.

COHEN, C. M., GUPTAROY, B., and FENNELL, R. (1990) Phosphorylation mediated associations of the red cell membrane skeleton. In: Cellular and Molecular Biology of Normal and Abnormal Erythroid Membranes. Cohen, C. M. and Palek, J. (Eds) Alan R. Liss, Inc. pp89-112,

COHEN, C. M., and LANGLEY, R. C. (1984) Functional characterization of human erythrocyte spectrin $\alpha$ and $\beta$ chains: Association with actin and erythrocyte protein 4.1.

Biochem. **23**, 4488-4495.

COHEN, C. M., TYLER, J. M., and BRANTON, D. (1980) Spectrin-actin associations studied by electron microscopy of shadowed preparations. Cell **21**, 875-883.

COLEMAN, T. R., FISHKIND, D. J., MOOSEKER, M. S., and MORROW, J. S. (1989) Functional diversity among spectrin isoforms. Cell Motility and the Cytoskeleton **12**, 225-247.

COLLIER, H. B., and LAM, A. (1970) Binding of $Ca^{2+}$ and $Mg^{2+}$ by 2,3-diphosphoglycerate. Biochim. Biophys. Acta **222**, 299-306.

CONBOY, J., KAN, Y. W., SHOHET, S. B., and MOHANDAS, N. (1986) Molecular cloning of protein 4.1, a major structural element of the human erythrocyte membrane skeleton. Proc. Natl. Acad. Sci. USA. **83**, 9512-9516.

CROALL, D. E. (1989) Proteolytic modification of calcium-dependent protease 1 in erythrocytes treated with ionomycin and calcium. Biochem. **28**, 6882-6888.

DAGHER, G., and LEW, V. L. (1988) Maximal calcium extrusion capacity and stoichiometry of the human red cell calcium pump. J. Physiol. **407**, 569-586.

DALE, G. L. and SUZUKI, T. (1988) Erythrocytes attached to a wheat germ agglutinin coated surface display an altered phospholipid metabolism. J. Cell. Biochem. **38**, 1-11.

DANILOV, Y. N., FENNELL, R., LING, E., and COHEN, C. M. (1990) Selective modulation of band 4.1 binding to erythrocyte membranes by protein kinase C. J. Biol. Chem. **265**, 2556-2562.

DANILOV, Y. N., and COHEN, C. M. (1989) Wheat germ agglutinin but not concanavalin A modulates protein kinase C-mediated phosphorylation of red cell skeletal proteins. FEBS Letters **257**, 431-434.

DAVIS, J. Q., and BENNETT, V. (1984) Brain ankyrin. J. Biol. Chem. **259**, 1874-1881.

DAVISON, M. D., and CRITCHLEY, D. R. (1988) Alpha-actinins and the DMD protein contain spectrin-like repeats. Cell **52**, 159-160.

DEDMAN, J. R., POTTER, J. D., JACKSON, R. L., JOHNSON, J. D., and MEANS, A. R. (1977) Physicochemical properties of rat testis $Ca^{2+}$-dependent regulator protein of cyclic nucleotide phosphodiesterase. J. Biol. Chem. **252**, 8415-8422.

DEUTICKE, B. (1968) Transformation and restoration of biconcave shape of human erythrocytes induced by amphiphilic agents and changes of ionic environment. Biochim. Biophys. Acta **163**, 494-500.

DEVAUX, P. F. (1991) Static and dynamic lipid asymmetry in cell membranes. Biochemistry **30**, 1163-1173.

DOWNES, C. P., and MICHELL, R. H. (1981) The polyphosphoinositide phosphodiesterase of erythrocyte membranes. Biochem. J. **198**, 133-140.

DRENCKHAHN, D., SCHLUTER, K., ALLEN, D. P., and BENNETT, V. (1985) Colocalization of band 3 with ankyrin and spectrin at the basal membrane of intercalated cells in the rat kidney. Science, **230**, 1287-1289.

EDER, P. S., SOONG, C.-J., and TAO, M. (1986) Phosphorylation reduces the affinity of protein 4.1 for spectrin. Biochemistry **25**, 1764-1770.

EDMONDSON, J. W., and LI, T.-K. (1976) The effects of ionophore A23187 on erythrocytes. Relationship of ATP and 2,3-diphosphoglycerate to calcium-binding capacity. Biochim. Biophys. Acta **443**, 106-113.

ELGSAETER, A., STOKKE, B. T., MIKKELSEN, A., and BRANTON, B. (1986) The molecular basis of erythrocyte shape. Science **234**, 1217-1223.

ENGELMANN, B., and DUHM, J. (1987) Intracellular calcium content of human erythrocytes: Relation to sodium transport systems. J. Membrane Biol. **98**, 79-87.

ENGELMANN, B., SCHUMACHER, U., and DUHM, J. (1990) Use of chlortetracycline fluorescence for the detection of Ca storing intracellular vesicles in normal human erythrocytes. J. Cell. Physiol. **143**, 357-363.

ENYEDI, A., FLURA, M., SARKADI, B., GARDOS, G., and CARAFOLI, E. (1987) The maximal velocity and the calcium affinity of the red cell calcium pump may be regulated independently. J. Biol. Chem. **262**, 6425-6430.

EVANS, E., and LEUNG, A. (1984) Adhesivity and rigidity of erythrocyte membrane in relation to wheat germ agglutinin binding. J. Cell Biol. **98**, 1201-1208.

FAIRBANKS, G., STECK, T. L., and WALLACH, D. F. H. (1971) Electrophoretic analysis of the major polypeptides of the human erythrocyte membrane. Biochemistry **10**, 2606-2616.

FALCHETTO, R., VORHERR, T., BRUNNER, J., and CARAFOLI, E. (1991) The plasma membrane $Ca^{2+}$ pump contains a site that

interacts with its calmodulin-binding domain. J. Biol. Chem. **266**, 2930-2936.

FEO, C. J., and LEBLOND, P. F. (1974) The discocyte -echinocyte transformation: Comparison of normal and ATP-enriched human erythrocytes. Blood **5**, 639-647.

FEO, C., and MOHANDAS, N. (1977) Clarification of role of ATP in red-cell morphology and function. Nature **265**, 166-168.

FERRELL, J. E., and HUESTIS, W. H. (1984) Phosphoinositide metabolism and the morphology of human erythrocytes. J. Cell Biol. **98**, 1992-1998.

FODER, B., and SCHARFF, O. (1981) Decrease of apparent calmodulin affinity of erythrocyte ($Ca^{2+}$ + $Mg^{2+}$)-ATPase at low $Ca^{2+}$ concentrations. Biochim. Biophys. Acta **649**, 367-376.

FOWLER, V. M. (1986) An actomyosin contractile mechanism for erythrocyte shape transformations. J. Cell. Biochem. **31**, 1-9.

FOWLER, V. M. (1990) Tropomodulin: A cytoskeletal protein that binds to the end of erythrocyte tropomyosin and inhibits tropomyosin binding to actin. J. Cell Biol. **111**, 471-482.

FOWLER, V. M., and BENNETT, V. (1984) Erythrocyte membrane tropomyosin. J. Biol. Chem. **259**, 5978-5989.

FRIEDERICHS, E., RADISCH, T., and WINKLER, H. (1989) Calcium content of the erythrocytes: A senstive and easy handling method for measuring free calcium ions, and modulation of the $Ca^{2+}$ ion concentration by the calcium antagonists nifedipine and pentoxifylline. Clin. Exper. Pharmacol. Physiol. **16**, 387-394.

FRIEDRICHS, B., KOOB, R., KRAEMER, D., and DRENCKHAHN, D. (1989) Demonstration of immunoreactive forms of erythrocyte protein 4.2 in nonerythroid cells and tissues. Eur. J. Cell Biol. **48**, 121-127.

GAFFNEY, J. (1985) Chemical and biochemical crosslinking of membrane components. Biochim. Biophys. Acta **822**, 298-317.

GARCIA-SANCHO, J., and LEW, V. L. (1988) Detection and separation of human red cells with different calcium contents following uniform calcium permeabilization. J. Physiol. **407**, 505-522.

GARCIA-SANCHO, J., and LEW, V. L. (1988a) Heterogeneous

calcium and adenosine triphosphate distribution in calcium-permeabilized human red cells. J. Physiol. **407**, 523-539.

GARCIA-SANCHO, J., and LEW, V. L. (1988b) Properties of the residual calcium pools in human red cells exposed to transient calcium loads. J. Physiol. **407**, 541-556.

GARDNER, K., and BENNETT, V. (1986) A new erythrocyte membrane-associated protein with calmodulin binding activity. J. Biol. Chem. **261**, 1339-1348.

GARDOS, G. (1958) The function of calcium in the potassium permeability of human erythrocytes. Biochim. Biochem. Acta **30**, 653-654.

GARRAHAN, P. J., and REGA, A. F. (1990) Plasma membrane calcium pump. In: Intracellular calcium regulation. F. Bronner (Ed.) Alan R. Liss, Inc., pp 271-303.

GASCARD, P., JOURNET, E., SULPICE, J.-C., and GIRAUD, F. (1989) Functional heterogeneity of polyphosphoinositides in human erythrocytes. Biochem. J. **264**, 547-553.

GIETZEN, K., TEJCKA, M., and WOLF, H. U. (1980) Calmodulin affinity chromatography yields a functional purified erythrocyte ($Ca^{2+}$ + $Mg^{2+}$)-dependent adenosine triphosphatase. Biochem. J. **189**, 81-88.

GLENNEY, J. R., Jr., GLENNEY, P., OSBORN, M., and WEBER, K. (1982) An F-actin- and calmodulin-binding protein from isolated intestinal brush borders has a morphology related to spectrin. Cell **28**, 843-854.

GOLDSCHMIDT-CLERMONT, P. J., MACHESKY, L. M., BALDASSARE, J. J., and POLLARD, T. D. (1990) The actin-binding protein profilin binds to $PIP_2$ and inhibits its hydrolysis by phospholipase C. Science **247**, 1575-1578.

GOODMAN, S. R., CASORIA, L. A., and COLEMAN, D. B. (1984) Identification and location of brain protein 4.1. Science **224**, 1433-1435.

GOODMAN, S. R., KREBS, K. E., WHITFIELD, C. F., RIEDERER, B. M., and ZAGON, I. S. (1988) Spectrin and related molecules. CRC Crit. Rev. Biochem. **23**, 171-234.

GOODMAN, S. R., and ZAGON, I. S. (1986) The neural cell spectrin skeleton: a review. Am. J. Physiol. **250**, C347-360.

GRASSO, M., MORELLI, A., and DE FLORA, A. (1986) Calcium-induced alterations in the levels and subcellular distribution of proteolytic enzymes in human red blood cells. Biochem. Biophys. Res. Commun. **138**, 87-94.

HALL, T. G., and BENNETT, V. (1987) Regulatory domains of erythrocyte ankyrin. J. Biol. Chem. **262**, 10537-10545.

HARMAN, A. W., NIEMINEN, A.-L., LEMASTERS, J. J., and HERMAN, B. (1990) Cytosolic free magnesium, ATP, and blebbing during chemical hypoxia in cultured rat hepatocytes. Biochem. Biophys. Res. Commun. **170**, 477-483.

HARRISON, D. G., and LONG, C. (1968) The calcium content of human erythrocytes. J. Physiol. **199**, 367-381.

HUSAIN, A., HOWLETT, G. J., SAWYER, W. H. (1985) The interaction of calmodulin with erythrocyte membrane proteins. Biochemistry International, **10**, 1-12.

HUSAIN-CHISHTI, A., LEVIN, A., and BRANTON, D. (1988) Abolition of actin-bundling by phosphorylation of human erythrocyte protein 4.9. Nature **334**, 719-721.

INOMATA, M., SAITO, Y., KON, K., and KAWASHIMA, S. (1990) Binding sites for calcium-activated neutral protease on erythrocyte membranes are not membrane phospholipids. Biochem. Biophys. Res. Commun. **171**, 625-632.

JAIN, S. K. (1988) Evidence for membrane lipid peroxidation during the *in vivo* aging of human erythrocytes. Biochim. Biophys. Acta **937**, 205-210.

JARRETT, H. W., and PENNISTON, J. T. (1978) Purification of the $Ca^{2+}$-stimulated ATPase activator from human erythrocytes. J. Biol. Chem. **253**, 4676-4682.

JENNINGS, M. L. (1989) Structure and function of the red blood cell anion transport protein. Ann. Rev. Biophys. Biophys. Chem. **18**, 397-430.

JEWELL, S. A., BELLOMO, G., THOR, H., and ORRENIUS, S. (1982) Bleb formation in hepatocytes during drug metabolism is caused by disturbances in thiol and calcium ion homeostasis. Science **217**, 1257-1259.

JINBU, Y., SATO, S., and NAKAO, M. (1984) Reversible shape change of Triton-treated erythrocyte ghosts induced by $Ca^{2+}$ and Mg-ATP. Nature **307**, 376-378.

JINBU, Y., SATO, S., NAKAO, T., NAKAO, M., TSUKITA, S., and ISHIKAWA, H. (1984a) The role of ankyrin in shape and deformability change of erythrocyte ghosts. Biochim. Biophys. Acta **773**, 237-245.

JINBU, Y., SATO, S., NAKAO, M., and TSUKITA, S. (1984b) $Ca^{2+}$-and Mg-ATP-dependent shape change of human erythrocyte ghosts and Triton shells. Exp. Cell Res. **151**, 160-170.

JINBU, Y., SATO, S., NAKAO, T., and NAKAO, M. (1982) Ankyrin is necessary for both drug-induced and ATP-induced shape change of human erythrocyte ghosts. Biochem. Biophys. Res. Commun. **104**, 1087-1092.

JOHNSON, P. (1990) Calpains (intracellular calcium -activated cysteine proteinases): Structure-activity relationships and involvement in normal and abnormal cellular metabolism. Int. J. Biochem. **22**, 811-822.

KARINCH, A. M., ZIMMER, W. E., and GOODMAN, S. R. (1990) The identification and sequence of the actin-binding domain of human red blood cell ß-spectrin. J. Biol. Chem. **265**, 11833-11840.

KAY, M. M. B., BOSMAN, G. J. C. G. M., JOHNSON, G. J., and BETH, A. H. (1988) Band-3 polymers and aggregates, and hemoglobin precipitates in red cell aging. Blood Cells **14**, 275-289.

KETIS, N. V., HOOVER, R. L., and KARNOVSKY, M. J. (1986) Isolation of bovine aortic endothelial cell plasma membranes: Identification of membrane-associated cytoskeletal proteins. J Cell. Physiol. **128**, 162-170.

KIM, H. D. (1990) Is adenosine a second metabolic substrate for human red blood cells? Biochim. Biophys. Acta **1036**, 113-120.

KING, C. E., STEPHENS, L. R., HAWKINS, P. T., GUY, G. R., and MICHELL, R. H. (1987) Multiple metabolic pools of phosphoinositides and phosphatidate in human erythrocytes incubated in a medium that permits rapid transmembrane exchange of phosphate. Biochem. J. **244**, 209-217.

KLEE, C. B., CROUCH, T. H., and RICHMAN, P. G. (1980) Calmodulin. Ann. Rev. Biochem. **49**, 849-515.

KORSGREN, C., and COHEN, C. M. (1988) Associations of human erythrocyte band 4.2. J. Biol Chem. **263**, 10212-10218.

KORSGREN, C., LAWLER. J., LAMBERT, S., SPEICHER, D., and COHEN, C. M. (1990) Complete amino acid sequence and homologies of human erythrocyte membrane protein band 4.2. Proc. Natl. Acad. Sci. USA **87**, 613-617.

KROCZEK, R. A., GUNTER, K. C., GERMAIN, R. N., and SHEVACH, E. M. (1986) Thy-1 functions as a signal transduction molecule in T lymphocytes and transfected B lymphocytes. Nature **322**, 181-184.

KUBOKI, M., ISHII, H., and KAZAMA, M. (1990)

Characterization of calpain I-binding proteins in human erythrocyte plasma membrane. J. Biochem. **107**, 776-780.

LAMBERT, S., YU, H., PRCHAL, J. T., LAWLER, J., RUFF, P., SPEICHER, D., CHEUNG, M. C., KAN, Y. W., and PALEK, J. (1990) cDNA sequence for human erythrocyte ankyrin. Proc. Natl. Acad. Sci. USA. **87**, 1730-1734.

LANGE, Y., HADESMAN, R. A., STECK, T. L. (1982) Role of the reticulum in the stability and shape of the isolated human erythrocyte membrane. J. Cell Biol. **92**, 714-721.

LASSING, I., and LINDBERG, U. (1985) Specific interaction between phosphatidylinositol 4,5-bisphosphate and profilactin. Nature **314**, 472-474.

LEMASTERS, J. J., DiGUISEPPI, J., NIEMINEN, A.-L., and HERMAN, B. (1987) Blebbing, free $Ca^{2+}$ and mitochondrial membrane potential preceding cell death in hepatocytes. Nature **325**, 78-81.

LEMASTERS, J. J., STEMKOWSKI, C. J., JI, S., and THURMAN, R. G. (1983) Cell surface changes and enzyme release during hypoxia and reoygenation in the isolated, perfused rat liver. J. Cell Biol. **97**, 778-786.

LEVINE, J., and WILLARD, M. (1981) Fodrin: Axonally transported polypeptides associated with the internal periphery of many cells. J. Cell Biol. **90**, 631-643.

LEW, V. L. (1990) Permeability and permeabilization of red cells to calcium. In: Intracellular calcium regulation. F Bronner (Ed.) Alan R. Liss, Inc. pp1-17.

LEW, V. L. and FERREIRA, H. G. (1978) Calcium transport and the properties of a calcium-activated potassium channel in red cell membranes. Current Topics in Membranes and Transport **10**, 217-277.

LEW, V. L., and GARCIA-SANCHO, J. (1989) Measurement and control of intracellular calcium in intact red cells. Methods in Enzynology **173**, 100-113.

LEW, V. L., HOCKADAY, A., SEPULVEDA, M.-I., SOMLYO, A. P., SOMLYO, A. V., ORTIZ, O. E., and BOOKCHIN, R. M. (1985) Compartmentalization of sickle-cell calcium in endocytic inside-out vesicles. Nature **315**, 586-589.

LEW, V. L., and SIMONSEN, L. O. (1980) Ionophore A23187 -induced calcium permeability of intact human red blood cells. J. Physiol. **308**, 60P.

LEW, V. L., TSIEN, R. Y., MINER, C., and BOOKCHIN, R. M. (1982) Physiological $[Ca^{2+}]_i$ level and pump-leak turnover

in intact red cells measured using an incorporated Ca chelator. Nature **298**, 478-481.

LING, E., DANILOV, Y. N., and COHEN, C. M. (1987) Regulation of red cell band 4.1 function by cAMP-dependent and Ca/phospholipid dependent phosphorylation. J. Cell Biol. **105**, 39a.

LIU, C.-M., and HERMANN, T. E. (1978) Characterization of ionomycin as a calcium ionophore. J. Biol. Chem. **253**, 5892-5894.

LIU, S.-C., DERICK, L. H., DUQUETTE, M. A., and PALEK, J. (1989) Separation of the lipid bilayer from the membrane skeleton during discocyte-echinocyte transformation of human erythrocyte ghosts. Eur. J. Cell Biol. **49**, 358-365.

LORAND, L., BJERRUM, O. J., HAWKINS, M., LOWE-KRENTZ, L., and SIEFRING, Jr., G. E. (1983) Degradation of transmembrane proteins in $Ca^{2+}$-enriched human erythrocytes. J. Biol. Chem. **258**, 5300-5305.

LOVRIEN, R. E., and ANDERSON, R. A. (1980) Stoichiometry of wheat germ agglutinin as a morphology controlling agent and as a morphology protective agent for the human erythrocyte. J. Cell Biol. **85**, 534-548.

LOW, P. S., WILLARDSON, B. M., MOHANDAS, N., ROSSI, M., and SHOHET, S. (1991) Contribution of the band 3-ankyrin interaction to erythrocyte membrane mechanical stability. Blood **77**, 1581-1586.

LU, P.-W., SOONG, C.-J., and TAO, M. (1985) Phosphorylation of ankyrin decreases its affinity for spectrin tetramer. J. Biol. Chem. **260**, 14958-14964.

LUNA, E. J., KIDD, G. H., and BRANTON, D. (1979) Identification by peptide analysis of the spectrin-binding protein in human erythrocytes. J. Biol. Chem. **254**, 2526-2532.

LUTHRA, M. G., and KIM, H. D. (1980) ($Ca^{2+}$ + $Mg^{2+}$)-ATPase of density-separated human red cells. Effects of calcium and a soluble cytoplasmic activator (calmodulin). Biochim. Biophys. Acta. **600**, 480-488.

LUTZ, H. U., LIU, S.-C., and PALEK, J. (1977) Release of spectrin-free vesicles from human erythrocytes during ATP depletion. J. Cell Biol. **73**, 548-560.

LUX, S. E., JOHN, K. M., and BENNETT, V. (1990) Analysis of cDNA for human erythrocyte ankyrin indicates a repeated structure with homology to tissue-differentiation and cell-cycle control proteins. Nature **344**, 36-42.

MANGEAT, P.-H. (1988) Interactions of biological membranes with the cytoskeletal framework of living cells. Biology of the Cell, **64**, 261-281.

MARCHESI, V. T. (1985) Stabilizing infrastructure of cell membranes. Ann. Rev. Cell Biol. **1**, 531-61.

McGOUGH, A. M., and JOSEPHS, R. (1990) On the structure of erythrocyte spectrin in partially expanded membrane skeletons. Proc. Natl. Acad. Sci. USA. **87**, 5208-5212.

McNAMARA, M. K., and WILEY, J. S. (1986) Passive permeability of human red blood cells to calcium. Am. J. Physiol. **250**, C26-C31.

MELLONI, E., SALAMINO, F., SPARATORE, B., MICHETTI, M., and PONTREMOLI, S. (1984) $Ca^{2+}$-dependent neutral proteinase from human erythrocytes: Activation by $Ca^{2+}$ ions and substrate and regulation by the endogenous inhibitor. Biochem. International **8**, 477-489.

MELLONI, E., SPARATORE, B., SALAMINO, F., MICHETTI, M., and PONTREMOLI, S. (1982) Cytosolic calcium dependent proteinase of human erythrocytes: Formation of an enzyme -natural inhibitor complex induced by Ca2+ ions. Biochem. Biophys. Res. Commun. **106**, 731-741.

MISCHE, S. M., MOOSEKER, M. S., AND MORROW, J. S. (1987) Erythrocyte adducin: A calmodulin-regulated actin-bundling protein that stimulates spectrin-actin binding. J. Cell Biochem. **105**, 2837-2845.

MONZON, C. M., PENNISTON, J. T., FAIRBANKS, V. F., and BURGERT, E. O. Jr. (1982) Erythrocytic calmodulin correlates with red cell age. Brit. J. Haematology **51**, 261-264.

MUALLEM, S., and KARLISH, S. J. D. (1982) Regulation of the $Ca^{2+}$-pump by calmodulin in intact cells. Biochim. Biophys. Acta **687** 329-332.

MUELLER, T. J., JACKSON, C. W., DOCKTER, M. E., and MORRISON, M. (1987) Membrane skeletal alterations during *in vivo* mouse red cell aging. J. Clin. Invest. **79**, 492-499.

MULLER, E., HEGEWALD, H., JAROSZEWICZ, K., CUMME, G. A., HOPPE, H., and FRUNDER, H. (1986) Turnover of phosphomonoester groups and compartmentation of polyphosphoinositides in human erythrocytes. Biochem. J. **235**, 775-783.

MURACHI, T. (1983) Calpain and calpastatin. Trends

Biochem. Sci. **8**, 167-169.

NAKAO, M., NAKAO, T., and YAMAZOE, S. (1960) Adenosine triphosphate and maintenance of shape of the human red cells. Nature **187**, 945-946.

NAKAO, M., NAKAO, T., YAMAZOE, S., and YOSHIKAWA, H. (1961) Adenosine triphosphate and shape of erythrocytes. J. Biochem. **49**, 487-492.

NELSON, G. A., ANDREWS, M. L., KARNOVSKY, M. J. (1983) Control of erythrocyte shape by calmodulin. J. Cell Biol. **96**, 730-735.

NICOTERA, P., HARTZELL, P., DAVIS, G., and ORRENIUS, S. (1986) The formation of plasma membrane blebs in hepatocytes exposed to agents that increase cytosolic $Ca^{2+}$ is mediated by the activation of a non-lysosomal proteolytic system. FEBS Letters **209**, 139-144.

NIEMINEN, A.-L., GORES, G. J., WRAY, B. E., TANAKA, Y., HERMAN, B., and LEMASTERS, J. J. (1988) Calcium dependence of bleb formation and cell death in hepatocytes. Cell Calcium **9**, 237-246.

NIGGLI, V., ADUNYAH, E. S., PENNISTON, J. T., and CARAFOLI, E. (1981) Purified ($Ca^{2+}$-$Mg^{2+}$)-ATPase of the erythrocyte membrane. J. Biol. Chem. **256**, 395-401.

OP DEN KAMP, J. A. F. (1979) Lipid asymmetry in membranes. Ann. Rev. Biochem. **48**, 47-71.

ORRENIUS, S., McCONKEY, D. J., BELLOMO, G., and NICOTERA, P. (1989) Role of $Ca^{2+}$ in toxic cell killing. Trends Pharmacol. Sci. **10**, 281-285.

PALEK, J., LIU, P. A., and LIU, S.C. (1978) Polymerisation of red cell membrane protein contributes to spheroechinocyte shape irreversibility. Nature **274**, 505-507.

PALEK, J., and LUX, S. E. (1983) Red cell membrane skeletal defects in hereditary and acquired hemolytic anemias. Semin. Hematol. **20**, 189-224.

PALMER, F. B. St. C. (1985) Polyphosphoinositide metabolism in aging human erythrocytes. Can. J. Biochem. Cell Biol. **63**, 927-931

PASTERNACK, G. R., ANDERSON, R. A., LETO, T. L., MARCHESI, V. T. (1985) Interactions between protein 4.1 and band 3. J. Biol. Chem. **260**, 3676-3683.

PASTERNACK, G. R., and RACUSEN, R. H. (1989) Erythrocyte

protein 4.1 binds and regulates myosin. Proc. Natl. Acad. Sci. USA **86**, 9712-9716.

PATEL, V. P., and FAIRBANKS, G. (1981) Spectrin phosphorylation and shape change of human erythrocyte ghosts. J. Cell Biol. **88**, 430-440.

PERCY, A. K., SCHMELL, E., EARLES, B. J., LENNARZ, W. J. (1973) Phospholipid biosynthesis in the membranes of immature and mature red blood cells. Biochemistry, **12**, 2456-2461.

PFEFFER, S. R., and SWISLOCKI, N.I. (1976) Age-related decline in the activities of erythrocyte membrane adenylate cyclase and protein kinase. Arch. Biochem. Biophys. **177**, 117-122.

POLLARD, T. D. (1984) Purification of a high molecular weight actin filament gelation protein from Acanthamoeba that shares antigenic determinants with vertebrate spectrins. J. Cell Biol. **99**, 1970-1980.

PONTREMOLI, S., and MELLONI, E. (1986) Extralysosomal protein degradaton. Ann. Rev. Biochem. **55**, 455-581.

PONTREMOLI, S., MELLONI, E., SALAMINO, B., SPARATORE, B., MICHETTI, M., BENATTI, U., MORELLI, A., and DE FLORA, A. (1980) Identification of proteolytic activites in the cytosolic compartment of mature human erythrocytes. Eur. J. Biochem. **110**, 421-430

PONTREMOLI, S., MELLONI, E., SPARATORE, B., MICHETTI, M., and HORECKER, B. L. (1984) A dual role for the $Ca^{2+}$-requiring proteinase in the degradation of hemoglobin by erythrocyte membrane proteinases. Proc. Natl. Acad. Sci. USA **81**, 6714-6717.

PONTREMOLI, S., MELLONI, E., SPARATORE, B., MICHETTI, M., SACCO, O., and HORECKER, B. L. (1985) Role of phospholipids in the activation of the $Ca^{2+}$-dependent neutral proteinase of human erythrocytes. Biochem. Biophys. Res. Commun. **129**, 389-395.

PONTREMOLI, S., SALAMINO, B., SPARATORE, B., MELLONI, E., MORELLI, A., BENATTI, U., and DE FLORA, A. (1979) Isolation and partial characterization of three acidic proteinases in erythrocyte membranes. Biochem J. **181**, 559-568.

PONTREMOLI, S., SALAMINO, F., SPARATORE, B., MICHETTI, M., SACCO, O., and MELLONI, E. (1985a) Following association to the membrane, human erythrocyte procalpain is converted and released as fully active calpain. Biochim. Biophys. Acta. **381**, 335-339.

PONTREMOLI, S., SPARATORE, B., MELLONI, E., MICHETTI, M., and HORECKER, B. L. (1984a) Activation by hemoglobin of the $Ca^{2+}$-requiring neutral proteinase of human erythrocytes: Structural requirements. Biochem. Biophys. Res. Commun. **123**, 331-337.

PORZIG, H., and STOFFEL, D. (1978) Equilibrium binding of calcium to fragmented human red cell membranes and its relation to calcium-mediated effects on cation permeability. J. Membrane Biol. **40**, 117-142.

PRESSMAN, B. C., and FAHIM, M. (1982) Pharmacology and toxicology of the monovalent carboxylic ionophores. Ann. Rev. Pharmacol. Toxicol. **22**, 465-490.

RASMUSSEN, H., and WAISMAN, D. M. (1983) Modulation of cell function in the calcium messenger system. Rev. Physiol. Biochem. Pharmacol. **95**, 111-148.

REED, P. W., and LARDY, H. A. (1972) A23187: A divalent cation ionophore. J. Biol. Chem. **247**, 6970-6977.

REID, M. E., CHASIS, J. A., and MOHANDAS, N. (1987) Identification of a functional role for human erythrocyte sialoglycoproteins ß and ɣ. Blood **69**, 1068-1072.

REID, M. E., TAKAKUWA, Y., CONBOY, J., TCHERNIA, G., and MOHANDAS, N. (1990) Glycophorin C content of human erythrocyte membrane is regulated by protein 4.1. Blood **75**, 2229-2234.

REINHART, W. H., SUNG, L. A., SCHUESSLER, G. B., and CHIEN, S. (1986) Membrane protein phosphorylation during stomatocyte-echincoyte transformation of human erythrocytes. Biochim. Biophys. Acta **862**, 1-7.

REPASKY, E. A., GRANGER, B. L., and LAZARIDES, E. (1982) Widespread occurrence of avian spectrin in nonerythroid cells. Cell **29**, 821-833.

RHODA, M. D., GIRAUD, F., CRAESCU, $C_{2+}$T., and BEUZARD, Y. (1985) Compartmentalization of $Ca^{2+}$ in sickle cells. Cell Calcium **6**, 397-411.

ROELOFSEN, B., and SCHATZMANN, $_{2+}$H. J. (1977) The lipid requirement of the ($Ca^{2+}$ + $Mg^{2+}$)-ATPase in the human erythrocyte membrane, as studied by various highly purified phospholipases. Biochim. Biophys. Acta **464**, 17-36.

ROSSI, J. P. F. C., and SCHATZMANN, $H_{2+}$ J. (1982) Trypsin activation of the red cell $Ca^{2+}$-pump ATPase is calcium-sensitive. Cell Calcium **3**, 583-590.

RUMSBY, M. G., TROTTER, J., ALLAN, D., and MICHELL, R. (1977) Recovery of membrane micro-vesicles from human erythrocytes stored for transfusion: A mechanism for the erythrocyte discocyte-to-spherocyte shape transformation. Biochemical Soc. Trans. **5**, 126-128.

RYBICKI, A. C., HEATH, R., WOLF, J. L., LUBIN, B., and SCHARTZ, R. S. (1988) Deficiency of protein 4.2 in erythrocytes from a patient with a Coombs negative hemolytic anemia. J. Clin. Invest. **81**, 893-901.

SARKADI, B., ENYEDI, A., FOLDES-PAPP, Z., and GARDOS, G. (1986) Molecular characterisation of the in situ red cell membrane calcium pump by limited proteolysis. J. Biol. Chem. **261**, 9552-9557.

SARKADI, B., SZASZ, I., and GARDOS, G. (1976) The use of ionophores of rapid loading of human red cells with radioactive cations for cation-pump studies. J. Membrane Biol. **26**, 357-370.

SCHANNE, F. A. X., KANE, A. B., YOUNG, E. E., FARBER, J. L. (1979) Calcium dependence of toxic cell death: A final common pathway. Science **206**, 700-702.

SCHARFF, O., and FODER, B. (1978) Reversible shift between two states of $Ca^{2+}$-ATPase in human erythrocytes mediated by $Ca^{2+}$ and a membrane-bound activator. Biochim. Biophys. Acta **509**, 67-77.

SCHATZMANN, H. J. (1983) The red cell calcium pump. Ann Rev. Physiol. **45**, 303-312.

SCHATZMANN, H. J., and BURGIN, H. (1978) Calcium in human red blood cells. Annals of N. Y. Acad. Sci **307**, 125-146.

SEAMON, K. B. (1980) Calcium-and magnesium-dependent conformational states of calmodulin as determined by nuclear magnetic resonance. Biochemistry **19**, 207-215.

SEARS, D. E., MARCHESI, V. T., and MORROW, J. S. (1986) A calmodulin and alpha-subunit binding domain in human erythrocyte spectrin. Biochim. Biophys. Acta **870**, 432-442.

SEIGNEURET, M., and DEVAUX, P. F. (1984) ATP-dependent asymmetric distribution of spin-labelled phoshpholipids in the erythrocyte membrane: Relation to shape changes. Proc. Natl. Acad. Sci. USA **81**, 3751-3755.

SHEETZ, M. P., FEBBRORIELLO, P., and KOPPEL, D. E. (1982) Triphosphoinositide increases glycoprotein lateral mobility in erythrocyte membranes. Nature **296**, 91-93.

SHEETZ, M. P., and SINGER, S. J. (1974) Biological

membranes as bilayer couples. A molecular mechanism of drug-erythrocyte interactions. Proc. Natl. Acad. Sci. USA. **71**, 4457-4461.

SHEETZ, M. P., and SINGER, S. J. (1976) Equilibrium and kinetic effects of drugs on the shapes of human erythrocytes. J. Cell Biol. **70**, 247-251.

SHEN, B. W., JOSEPHS, R., and STECK, T. L. (1986) Ultrastructure of the intact skeleton of the human erythrocyte membrane. J. Cell. Biol. **102**, 997-1006.

SHOTTON, D. M., BURKE, B. E., and BRANTON, D. (1979) The molecular structure of human erythrocyte spectrin. J. Mol. Biol. **131**, 303-329.

SIEGEL, D. L., and BRANTON, D. (1985) Partial purification and characterisation of an actin-bundling protein, band 4.9, from human erythrocytes. J. Cell. Biol. **100**, 775-785.

SIEGEL, D. L., GOODMAN, S. R., and BRANTON, D. (1980) The effect of endogenous proteases on the spectrin binding proteins of human erythrocytes. Biochim. Biophys. Acta **598**, 517-527.

SIMONSEN, L. O. (1981) Binding of ionophore A23187 by bovine plasma albumin. J. Physiol. **313**, 34P-35P.

SIMONSEN, L. O., GOMME, J., and LEW, V. (1982) Uniform ionophore A23187 distribution and cytoplasmic calcium buffering in intact red cells. Biochim. Biophys. Acta. **692**, 431-440.

SMITH, L., and HOCHMUTH, R. M. (1982) Effect of wheat germ agglutinin on the viscoelastic properties of erythrocyte membrane. J. Cell Biol. **94**, 7-11.

SOONG, C.-J., LU, P.-W., and TAO, M. (1987) Analysis of band 3 cytoplasmic domain phosphorylation and association with ankyrin. Arch. Biochem. Biophys. **254**, 509-517.

SPIEGEL, J. E., BEARDSLEY, D. S., SOUTHWICK, F. S., and LUX, S. E. (1984) An analogue of the erythroid membrane skeletal protein 4.1 in nonerythroid cells. J. Cell Biol. **99**, 886-893.

STECK, T. L. (1989) Red cell shape. In: Cell Shape: Determinants, regulation, and regulatory role. Stein, W. and Bronner, F. (Eds.) Academic Press, Inc. pp 205-246.

SUNG, L. A., CHIEN, S., CHANG, L.-S., LAMBERT, K., BLISS, S. A., BOUHASSIRA, E. E., NAGEL, R. L., SCHWARTZ, R. S., and RYBICKI, A. C. (1990) Molecular cloning of human

protein 4.2: A major component of the erythrocyte membrane. Proc. Natl. Acad. Sci. USA **87**, 955-959.

TAKAKUWA, Y., and MOHANDAS, N. (1988) Modulation of erythrocyte membrane material properties by $Ca^{2+}$ and calmodulin. J. Clin. Invest. **82**, 394-400.

TANAKA, T., KADOWAKI, K., LAZARIDES, E., and SOBUE, K. (1991) $Ca^{2+}$-dependent regulation of the spectrin/actin interaction by calmodulin and protein 4.1. J. Biol. Chem. **266**, 1134-1140.

TANG, K.-Y. (1988) An investigation of the effects of antitumour and other drugs on cell morphology and the cytoskeleton of erythrocytes. PhD Thesis. The University of Aston in Birmingham.

TAYLOR, D., BAKER, R., and HOCHSTEIN, P. (1977) The effect of calcium ionophore A23187 on the ATP level of human erythrocytes. Biochem. Biophys. Res. Commun. **76**, 205-211.

THOMPSON, M. G., CHAHWALA, S. B., and HICKMAN, J. A. (1987) Inhibition of human erythrocyte inositol lipid metabolism by Adriamycin. Cancer Res. **47**, 2799-2803.

TIFFERT, T., GARCIA-SANCHO, J., and LEW, V. L. (1984) Irreversible ATP depletion caused by low concentrations of formaldehyde and of calcium-chelator esters in intact human red cells. Biochim. Biophys. Acta **773**, 143-156.

TIFFERT, T., SPIVAK, J. L., and LEW, V. L. (1988) Magnitude of calcium influx required to induce dehydration of normal human red cells. Biochim. Biophys. Acta **943**, 157-165.

TYLER, J. M., HARGREAVES, W. R., and BRANTON, D. (1979) Purification of two spectrin-binding proteins: Biochemical and electron microscopic evidence for site-specific reassociation between spectrin and bands 2.1 and 4.1. Proc. Natl. Acad. Sci. USA **76**, 5192-5196.

UNGEWICKELL, E., BENNETT, P. M., CALVERT, R., OHANIAN, V., and GRATZER, W. B. (1979) *In vitro* formation of a complex between cytoskeletal proteins of the human erythrocyte. Nature **280**, 811-814.

UNGEWICKELL, E., and GRATZER, W. (1978) Self-association of human spectrin. Eur. J. Biochem. **88**, 379-385.

WAGNER, G. M., CHIU, D. T.-Y., YEE, M. C., and LUBIN B. H. (1986) Red cell vesiculation - a common membrane physiologic event. J. Lab. Clin. Med. **108**, 315-324.

WANG, K. W. K., VILLALOBO, A., and ROUFOGALIS, B. D. (1988) Activation of the $Ca^{2+}$-ATPase of human erythrocyte membrane by an endogenous $Ca^{2+}$-dependent neutral protease. Arch. Biochem. Biophys. **260**, 696-704.

WEED, R. I., LACELLE, P. L., and MERRILL. (1969) Metabolic dependence of red cell deformability. J. Clin. Invest. **48**, 795-809.

WHITE, J. G. (1974) Effects of an ionophore, A23187, on the surface morphology of normal human erythrocytes. Am. J. Path. **77**, 507-518.y

WINKELMANN, J. C., CHANG, J.-G., TSE, W. T., SCARPA, A. L., MARCHESI, V. T., and FORGET, B. G. (1990) Full-length sequence of the cDNA for human erythroid ß-spectrin. J. Biol. Chem. **265**, 11827-11832.

WONG, A. J., KIEHART, D. P., and POLLARD, T. D. (1985) Myosin from human erythrocytes. J. Biol. Chem. **260**, 46-49.

YONEZAWA, N., NISHIDA, E., IIDA, K., YAHARA, I., and SAKAI, H. (1990) Inhibition of the interactions of cofilin, destrin, and deoxyribonuclease I with actin by phosphoinositides. J. Biol. Chem. **265**, 8382-8386.

YU, J., FISCHMAN, D., A., and STECK, T. L. (1973) Selective solubilization of proteins and phospholipids from red blood cell membranes by nonionic detergents. J. Supramol. Struct. **1**, 233-248.

YU, J., and GOODMAN, S. R. (1979) Syndeins: The spectrin-binding protein(s) of the human erythrocyte membrane. Proc. Natl. Acad. Sci. **76**, 2340-2344.

# APPENDIX I: SHAPE REVERSAL FROM THE ECHINOCYTE FORM IN ERYTHROCYTE POPULATIONS ENRICHED IN EITHER YOUNG OR OLD CELLS

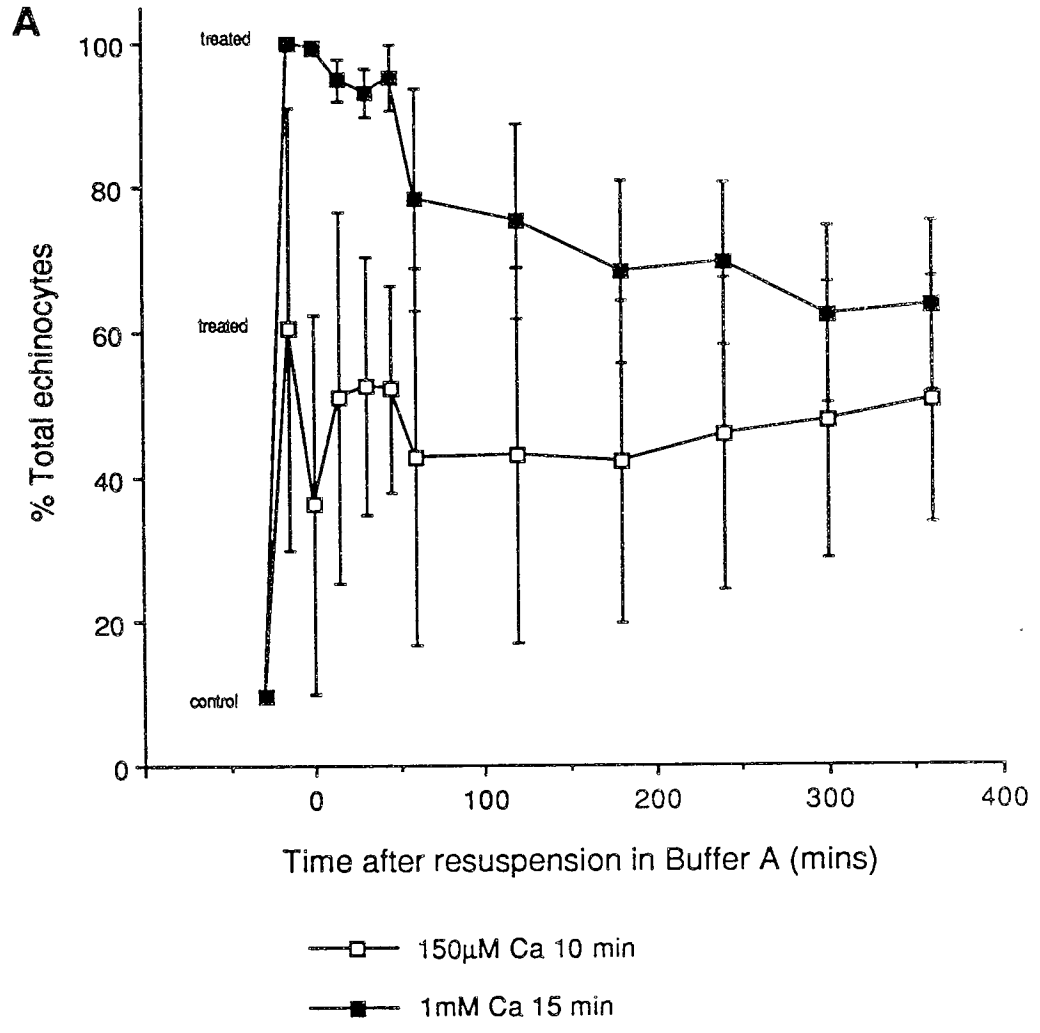


**Figure 42** The quantitation of cell morphologies during reversal from echinocytosis induced in an erythrocyte population enriched in young cells while held in buffer B; shape recovery attempted in buffer A.
Following density separation erythrocyte populations enriched in young cells and held in buffer B were loaded with either 150µM calcium for 10 minutes or 1mM calcium for 15 minutes. After removal of the calcium and A23187, cells were resuspended in buffer A and shape recovery examined by the quantitation of morphology at the time intervals specified.
**A** Total echinocyte levels. Results expressed as mean -SD (n=4).
**B** Analysis of the changes in the levels of different stage echinocytes in cells initially loaded with 150µM calcium. Results expressed as mean of n=4.
**C** Analysis of the changes in the levels of different stage echinocytes in cells initially loaded with 1mM calcium. Results expressed as mean of n=4.

**42B**

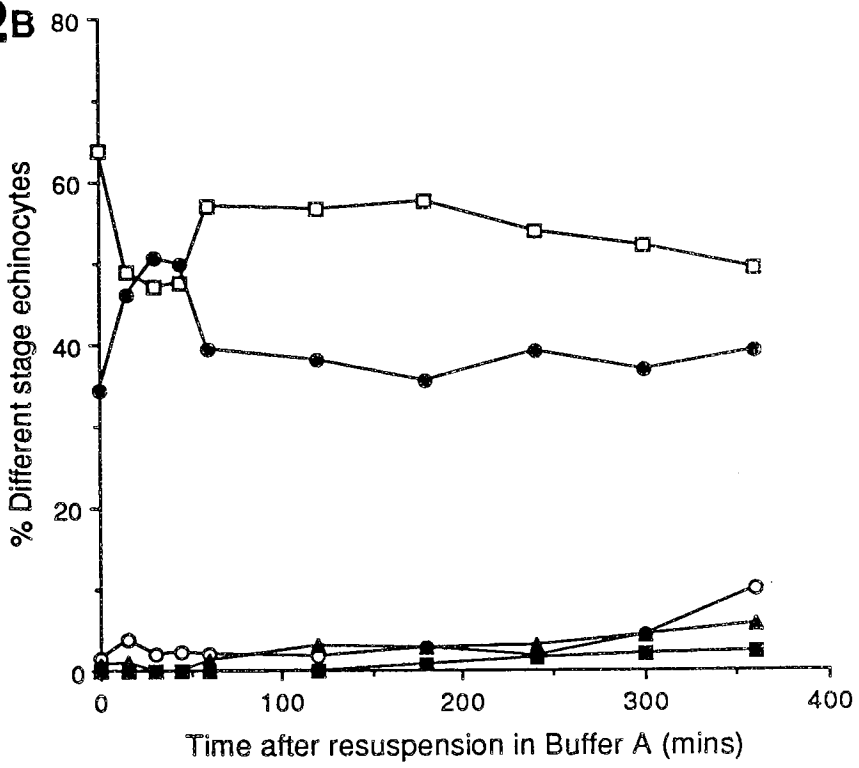
% Different stage echinocytes
0
20
40
60
80
0
100
200
300
400
Time after resuspension in Buffer A (mins)

**42C**

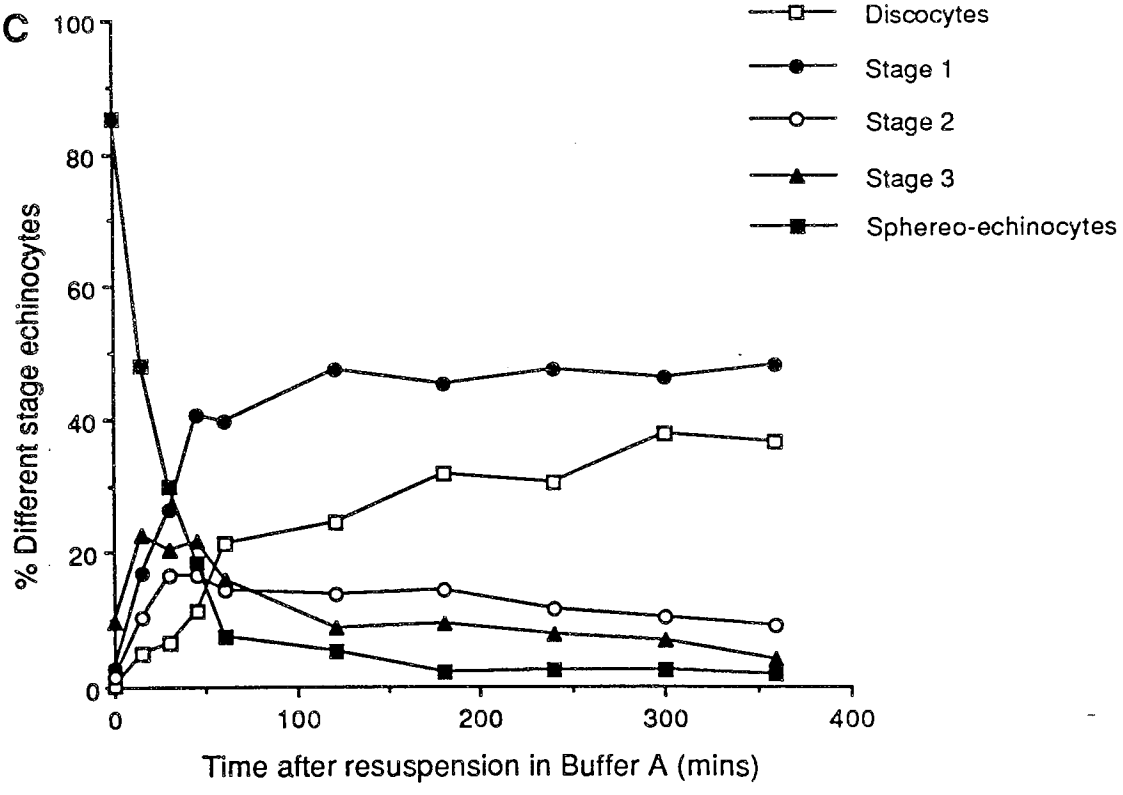
Discocytes
Stage 1
Stage 2
Stage 3
Sphereo-echinocytes
% Different stage echinocytes
0
20
40
60
80
100
0
100
200
300
400
Time after resuspension in Buffer A (mins)

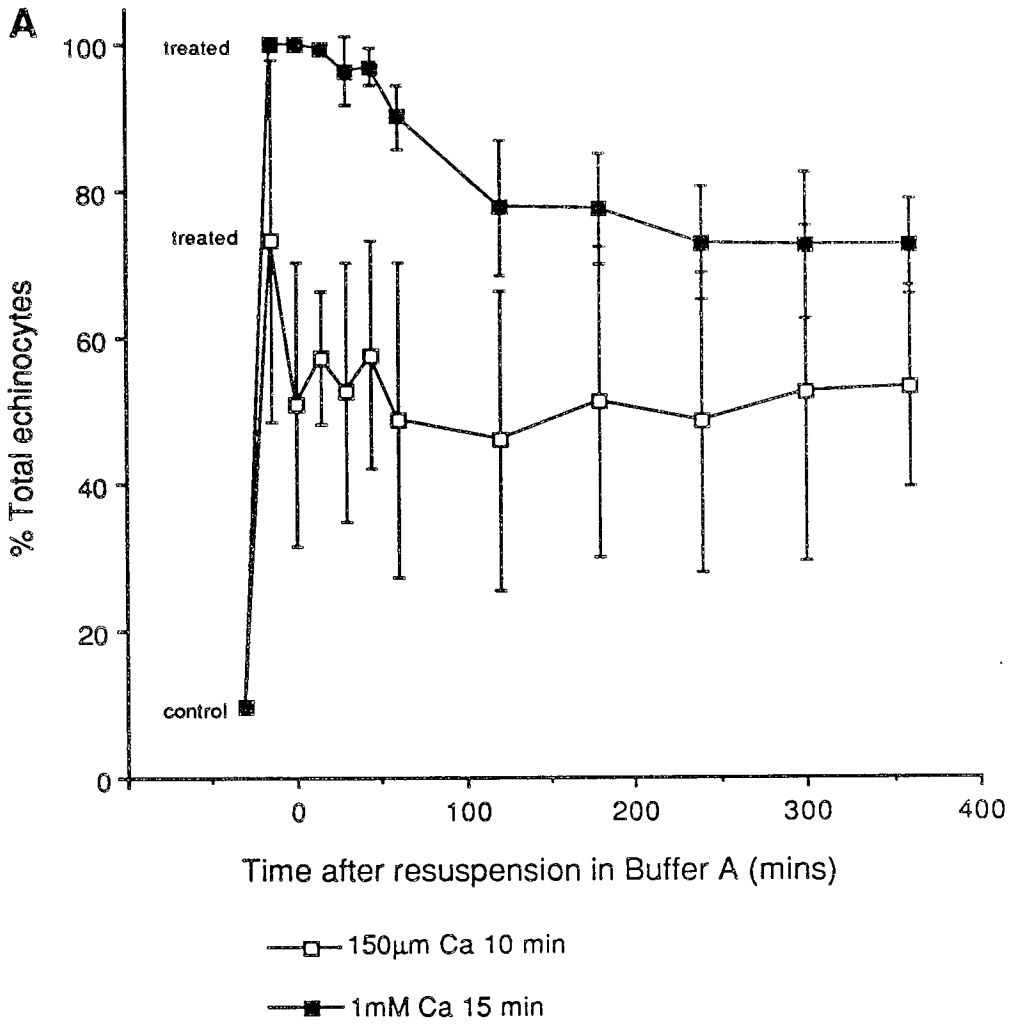


**Figure 43** The quantitation of cell morphologies during reversal from echinocytosis induced in an erythrocyte population enriched in old cells while held in buffer B; shape recovery attempted in buffer A.
Following density separation erythrocyte populations enriched in old cells and held in buffer B were loaded with either 150µM calcium for 10 minutes or 1mM calcium for 15 minutes. After removal of the calcium and A23187, cells were resuspended in buffer A and shape recovery examined by the quantitation of morphology at the time intervals specified.
**A** Total echinocyte levels. Results expressed as mean -SD (n=4).
**B** Analysis of the changes in the levels of different stage echinocytes in cells initially loaded with 150µM calcium. Results expressed as mean of n=4.
**C** Analysis of the changes in the levels of different stage echinocytes in cells initially loaded with 1mM calcium. Results expressed as mean of n=4.

**43B**

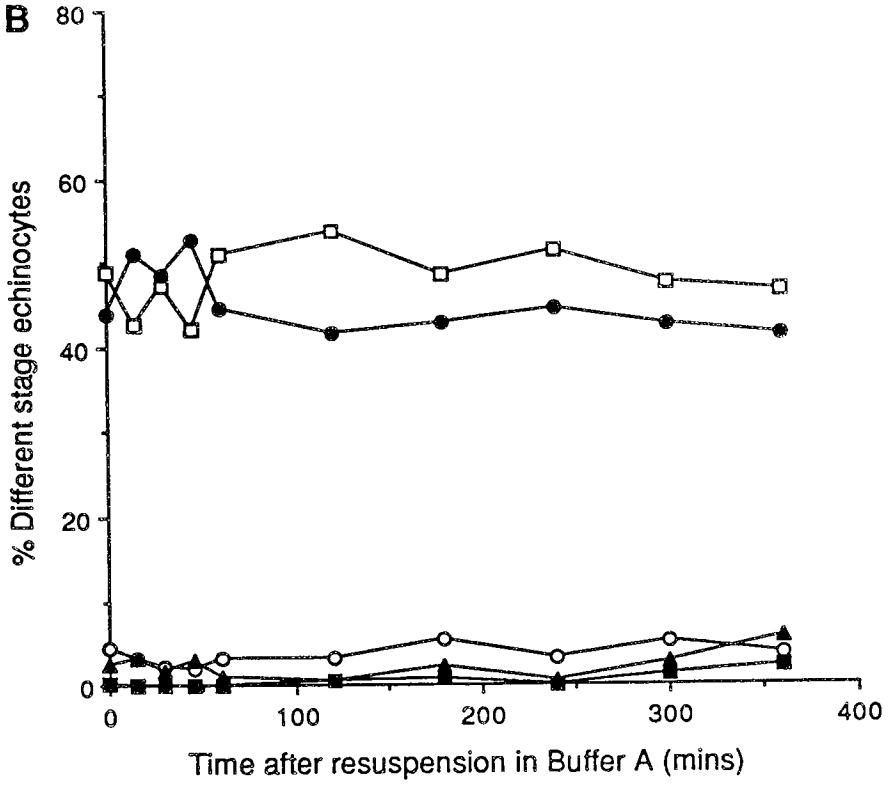
80
60
40
20
0
% Different stage echinocytes
0
100
200
300
400
Time after resuspension in Buffer A (mins)

**43C**

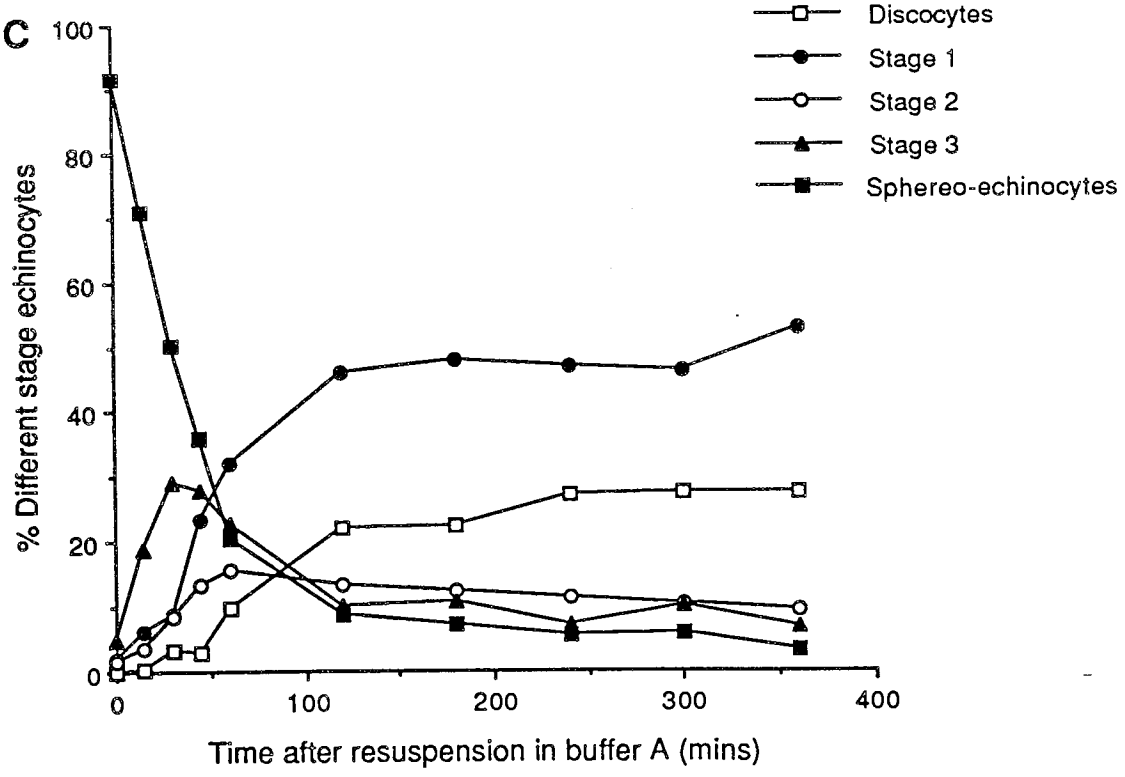
Discocytes
Stage 1
Stage 2
Stage 3
Sphereo-echinocytes
100
80
60
40
20
0
% Different stage echinocytes
0
100
200
300
400
Time after resuspension in buffer A (mins)

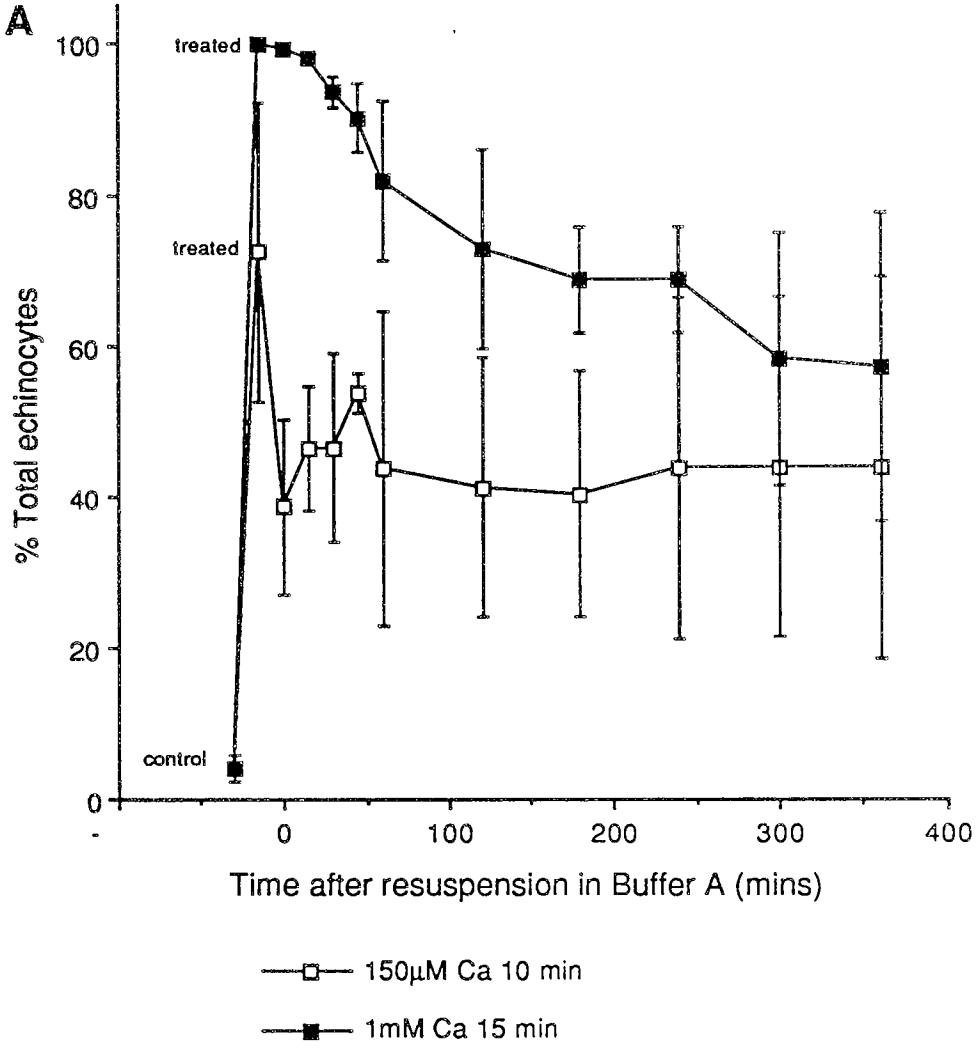


**Figure 44** The quantitation of cell morphologies during reversal from echinocytosis induced in an erythrocyte population enriched in young cells while held in buffer A; shape recovery also attempted in buffer A.
Following density separation erythrocyte populations enriched in young cells and held in buffer A were loaded with either 150µM calcium for 10 minutes or 1mM calcium for 15 minutes. After removal of the calcium and A23187, cells were resuspended in buffer A and shape recovery examined by the quantitation of morphology at the time intervals specified.
**A** Total echinocyte levels. Results expressed as mean -SD (n=4).
**B** Analysis of the changes in the levels of different stage echinocytes in cells initially loaded with 150µM calcium. Results expressed as mean of n=4.
**C** Analysis of the changes in the levels of different stage echinocytes in cells initially loaded with 1mM calcium. Results expressed as mean of n=4.

**44B**

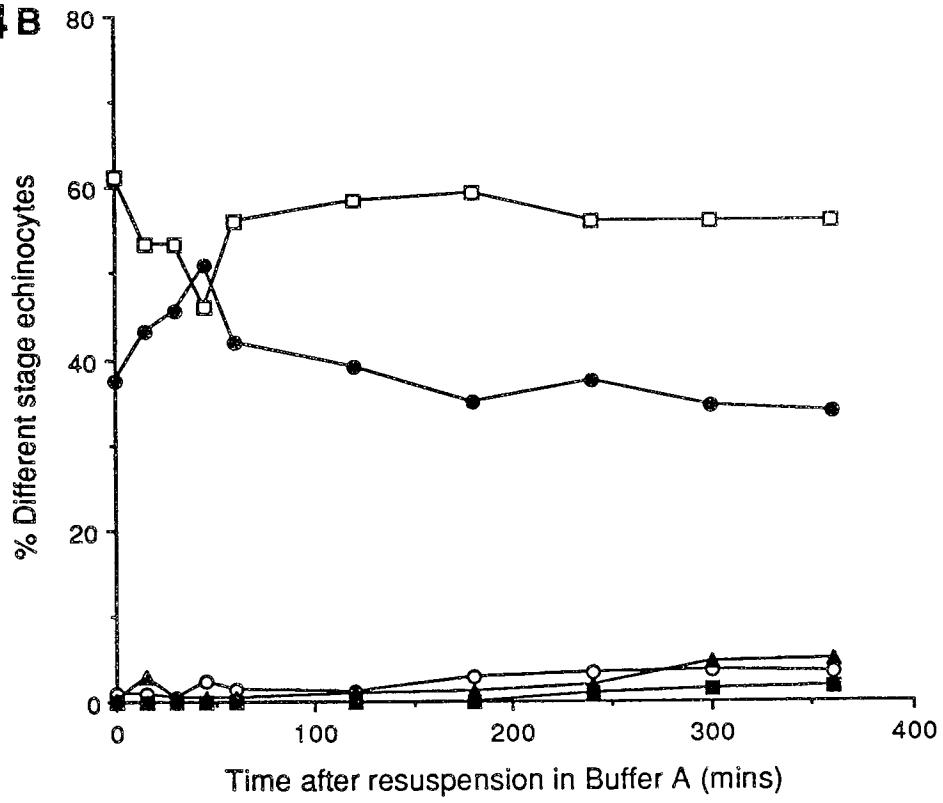
% Different stage echinocytes
0
20
40
60
80
0
100
200
300
400
Time after resuspension in Buffer A (mins)

**44C**

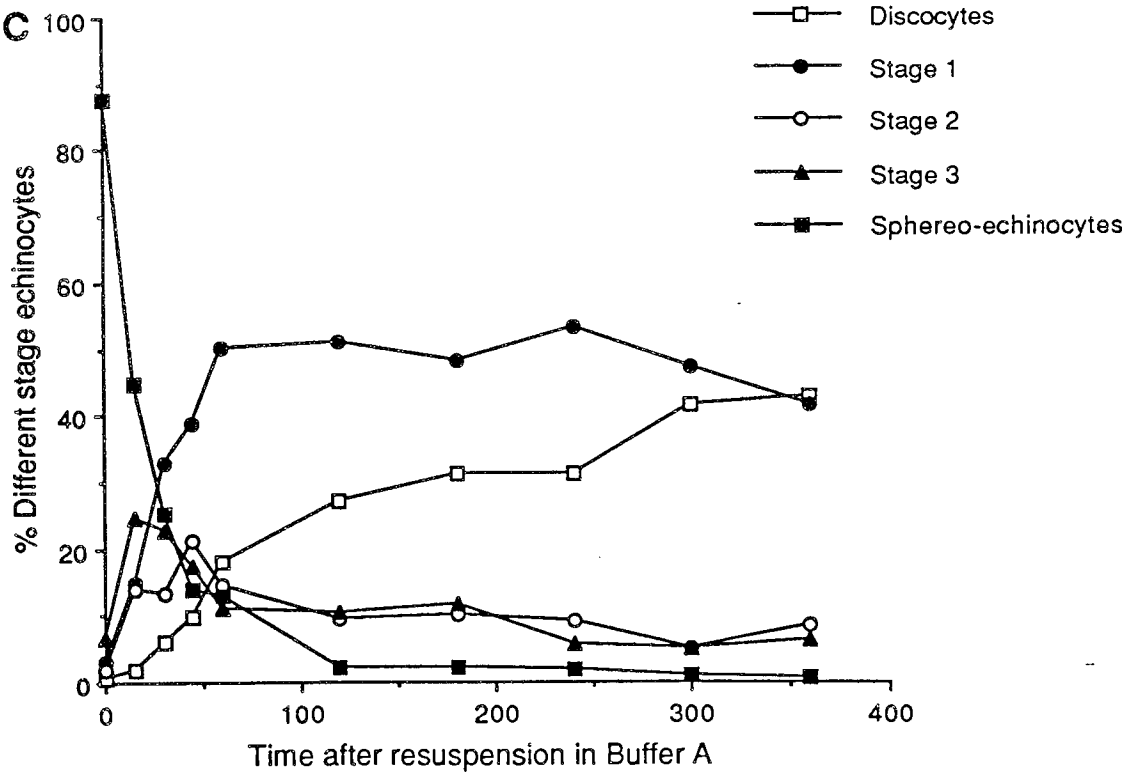
Discocytes
Stage 1
Stage 2
Stage 3
Sphereo-echinocytes
% Different stage echinocytes
0
20
40
60
80
100
0
100
200
300
400
Time after resuspension in Buffer A

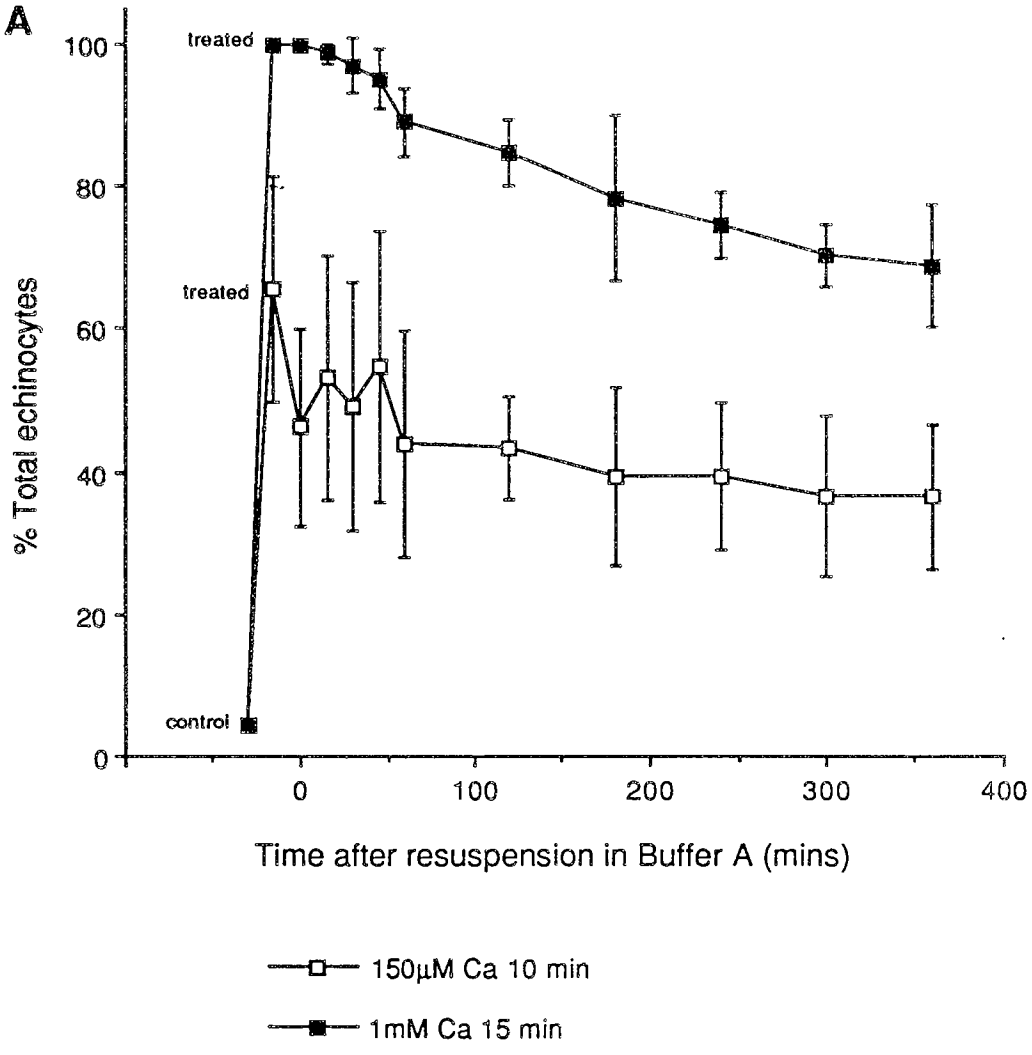


**Figure 45** The quantitation of cell morphologies during reversal from echinocytosis induced in an erythrocyte population enriched in old cells while held in buffer A; shape recovery also attempted in buffer A.
Following density separation erythrocyte populations enriched in old cells and held in buffer A were loaded with either 150µM calcium for 10 minutes or 1mM calcium for 15 minutes. After removal of the calcium and A23187, cells were resuspended in buffer A and shape recovery examined by the quantitation of morphology at the time intervals specified.
**A** Total echinocyte levels. Results expressed as mean -SD (n=4).
**B** Analysis of the changes in the levels of different stage echinocytes in cells initially loaded with 150µM calcium. Results expressed as mean of n=4.
**C** Analysis of the changes in the levels of different stage echinocytes in cells initially loaded with 1mM calcium. Results expressed as mean of n=4.

**45B**

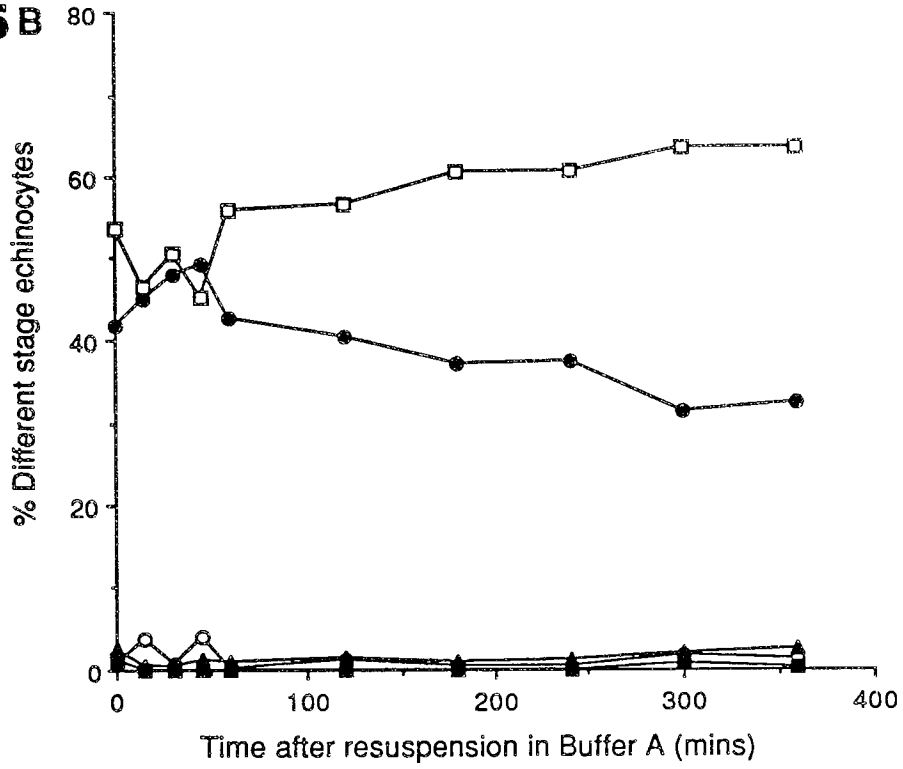
% Different stage echinocytes
80
60
40
20
0
0
100
200
300
400
Time after resuspension in Buffer A (mins)

**45C**

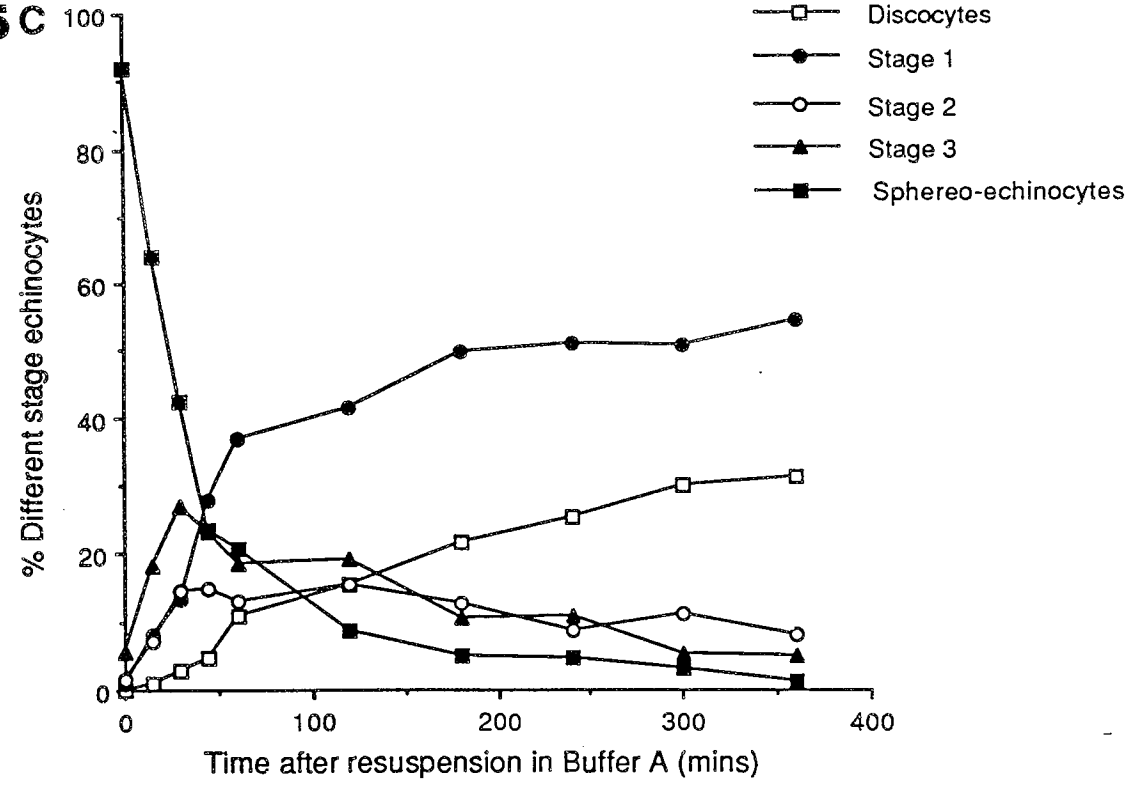
Discocytes
Stage 1
Stage 2
Stage 3
Sphereo-echinocytes
% Different stage echinocytes
100
80
60
40
20
0
0
100
200
300
400
Time after resuspension in Buffer A (mins)